Modelling and design of a general purpose, vertical shaft conveyance, all level docking device.

A.J.H. Lamprecht
20559313

Dissertation submitted in partial fulfilment of the requirements for the degree *Magister* in Mechanical Engineering at the Potchefstroom Campus of the North-West University

Supervisor: Prof. J. Markgraaff

May 2015

NORTH-WEST UNIVERSITY
YUNIBESITI YA BOKONE-BOPHIRIMA
NOORDWES-UNIVERSITEIT

It all starts here ™

ACKNOWLEDGEMENTS

ABSTRACT

Deep level mining is widely practised throughout South Africa, particularly in the gold sector, where the extraordinary depths of vertical hoisting present an array of challenges. The accurate and secure positioning of a conveyance next to a station has been and continues to be one of the unresolved challenges that have led to many serious injuries and equipment damage. The literature study presented in this dissertation highlights some of the complexities associated with properly docking a conveyance and investigates some current, proposed and similar systems to address the issue. From the study it was found that no satisfactory device existed prompting a systematic design of a conveyance arresting device capable of securing a conveyance in a vertical shaft at any level.

Proper definition of the system requirements was obtained and summarised into 16 groups. The system requirements play an important role in the design process by setting the direction but also featuring in concept screening and evaluation. In order to generate concepts a variety of creativity inspiring techniques were employed facilitating a systematic search for a solution. Application of the techniques, Brainstorming, Synectics, TRIZ, 2500 Engineering Principles, Sourcebooks and a Morphological chart resulted in the synthesis of 9 concepts. Screening and evaluation was performed on these concepts and the most suitable concept identified.

The proposed concept is a simple system where two sets of beams are extended into the shaft in order to have the conveyance settle onto the supporting shaft steelwork. Once the conveyance came to a rest on the steelwork a second set of beams are extended beneath the steelwork to positively lock the conveyance in position. This required the geometric design of the system to ensure adequate strength to satisfy a factor of safety of ten. Design decisions were made on the section properties of the clamp beam by comparing a solid section and a box section. A supporting frame is used to guide the beams, with consideration given to the most appropriate method of attaching this support frame to the conveyance. The first choice was to have the beams extend from the rear of the conveyance but due to the moments and forces involved the conveyance roof structure could not support this configuration. The support frame was instead affixed directly to the conveyance Transom.

In order to support the findings of the conventional calculations performed on the system components the system was subjected to finite element analysis. The results obtained from the simulation corresponded well for the simple components and varied somewhat in the more complex shapes attributed to the assumptions made to ease the conventional calculations. Weight and reliability in a harsh shaft environment was identified as critical design parameters and motivated the use of exotic high strength materials. The high strength of the materials made is possible to design a system with practical dimensions of adequate strength supported by the conventional and modelled calculations.

Even though high strength materials were used in the design the overall system weigh is dissatisfying. A potentially successful and practical device was designed but certain factors such as weight, cost, conveyance structure and infrastructure modifications threaten the implementation of the design. This dissertation sets a sound foundation for future development and the continued search for a practical simple solution to this age old challenge.

Keywords: Vertical shaft, conveyance docking/arresting, Alignment device, keps, Levelok.

TABLE OF CONTENTS

LIST OF TABLES

LIST OF FIGURES

NOMENCLATURE

WED:	Winding engine driver
DMR:	Department of Mineral Resources
m:	Meter
PDR:	Product Design Requirements
TRIZ:	Teoriya Resheniya Izobreatatelskikh Zadatch
	Theory of Inventive Problem Solving
MAI TRIZ:	Meta Algorithm of Inventive TRIZ
IFM	Ideal Final Result
FIM	Functional Ideal Model
SITO+	Single In Tuple Out - Positive
SITO-	Single In Tuple Out- Negative
BICO	Binary In Tuple Out
RICO	Radical In Cluster Out
MITO	Multiple In Tuple Out
PLC	Programmable Logic Controller
kg	Kilogram
N	Newton – Measure of force
EES	Engineering Equation Solver
bar	Measure of pressure equal to 100 kPa
Pa	(Pascal) SI unit for pressure.
l	(Litre) Unit of volume equal to 1 dm^3
CAD	Computer Aided Design
FEA	Finite Element Analysis
3D	Three Dimensional
PES	Project Engineering Services
NDT	Non Destructive Test

DECLARATION OF DEFINITIONS

Onsetter: Means the person who shall be the holder of an onsetters certificate issued by the Principle Inspector of Mines or who has been assessed competent against a skills program recognised by the Mining Qualifications Authority for this purpose, appointed by the manager to be in charge of a cage, skip or other means of conveyance underground in which persons are being raised or lowered and to give the necessary signals.

Haulages: An underground tunnel excavation leading from the shaft to the development end.

Cross cuts: An underground tunnel excavation splitting from the haulage to enable travel towards the reef.

Raise line: An underground tunnel excavation developed on the reef following the same inclination.

Stoping: The process where the reef is broken and cleaned.

Gullies: Excavations towards the panel broken off from the Raise line.

Kingpost: The main vertical load carrying member on a shaft station.

Bunton: Steel segments dividing the shaft into compartments and onto which the shaft guides are fastened.

Transom: The structural member from which the conveyance brindle is suspended.

Bridle: The structural member carrying the conveyance.

CHAPTER 1. INTRODUCTION

1.1.   PREFACE

Deep level gold mines require men and material to be transported to the underground workings down a vertical shaft, in a multi deck conveyance, through the process of hoisting. The position and speed of the conveyance is controlled from the hoist, operated by a certificated winding engine driver (WED), through the manipulation of the hoist's brakes and power [1].The WED is tasked to properly position the conveyance next to a level in order to load and unload men and material.

The accurate positioning and the stable suspension of the conveyance is a complex task influenced by multiple factors, such as rope stretch, conveyance load, reaction times, multi-layer coiling and conveyance arresting device efficiency. The conveyance is therefore frequently misaligned with the level. Without a proper docking system the conveyance is also likely to oscillate relative to the level.

Misaligned cages, failed arresting devices and rope stretch related accidents are therefore an unfortunate reality. Information from the Department of Mineral Resources (DMR) [2] disclosed that there have been 19 serious accidents between 2004 and 2012 directly related to conveyance position and stability. Failed arresting devices also led to the loss of life of three mineworkers [3], [4] at AngloGold Ashanti's Tau Tona mine.

The conveyance can be aligned higher or lower than the level each presenting its own risks. A conveyance positioned too high creates a step from which the workers must step down, when disembarking, creating the potential to fall and step up, when embarking, creating the potential to trip. The higher conveyance position imparts potential energy to the material cars loaded in the conveyance, when unloading these fall down to the level and exit with excessive speed posing a hazard to the workers unloading the conveyance. This fall further causes damage to the rails, car wheels and bearings, car content and greatly increases the chance of a derailment. When loading the cars need to be ramped into the cage requiring excessive energy to be expended.

Alternatively the conveyance can be positioned too low in which case workers disembarking need to step up, creating a tripping hazard, onto the level while at the same time the exit opening has decreased due to the upper deck being closer to the level. Hand injuries are common as the onsetter needs to lock and unlock the latches in the confined space between the level and the conveyance door. Difficulty is further experienced when attempting to unload material cars and the cars are again caused to fall into the cage when loading.

The rope suspending the conveyance is an elastic member which complicates the process further. With an abrupt stop next to the level the conveyance will oscillate excessively. As the mass in the conveyance increase the rope will stretch and as it decreases the rope shortens. The position of the conveyance, therefore constantly varies as the load changes and the conveyance oscillates. The change in position from too high to too low magnify the hazards listed in the previous paragraph.

A case study involving the capture and analysis of 9 hours of video material over 3 days at Mponeng mine [5] provided insight into the magnitude and frequency of conveyance misalignment. A total of 110 trips were done of which 4 were properly aligned and 4 misaligned to such an extent that it had to be realigned, a timely process. The graph provided below summarises the number of misalignments between set elevation difference brackets. The conveyances were misaligned higher than the level on 88 instances with a maximum misalignment exceeding 350 mm and lower than the landing on 18 instances.

Distribution profile of conveyance misalignment
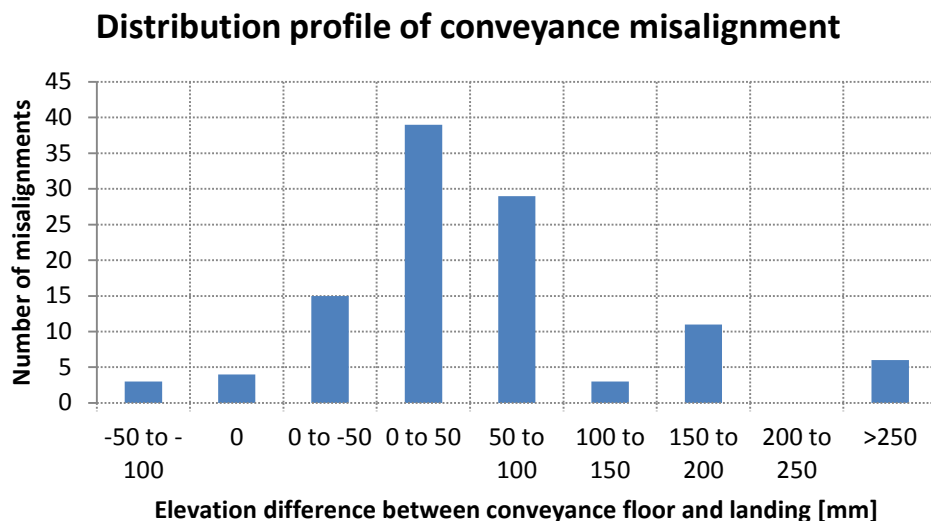
FIGURE 1 GRAPH SUMMARISING THE EXTEND AND FREQUENCY OF CONVEYANCE MISALIGNMENT FROM A CASE STUDY AT MPONENG MINE.

A misaligned and moving conveyance is a serious problem in deep level mines as it introduces risks to safety, time and equipment condition. These risks can escalate into severe financial losses and impaired quality of life of workers.

1.2. PROBLEM STATEMENT

The problem is that a conveyance in a vertical shaft is frequently misaligned with the station as a result of the multitude of factors that influence the ability to align the conveyance properly. The problem is further that the conveyance is able to move relative to the station during loading and unloading operations.

1.3. SCOPE

The scope of the project is to systematically search for and identify a means of ensuring that a conveyance is aligned properly with a level to such an extent that the floor of the conveyance line up with the rails on the station and remain stationary in that position. The literature study covers factors affecting the alignment, present cage arresting systems and proposed and patented ideas. The remainder of the dissertation covers the systematic design of a conveyance arresting device.

CHAPTER 2. LITERATURE REVIEW

2.1. GOLD MINING BACKGROUND

Gold mines require infrastructure and processes to reach the reef from where gold bearing ore is extracted. Vertical shafts are sunk to raise and lower men and material to the necessary levels from which mining takes place. Horizontal excavations known as haulages are developed parallel to the reef extending from the shaft. Cross cuts are tunnels breaking away from the haulages to develop towards the reef. At the reef intersection raise lines are developed, following the reef inclination, out of the cross cuts. Stoping the term used for the cyclic mining process of breaking and cleaning ore is then done from the raise lines. Gullies are left to allow access to the panel being mined. Figure 2 below gives an illustration of the underground excavations required for mining.
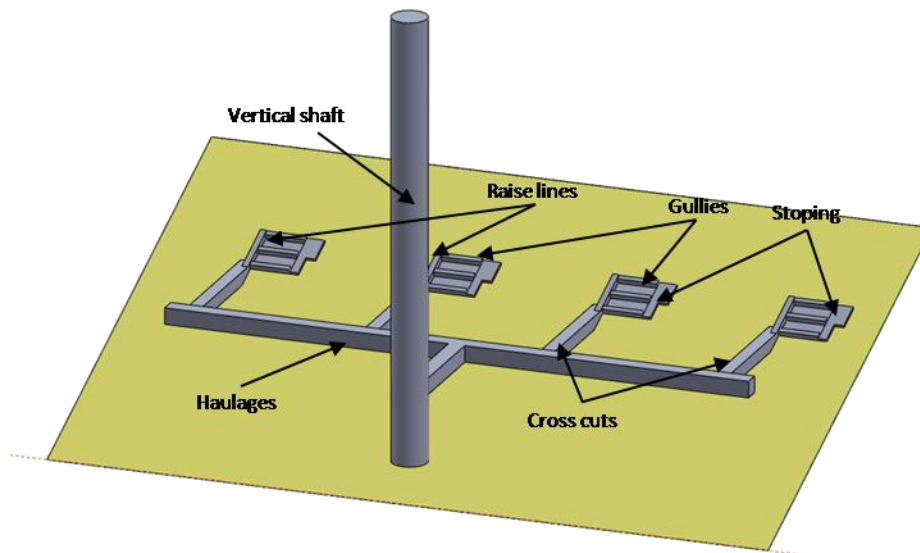
FIGURE 2 BASIC 3D ILLUSTRATION OF A MINE DESIGN

2.2. HOISTING DYNAMICS

Hoisting is the process where a conveyance is raised or lowered, in a vertical shaft, through the action of a hoist for the purpose of transporting men, material or rock. The position of the multi-deck conveyance suspended from a rope is dependent upon the amount of rope spooled out or reeled in by the hoist, under the control of the WED. A winding cycle as shown below illustrates the process of moving from one level to another [6].
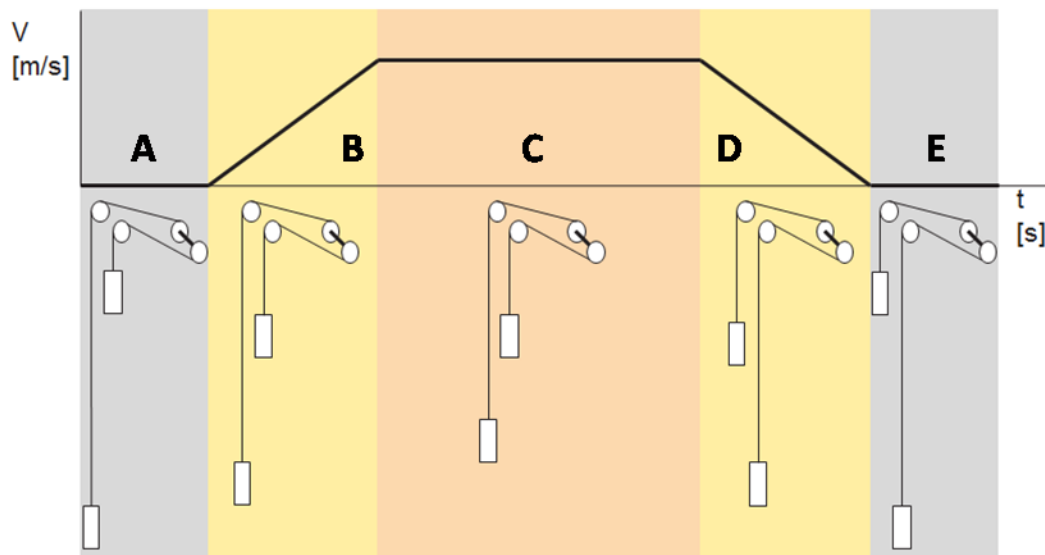
FIGURE 3 DIAGRAMATIC ILLUSTRATION OF A WINDING CYCLE [6]

At position A the conveyance is stationed at the bank with the brakes locked and the full number of layers of rope coiled on the underlay drum. The conveyance is called to position E, by the onsetter, through the exchange of the necessary bells on the lock bell system. The signal from the onsetter unlocks the hoist's brakes and allows the WED to lift his brakes. By applying power to the hoist the rope is spooled off the underlay drum and the conveyance in the underlay compartment accelerates down the shaft. Simultaneously rope is coiled onto the overlay drum and the conveyance in the overlay compartment is raised. The conveyance is accelerated at position B to full travelling speed at position C on the figure above. The conveyance is run at full speed at position C from where it is decelerated at position D to come to a stop at the desired position E.

The WED makes use of his depth indicator which is simply an indexed dial and pointer to judge his position in the shaft and commence braking; decreasing the conveyance speed until it nears the level. The indexed dial depth indicator is too crude to allow accurate alignment so the WED makes use of his second indication. To more accurately align the conveyance the WED allows the hoist to undergo more revolutions referencing numbers painted on the drum. The drum is thus indexed to allow the WED to only rotate it in discrete fractions of a revolution. Because the number of layers of rope on the drum changes, causing a difference in the effective drum diameter, as the conveyance moves through the shaft the discrete fractions on the drum will correspond to different linear movements at different positions in the shaft. This hinders the accurate alignment of the conveyance at different positions. To overcome this the WED often depend on the onsetter giving him a signal to stop at the level. Reaction time of the onsetter and WED therefore influences the final positioning.

2.3.   ROPE CONSIDERATIONS

With the hoist stationary the position of the conveyance can only change if the rope length changes. There are two ways in which a rope can affect the position of the conveyance. A rope is an elastic member with a noticeable spring effect which is magnified when the conveyance is brought to an abrupt stop.

The rope also experiences stretch as described in the African wire ropes limited publication [7], Steel wire ropes for cranes and general engineering [8] and Haggie steel wire ropes for mining technical training manual [9]. A wire rope does not only experience elastic stretch but also a permanent stretch after the removal of a load due to the "bedding down" of the rope. The "bedding down" of a rope is dependent upon various parameters such as the quality of core, pre-forming and rope construction. The rope characteristics are thus based on the behaviour of the strands from which it is constructed. Common winding ropes such as 6 strand triangular ropes and non-spin ropes can stretch permanently between 0.5% and 0.75 %. This stretch takes a time to settle in properly and as such a newly installed rope continues to stretch for a couple of days.

The rope also undergoes elastic stretch which can be calculated from the equation below given in manufacturer's documents.

$$\Delta L = \frac{FL}{AE}$$

Where ΔL = Elongation (Stretch) [Meter]

F = Tension in rope [Newton]

L = Length of member (Rope) [Meter]

A = Area of member (Metallic area of rope) [Meters squared]

E = Elastic modulus of rope [Pascal]

A change in any of the parameters on the right hand side of the equation results in a change of rope length. The tension in the rope depends on the mass of the conveyance and the mass of the expelled rope. The tension is therefore different at different positions in the shaft and as mass is added or removed from the conveyance. The length of rope expelled is different for different levels and thus the stretch differs. The metallic area of the rope is the only load carrying member and constitutes the area of the member. Values for the area and elastic modulus are available in manufacturers' tables.

Complicating the matter further is that the elastic modulus for a rope is inconstant especially for ropes loaded to less than a quarter of their breaking strength. The modulus of elasticity for a rope is roughly linear when the rope is loaded between 25 % and 60 % of its breaking strength. The modulus of elasticity decrease as the load in the rope decreases below 25 %. The modulus of elasticity is then also linked to the permanent elongation. As the permanent elongation increases so does the modulus of elasticity. Simply put the more the rope "beds down" the higher the modulus of elasticity become.

The Minerals Act [10] requires that a winding rope used for the conveyance of men should have a safety factor of 8, implicating that a rope is never loaded to more than 12.5 % of its breaking strength. The load is therefore always below 25% of the breaking strength and all operation occurs in the load range where the elastic modulus is very inconsistent.

2.4.   CONVEYANCE ARRESTING DEVICES

2.4.1. LEVELOK

Levelok is a conveyance arresting system currently used by AngloGold Ashanti and explained in the AngloGold Ashanti specifications AngloGold AG ENG 063[11] and Anglogold AG ENG 064[12]. The system operates by having the WED position the conveyance next to the level. The onsetter connects compressed air to the power pack which drives a hydraulic pump to engage the clamps. Clamps with specially fitted friction shoes are pivoted to clamp onto the, 152 mm by 102 mm, steel top hat guides through which the conveyance runs. The system is mounted above or beneath the conveyance and can thus operate from any level. The conveyance is suspended in the shaft by clamping the guides strong enough to have friction keep the conveyance in position. The figure below shows the basic functionality of the system.
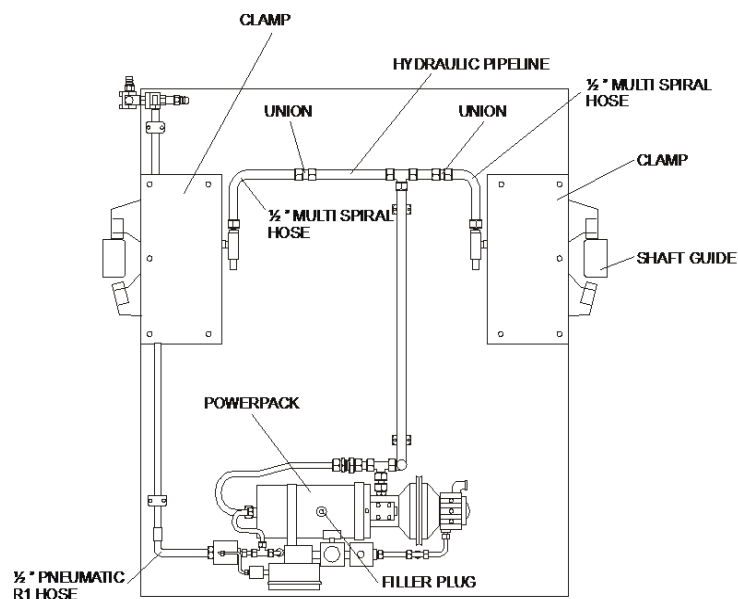
FIGURE 4 ILLUSTRATION OF A LEVELOK CAGE ARRESTING SYSTEM. ANGLOGOLD AG ENG 063 [12]

The Levelok system has primarily three drawbacks which have resulted in the reduced usage thereof. The system is time consuming to operate as the hydraulic pump must first build up sufficient pressure. The system merely supports a conveyance and does not work in aligning it. When disengaging the load must be transferred back to the rope and it often happens that the clamps release too quickly resulting in the load being rapidly transferred to the rope and the rope experiencing a dramatic amount of stretch.

2.4.2. CONVEYACE ARRESTING HOOK KNOWN AS KEPS

Another conveyance arresting device known as the KEPS device is currently used by AngloGold Ashanti and explained in AngloGold Ashanti specifications Anglogold AG ENG 218 [13] and Anglogold AG ENG 350 [14].The KEPS device works by having the conveyance lowered into the hook and then transferring the load to the kingpost, the main vertical support beam on the station. The figure below aids in the description of the process.
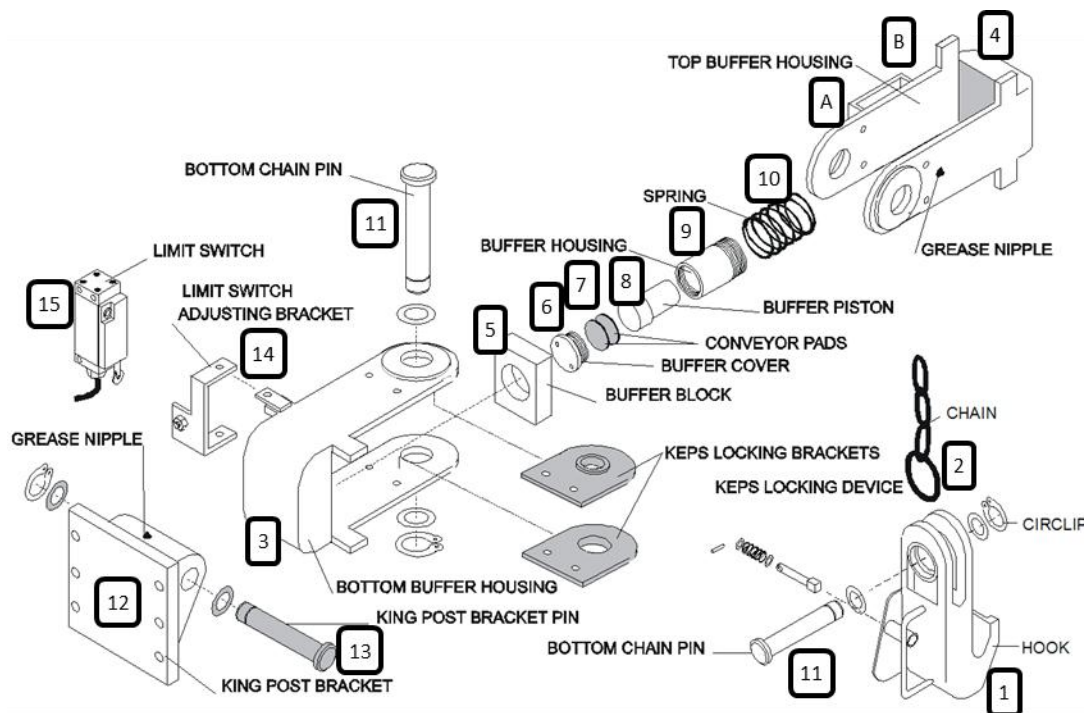
FIGURE 5 ILLUSTRATION OF THE COMPONENTS OF A KEPS CAGE ARRESTING SYSTEM. ANGLOGOLD AG ENG 218 [13].

As the conveyance approaches a level the onsetter signals the WED to reduce the speed. The onsetter's assistants hold the hook (1) into the path of the conveyance which engages with the hook on a strengthened slotted plate known as the perimeter plate. The system is used in duplicate to handle the weight and balance the load requiring the onsetter assistants to engage both hooks. The weight of the conveyance pulls the bottom buffer housing (3) down which is connected with a chain (2) to the hook (1). The bottom buffer housing (3) is thus pulled towards the top buffer housing (4) which is connected to the Kingpost through the Kingpost bracket (12). As the two buffer housings are pulled towards each other the buffer assembly components (5 to 10) are compressed damping the impact of the engagement. The conveyance rests in the hook and the load is transferred through all the components to the Kingpost.

The system further indicates when the conveyance is placed in the hook. A limit switch (15) is connected to the bottom buffer housing (3) through a limit switch adjusting bracket (14). The wheel of the limit switch (15) runs in the guide on the top buffer housing (4). If there is no weight on the hook the spring (10) will force the top and bottom buffer housings (3, 4) apart and the limit switch (15) contacts the guide on the A side. This gives an indication that there is no weight on the hook (1) and that there is thus no conveyance in the hook (1). When the buffer housings (3,4) are pulled together under the weight of the conveyance the limit switch makes contact with the B side of the guide indicating that there is a conveyance in the hook. The limit switch activates lights in a display panel on the station and at the WED cabin to indicate whether the conveyance is engaged or not. Newer systems use a laser in the throat of the hook to give an indication of the conveyance engagement following a fatal accident [3], [4]. With the conveyance engaged the WED spools out slack necessary to prevent the conveyance lifting out of the hooks when the rope stretch reduces as the conveyance is unloaded.

The KEPS device has a few drawbacks. In order to function properly both hooks must be engaged simultaneously and into the slots, a challenge with inexperienced or insuficient labour. The device requires that slack rope be spooled out where excessive slack can cause damage to the rope. Insufficient slack will cause the conveyance to rise out of the device when the conveyance is unloaded. The device also requires the conveyance to approach from above.

2.4.3. RACK AND PINION CAGE ARRESTING DEVICE

A rack and pinion cage arresting device is presented in the thesis by R. Austin [15] and a subsequent interview [16] with the engineer details the concept illustrated below.
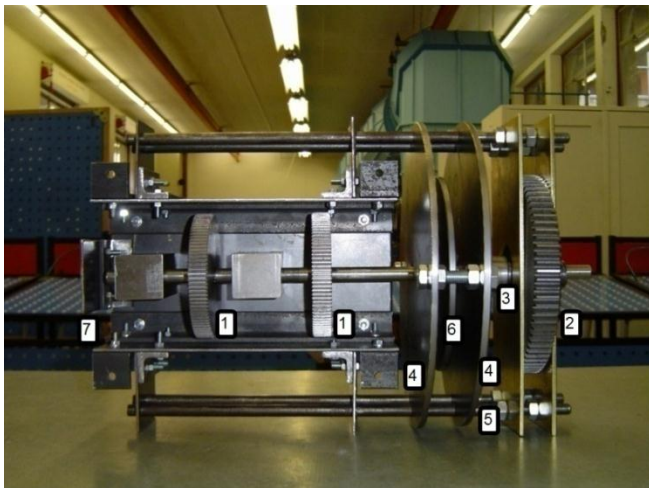
FIGURE 6 PHOTOGRAPH OF A MODEL OF A PROPOSED RACK AND PINION OPERATED CAGE ARRESTING DEVICE. R.AUSTIN [15].
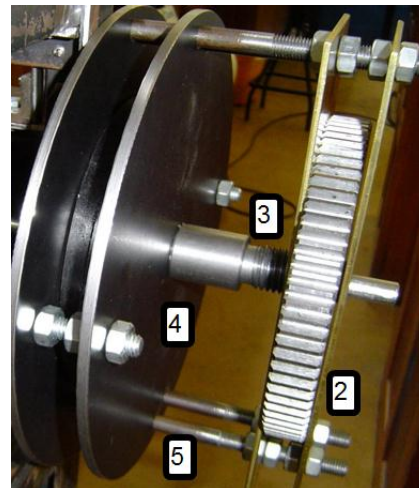
FIGURE 7 PHOTOGRAPH DETAILING THE DRIVE COMPONENTS OF A PROPOSED RACK AND PINION OPERATED CAGE ARRESTING DEVICE. R.AUSTIN [15].

The concept requires a rack to be placed on the conveyance which interacts with the pinion of the device (1). The conveyance is decelerated and secured by slowing the relative speed between the rack and pinion (1).

The concept uses a pinion (1) on a sliding shaft allowing it to be disengaged from the rack. In the disengaged position the conveyance is free to pass when the system, placed on the station, isn't in use. The system works by moving the shaft with the pinions (1) axially until it engages with the racks and then braking the shaft. The gear (2) seen in figure 7 is driven by a motor inducing axial movement on the threaded boss (3).

Axial movement of the threaded boss (3) moves both the discs (4) connected together and placed on guides (5). In-between the two discs (4) a third smaller disc (6) is mounted on the same shaft as the pinions (1). As the discs (4) are moved by the boss (3), it pushes against the middle disc (6) displacing it axially. This continues until the shaft is pushed against a stopper (7) at which stage the pinions (1) should be in the engagement position. The stopper (7) prevents any further movement of the shaft and a continued rotation of the gear (2) on the right only serves to increase the pressure between the discs (4) and the middle disc (6) connected to the shaft. This interference between the discs (4, 5) works like a clutch generating the braking action. More braking force is obtained by rotating the gear (2) further as it results in a greater pressure between the discs (4, 5) and therefore more friction.

The prototype was tested in a replica model of a shaft where it managed to decelerate and suspend a cage. The engagement between the rack and pinion however struggled on occasion with a particular incident seeing the cage jump up, proving difficulty in engaging at high speeds. The prototype further failed as final calculations showed that the size of the pinion gear required is too large. The strength of the gear and rack teeth is insufficient even with the use of high strength materials. A critical flaw in the concept was that the shaft onto which the pinion is mounted needs to pass through the Kingpost, a major structural member.

2.4.4. PATENTS SEARCH

A search for patents addressing the issue of docking a conveyance delivered no results. Two patents addressing the chairing of elevator cars, which is similar to a conveyance, were found.

Patent 1 has an elevator car mounted on top of a beam referred to as the arrestor. Between the car and the beam damping elements (13) are placed to absorb the impact to the car when the arrestors are engaged. The arrestors are simply latches (20) which are kicked out into the path of stop blocks (26). These latches (20) are kicked out by having a magnetic actuator (21) extend rotating bar (23) and lifting lever (24) which kicks out the latch. [17].
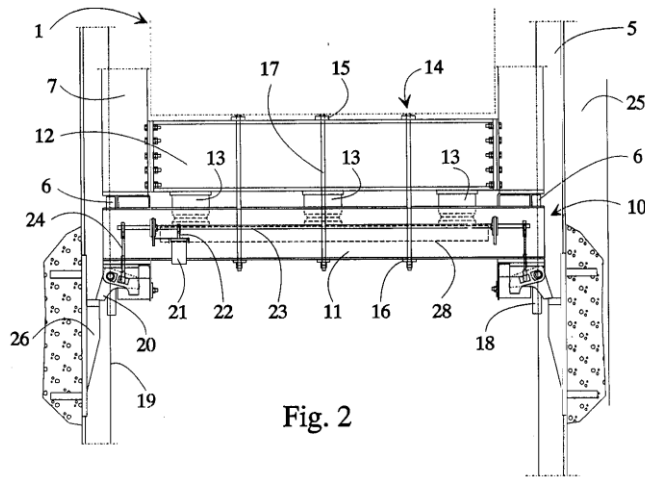
Fig. 2

FIGURE 8 ILLUSTRATION SHOWING THE LATCH ARRANGEMENT FROM PATENT US: 5,411,117 [17].

Patent 2 has an elevator car (18) connected to a beam (17) at the bottom of the car (18). From this beam (17) the car (18) is locked in a elevator hatchway by extending pins (37 / 47) into holes (39) located in the elevator hatchway. The embodiments are to either engage the pins (37 / 47) through the use of a jack screw (43) or a solenoid (60) . When the pins (37 / 47) are engaged the car (18) is secured and unable to move vertically. The pins (37 / 47) aren't able to retract as they experience a large frictional force due to the movement of the car (18) brought about by rope stretch. In order to release the car (18) load cells (62) or strain gauges (65) are placed on the pins (37 / 47). These measurements are send to a control unit that control the elevator driving sheaves to raise or lower the car (18) in order to release the pressure on the pins (37 / 47). The pins (37 / 47) are then retracted and the elevator car released.[18].
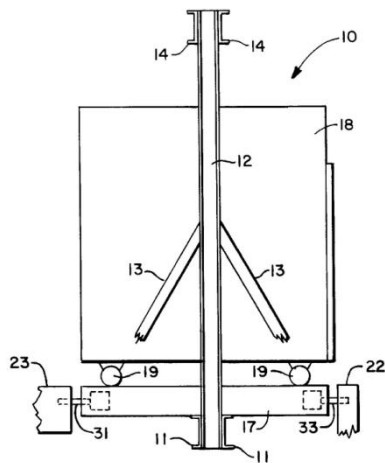
FIGURE 9 SIDE VIEW OF AN ELEVATOR CAR ILLUSTRATING THE POSITION OF THE LOCKING PINS BASED ON THE PATENT US: 5,862,886 [18].
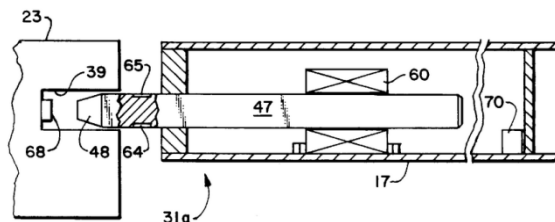
FIGURE 10 ILLUSTRATION FROM PATENT US: 5,862,886 SHOWING THE LOCKING PIN EMBODIMENT USING A SOLENOID AND STRAIN GAUGES. [18]
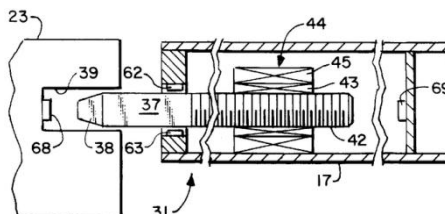
FIGURE 11 ILLUSTRATION FROM PATENT US: 5,862,886 SHOWING THE LOCKING PIN EMBODIMENT USING A JACK SCREW AND LOAD CELLS. [18]

CHAPTER 3.   TASK CLARIFICATION

Task clarification is one of the most important aspects of design. A detailed list of Product Design Requirements (PDR) was derived using the objectives tree method and the functional analysis method.

The objectives tree method based on the book, Engineering design methods, by N Cross [19] facilitated the generation of a hierarchal breakdown of the objectives and sub-objectives that must be addressed by the design. The main objectives to be satisfied are to ensure that the cage approaches the station smoothly and that the system operates reliably while being compatible with current systems. The system has to be safe and assist when the cage is repositioned to the next deck. The final product has to ensure that the cage aligns accurately and that it remains stationary while aligned. After the loading and unloading process the cage must accelerate away smoothly. The final objective is to improve efficiency without extreme costs. These objectives are listed in green blocks in the detailed objectives tree hierarchy presented in Appendix A with their sub-objectives in red, blue and black respectively.

The functional analysis method based on the book, Engineering design a systematic approach, by G Pahl, W Beitz, J Feldhusen and K.H Grote [20], suggests that any system functions by transforming material, energy and information from its input form into a desired output form. By studying the material, energy and information sources available and defining the desired output form thereof the sub-functions that catalyse this transformation are identified. The system is then designed with features to perform these functions. From the detailed process illustrated in Appendix A it is seen that the designed system must decelerate the conveyance, stop it, align it, secure it and then release it.

A summarised form of the Product Design Requirements is given in the figure below. The requirements are based on the findings of the above mentioned procedures as well as a checklist proposed in the book; Engineering design a systematic approach, by G Pahl, W Beitz, J Feldhusen and K.H Grote [20]. Appendix A contains the detailed table of quantitatively defined PDR in the format proposed by the abovementioned book. The PDR considers 16 topics namely geometry, kinematics, forces, energy, material, signals, safety, ergonomics, production, quality control, assembly, transport, operation, maintenance, costs and schedules. Each of these topics is briefly explained in the PDR summary below.

TABLE 1 SUMMARISED PRODUCT DESIGN REQUIREMENTS FOR A GENERAL PURPOSE, VERTICAL SHAFT CONVEYANCE, ALL LEVEL DOCKING DEVICE.

Summarised Product Design Requirements	
Geometry The geometry of the system should be such that it doesn't protrude into the shaft compartments or obstruct the conveyance door opening.	**Kinematics** The conveyance should arrive, engage and depart from the system with a velocity sufficiently low to minimise oscillations or damaging impact. The system should accommodate rope stretch and minimize conveyance movement when disengaging.
Forces The system should be sufficiently strong to support the conveyance in an upward or downward direction without imparting damage to the conveyance or infrastructure.	**Energy** The system should handle any impact energy and utilise the standard available energy sources, such as electricity, air and water for its operation.
Material The materials used in the system must be of adequate strength and suited to the application. It is desired to be wear and corrosion resistant and easily formable.	**Signals** The system must be fully integrated with the mine systems including the lock bell, call bell, slack-tight rope and stopping devices. It must indicate the engaged and disengaged status.
Safety The system must improve safety and operate on a failsafe principle. It must further be configured such that it discourages misuse and unauthorised access.	**Ergonomics** The system must simplify the work processes and require the minimum human input.
Production The system should be easy to manufacture and install. The operation and maintenance must be such to minimise idle time.	**Quality control** The system should contain a large safety factor, verified by a computer model, and manufactured by an accredited workshop.
Assembly The system should be easily assembled and disassembled on site.	**Transport** The system should be movable with standard mine lifting equipment.
Operation The system should be able to operate in a shaft environment, by being resistant to water, dust and falling debris. It should not make normal shaft procedures cumbersome.	**Maintenance** The system should have features to ease and minimise maintenance while highlighting component deterioration.
Costs The design should be completed at a minimum development cost and consideration given to obtain a low manufacturing cost.	**Schedule** A final design verified by a computer model should be presented in a dissertation for submission in November 2014.

CHAPTER 4.   CONCEPT GENERATION

Conceptual design involves the synthesis of potential solutions to a problem. The first step in the solution of the overall problem is to obtain solutions to the sub-functions identified through the functional analysis process in the preceding chapter. Methods are identified to decelerate a conveyance, damp the engagement forces, align the conveyance, secure the conveyance, indicate the status of the secured conveyance and equalise the rope tension. The solutions to these 6 sub-functions are combined to form a system that solves the overall problem. The 5 techniques used in this chapter to obtain solutions to the sub functions are, Brainstorming, Synectics, TRIZ, 2500 Engineering Principles and Mechanical Sourcebooks. The sub-function solutions are joined through a Morphological chart to synthesise concept solutions to the overall problem.

4.1.   BRAINSTORMING

Brainstorming was performed through the generation of a mind map. The process involved putting the topic of concern in the centre of a page and branching any sub-topics from there. These sub-topics are further branched off until the ends of the branches indicate possible solutions. The centre topic for the mind map presented on the next page is a conveyance alignment and arresting device which branches off into the 6 sub functions identified by the functional analysis process. One extra sub-topic namely the release of the conveyance is presented. The table below summarises the potential solutions generated through the use of the mind map for each of the sub functions.

TABLE 2 SUMMARY OF THE POTENTIAL SOLUTIONS FOR EACH PROBLEM SUB-FUNCTION GENERATED THROUGH THE USE OF A MIND MAP.

Decelerate the conveyance				
Forced creep	Control programme on PLC	Control Cam	Manual control according to an indicated rate	Engagement with a device and device retardation
Energy of engagement				
Impact onto a Spring	Winder deceleration to limit speed	Impact onto an elastomer	Impact onto an airbag (Compression of a compressible gas)	Impact onto a hydraulic damper
Alignment / vertical positioning				
Lever arrangement	Screw drive	Climber arrangement	Bellows	Piezoelectric
Aerodynamic lift	Lift using the hoist rope	Magnetic levitation	Hydraulic cylinder	Wedge action
Sprocket and chain	Pneumatic cylinder	Linear motor	Thermal expansion	Rack and pinion
Cam and follower	Counter movement			
Continued on next page...				

Securing				
Interference / Geometric interaction	Support / Geometric constraint	Magnetism	Suction (Pressure differential)	Bonding
Friction	High inertia			
Indication				
Magnetic switches	Pressure switches	Visual and manual signal	Load cells	Laser sensors
Slack and tight rope device	Linkages and whisker switches	Inductive switches	Camera with image identification	
Controlling rope tension / rope stretch				
Compensating link (Change rope length)	Rotate the winder drum	Control the sheave position	Release when load is normalised due to normal hoisting	Alignment / vertical positioning device move to normalise load

Brainstorming has led to the generation of multiple potential solutions to the sub-functions of the problem. The results illustrated in the table form the majority of the entries in the Morphological chart used later in the chapter. The remaining four techniques are used to supplement the concept solutions from this section.
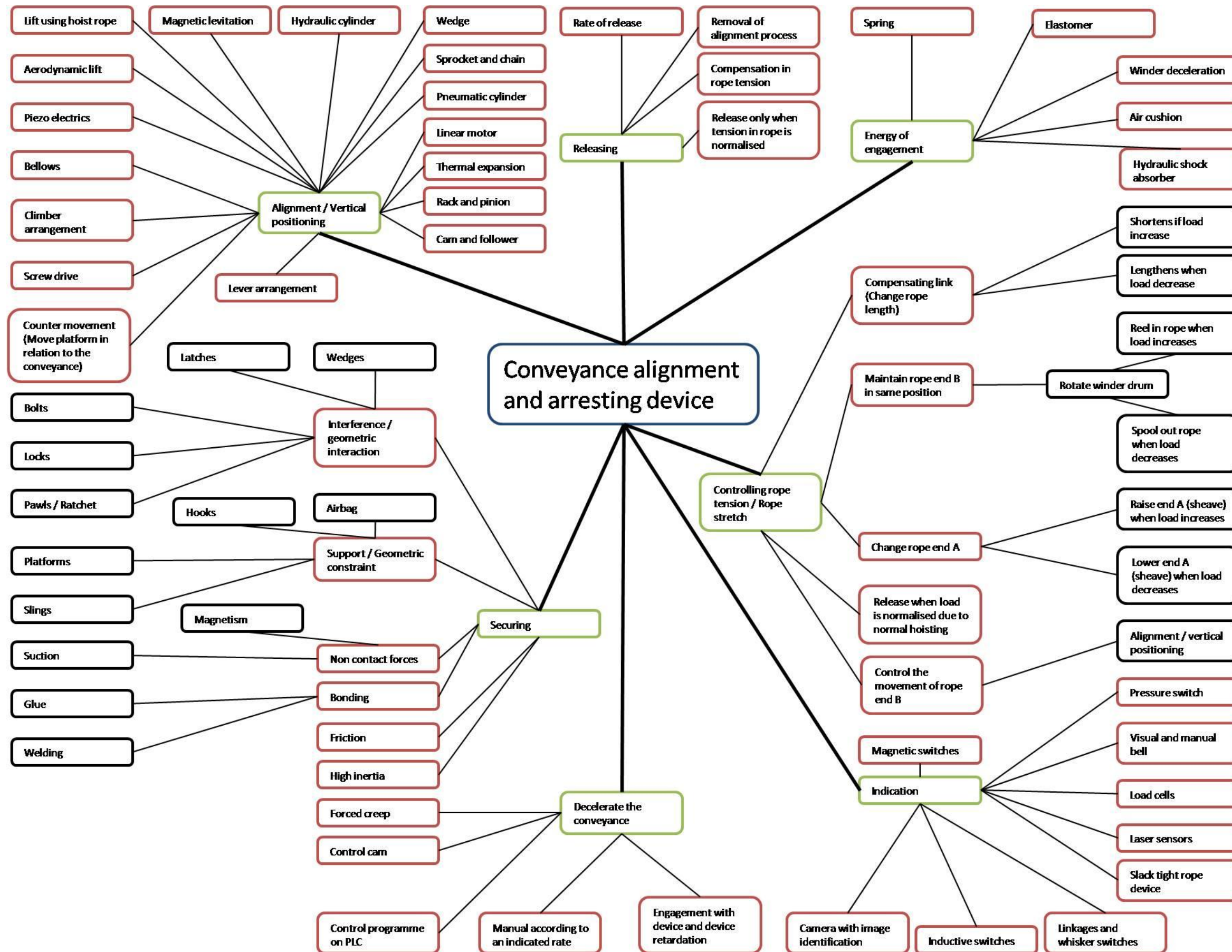
FIGURE 12 MIND MAP ILLUSTRATING POTENTIAL SOLUTIONS TO THE SUB FUNCTIONS ASSOCIATED WITH THE DESIGN OF A CONVEYANCE ALIGNMENT AND ARRESTING DEVICE.

4.2.   SYNECTICS

Synectics is a concept based on the knowledge that the brain works by creating links between thoughts, feelings, experiences and knowledge. Normally the brain group thoughts together based on similarities. Synectics however requires and promotes the realisation that complex and apparently contradicting thoughts, feelings, experiences and knowledge can also be grouped together. By forcing the mind to find a similarity between things thought unalike stimulates innovation. To start the process a Synectics trigger is required to initiate the generation of new ideas and combinations based on disruptive thinking where anything is made relevant to the problem. It is further necessary to then question why things are considered similar or dissimilar and how they were eventually related to each other. This is a difficult thought process and as such the heuristic devices proposed in the book, Design synectics: stimulating creativity in design [22], were used.

The first heuristic device used was "repeat" meaning to do something over and over. Forcing the mind to think of something that happens over and over inspired the thought of a person swallowing, the Synectics trigger, and the food being transported through the process of peristalses. It could be possible to have bladders expand to clamp the conveyance then move down and contract as soon as the bladders above them have expanded and in the process lift or lower the conveyance. It is possible to make use of a climber mechanism such as in a farm jack where one lifting lug transfers the load to the next lug; this action could also be obtained through wedges working on opposite sides of the conveyance. Alternatively the function of the bladders can be performed by a set of clamps that engage lift and disengage from the conveyance.

The second heuristic device used was "combine" where existing ideas should be joined together. The Synectics trigger is the two most popular conveyance arresting devices namely KEPS and Levelok. The concept is to use the KEPS device to align the conveyance and then activate the Levelok device to hold it in place.

The third heuristic device used was "add" where it is asked what can be done extra. The two current devices are again the Synectics trigger. Considering the KEPS device the hook can be altered by giving it a clamping feature or a locking pin to lock onto the conveyance. The device can then be made to move up or down to equalise the rope tension by connecting it to a rope loop or hydraulic cylinder. The Levelok system can be mounted on a controllable sliding frame which would afford manageability over the release rate.

The fourth heuristic device used was "empathise" meaning to relate to the subject. A common image of sharing feelings is to hug. The idea to have a device surround the conveyance and squeeze is therefore inspired. It is possible to have the guides move and press against the conveyance to secure it, by using the guides as a friction clamp.

The fifth heuristic device used was "animate" where motion is given to something stationary. The image of a trampoline inspired having the conveyance drop onto a mat or structure supported by springs or dampers.

The sixth heuristic device used was "change scale" requiring the object to be made smaller or larger. Downscaling a lot brings to mind ants working together to carry a large breadcrumb. Using multiple objects in unison will reduce the size of the units required, example smaller lifting lugs.

The seventh heuristic device "analogize" meaning to draw associations between dissimilar objects was used. Sitting thinking about this device prompted the Synectics trigger of a chair. A chair possesses a few features that can be transferred to the problem of arresting a cage. The height is adjusted through a screw mechanism and the impact absorbed through a spring, piston and cushion.

The eighth and last heuristic device used "borrow" suggests taking a feature from an object with a similar function. To address the issue of locking a conveyance in place the "space case" (pencil case) borrowed the idea of using a sliding lock.

The Synectics method is an innovation inspiring technique that broadens the normal way of thinking. It was used to generate 12 potential solutions which were broken down and generalised to add into the Morphological chart. With the working principles identified and generalised 7 of the potential solutions were already included in the Morphological chart populated thus far with the results of the brainstorming technique. The 5 potential solutions added to the chart are illustrated in the table below.

TABLE 3 POTENTIAL SOLUTIONS GENERATED THROUGH THE SYNECTIC PROCESS.

Bladders expand and contract to raise and lower the conveyance	Clamps activate and release to raise or lower the conveyance	Lower conveyance onto a fixed stop	Raise or lower the attached device by rotating a rope loop	Use the guides to squeeze the conveyance

4.3.   TRIZ

TRIZ is a Russian acronym, for Teoriya Resheniya Izobreatatelskikh Zadatch, translated into English as the Theory of Inventive Problem Solving. TRIZ is a method of solving problems, where the root of the problem lays in technical contradictions, proposed by Genrich Altshuller. Altshuller discovered after studying thousands of patents that there were a limited number of contradictions that had to be solved and that inventors only used some 40 methods to solve these defined as the transition models. TRIZ has been developed over many years and the books, TRIZ for Engineers by Karen Gadd [23] and Modern TRIZ A Practical Course with EASyTRIZ Technology by Michael Orloff [24], were used to study the technique applied in this section to develop further potential solutions to the sub-functions identified in chapter 3. The Meta Algorithm of Inventive TRIZ (MAI TRIZ), proposed by M. Orloff, which has the names of the steps conveniently linked to the letters of the acronym TRIZ, is applied in this section and summarised in figure13.

The TREND step involves finding the root of the problem (hypocentre) and distinguishing it from the symptoms of the problem (epicentre). This is done by asking probing questions to understand the essence of the problem and to obtain the factor, which could be 1 of 39 factors identified by Altshuller, desired to be solved. It is then attempted to solve for this factor by applying professional knowledge. If the factor cannot be solved through normal practices a contradicting factor is normally present, meaning that by improving one factor a second factor or property is negatively influenced, and the rest of the contradicting factors must then be identified.

The contradictions are defined by identifying which factors must be improved and which are negatively affected. It is possible to have one of four contradictions. An ordinary contradiction is where a particular property or requirement must be maximised or minimised to deliver the desired result. A standard contradiction (technical contradiction) is where incompatible properties or requirements reside between different functional features of the artefact. A radical contradiction (physical contradiction) is where opposing properties or requirements are required of the same functional feature. A compositional contradiction is where there are more negative features to the required positive feature and thus a composition of standard contradictions.

The REDUCE step requires the definition of the Ideal Final Result (IFM) which is simply the final desired condition of the factors identified in the TREND step. The Functional Ideal Models (FIM's) are the transitional models that aids in transforming the factor into the desired factor. These transformation models are identified based on the type of contradiction where the SITO+ (Single In Tuple Out - Positive) or SITO- (Single In Tuple Out- Negative) methods are used on ordinary contradictions, the former where the factor must improve and the latter where the factor must decrease. The BICO (Binary In Tuple Out) method is used to solve standard contradictions, the RICO (Radical In Cluster Out) method to solve radical contradictions and the MITO (Multiple In Tuple Out) method to solve compositional contradictions. All these methods employ a different approach to identify the few most likely transformation models, out of the 40 possible models identified by Altshuller, that will aid in overcoming the contradictions associated with the factors identified in the TREND step.

The transitional models suggested from the various methods are now used in the INVENTING step. An individual now applies the transition models and come up with a solution to the contradiction that will resolve the problem and deliver an answer that can be applied in the artefact in which the contradiction exist.

The ZOOMING step requires the final artefact, in which the answer obtained in the previous step has been implemented, to be reviewed. It is studied to see if the problem is resolved, if application of the method has brought about any major improvements (super effect) or severely damaged another feature (negative effect). If the solution is implementable in practise the artefact can thus be developed into a working system. The figure below summarises the methodology used when applying MAI TRIZ.

TREND:	Define the objective of the problem and obtain a direction for the solution			

Initial Problem	→	Identify contradicting factor 1	→	Attempt solutions	→	Identify contradicting factor 2
Ask the questions: What? Where? When? Who?		Determine the purpose of the project. What must be done and what is desired.		Here traditional solutions are attempted. If no solution is found the process must be continued.		What is the cause of the problem? Why is the contradiction present?

REDUCE: Define the Ideal Final Result and Functional Ideal Model Re-write the informal contradiction into a standard or radical contradiction.				INVENTING: Apply professional knowledge, creativity and psychological skills to generate ideas. Make use of the transformation models proposed from the various methods.

Contradiction type	Factor 1	Factor 2	→	
Ordinary	Factor to improve or weaken		→	SITO Single In Tuple Out
Standard	Positive factor	Negative factor	→	BICO Binary In Cluster Out
Radical	Factor 1 increase	Factor 1 decrease	→	RICO Radical In Cluster Out
Compositional	Positive factor	Negative factor 1 to n		MITO Multiple In Tuple Out

ZOOMING: Verify suitability and ensure that the problem is resolved. Evaluate the efficiency. Judge the implement ability. Look for any super or negative effects.

FIGURE 13 ILLUSTRATION SUMMARISING THE METHODOLOGY OF THE META ALGORITHM OF INVENTIVE TRIZ.

During application of the method the factors used are identified through the letter F followed by a hash and the factor number, which corresponds to one of the 39 factors identified by Altshuller, enclosed by brackets. The transitional models used are identified through the letters TM followed by a hash and the transition model number, which corresponds to one of 40 models identified by Altshuller, enclosed in brackets.

To limit the impact when a conveyance engages with an arresting device the factor speed (F#22) must be decreased but doing so will negatively influence the factors forces (F#30), complexity of construction (F#7), surface of the object (F#17 + F#18) and reliability (F#4). The MITO process proposed the use of the transitional models; replacing mechanical matter (TM#4), aggregate state of an object (TM#1), periodic action (TM#8), inexpensive short life object as a replacement for an expensive long life item (TM#13), discard and renewal of parts (TM#15) and previously installed cushion (TM#28). The application of these transition models prompted the potential solutions tabled below. The entries crossed out are potential solutions already included in the Morphological chart.

TABLE 4 POTENTIAL SOLUTIONS TO THE PROBLEM, ENGAGING A MOVING CONVEYANCE, GENERATED THROUGH THE MAI TRIZ METHODOLOGY.

Interact with a magnetic field	Impact onto springs	Impact onto an elastomer	Impact onto a compressible gas	Impact onto a non-Newtonian fluid
Impact onto clay	Impact onto a flexible Bunton	Impact onto a cylinder of which the release rate of pressure is controlled	Use shear pins to prevent subjecting the system to excessive forces	Impact onto a collapsible structure (Crush a can)

Since TRIZ was developed primarily for the manufacturing industry the factor to be improved to ensure proper alignment of a conveyance is precision of manufacture (F#5) as this suggests accurately positioning a moving object next to a stationary one. Using the MITO method the transitional models aggregate state of an object (TM#1), segmentation (TM#3), local property (TM#12) and the use of pneumatic or hydraulic constructions (TM#14) were identified. The potential solutions tabled below were generated through the application of these models.

TABLE 5 POTENTIAL SOLUTIONS TO THE PROBLEM, ALIGNING A CONVEYANCE NEXT TO A STATION, GENERATED THROUGH THE MAI TRIZ METHODOLOGY.

Arresting device collapse until the conveyance is aligned	Remove the rope from the conveyance during alignment	Move the floor into position	Change the length of the attachment hydraulically	Raise or lower the sheave hydraulically

4.4. 2500 ENGINEERING PRINCIPLES

TRIZ has been studied over many years and the concept of analysing patents and extracting the engineering principles used has continued into modern days. This has led to the compilation of 2500 engineering principles commonly applied in artefacts into a database which fortunately is in an electronic format today. These principles were then joined with common functions required in artefacts. Searching for a function in the database would then return the engineering principles commonly used to achieve the function.

In order to make the effects database [25] applicable to all fields the functions are kept very general. A search for "Hold Solid" was therefore used to search for engineering principles that can be applied to keep a conveyance in place. The search delivered 107 engineering principles many of which were irrelevant as they applied to specific processes. The physical effects found that could be applied to the problem were adhesive, chain, elastic recovery, electromagnet, ferromagnetism, force, gravitation, groove, holes, hook, hydraulic press, Lewis, Maglev, shape memory alloy, mechanical fastener, physical containment, pin, screw, solenoid, static friction, interlocking, thermal expansion and wedge. Many of these principles were already included in the Morphological chart in a more general format and those tabled below added.

TABLE 6 POTENTIAL SOLUTIONS FOR THE PROBLEM; HOLD A CONVEYANCE, OBTAINED FROM THE EFFECTS DATABASE AT WWW.TRIZ4ENGINEERS.COM.

Elastic recovery	Shape memory alloy	Thermal expansion		

4.5.   MECHANICAL SOURCEBOOKS

Throughout the years many ingenious mechanisms have been designed some of which are commonly used in applications. Databases and sourcebooks provide access to these existing treasures which might be used to perform one of the sub-functions from chapter 3. The illustrated sourcebook of mechanical components [26] was studied in depth to search for solutions to the sub-functions.

A multitude of mechanisms exist to produce linear motion which should be transferable to the problem of aligning a conveyance. The book reveals mechanisms using a screw and travelling nut which can be used in a jacking application, an application where a hook or clamping device is lifted or a turnbuckle changing the rope length. Wedges and cams can be used to generate reciprocating lifting actions. Sprockets and chains, friction drives and rack and pinions also produce linear motion. Gears used in parallel motion mechanisms or a Scotch Yoke can also transform rotational motion into linear motion. Hydraulics see application in a variety of styles from direct lifting to driving climber or lever mechanism arrangements. Linkages can be configured to generate collapsible structures, toggle arrangements or to magnify forces.

The book further gives solutions to the issue of damping by illustrating a variety of elastomeric shapes and springs, ranging from helical, Bellville, leaf and torsional springs. Damping is further possible through compressing a compressible fluid or through the controlled escape of an incompressible fluid.

Novel ideas on damping involve the dissipation of energy through the deformation of elements. Some concepts involve the bending of a strip of steel as it passes between rollers or the deformation of a ring as it is rolled over a cylinder. A concept for a frictional damper is also given where the compression of a spring in a cylinder pushes wedges placed between the coils of the spring against the side of the cylinder resulting in an increased normal force between the wedge and the cylinder wall increasing the friction. There is further a variety of snap action devices, detents, clamps and ratchet and pawl systems. After studying the book 7 potential solutions tabled below were added to the Morphological chart.

TABLE 7 POTENTIAL SOLUTIONS FOR THE PROBLEM, ALIGN AND SECURE A CONVEYANCE, BASED ON MECHANISMS FROM SOURCEBOOKS.

Deforming elements	Friction damper	Friction drive	Rope puller	Parallel motion linkage
Over-toggle arrangement	Ratchet and pawl			

4.6. MORPHOLOGICAL CHART

A morphological chart, as explained in the book Engineering design a systematic approach [20], is a powerful tool in the development of concepts. The chart contains all the potential solutions identified through the techniques discussed in this chapter. Functional analysis showed that to obtain an aligned and secured conveyance the concept system had to address the six sub-functions; decelerate the conveyance, damp the impact, align the conveyance, secure the conveyance and equalise the rope tension before releasing the conveyance. These sub-functions are listed in rows beneath each other in the second column of the chart; with the sub-function align the conveyance given twice due to the number of potential solutions identified. The first column assigns a number to each entry in the second column so that a number index can be used to identify a certain solution principle. The solution principles identified through each of the techniques were then entered in columns next to each other in the row of the sub-function to which it applies. The top row assigns a number to each of these potential solutions so that they can be identified though a number index.

To develop a system concept a potential solution from each of the sub functions must be identified and joined into a concept. The potential solutions which will be ill-suited for use in the system are eliminated first by crossing it off.

The sub-function, decelerate the conveyance, in row 1 has 5 potential solutions listed. The first four potential solutions all suggest slowing the hoist and the fifth having the conveyance slowed by the system it engaged with. Having the hoist slow to creep speed (PS#1) for each station isn't sensible as there are many stations passed before reaching the desired station which will influence the hoisting cycle negatively. Using a control cam (PS#2) to slow the hoist is only practical on older type hoists and will be difficult to select the cam that should control the winder for the specific stations; it is normally only used for end of wind control. Controlling the hoist through a Programmable Logic Controller (PLC) (PS#3) is only practical on hoists with modern control systems. To have the conveyance decelerated by engaging with a device (PS#5) is potentially dangerous as very large forces may be involved. The hoist will need to decelerate at the same rate as the potential is otherwise created to damage the rope by inducing slack. Potential Solutions 1 to 3 and 5 therefore aren't preferred and are removed from consideration. The concept systems requires the WED to control the speed (PS#4) coming into the station. To aid him in the process indication is provided to show him when to start decelerating and warn if he is approaching too fast.

The sub-function, damp the impact onto the system, listed in row 2 has 14 potential solutions listed. The approaching conveyance will already have a greatly reduced speed, because of the control from the WED and the controls implemented to warn him and trip the hoist should his speed still be too great, reducing the forces that need to be damped. The concepts therefore makes use of potential solution 2 which requires an adequately decelerated conveyance in conjunction with either one of the following simple to implement potential solutions; Impact onto an hydraulic damper (PS#5), impact onto an elastomer (PS#3), impact causing the compression of a compressible gas (PS#4) or impact onto a cylinder of which the release rate is constantly controlled (PS#10). It is also considered to make use of flexible supports (PS#9), collapsible structures (PS#12) or deformable elements (PS#13).

Having the conveyance interact with a magnetic field (PS#6) is impractical as the majority of the conveyance is constructed from Aluminium, a non-magnetic material, and the required magnitude of the magnetic field. Impact onto a non-Newtonian fluid (PS#7) would present difficult containment issues and is also disregarded. Having the conveyance impact onto clay (PS#8) would permanently deform the clay, and incorporating a system to re-mould the clay would be impractical. The generated concepts therefore makes use of 6 of the 10 remaining practical potential solutions listed in row 2.

The sub-function, align the conveyance, is listed in row 3 and 4 due to the number of potential solutions where row 3 and 4 both provide 14 potential solutions. Considering the entries in row 3 the potential solution bellows (PS#4) is discarded as a bellow will require excessive pressure to lift the conveyance and will be prone to damage should a piece of debris fall down the shaft. Piezoelectric (PS#5) is also discarded as it won't be able to provide the lift required. Aerodynamic lift (PS#6) suggests passing a stream of air over an aerofoil to generate lift; it is impractical as it will require a controlled flow of air over a large aerofoil. Using the rope to lift the conveyance (PS#7) lacks accuracy and using a magnetic field (PS#8) is impractical as mentioned in the previous section. The use of a linear motor (PS#12) will greatly increase power consumption and will present maintenance and reliability issues in a dusty and wet shaft, while thermal expansion (PS#13) is also disregarded due to fire risks and the amount of lift it should be able to effect. Seven potential solutions remain in row three where the potential solutions lever arrangement (PS#1), lead screw drive (PS#2), hydraulic / pneumatic cylinder (PS#9) and sprocket and chain (PS#11) are incorporated into concepts.

Row four has another 14 potential solutions where the following were discarded. To counter the movement of the conveyance (PS#2) to maintain it in an aligned position would be incredibly difficult due to the unpredictable nature of the rope and the near infinite combination of loads that can be applied to the conveyance once in position. To have bladders expand and press against the side of the conveyance (PS#3) is discarded for the same reasons as in the previous section. Raising or lowering the alignment device connected to the conveyance by rotating a rope loop (PS#6) will be unreliable as rope slip is likely. Removing the rope from the conveyance (PS#8) will struggle to find acceptance in the industry as proper reconnection will be questioned. To move the floor toward the conveyance position (PS#9) will be very complex as the floor needs to be removable to allow access to the shaft during slinging operations. To pull the rope through a rope puller (PS#13), similar to a Tirfor, might damage the rope and is an unnecessary risk. Eight potential solutions remain in row four where the potential solution lowering the conveyance onto a fixed stop (PS#5) is considered in the system concepts.

The sub-function, secure the conveyance, listed in row 5 has 13 potential solutions. To use magnetism (PS#3) to secure a conveyance is impractical as mentioned previously. A tremendous pressure differential is required to secure a conveyance through suction (PS#4) along with complex machinery. To secure the conveyance with adhesive or other bonding (PS#5) techniques isn't practical due to the strengths required and the difficulty to remove the joint. Increasing the inertia (PS#7) of the conveyance will simply reduce the acceleration rates but won't keep it in position. To use a shape memory alloy (PS#10) to interact with the conveyance is very complex and does not appear to be a sensible solution. Thermal expansion (PS#11) is also discarded as discussed previously. Having discarded the potential solutions above only seven remain in row 5 where the potential solutions interference / geometric interaction (PS#1), support / geometric constraint (PS#2), elastic recovery (PS#9) and over-toggle arrangement (PS#12) are used in the system concepts.

The sub-function, indicate the state of engagement, listed in row 6 has 10 potential solutions. The potential solution to use the slack and tight rope device (PS#6) to give an indication is discarded as the system should be such that no excessive slack or tight rope condition exist, so that depending on the device would be unreliable. Inductive switches (PS#8) have a very narrow operating range and would require too narrow tolerances and are therefore also discarded. To make use of a camera with image identification (PS#9) is too elaborate and complex for a practical solution. The remaining 7 potential solutions could all be viable depending on the final system. In the creation of the concepts the potential solutions linkages and whisker switches (PS#7), load cells (PS#4), pressure switches (PS#2), magnetic switches (PS#1) and strain gauges (PS#10) were considered.

The sub-function, equalise the tension in the rope, listed in row 7 has 4 potential solutions. The sub-function requires the vertical movement of the conveyance to equalise the rope tension and therefore most of the potential solutions in row 3 and 4 is also applicable. The system concepts make use of all of the potential solutions namely control the sheave position (PS#1), release the conveyance when the load has equalised due to normal hoisting (PS#2), use the alignment device to equalise the rope tension (PS#3) and change the length of the attachment (PS#4).

The Morphological chart for the project is provided below listing all the potential solutions in the rows of the sub-functions to which they apply. The rejected potential solutions discussed in the preceding paragraphs are crossed off and the remainder of the potential solutions considered for use in concepts. Concepts were generated from the chart indicating the potential solution used under each sub function with a number in curled brackets. Concept 1 thus utilises all the potential solutions marked **{1}**.

TABLE 8 MORPHOLOGICAL CHART DETAILING THE POTENTIAL SOLUTIONS AND SUB-FUNCTIONS CONSIDERED FOR CONCEPT GENERATION.

	Sub-functions	Potential Solutions													
		PS#1	PS#2	PS#3	PS#4	PS#5	PS#6	PS#7	PS#8	PS#9	PS#10	PS#11	PS#12	PS#13	PS#14
1	Decelerate the conveyance	Forced creep	Control Cam	Control programme on PLC	Manual control according to an indicated rate {1}{2}{6}{4}{5}{3}{7}{8}{9}	Engagement with a device and device retardation									
2	Damp the impact onto the system	Impact onto a Spring {5}{3}	Winder deceleration to limit speed {2}{6}{1}{4}{5}{3}{9}	Impact onto an elastomer {9}	Impact onto an airbag (Compression of an compressible gas)	Impact onto a hydraulic damper {2}{3}	Interact with a magnetic field	Impact onto a non-Newtonian fluid	Impact onto clay	Impact onto flexible supports {7}{9}	Impact onto a cylinder of which the release rate of pressure is controlled {6}{4}{8}	Use shear pins to prevent subjecting the system to excessive forces	Impact onto a collapsible structure (Crush a can) {4}	Make use of deforming elements {5}	Make use of a friction damper
3	Align the conveyance	Lever arrangement {4}	Lead screw drive {1}	Climber arrangement	Bellows	Piezoelectric	Aerodynamic lift	Lift using the hoist rope	Magnetic levitation	Hydraulic / Pneumatic cylinder {6}{8}	Wedge action {5}	Sprocket and chain {3}	Linear motor	Thermal expansion	Rack and pinion
4		Cam and follower	Counter movement	Bladders expand and contract to raise and lower the conveyance	Clamps activate and release to raise or lower the conveyance.	Lower conveyance onto a fixed stop {1}{2}{6}{7}{8}{9}	Raise or lower the attached device by rotating a rope loop	Arresting device collapse until the conveyance is aligned {6}{4}{5}{3}	Remove the rope from the conveyance during alignment	Move the floor into position	Change the length of the attachment hydraulically	Raise or lower the sheave hydraulically.	Friction drive	Rope puller	Parallel motion linkage
5	Secure the conveyance	Interference / Geometric interaction {1}	Support / Geometric constraint {2}{6}{4}{5}{3}{7}{8}{9}	Magnetism	Suction (Pressure differential)	Bonding or adhesive	Friction	High inertia	Use the guides to squeeze the conveyance	Elastic recovery	Shape memory alloy	Thermal expansion	Over-toggle arrangement {6}	Ratchet and pawl {2}{5}{7}	
6	Indicate the state of engagement	Magnetic switches {6}{3}	Pressure switches {2}{6}{4}{8}	Visual and manual signal	Load cells {1}	Laser sensors {9}	Slack and tight rope device	Limit and whisker switches {4}{5}{7}{8}{9}	Inductive switches	Camera with image identification	Strain gauges				
7	Equalise the tension in the rope	Control the sheave position {7}	Release when load is normalised due to normal hoisting {9}	Alignment / vertical positioning device move to normalise load {1}{2}{6}{4}{5}{3}	Change the length of the attachment {8}										

4.7.   CONCEPTS

The potential solutions selected in the Morphological chart are combined to form system concepts that will align and secure a conveyance. The nine concepts generated are displayed and discussed in this section before being subjected to screening.
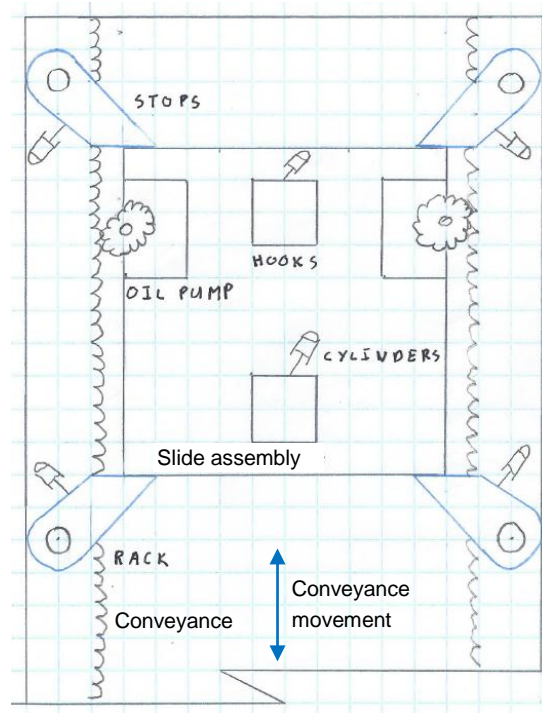
Concept 1 {1}

Concept 1 relies on the WED slowing the conveyance according to an indicated rate and lowering it onto a hook. The hook is connected to a lead screw through a bracket and positioned at a fixed height to ensure the conveyance is aligned when it comes to rest on this fixed stop position. As soon as the conveyance enters the hook a pin is inserted from the hook to lock the conveyance and the hook through geometric interference. The conveyance is aligned and secured and can be loaded or unloaded after which the lead screw is rotated to have the position of the hook change to a position where the tension in the rope is released. The pin is then removed from the hook and the conveyance released. The indication is obtained by having the lead screws rest on load cells where the load values is used to determine the instance when the conveyance is in the hook and also when the tension in the rope is equalised.
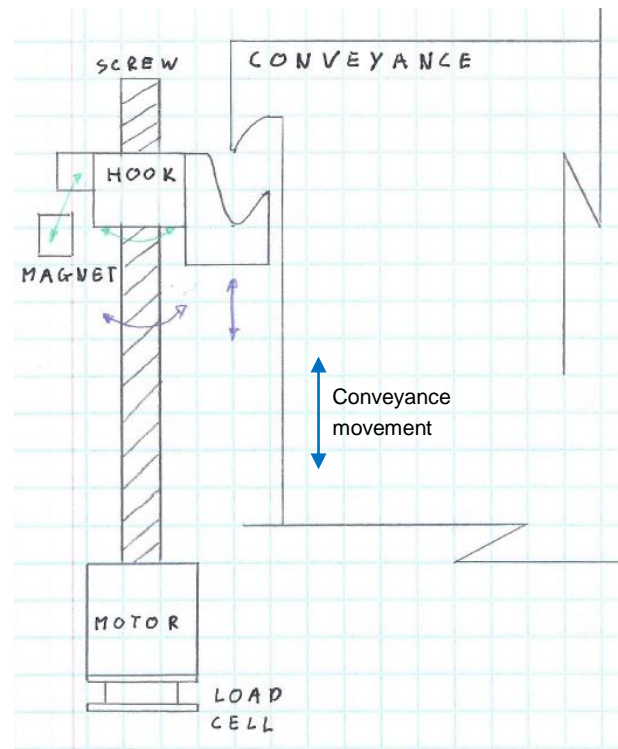
FIGURE 14 HAND DRAWING OF A CAGE ARRESTING DEVICE CONCEPT USING AUTOMATED KEPS HOOKS.
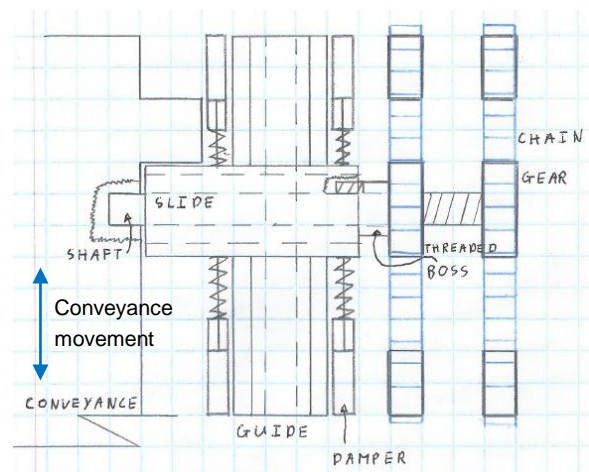
Concept 2 {2}

Concept 2 relies on the decelerated conveyance locking with a sliding assembly onto the station steelwork through geometric containment. The sliding assembly will remain stationary while the conveyance then slides relative to the sliding assembly rotating a gear pump in the process to charge up the hydraulic system powering the device. This relative motion and energy input into the hydraulic system damps the impact of the conveyance. The sliding assembly moves in this slide until it reaches a hydraulically activated stop pawl at which stage the conveyance is fully secured. After loading operations the stopping pawl is retracted and the conveyance slides relative to the still locked sliding assembly again powering the gear pump resulting in a controlled rate of rope tension equalisation. When the slide comes to a standstill the sliding assembly is released and the conveyance can move away freely. Due to the hydraulic design pressure switches is used to provide the necessary indication.

FIGURE 15 HAND DRAWING OF A CAGE ARRESTING DEVICE CONCEPT USING A HYDRAULICALLY DAMPED SLIDING MECHANISM.

Concept 3 {3}

Concept 3 has a slide, mounted on a vertical guide, supported by four spring-damper units on the station. The slide then has a beam mounted on a slide transverse to the first slide. The beam is connected with a hollow shaft to a sprocket which has one side of the sprocket teeth engaged with a chain. The spring damper units maintain the beam at the centre of the guide when it is disengaged. When a conveyance arrives the sprocket drive powering the front chain is started and as the chain rotates it rotates the sprocket. The hollow shaft is threaded so that it extends as it is rotated pushing the beam into the path of the conveyance. When the conveyance lowers onto the beam it displaces it along the guide compressing and extending the spring damper units. The inner shaft running through the beam and connected to a sprocket on the rear chain also has a threaded section.
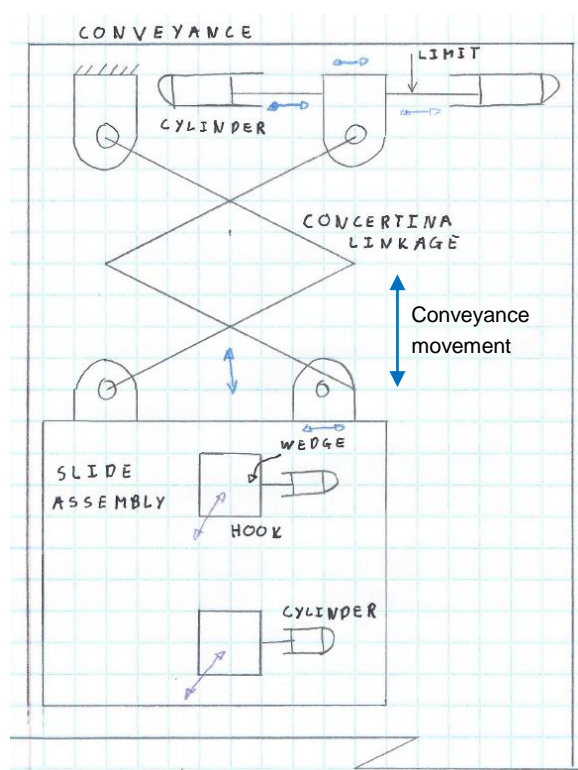

FIGURE 16 HAND DRAWING OF A CAGE ARRESTING DEVICE CONCEPT USING A SCREW JACK ACTUATED LOCKING BEAM.

The rear chain is kept in a locked position and the movement of the sprocket relative to the stationary chain drives the threaded shaft pushing it into an opening on the conveyance. The conveyance which is now locked is secured as soon as the front chain is locked preventing further vertical travel. The beam is kept from screwing out under the force when both chains are locked by having the sprocket faces engage on different sides of the chains causing the beam and shaft to behave similar to a lock nut. To release the conveyance both chains are unlocked and the conveyance settles in a position where the rope tension is equalised. The chains are then rotated to retract the shaft and the beam, freeing the conveyance. Indication is achieved through magnetic switches.

Concept 4 {4}

Concept 4 uses a sliding assembly mounted on the conveyance. The sliding assembly locks onto the station steelwork through clamps that pass above and below the beams. The clamps are engaged and disengaged by hydraulic cylinders mounted on top of the conveyance and linkages passing to the slide assembly. The slide assembly is supported by a concertina arrangement of linkages that has the top linkages connected to a hydraulic cylinder. As the conveyance move with the slide assembly locked the concertina arrangement of linkages collapse increasing the distance between the top linkage legs which extends the cylinder. This causes a damping effect and controls the extent to which the system may collapse. The system thus collapses to the aligned position and remains secured due to the locking effect of the cylinder and linkages. After loading the cylinder is allowed to dump again and the slide assembly moves until the rope tension is equalised. The clamps are retracted and the conveyance released. The indication is obtained from pressure switches and whisker switches.

FIGURE 17 HAND DRAWING OF A CAGE ARRESTING DEVICE CONCEPT USING A COLLAPSIBLE CONCERTINA ARRANGEMENT.
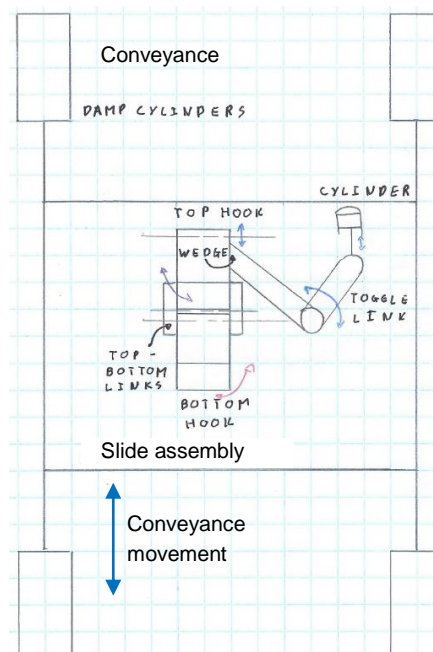
Concept 5 {5}

Concept 5 has a sliding assembly where two wedge shaped clamps are made to protrude into the path of the station steelwork. As the conveyance lower the lower wedge clamp is pressed back against the spring and allows the support to pass. The support comes to a rest against the top clamp where the wedge face is now on the opposite side of the clamp. As soon as the support clears the bottom clamp it is pushed out beneath the support due to the spring. The now secured slide assembly runs in a slide where it compresses a spring and deforms rolling elements to absorb energy. The sliding assembly comes to a rest when it engages pawls which are also spring loaded. The conveyance is secured and can be loaded or unloaded. To release the tension in the rope the pawls are retracted through a lever allowing the slide assembly to again slide against a spring and deforming rollers. The clamps are then retracted by rotating the supports of the spring extending the clamps releasing the conveyance. Indication is provided through whisker switches.
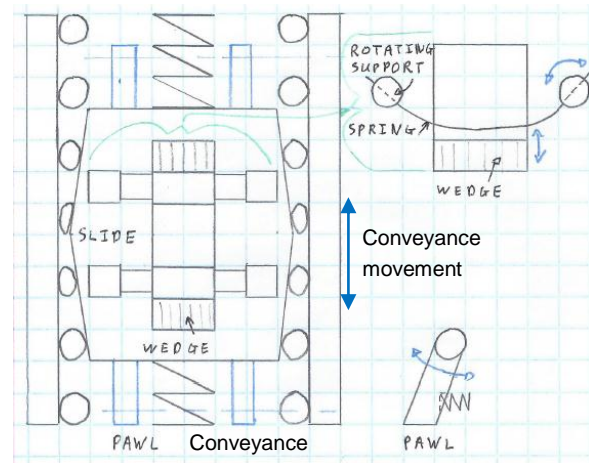
FIGURE 18 HAND DRAWING OF A CAGE ARRESTING DEVICE CONCEPT USING A SPRING APPLIED WEDGE PRINCIPLE.

Concept 6 {6}

Concept 6 has a similar philosophy as concept 2 where a sliding assembly is installed on the conveyance. The sliding assembly locks onto the station supporting steelwork by clamping a hook above and beneath the support beam. The hooks are activated hydraulically and locked with an over-toggle arrangement. The secured sliding assembly will remain in position while the conveyance moves. The assembly which is connected to four hydraulic cylinders displace the hydraulic fluid until the flow is stopped and the sliding assembly is locked from further movement. The conveyance is secured and held in position through the hydraulics and locked sliding assembly. To release, the cylinders are allowed to dump and the assembly moves to a position where the rope tension is equalised. The sliding assembly can then be released to free the conveyance. Indication is achieved using pressure switches and magnetic switches.

FIGURE 19 HAND DRAWING OF A CAGE ARRESTING DEVICE CONCEPT USING CONVEYANCE MOUNTED HYDRAULICALLY ACTUATED CLAMP BEAMS.
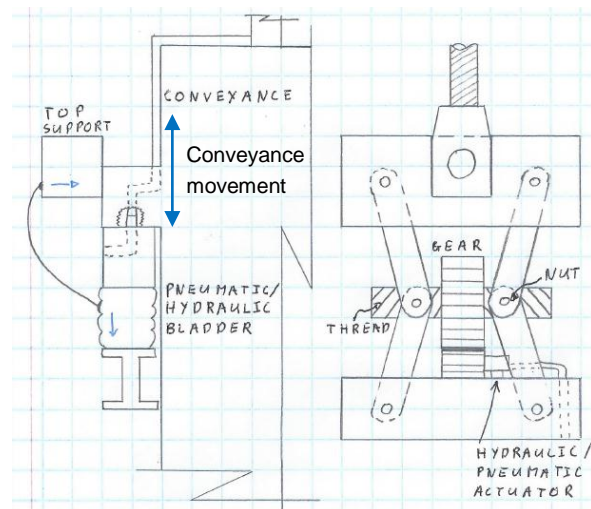
Concept 7 {7}

Concept 7 has a support protruding from the conveyance. As the conveyance is lowered to a station it passes through a pawl which is engaged through a weight. This pawl will prevent any upward motion and can be removed by pushing release pins down to open the pawl. The conveyance then lowers onto a flexible support, made from a collection of leaf springs. The flexible support is brought into the path of the lowering conveyance through a rigid beam. The conveyance is now secured and can be unloaded or loaded. To equalise the rope tension the sheave supporting the conveyance is raised or lowered hydraulically. Indication is obtained by using whisker switches.
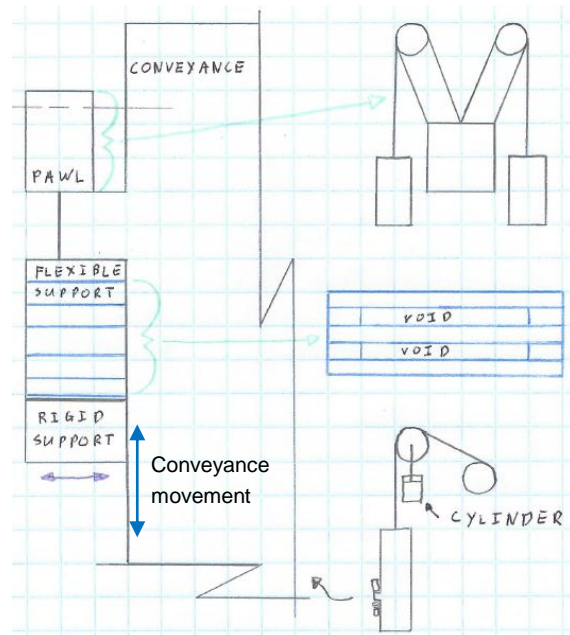
FIGURE 20 HAND DRAWING OF A CAGE ARRESTING DEVICE CONCEPT USING A STATION MOUNTED PAWL AND FLEXIBLE SUPPORTS.

Concept 8 {8}

Concept 8 has a hydraulic cylinder positioned on a rigid beam which is placed in line with the support protruding from the descending conveyance. As the conveyance is lowered onto the cylinder the oil displaced pushes out another cylinder that passes above the protruding support to secure the conveyance. The hydraulic action damps the impact and ensures that the conveyance remains secured. After loading operations are completed a valve opens to drive a hydraulic motor mounted on top of the conveyance. The motor rotates a gear through which a screw passes. As the gear rotates the screw rotates and travelling nuts mounted on the two ends of the screw is displaced horizontally. The travelling nuts are connected to diagonal links between the attachment block and the conveyance. The displacement of the nuts changes the linkage angles and elongates or shortens the attachment to equalise the rope tension. The system concept uses pressure and whisker switches for indication.

FIGURE 21 HAND DRAWING OF A CAGE ARRESTING DEVICE CONCEPT USING A HYDRAULIC BUFFER TO ACTUATE A CLAMP BEAM.

Concept 9 {9}

Concept 9 has two beams mounted on top of the conveyance. As the conveyance lowers to a station the top beam is extended by a pneumatic cylinder. The protruding beam comes to a rest on the station steelwork supported in a box filled with a rubber compound to absorb the impact. As soon as the beam makes contact the laser mounted in the support beam activates a contact actuating the cylinder pushing the bottom beam. The bottom beam is extended beneath the support steelwork and the conveyance is secured. After loading and unloading, the conveyance is lowered to ensure the conveyance rests on the top beam where the bottom beam can be removed. The conveyance is then lifted allowing the top beam to be retracted. The system concept can be configured to secure a conveyance coming up as well by first extending the bottom beam. Indication is obtained through the use of lasers and magnetic switches.
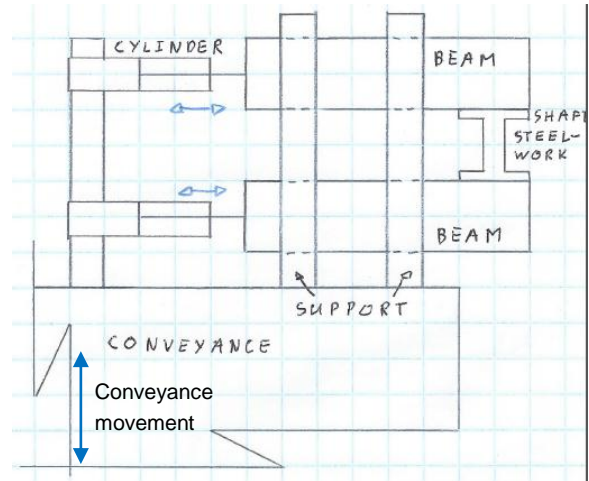
FIGURE 22 HAND DRAWING OF A CAGE ARRESTING DEVICE CONCEPT USING BEAMS THAT EXTEND ABOVE AND BELOW SUPPORTING STEELWORK.

4.8.   CONCEPT SCREENING

Nine concepts were created through the application of the Morphological chart and the potential solution identification techniques. The concepts are reduced through a process of screening to obtain the most promising concepts. The selection table given below is used to measure the suitability of the concepts.

TABLE 9 CONCEPT SCREENING TABLE

Selection chart for: A general purpose, vertical shaft conveyance, all level docking device.

Selection Criteria:	Decision:
(Y) Yes	(Y) Continue with concept
(N) No	(N) Eliminate concept
(?) Require further investigation	(?) Investigate concept in more depth
Realisable in practise	(!) Investigate possibility to change PDR

Solution Concept	Realisable in practise	Universality	Robustness	low complexity	Do not compromise safety	Compatible with existing infrastructure	Fulfils demands of requirements list	Remarks:	Decision:
C 1	Y	Y	Y	Y	Y	Y	Y		Y
C 2	?	Y	Y	Y	Y	?	?	Unsure of dimensions. Concept must undergo embodiment.	?
C 3	Y	N	N	Y	Y	?	?	Mounted to station. Cantilever action will cause guide to wedge.	N
C 4	Y	Y	N	Y	N	Y	Y	Cylinder failure poses too great a risk.	N
C 5	Y	Y	N	N	Y	Y	Y	Warpage or tear of the metal sheet is likely.	N
C 6	Y	Y	Y	Y	Y	Y	Y		Y
C 7	Y	N	Y	N	Y	N	Y	Mounted to station. Insufficient space beneath the sheave.	N
C 8	Y	N	N	Y	Y	?	Y	Mounted to station. Compressible bladder likely to fail.	N
C 9	Y	Y	Y	Y	Y	Y	Y		Y

The table lists the concepts as discussed in the section above in the first column. Each concept forms a new row. The next 7 columns list the criteria against which the concept is evaluated. The cell obtained at the junction of a row and column receives a (Y) -Yes status if the concept meets the criteria, a (N) - No status if it fails the criteria and a (?) - Uncertain status if the concepts require more in depth investigation based on some embodiment of the design. Next to the criteria columns a column is left for remarks where comments are entered explaining why a concept received a (N) or (?) status. The rightmost column displays the result of the decision process. If a row contains only (Y) entries it is deemed suitable for further investigation and the decision column displays a (Y) verdict. Any row that contains a (N) status in any column is deemed unsuitable and a (N) verdict is given in the decision column, discarding the concept from further investigation. If a row contains a (?) status along with only (Y) statuses the concept is assumed at first to be suitable but requires further embodiment before it can be accepted or discarded.

The second column lists the first criteria, realisable in practise. Concept 1 received an (Y) status as it is based on the proven KEPS system with modifications using commercially obtainable components. Concept 2 received an (?) status since the hydraulic nature of the concept required further investigation. Concept 3 received an (Y) status as it is based on the same working principle as the slide assembly of a lathe seen commonly in industry. Concept 4 received an (Y) status as the links are thin and don't protrude into the shaft compartments while the hydraulics are mounted on top of the conveyance where there is space. Concept 5 received an (Y) status as it is constructed from known mechanical components such as pawls and rollers. Concept 6 received an (Y) status since the components can be manufactured using existing methods. Concept 7 received an (Y) status since sheaves are currently lifted hydraulically and the flexible beam only requires the joining of multiple spring steel plates. Concept 8 received an (Y) status since the attachment mechanism works the same as the mechanism spreading the legs of a protractor whereas the hydraulic stop is simply a cylinder of which the oil is directed to another cylinder. Concept 9 received an (Y) as it is a simple beam supported on standard linear slides.

Column three lists the second criteria, universality, which requires that the system can be easily used on multiple stations. Concept 1 received an (Y) since the concept is simple enough to be installed on all stations. Concept 2, 4, 5, 6 and 9 received an (Y) status as they are conveyance mounted and requires the minimum infrastructure upgrade on the stations. Concept 3, 7 and 8 received a (N) status since they all require elaborate installations on the station.

Column four lists the third criteria, robustness, which requires that the system is able to withstand the harsh operating conditions including debris, water, dust and repetitive operation. Concepts 1, 2, 6, 7 and 9 all received (Y) statuses since they are all constructed from heavy sections with the sensitive components well hidden. Concept 3 received an (N) status since the slide running on the guide will be prone to jamming when a force is placed on the cantilever end. Concept 4 received a (N) status as the cylinder mounted on the conveyance is exposed and the thin links will experience wear on the pin joints. Concept 5 received a (N) status since the pawls that retain the slide needs to be mounted in the thin side panels of the conveyance where tear out is likely, the springs that will operate the beams will wear out the mountings and might snap under repeated use. Concept 8 received a (N) status since the hydraulic cylinder rod can easily bend when the conveyance impacts too fast with the impact also causing excessive pressure in the pipes. The compensating attachment is also sensitive to dust that will hinder the movement of the travelling nut.

Column five list the fourth criteria, low complexity, which requires that the system should be easily understood, operated, manufactured and maintained. Concepts 1,2,3,4, 6, 8 and 9 all received an (Y) status as they are relatively simple to operate. The concepts are either well protected or easily accessible for maintenance. Although the hydraulic systems are more complex, they are understandable and serviceable by skilled artisans. Concept 5 received a (N) status as it requires the operation of levers in too many planes where the system requires pawls to be retracted and the springs to be rotated for every station it passes. Concept 7 received a (N) status as it requires the sheave to be raised or lowered by a height difficult to determine.

Column six lists the fifth criteria, do not compromise safety a non-negotiable feature. All the concepts received an (Y) status except concept 4. All the concepts use rigid components that are unlikely to fail, should any of them fail however the designs are such that the associated movement will either be slow as it is still damped or slight as the travel is restricted with a maximum movement equal to the rope stretch which is similar to the Levelok system. Concept 4 however received an (N) status as a failure of the cylinder will cause a movement of the conveyance when the concertina links collapse resulting in an unacceptably fast and large movement.

Column seven lists the sixth criteria, compatible with existing infrastructure. Concept 1 received an (Y) status as it is similar to the existing KEPS and can be readily adopted. Concept 2, 5 and 6 received (?) statuses as it is unsure of the clearances until embodiment designs are done. Concept 3 received an (?) as the complexity of the system to be mounted on the station influences its adoptability, more embodiment is required. Concept 4 received an (Y) status as it is mounted on the conveyance in such a position as not to disturb normal operations. Concept 7 received a (N) status since the sheaves do not have space to install a jacking system. Concepts 8 and 9 received an (Y) status as they are self-contained units that take up the minimum space.

Column eight lists the last criteria which require the concept to fulfil the demands of the requirements list. At this stage the concepts were developed based on the Product Design Requirements and all are assumed to meet them. Concepts 2, 3, 5 and 6 however required embodiment before the clearance and strength specifications can be judged.

The decision table illustrates that the five concepts; concept 3, 4, 5, 7 and 8 failed on one or more criteria and is discarded from further design. Concept 1 and 9 has no foreseen reasons why it will not be viable solutions and can proceed to the embodiment phase. Concepts 2 and 6 appear to be suitable but require embodiment before a decision is made.

4.9.   CONCEPT EMBODIMENTS

4.9.1. CONCEPT 1

The design of concept 1 is similar to that of KEPS with modifications to overcome some of the inadequacies. The system is mounted on each station which allows easier maintenance and access to energy sources.

Figure 23 gives an overall look at the system constructed on the station with a zoomed in detailed view of the primary working components. Figure 24 presents a look from beneath focussing on the components connected to the support beams. Figure 25 shows the engagement hook (3) in the retracted position and figure 26 shows it in the activated position. The operation of the system is discussed below.

The onsetter positioned at the station signals, the WED to slow the conveyance when he sees it approaching the station, on the lock bell system activating the electromagnet (1) and pulling the engagement bracket (2) towards the magnet. As the engagement bracket (2) moves towards the magnet (1) it pulls the engagement hook (3) from its position illustrated in figure 25 into the path of the descending conveyance shown in figure 26. The electromagnet (1) overcomes the torque of the torque spring (4); installed to retract the hook (3) and keep it retracted during normal hoisting, to pivot the engagement hook (3) into position.

The descending conveyance settles into the engagement hook (3) increasing the load on the load cells placed beneath the lead screws. The increased load activates the solenoid pushing the locking pin (5) into its slot on the conveyance. The conveyance is now aligned because of the engagement hook's (3) position on the lead screw (6) and secured by the engagement hook (3) and locking pin (5).

The secured conveyance is loaded or unloaded causing a change in weight that must be taken up by the rope before the conveyance is released. The load is transferred to the rope by rotating the lead screw (6) with electric motors (7) which changes the vertical position of the threaded engagement hook brackets (8). With the load transferred to the rope the locking pin (5) is retracted followed by the engagement hook (3).
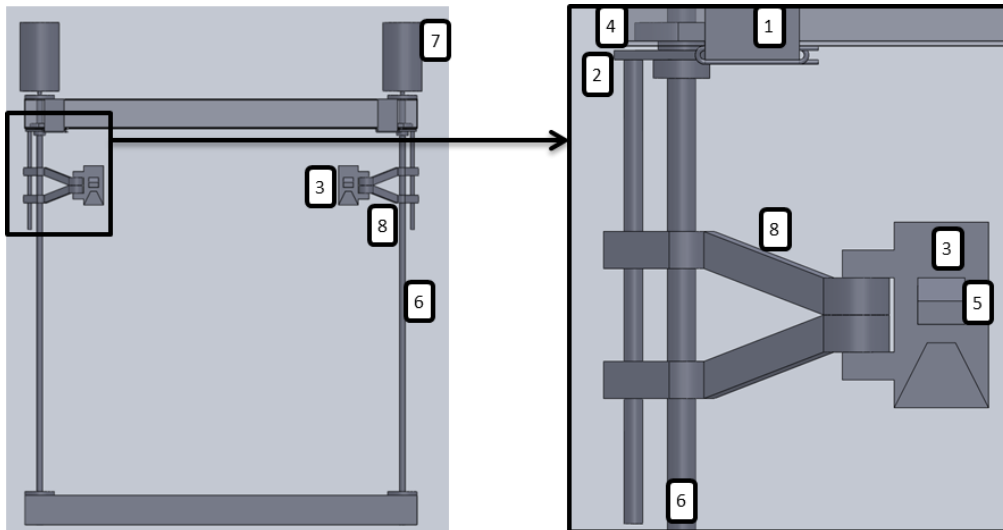
FIGURE 23 FRONT VIEW OF A CAGE ARRESTING DEVICE CONCEPT USING AUTOMATED KEPS HOOKS WITH AN ENLARGED VIEW OF THE HOOK MECHANISM.
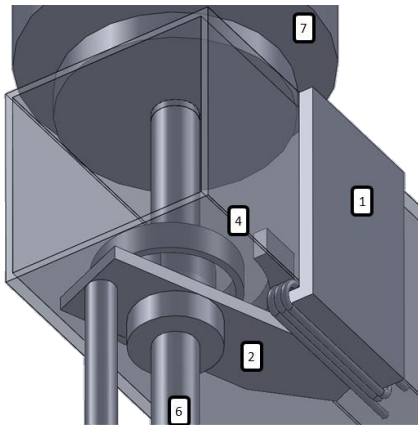
FIGURE 24 3D MODEL DETAILING THE COMPONENTS CONNECTED TO THE SUPPORT BEAM OF A CAGE ARRESTING DEVICE CONCEPT USING AUTOMATED KEPS HOOKS.
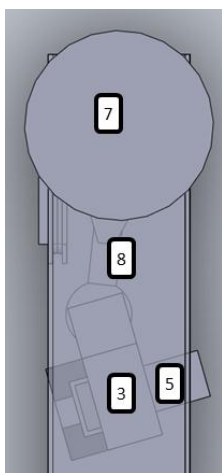
FIGURE 25 TOP VIEW OF A CAGE ARRESTING DEVICE CONCEPT USING AUTOMATED KEPS HOOKS IN THE RETRACTED POSITION.
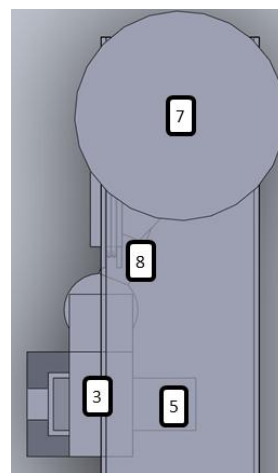
FIGURE 26 TOP VIEW OF A CAGE ARRESTING DEVICE CONCEPT USING AUTOMATED KEPS HOOKS IN THE ACTIVATED POSITION.

The conveyance is now free from the system and can continue on its way to the next station. The system eliminates the need for onsetters to place their arms into the line of fire, as with the engagement of the KEPS hooks, by providing an automated system that is activated through the use of the lock bell system. It also ensures that the conveyance remains secure in position and that the tension in the rope is controlled before release post loading or unloading operations.

4.9.2. CONCEPT 2

The second system concept is mounted on the conveyance in order to ensure its usability at any station. The design makes use of methods to store energy during docking which can be used to operate some of the features removing the need to rely on externally supplied energy.

Figure 27 shows the hydraulic slide assembly (1) located to the lower end of the sides of the conveyance with the equipment necessary to secure the conveyance to the hydraulic slide assembly at the top. Figure 28 gives a close up view of the components in the hydraulic slide assembly (1). The operation of the system is discussed below.
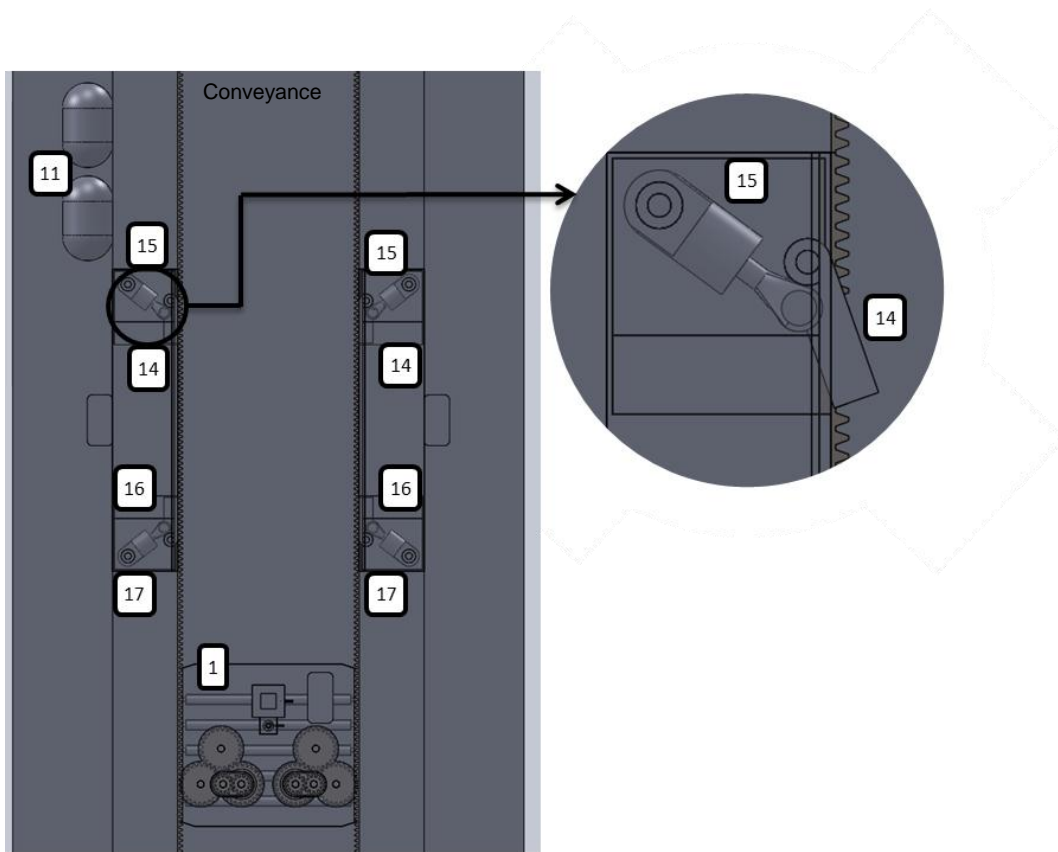
FIGURE 27 FRONT VIEW OF A CAGE ARRESTING DEVICE CONCEPT USING A HYDRAULICALLY DAMPED SLIDING MECHANISM WITH AN ENLARGED VIEW OF THE UPPER STOPPING BLOCKS.
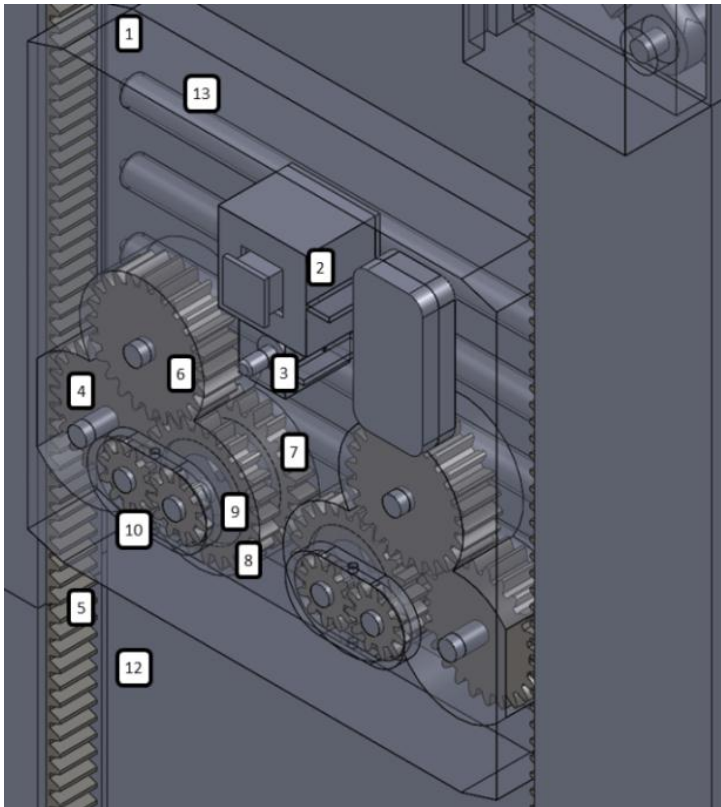
FIGURE 28 DETAILED 3D MODEL OF THE SLIDE ASSEMBLY COMPONENTS OF A CAGE ARRESTING DEVICE CONCEPT USING A HYDRAULICALLY DAMPED SLIDING MECHANISM.

When the conveyance descend to the station the onsetter signals the WED , on the lock bell system, to decrease his speed and by doing so activates the hydraulic cylinder that actuates the engagement lock (2). The actuated engagement lock (2) will come to a rest on the supporting station steelwork at which time the locking hook (3) is actuated. The locking hook which is also actuated hydraulically work with the engagement hook to secure the slide assembly to the station steelwork.

As the conveyance continue to move downwards the hydraulic slide assembly (1), now secured to the station steelwork, moves relative to the conveyance resulting in a rotation of gear A (4) which is meshed with the rack (5) mounted to the conveyance. Gear A (4) is meshed both with gear B (6) and gear C (7). Both gears B (6) and C (7) therefore rotate causing gear C (7) to transmit power to the common shaft of gear C (7) and gear D (8). Gear D (8) is however also meshed with gear B (6). Gear C (7) and gear D (8) therefore need to rotate in opposite directions. Both gears are however fitted with free-wheeling clutches (9). It can be seen that the free-wheeling clutch (9) inside gear D (8) disengage the gear from the shaft as the gear rotate in an anti-clockwise direction. The pawl inside the free-wheeling clutch rolls out of the wedged position disengaging the gear and the shaft. The free-wheeling clutch on gear C (7) is installed the same way around and since the gear is driven from gear A (4) it rotates in a clockwise direction. The shaft and the gear is thus connected and torque is transferred to the gear pump (10) mounted on the hydraulic slide assembly.

The relative motion between the hydraulic assembly (1) and the conveyance therefore results in a gear pump to be driven which fills the accumulators (11) mounted on the cage. The energy required to drive the gear pumps is obtained from the relative movement between the now stationary hydraulic slide assembly and the conveyance. This results in the velocity of movement decreasing and providing a small damping ability. The reason for the free-wheeling arrangement on the gears is to ensure that the gear pump is always rotated in the clockwise direction regardless of the direction of movement of the hydraulic slide assembly (1). The hydraulic slide assembly is designed to run in a guide (12) beneath the rack (5) to keep it affixed to the conveyance. The motion of the hydraulic slide assembly is then eased by having the assembly run on rollers (13) between the conveyance and the assembly. The gear pump assembly is duplicated on the right hand side in order to double the flow of oil to the accumulator (11).

The cage continues to move through the hydraulic assembly until it comes into contact with the upper stopping blocks (14) mounted on both sides of the cage. These upper stopping blocks (14) are actuated by a hydraulic cylinder (15) at the same time as the engagement hook (2). The upper stopping blocks (14) which now protrude into the path of the hydraulic slide assembly (1) forces the conveyance to come to a rest against the hydraulic slide assembly (1). As soon as the contact is made between the hydraulic slide assembly and the upper stopping blocks (14) the lower retaining blocks (16) are actuated through a hydraulic cylinder (17). This positively locks the conveyance to the hydraulic slide assembly (1) by constraining the assembly in the vertical direction between the upper stopping blocks (14) and the lower retaining blocks (17).

The hydraulic slide assembly (1) is secured to the supporting steelwork through containment by the engagement hook (2) and locking hook (3) and can thus not move relative to the station. The cage is now also secured to the hydraulic slide assembly (1) through the containment by the upper stopping blocks (14) and the lower retaining blocks (16). The support steelwork is installed at the correct height to ensure that the cage is secured at the correct elevation. A properly aligned and secured cage is obtained allowing the safe loading and unloading of the conveyance.

To release the conveyance after the loading or unloading process the upper stopping blocks (14) and the lower retaining blocks (16) are retracted through the action of the hydraulic cylinders (15, 17). The conveyance is now free to move relative to the hydraulic slide assembly (1) which is still connected to the supporting steelwork. This relative motion is required in order to equalise the stress in the rope due to the change in weight of the conveyance. The relative movement between the conveyance and the hydraulic slide assembly (1) drives the gear pump which requires energy and thus hinders the motion to obtain a smooth controlled movement of the conveyance. After a given time the engagement hook (2) and the locking hook (3) is retracted and the entire system is freed from the supporting steelwork. During the subsequent travel of the conveyance the hydraulic slide assembly (1) is returned to its original starting position due to the weight off the assembly.

4.9.3. CONCEPT 6

The sixth system concept is mounted to the conveyance ensuring that it can be utilised at any station. The system stores hydraulic energy during docking, which is used to power the necessary components. It is a fairly complex design and a variety of illustrations are used to explain the workings of the concept.
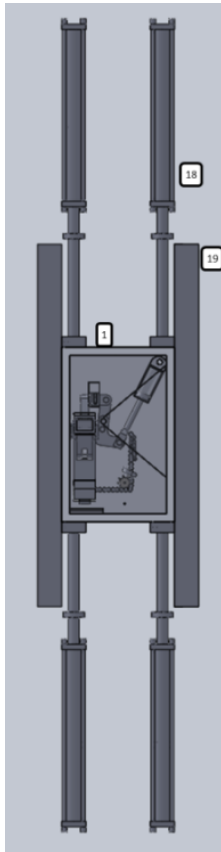
FIGURE 29 FRONT VIEW OF A CAGE ARRESTING DEVICE CONCEPT USING CONVEYANCE MOUNTED HYDRAULICALLY ACTUATED CLAMP BEAMS.

The slide assembly (1) shown above is responsible for locking the conveyance to the supporting steelwork with its internal components illustrated below.
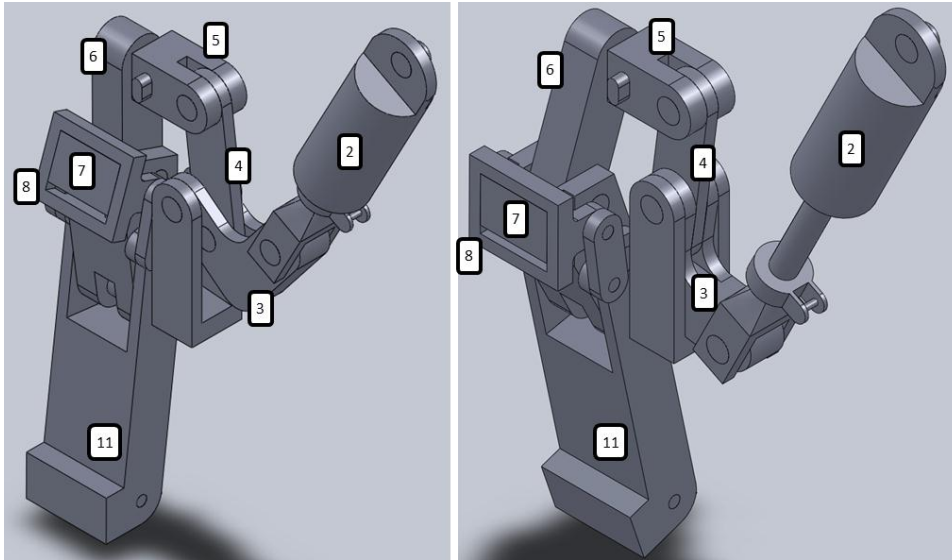
FIGURE 30 DETAILED 3D MODEL OF THE CLAMPING MECHANISM, OF A CAGE ARRESTING DEVICE CONCEPT USING CONVEYANCE MOUNTED HYDRAULICALLY ACTUATED CLAMP BEAMS, SHOWING THE MECHANISM IN THE DISENGAGED POSITION ON THE LEFT AND ENGAGED POSITION ON THE RIGHT.

During the conveyance's travel through the shaft the locking arrangement is in the retracted position shown in the figure on the left. When the onsetter positioned at the station sees the descending conveyance he signals the WED, on the lock bell system, to decelerate the conveyance. When the signal is given the engagement cylinder (2) extends causing the toggle link (3) to rotate in a clockwise direction around the top pivot point secured to the slide assembly housing through a strengthening web (17). The rotation around the top pivot point causes the transfer link (4), connected to the vertical transfer boss (5) running in guides on the slide assembly, to be pulled downwards. The downward pull on the vertical transfer boss (5) pushes on the engagement hook actuation link (6) to kick the engagement hook (7) out into the path of the station steelwork. The engagement cylinder (2) extends to full stroke to rotate the toggle link (3) into an over-toggle position where it prevents the engagement hook (7) from being hit back into the housing when it comes into contact with the supporting steelwork. As the engagement hook (7) moves to the activated position the locking hook (11) is kept inside the housing through a spring between the catchment surface of the engagement hook (7) and the inner surface of the locking hook actuation boss (8). The position of the engagement hook (7) after the extension of the engagement cylinder (2) can be seen on the right hand side of figure 30.

The conveyance is lowered until the locking hook actuation boss (8), mounted over the engagement hook (7) in guides (9), settles on the supporting station steelwork. The engagement hook remains in position because of the over-toggle at the toggle link (3) causing the locking hook actuation boss (8) to be pushed upwards until it press against the engagement hook (7). The upwards movement of the locking hook actuation boss (8) connected to the locking hook links (10) pull the locking hook (11), illustrated in figure 31, into the locking position beneath the supporting steelwork. As the locking hook (11), illustrated in figure 32, moves forward the pawl (12) connected to the bottom of the locking hook (11) drops into the locking position in front of the retainer block (13) preventing the locking hook (11) from being pushed back into the slide assembly (1) when a force is applied to the locking hook.
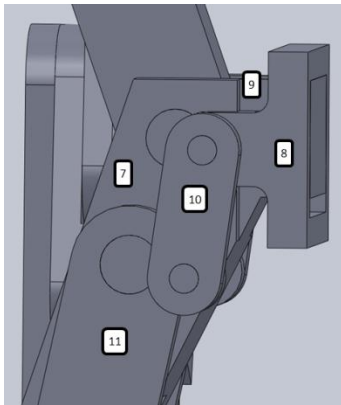
FIGURE 31 DETAILED 3D MODEL OF THE LOCKING HOOK USED IN A CAGE ARRESTING DEVICE CONCEPT USING CONVEYANCE MOUNTED HYDRAULICALLY ACTUATED CLAMP BEAMS.
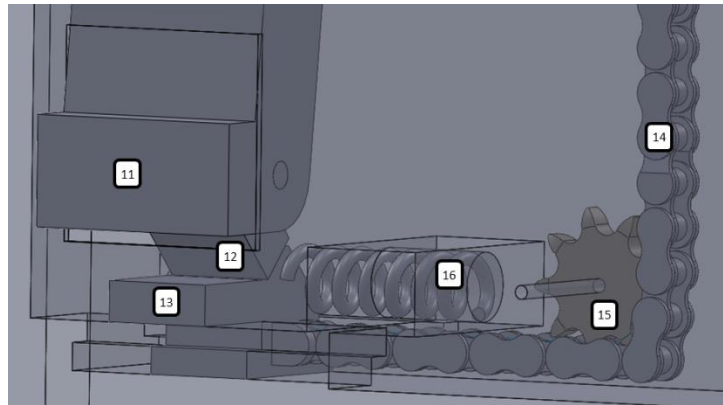
FIGURE 32 DETAILED 3D MODEL OF THE LOCKING HOOK, PAWL AND RETAINER BLOCK OF A CAGE ARRESTING DEVICE CONCEPT USING CONVEYANCE MOUNTED HYDRAULICALLY ACTUATED CLAMP BEAMS.

The slide assembly is thus secured by the engagement hook (7) retained by the over-toggle position and the locking hook (11) retained by the pawl (12) pressing against the retainer block (13) enfolding the station steelwork.

The slide assembly, locked onto the station steelwork through the components described above, is mounted in guides between four damping cylinders to the side of the conveyance shown in figure 29. With the damping cylinders (18) hydraulically locked the conveyance is secured and aligned next to the station allowing safe loading and unloading operations. On completion of these operations the damping cylinders (18) are unlocked to discharge oil through an orifice resulting in a controlled relative motion between the slide assembly (1) and the conveyance to transfer the conveyance load gradually to the rope.

Once the tension is equalised in the rope the slide assembly (1) is disconnected from the station steelwork and the conveyance released. To achieve this release the pawl (12) is disengaged from the retainer block (13) and the toggle link (3) removed from the over-toggle position by retracting the engagement cylinder (2).Retracting the engagement cylinder (2) pulls the toggle link (3) out of the over-toggle position and the chain (14) over the sprocket (15) to remove the retainer block (13) from the path of the pawl (12). With the retainer block (13) pulled back against the spring (16) the locking hook (11) returns back into the slide assembly housing. Figure 33 shows the entire slide assembly (1), with the associated components in the engaged position.
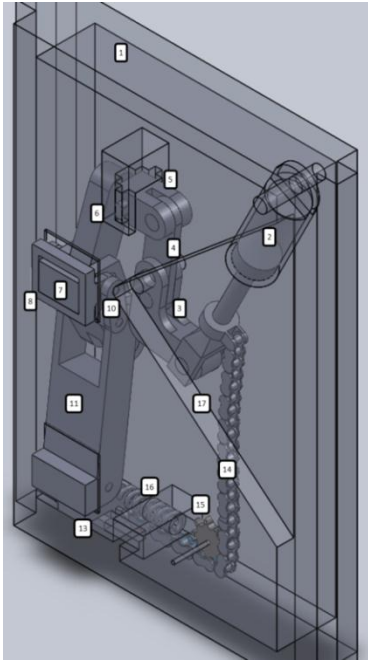
FIGURE 33 DETAILED 3D MODEL OF THE SLIDE ASSEMBLY EMPLOYED IN A CAGE ARRESTING DEVICE CONCEPT USING CONVEYANCE MOUNTED HYDRAULICALLY ACTUATED CLAMP BEAMS.

With all the locking components released the conveyance is fully disconnected from the supporting steelwork and free to move. During the travelling portion of the hoisting cycle the slide assembly (1) is returned to its original position, resetting the system for its next engagement, by equalising the pressure in the damping cylinders (18).

4.9.4. CONCEPT 9

Concept 9 is a simple design based on the working principles of the KEPS system. The device is designed to enfold the supporting station steelwork preventing movement of the conveyance. The device is mounted on the conveyance roof to facilitate usability at any shaft station. Consideration is given to storing energy for use at different levels.

Figure 34 below illustrates a set of bottom beams (1) and top beams (2) in the disengaged position passing through a supporting frame (3). As the conveyance descend towards a station the onsetter signals the WED on the lock bell system to decelerate the conveyance and in the process activates a magnetic switch (4) positioned above the station in the shaft. As the conveyance pass the activated electromagnet (4) it opens a switch to activate the solenoid actuating a valve. By opening the valve compressed air is released from a storage reservoir to extend a cylinder (5) and push the top beams (2) into the path of the steelwork (6) being approached shown in figure 35.
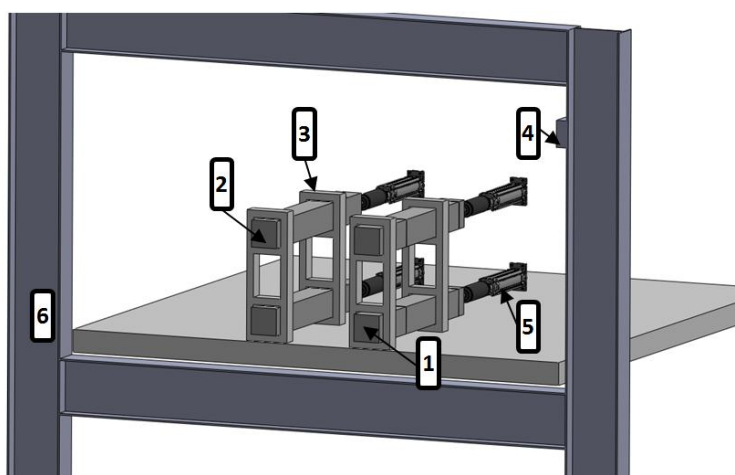
FIGURE 34 3D MODEL OF A CAGE ARRESTING DEVICE CONCEPT USING BEAMS THAT EXTEND ABOVE AND BELOW SUPPORTING STEELWORK WITH ALL BEAMS IN THE RETRACTED POSITION.
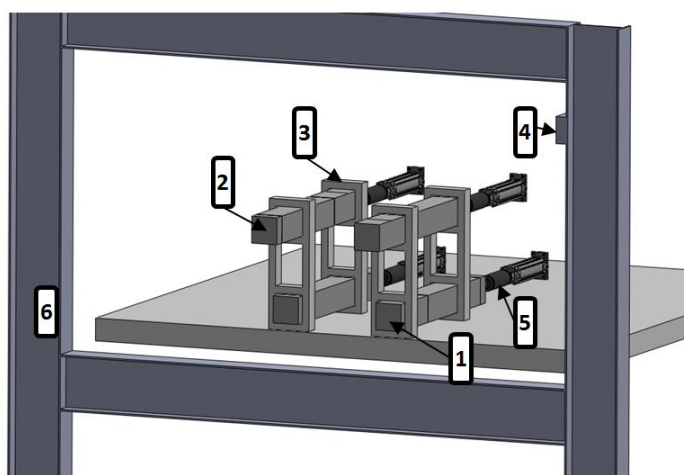
FIGURE 35 3D MODEL OF A CAGE ARRESTING DEVICE CONCEPT USING BEAMS THAT EXTEND ABOVE AND BELOW SUPPORTING STEELWORK WITH THE TOP BEAMS EXTENDED TO ENGAGE THE SUPPORTING STEELWORK.

The conveyance descends until the top beams (2) come to rest on the supporting steelwork (6) at which time a pneumatic and data transfer connection is made. The engagement indicates at the WED that the conveyance has lowered onto the steelwork (6) in the same manner as the KEPS device. With the data linkage and pneumatic connection made the device is supplied with pressurised air which is used to activate the bottom beams (1). The conveyance is secured by having beams (1+2) pass above and below the station steelwork (6) and constraining the conveyance from moving as illustrated in figure 37 below. Loading or unloading operations commences. Upon completion of the operations the onsetter signals the conveyance away, which transfers a signal to the bottom beams (1) to retract. Upon complete retraction proven by a position sensor on the actuation cylinder (5) the signal is passed on to the WED. The WED lifts the conveyance off the supporting steelwork (6) removing any slack from the rope. As soon as the pneumatic and data linkage is broken the top beams (2) retract and the conveyance is free to be moved to the next station. The air stored in the reservoir is used to power the system at the next station restarting the cycle. A battery provided on the conveyance roof provides power to all the sensors and transmitters.
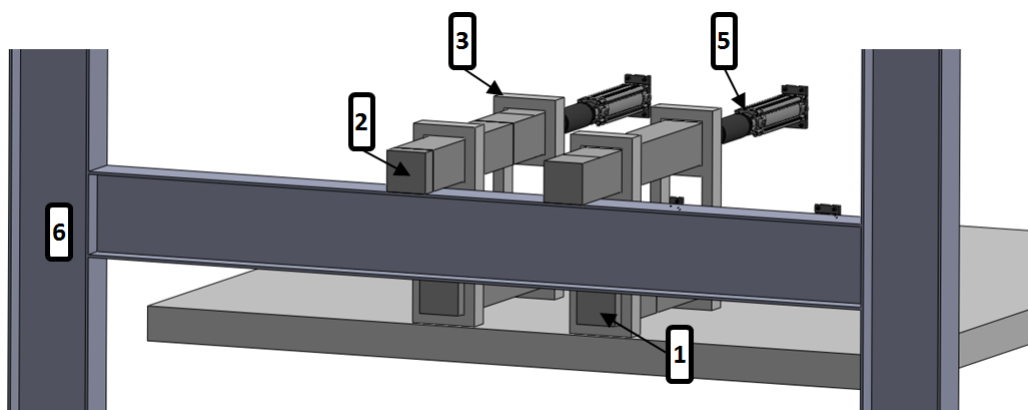
FIGURE 36 3D MODEL OF A CAGE ARRESTING DEVICE CONCEPT USING BEAMS THAT EXTEND ABOVE AND BELOW SUPPORTING STEELWORK WITH THE TOP BEAMS SETTLED ON THE STEELWORK.
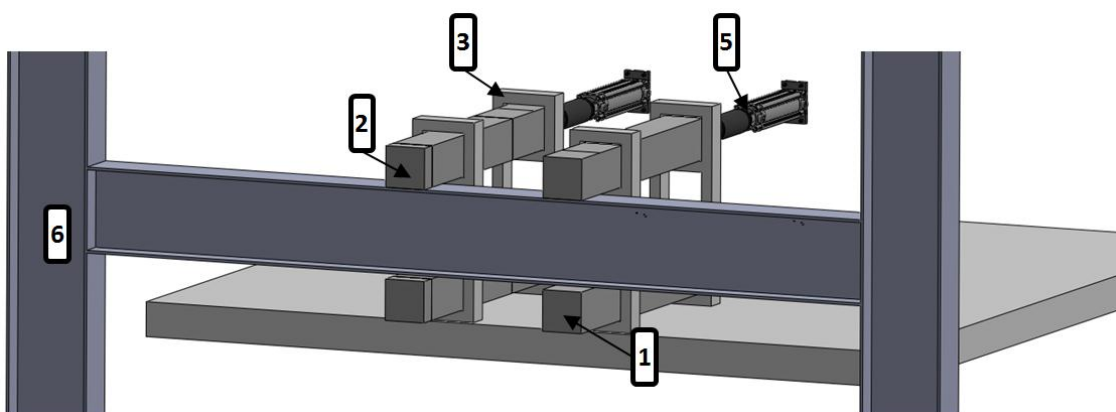
FIGURE 37 3D MODEL OF A CAGE ARRESTING DEVICE CONCEPT USING BEAMS THAT EXTEND ABOVE AND BELOW SUPPORTING STEELWORK WITH THE BEAMS ENFOLDING THE STEELWORK.

4.10.   CONCEPT EVALUATION

The four embodied concepts provides a better feel for the concepts' capabilities and complexities allowing a comparison to be made between them in order to select the most suitable concept for further development. Concept 2 required preliminary embodiment as it was uncertain at the screening stage if it would meet the requirements. Following the embodiment concept 2 is eliminated because it is a too complex and heavy design that exceeds the space requirements of the shaft.

The remaining three concepts are evaluated in a comparison table where the lowest level functional requirements, which are used as measurement criteria, are listed in the first column. The functional requirements used are the lowest level entries in the objectives tree hierarchy provided in Appendix A. A weighted value is assigned to each functional requirement in the second column.

The weighted values are obtained by assigning relative values to the ten sub topics, shown in the green blocks, based on their relative importance such that the assigned values sum to 1. The process is repeated downward for the sub topics such that the summation of the values assigned to the lower level blocks add to 1 for the associated higher level block ending with the black blocks.

The overall weighting of each block, containing a functional requirement, is obtained by multiplying the weighting of the block with the overall weighting of the block immediately above it in the hierarchical structure. The overall weighting for a red block would thus be obtained by multiplying the weighting of the red block with the overall rating of the green block to which it belongs. The overall weighting of the functional requirement listed in column 1is listed in column 2 where the summation of their weights add to 1 illustrating their calculated relative importance.
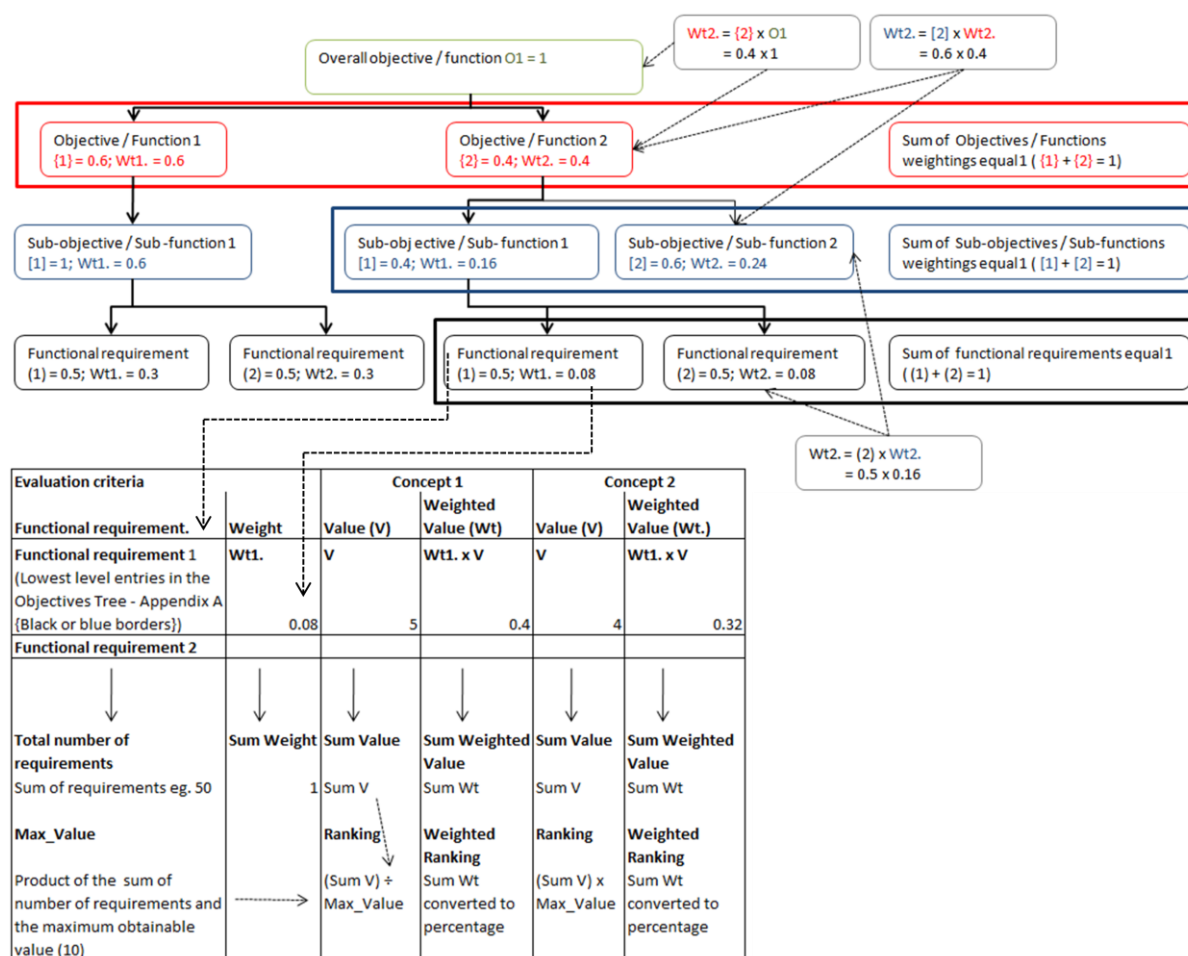
FIGURE 38 ILLUSTRATION EXPLAINING THE PROCESS OF EVALUATING CONCEPTS FROM THE FUNCTIONAL REQUIREMENTS DETERMINED IN THE OBJECTIVES TREE.

The concepts are compared by assigning two columns to each concept next to each other in the evaluation table. The first column beneath a concept contains a number, between 0 and 10, based on the expected performance of the concept when considering the functional requirement. The table used to assign the numerical values is shown below.

TABLE 10 VALUE SCALE USED IN THE CONCEPT EVALUATION PROCESS.

Value scale	
Meaning	Value
Absolutely useless solution	0
Very inadequate solution	1
Weak solution	2
Tolerable solution	3
Adequate solution	4
Satisfactory solution	5
Good solution with a few drawbacks	6
Good solution	7
Very good solution	8
Solution exceeding the requirements	9
Ideal Solution	10

The second column beneath a concept contains the weighted value calculated by multiplying the value in the first column beneath the concept with the weight of the functional requirement listed in column 2 of the evaluation table. The concepts are thus compared by giving them different numerical values based on their expected performance and then calculating the weighted value for the functional requirements.

At the bottom of the table the overall value and overall weight for each concept is calculated by summing the values in the rows. A ranking for each concept (R1, R6 and R9) is calculated by dividing the overall value with the maximum obtainable value (740) obtained by multiplying the number of functional requirements (74) with 10 (because the scale used goes up to 10). This gives the ranking of the concepts if all the functional requirements carried the same weight. The weighted ranking for each concept (WR1, WR6 and WR9) is simply the overall percentage calculated for the concept based on the relative importance of the functional requirements and is obtained by dividing the weighted value by 10.

Looking at an extract (showing only the functional requirements from the financial sub topic) of the evaluation table, provided in Appendix B where the evaluation was performed, it is seen that concept 9 is the best option as it obtained a weighted ranking of 64 % in comparison to the weighted ranking of concept 1 which was 54 % and concept 6 which was 62 %.

TABLE 11 EXTRACT OF THE FINANCIAL PORTION OF THE EVALUATION TABLE, PROVIDED IN APPENDIX B, SHOWING THE RELATIVE RANKINGS OF CONCEPT 1, 6 AND 9.

Evaluation Criteria		Concept 1		Concept 6		Concept 9	
	Weight	Value	Weighted Value	Value	Weighted Value	Value	Weighted Value
Financial							
Minimize parts	0.013	6	0.076	5	0.063	6	0.076
Local manufacturing	0.008	6	0.050	6	0.050	6	0.050
Material choices	0.014	5	0.072	5	0.072	4	0.058
Labour costs	0.010	7	0.067	7	0.067	7	0.067
Elimination of outside resources including power draw	0.013	3	0.038	7	0.090	7	0.090
Minimize maintenance	0.010	6	0.058	6	0.058	6	0.058
	Sum Wt	**OV 1**	**OWV 1**	**OV 6**	**OWV 6**	**OV 9**	**OWV 9**
	1.000	404	5.41	447	6.16	456	6.39
		R 1	**WR 1**	**R 6**	**WR 6**	**R 9**	**WR 9**
		0.546	0.54	0.60	0.62	0.62	0.64

CHAPTER 5.   DESIGN

Concept 9, identified as the best system concept in the preceding chapter, is developed into the Quadro-cage-clamp in this chapter. This chapter discusses the components used and the calculations methodology.

5.1.   CONVEYANCE CLAMP BEAM

In this sub-section the beams shown below in blue of the Quadro-cage-clamp is considered. The calculations and decisions made are discussed.
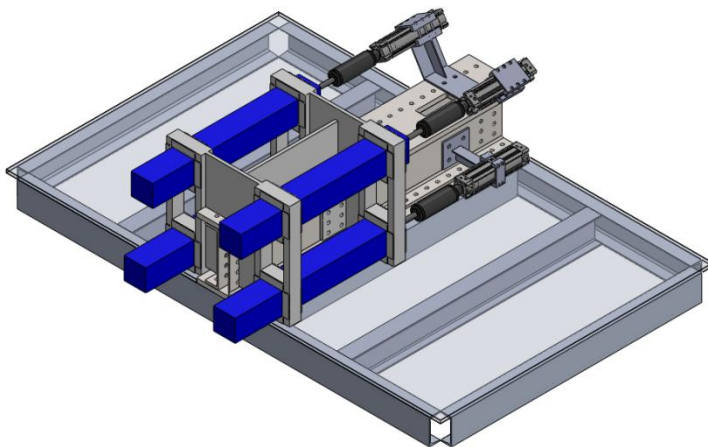
FIGURE 39 3D MODEL ILLUSTRATING THE CLAMP BEAMS OF THE QUADRO-CAGE-CLAMP

Tau Tona Mine's main shaft man winder is used as a model shaft for the design of the system. The winder, with permit number 3957 [27], may hoist a conveyance with a mass of 6,800 kg including attachments and 11,200 kg payload. To promote a stable suspension of the conveyance when docked and to provide redundancy the conveyance arresting device is mounted to the conveyance in duplicate. Each device is designed to support a load of 883 kN (F1) calculated by adding the payload and the conveyance mass and multiplying it with gravity and the required safety factor of 10 [28] before dividing it by 2 for the two devices. With the force applied to the end of the beam known; the distance between the beam supports is required to calculate the forces and ultimately the stresses in the beam.

A decision was made to mount the devices on top of the conveyance such that the clamp beams extend to protrude into the shaft compartment from the side of the conveyance in order to settle on the Buntons. The device cannot be practically mounted to the front of the conveyance as it requires the addition of station steelwork, therefore obstructing the entrance to the conveyance and also hindering the pulling of equipment into the shaft during slinging operations. Mounting the device to the rear of the conveyance was considered but rejected because the associated stresses are too great. Appendix F provides the calculations and description of the rear mount arrangement while Appendix G shows that the forces obtained in Appendix F exceeds the allowable forces provided in Appendix G.

The most suitable orientation of the device is therefore to have the clamp beams extend to settle onto the 305x165x54 kg/m beams dividing the shaft compartments. The section properties of steel profiles database from the South African Institute of Steel Construction [29] shows that this beam has a flange width of 166 mm and from the drawing titled; TYPICAL CROSS SECTION THROUGH SHAFT SHOWING BUNTON STEELWORK (Drawing number 346-SO1-RM0383) [30] it is seen that the centre of this beam is 216 mm from the side of the conveyance. The stroke by which the beam is extended to settle onto the support beam is equal to this clearance plus half the flange width; rounded up to 300 mm. The beam is supported by two 80 mm wide supports placed x mm between centres and the decision is made to have the conveyance overlap with 30 mm when it is extended or retracted. The minimum distance between the support centres x is found as 420 mm to allow for the two halves of the supports, a stopper on the beam of 40 mm and the stroke. The retracted beam must be shorter than 1882 mm, obtained from the drawing entitled ARRGT & DETAILS OF ROOF & TOP TRANSOM FOR 4 DECK MAN CAGE (Drawing number 349-000-M0574 revision 18) [31], to fit between the sides of the conveyance. The maximum distance between the supports is 1442 mm calculated by subtracting the two support halves, stroke and two overlaps from the maximum allowable beam length. The Excel program attached in Appendix C is used to vary the value of x, by dragging the scroll bar next to the graphs, to calculate the reaction forces at the supports.

The distance between supports, x, was altered and the forces obtained fed into the Engineering Equation Solver (EES) program Side Mount Supports Same Side Extended Base, provided in appendix D, to calculate the forces on the supports. The program delivers the number of bolts that need to be fitted to the support to secure it and considering the required spacing between bolts the length between the supports, x, must be adjusted to accommodate the required number of bolts. By increasing the distance between the supports the reaction forces are lowered and the number of bolts required reduced. A distance between supports of 720 mm was decided upon resulting in a total beam length of 1160 mm.

The Clamp Beam Two Supports Side Mount Extended Base program is used to calculate the forces at the supports in the force analysis section. The support nearest the conveyance edge, F2, experiences an upward pull of 1235 kN and the support closest to the Transom, F3, a push of 352 kN. The associated shear force and moment diagrams for the beam are shown below.
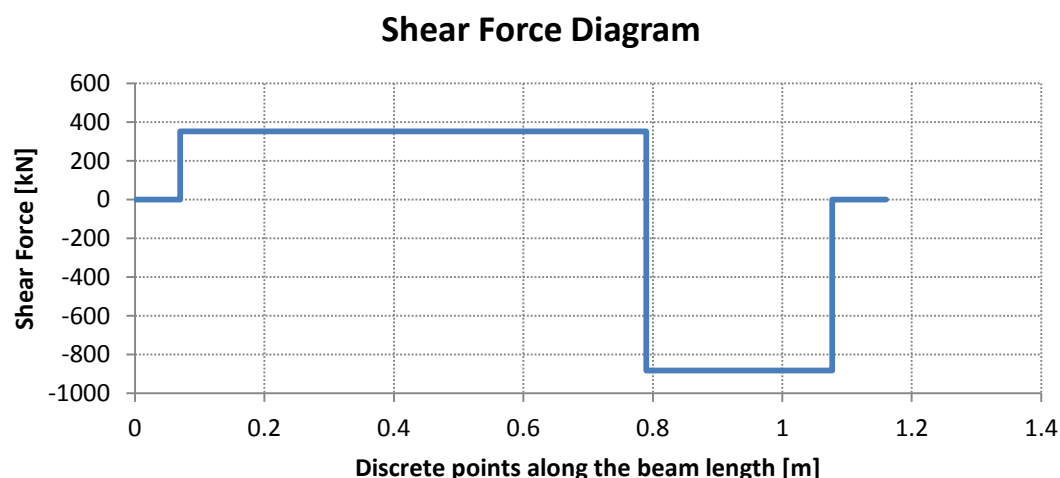
FIGURE 40 SHEAR FORCE DIAGRAM OF THE CLAMP BEAM.

Moment Diagram
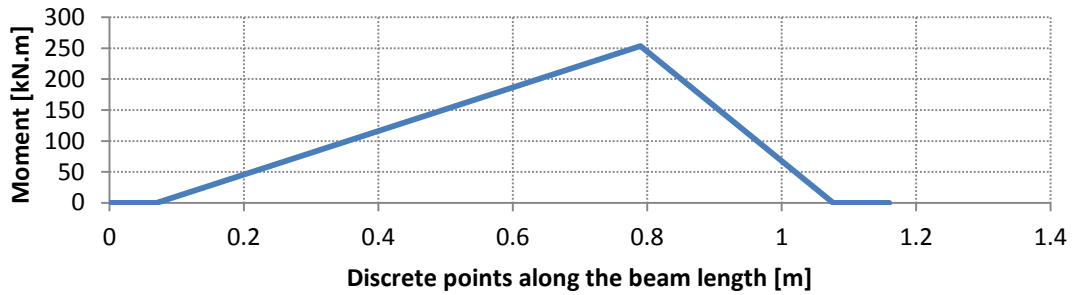
FIGURE 41 MOMENT DIAGRAM OF THE CLAMP BEAM.

The loadings on the beam creates a combined tensile and shear stress in the beam. The beam geometry influences the stresses in the beam and a suitable beam profile is selected by considering a solid beam and a box beam. The Von Misses stresses are calculated in the beam and the geometry specified as not to exceed the yield limit.

The Maximum Distortion Energy Theory (Von Misses) requires the left hand side of the equation, given in the book Mechanics of Materials by R.C. Hibbeler [32], and reproduced below to be less than the right hand side of the equation to prevent yielding of the material.

$$\sigma_1^2 - \sigma_1\sigma_2 + \sigma_2^2 = \sigma_Y^2 \qquad ...(1)$$

A Mohr circle as shown below can be used to calculate the values of the principal stresses required for the Maximum Distortion Energy equation above.
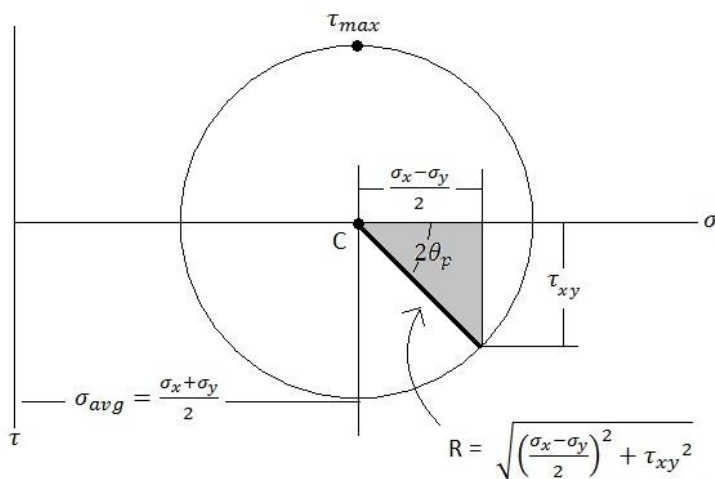
FIGURE 42 2 DIMENSIONAL MOHR CIRCLE [56]

Considering the Mohr circle shown above it can be seen that the first principle stress can be written as follow.

$$\sigma_1 = \sigma_{avg} + R \qquad \text{...(2)}$$

Where σ_{avg} is the centre of the Mohr circle and R the radius. The second principle stress can be written as follow.

$$\sigma_2 = \sigma_{avg} - R \qquad \text{...(3)}$$

Substituting these equations into the first equation and simplifying yields:

$$\sigma_{avg}^2 + 3R^2 = \sigma_Y^2 \qquad \text{...(4)}$$

It is known that:

$$\sigma_{avg} = \frac{\sigma_x + \sigma_y}{2} \qquad \text{...(5)}$$

When considering the case of plane stress; $\sigma_y = 0$. Further it is known that:

$$R^2 = \left(\frac{\sigma_x - \sigma_y}{2}\right)^2 + \tau_{xy}^2 \qquad \text{...(6)}$$

Substituting equations (5) and (6) into equation (4) and simplifying yields:

$$\sigma_x^2 + 3\tau_{xy}^2 = \sigma_Y^2 \qquad \text{...(7)}$$

The left hand side of the formula is used to calculate the combined stress at any given point on the cross section and defined as $\sigma_{element}$. As long as $\sigma_{element}$ is less than σ_Y^2 the yield stress isn't exceeded and the design is safe. By dividing $\sigma_{element}$ with σ_Y^2 the safety factor at any point in the cross section is obtained.

5.1.1. SOLID BEAM

The beam section next to the support closest to the conveyance edge (x = 0.79 m) experiences both the largest moment and shear force. The shear force and moment distribution through this section for a rectangular beam profile with dimensions 80x130 mm is calculated and shown in figure 43 and figure 44 below. The y-axis gives the stress magnitude and the x-axis the height of the beam at discrete distances from the bottom of the beam throughout the section.

Shear Stress Diagram
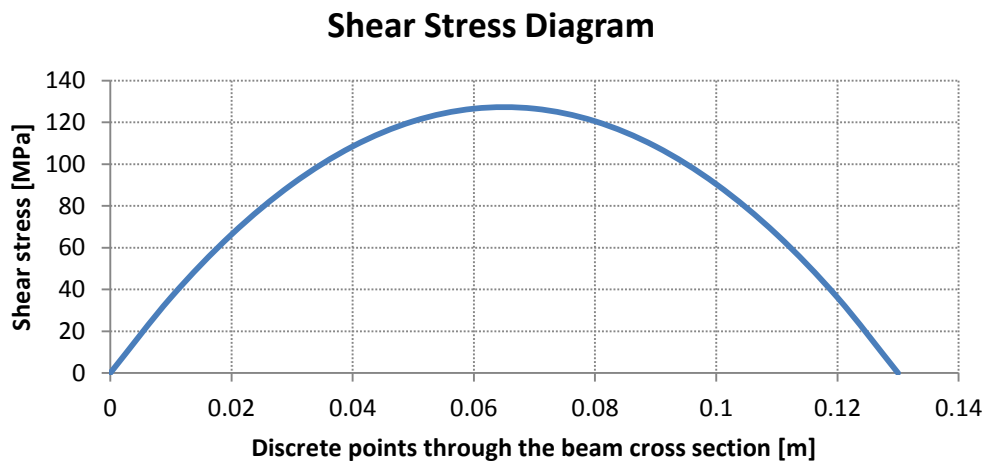
FIGURE 43 SHEAR STRESS DIAGRAM FOR A SOLID CLAMP BEAM.

Tensile Stress Diagram
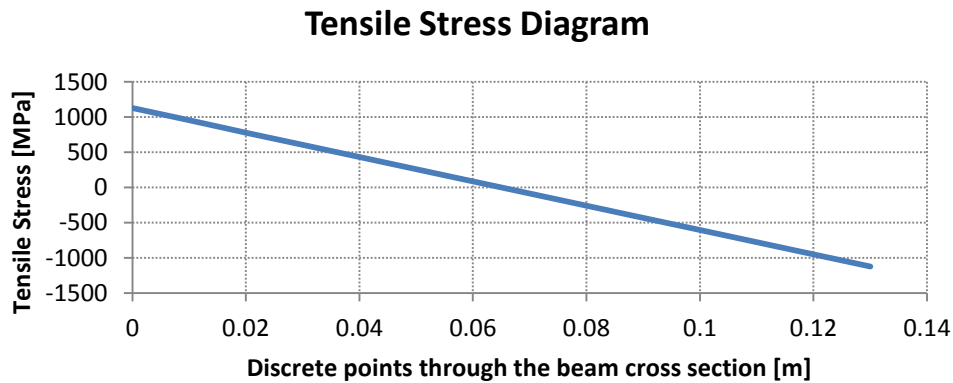
FIGURE 44 TENSILE STRESS DIAGRAM FOR A SOLID CLAMP BEAM.

The tensile stress and shear stress varies across the beam and a combined stress results. The Von Misses stresses are found by calculating $\sigma_{element}$, plotted as a red curve on the graph in figure 45 below, for various points across the section. σ_Y^2 is calculated for various points across the section and plotted as a blue line on the graph below. As long as the red curve remains below the blue line the design doesn't exceed the yield stress.
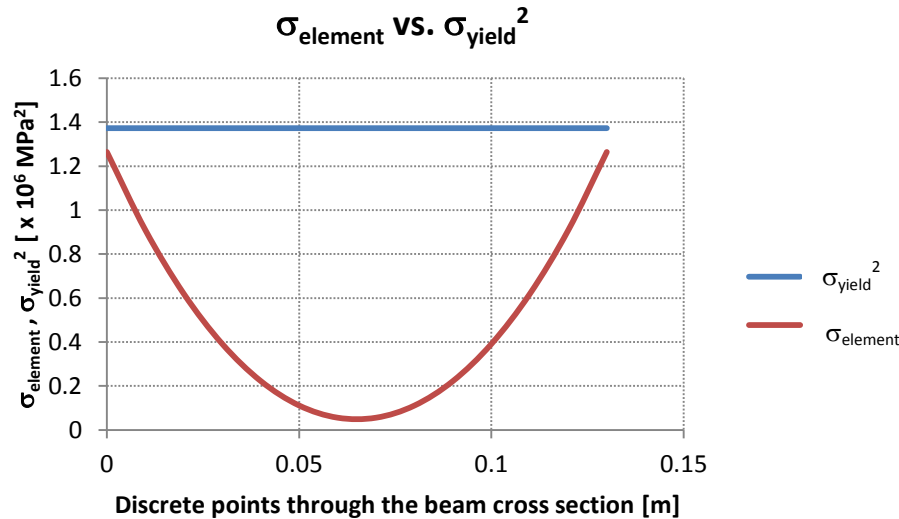
FIGURE 45 GRAPH OF THE ELEMENT STRESS VS. THE SQUARE OF THE YIELD STRESS ACROSS A CROSS SECTION OF A SOLID CLAMP BEAM.

The material specified for the beam is 17-4 PH stainless steel as it will resist corrosion in the wet shaft and has a massive yield strength of 1172 MPa when given H900 heat treatment according to AK Steel's Product Data Bulletin [33]. This high yield strength is important as it allows the size of the beam to be reduced lowering the beam mass which is calculated as 94 kg. The geometry of the beam is altered which changes the red curve until it is as close as possible to the blue line. To prevent the beam becoming too thin the width of the beam is limited to 80 mm, also the maximum standard thickness plate 17-4 PH is sold in [34], and the height adjusted to the minimum value of 130 mm where the lowest safety factor of 1.09 is achieved. The safety factor of 1.09 implies that the true factor of safety is in excess of 10 since the load used in the calculations already contains a factor of safety of 10.

5.1.2. BOX BEAM

In order to reduce the beam weight a box beam section is considered. The forces acting on the beam is the same as with the solid beam. The Excel program Clamp Beam Two Supports Side Mount Extended Base has a tab titled Box Beam 17-4 PH H900 where the forces and stresses in the beam are calculated. The program has two scrolls which changes the thickness of the top plate and side plates. Changing the overall beam dimensions and the plate thicknesses allows a beam with a balanced stress to be designed. Reducing the thickness of the side plates increases the shear stress. A high beam is also required to handle the tensile stresses brought about by the moment. The variables are thus altered to minimise the beam mass and to obtain a near equal stress distribution. The tensile stress diagram for the beam is given below.

Tensile Stress Diagram
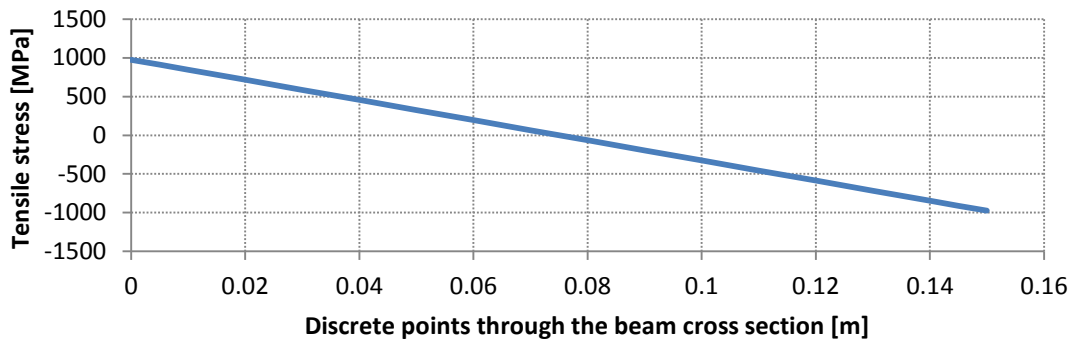
FIGURE 46 TENSILE STRESS DIAGRAM FOR A BOX SECTION CLAMP BEAM.

The shear stress for a box beam is slightly different, where the shear stress distribution is linear for horizontal segments and parabolic for vertical sections as explained in the book Mechanics of Materials by R.C. Hibbeler [32]. The stress therefore doesn't start off from zero at the beam edge but from 334 MPa at the middle of the top flange. The shear stress diagram is provided below.

Shear Stress Diagram
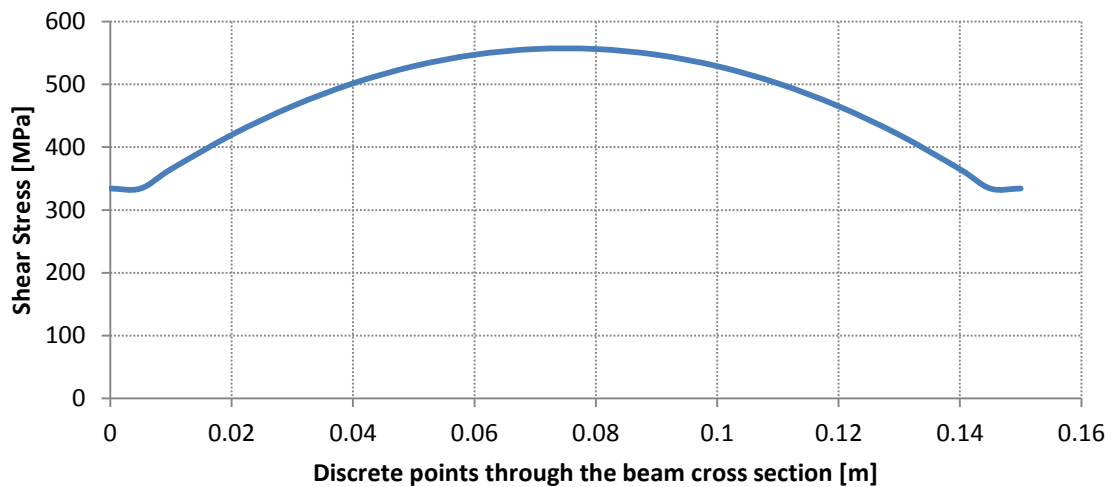
FIGURE 47 SHEAR STRESS DIAGRAM FOR A BOX SECTION CLAMP BEAM.

The combined stress in the beam, $\sigma_{element}$, is calculated and plotted as a red curve in the graph below. The square of the yield stress, σ_Y^2, is also calculated and plotted as a blue line on the graph below. As long as the red curve is below the blue line the yield stress isn't exceeded and the design is safe. The square of the yield strength is also divided by the combined stress to obtain a minimum safety factor of 1.07. Because the applied load is ten times larger the safety factor is in fact ten times larger.

$\sigma_{element}$ **vs.** σ_{yield}^2
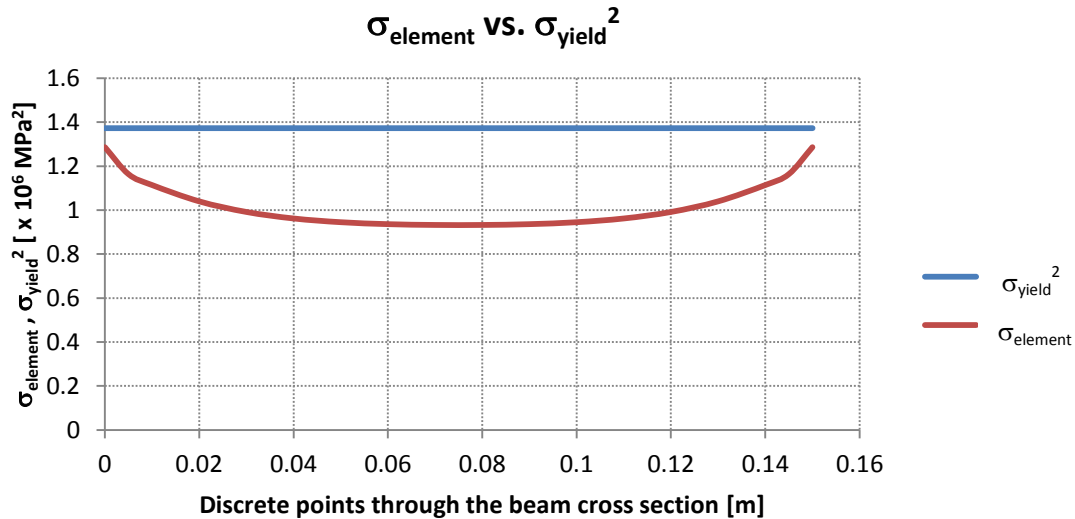
FIGURE 48 GRAPH OF THE ELEMENT STRESS VS. THE SQUARE OF THE YIELD STRESS ACROSS A CROSS SECTION OF A BOX SECTION CLAMP BEAM.

The graph indicates that the material is used better in a box beam in comparison to a solid beam since the two graphs are closer to each other indicating that the stress is more equally distributed throughout the section. Comparing the safety factors it can be seen that the smallest safety factor, throughout the section at the point where the maximum shear force and moment is present, is 1.09 for the solid beam and 1.07 for the box beam whereas the maximum safety factor for the solid beam is 24.7 and for the box beam 1.47. This near equal distribution of stress results in a lighter beam where the weight of the box beam is calculated as 57.7 kg; 36.4 kg lighter than the solid beam.

The final design of the clamp beam is a box beam with a length of 1160 mm and welded together from 13 mm plates on the sides and 10 mm plates at the top and bottom. The overall height of the beam is 150 mm and its width 150 mm. The beam is shown below with a cut out on the corner to illustrate the inside.
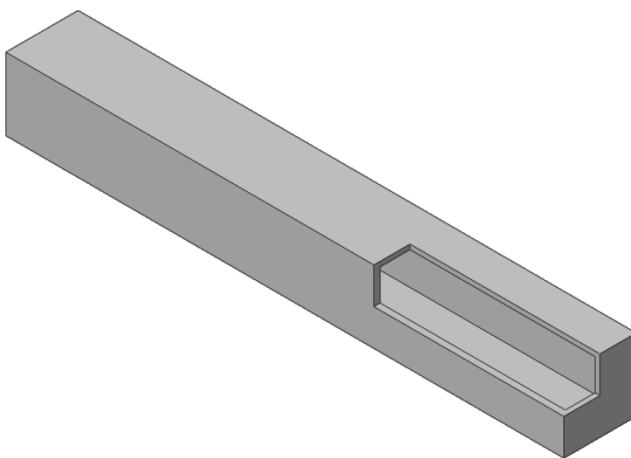
FIGURE 49 3D MODEL OF A BOX SECTION CLAMP BEAM.

5.2.   SUPPORT STRUCTURE

In this sub-section the support frame shown below in blue of the Quadro-cage-clamp is considered. The calculations and decisions made are discussed.
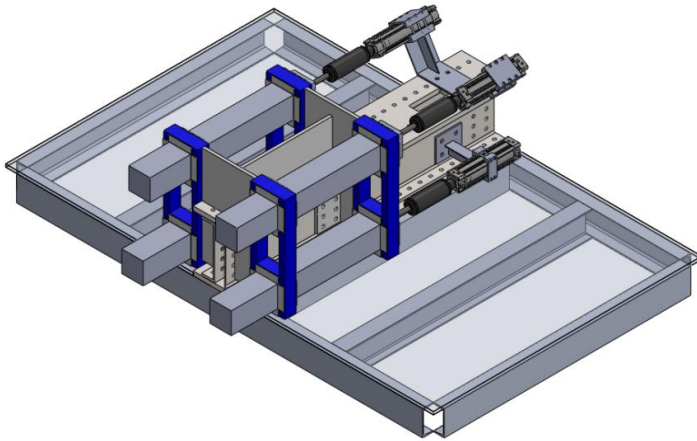
FIGURE 50 3D MODEL ILLUSTRATING THE SUPPORT FRAME OF THE QUADRO-CAGE-CLAMP.

The box beam is supported by a support frame connected to the conveyance Transom through a support fixture. The clamp beams pass through the top and bottom opening of the support shown below with a distance of 330 mm between them to allow the supporting Bunton to be easily enfolded. The openings are 160 mm high and wide to fit the clamp beam and a 5 mm thick liner plate at all sides.
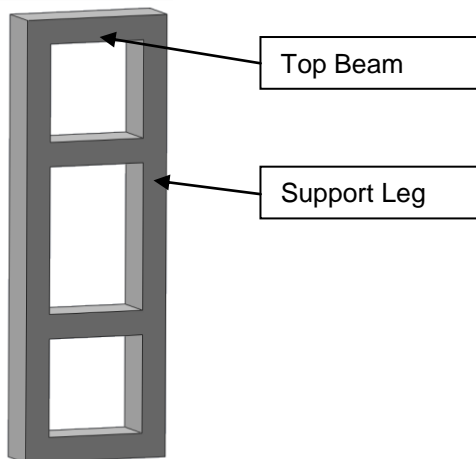
FIGURE 51 3D MODEL OF THE QUADRO-CAGE-CLAMP'S SUPPORT FRAME.

The force at the support closest to the conveyance edge must push down on the clamp beam with a force of 1.2×10^3 kN calculated as a distributed load of 7.7×10^3 kN/m acting over a 160 mm long beam clamped at both ends [35]. The distributed load creates a maximum shear stress of 617 kN and a moment of 17 kN.m at the legs of the support connected to the top beam. The resultant shear force and moment diagrams are provided below. In the graphs below the Y-axis displays the magnitude of the shear force and the moment while the X-axis displays the length from the left beam-leg juncture of the support frame in meters.

Shear Force Diagram
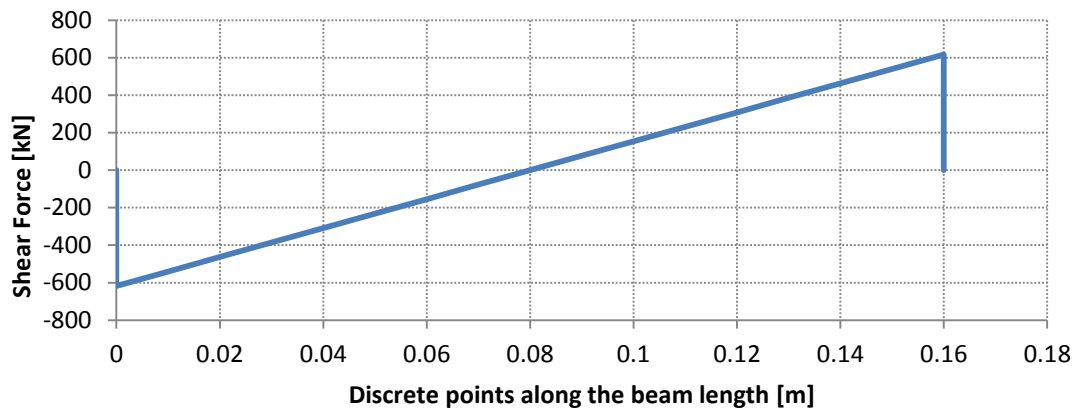
FIGURE 52 SHEAR FORCE DIAGRAM FOR THE TOP BEAM OF THE QUADRO-CAGE-CLAMP'S SUPPORT FRAME.

Moment Diagram
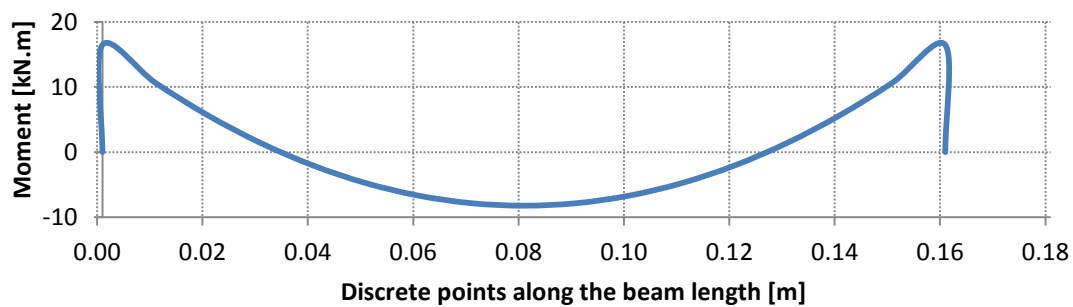
FIGURE 53 MOMENT DIAGRAM FOR THE TOP BEAM OF THE QUADRO-CAGE-CLAMP'S SUPPORT FRAME.

The Excel program Side Mount Support Calculations, provided in appendix E, was used to calculate the tensile and shear stress at the cross section adjacent to the support as this is where both the moment and shear force is the greatest. The tensile and shear stresses are plane stresses and are therefore added together to obtain $\sigma_{element}$, plotted as a red line in the graph below, as described earlier. The square of the yield stress is plotted as a blue line and the thickness of the beam adjusted to keep the red curve below the blue line indicating a satisfactory safety factor. The minimum required thickness of the beam is found as 33 mm. The legs attached to the top beam must have an adequate area to handle the tensile stress developed by the vertical support reaction force and tensile stress of the moment. The two tensile stresses are added and the thickness of the leg increased until a safety factor of 1 is obtained at 36 mm. The decision was thus made to construct the entire support from 40 mm plates welded together as it exceeds the required minimum thicknesses and reduces the number of different thickness plates needed, lowering cost. The combined stresses in the beam and support legs are provided in the graphs below.

$\sigma_{element}$ vs. σ_{yield}^2
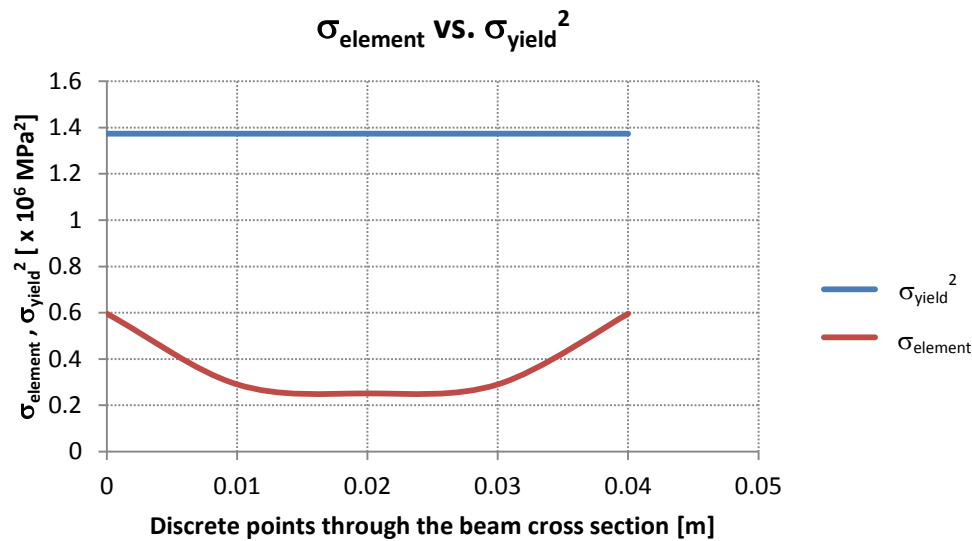
FIGURE 54 GRAPH OF THE ELEMENT STRESS VS. THE SQUARE OF THE YIELD STRESS FOR THE TOP BEAM OF THE QUADRO-CAGE-CLAMP'S SUPPORT FRAME.

Support Frame Leg Stresses
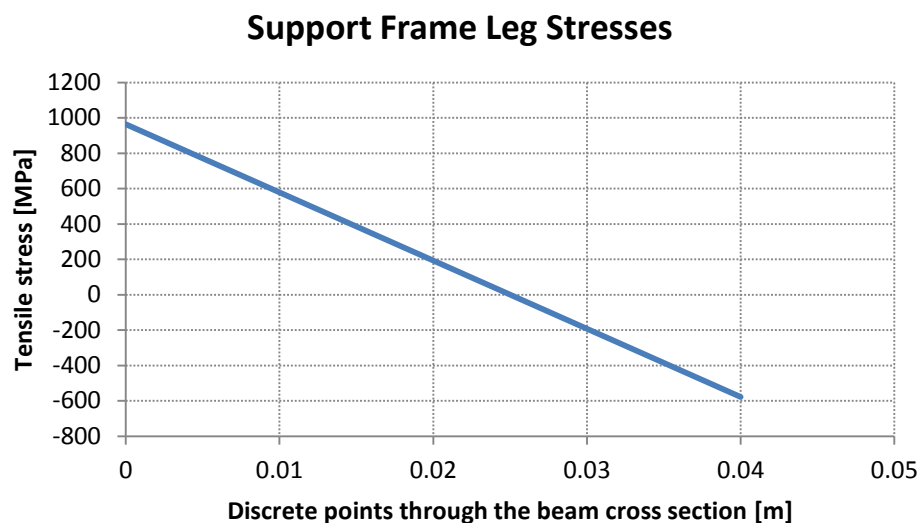
FIGURE 55 GRAPH ILLUSTRATING THE TENSILE STRESS IN THE LEGS OF THE QUADRO-CAGE-CLAMP'S SUPPORT FRAME.

The beams beneath the top clamp beam, above the bottom clamp beam and beneath the bottom clamp beam is also constructed from 40 mm plates to standardise on the size reducing cost and easing assembly. The thickness is considered sufficient as the forces applied to the beams is far less than that applied to the top beam.

The beam beneath the top clamp beam on the rear support experiences a downwards push of 352 kN calculated as a distributed load of 2.2×10^3 kN/m acting over a 160 mm long beam clamped at both ends. The distributed load creates a maximum shear stress of 176 kN and a moment of 5 kN.m at the legs of the support connected to the beam. The resultant shear force and moment diagram is provided below.

Shear Force Diagram
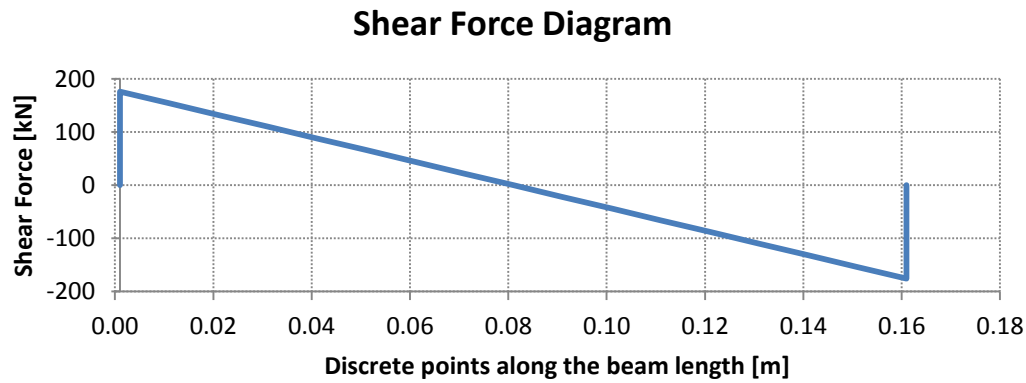
FIGURE 56 SHEAR FORCE DIAGRAM FOR THE BEAM BENEATH THE TOP CLAMP BEAM OF THE QUADRO-CAGE-CLAMP'S REAR SUPPORT FRAME.
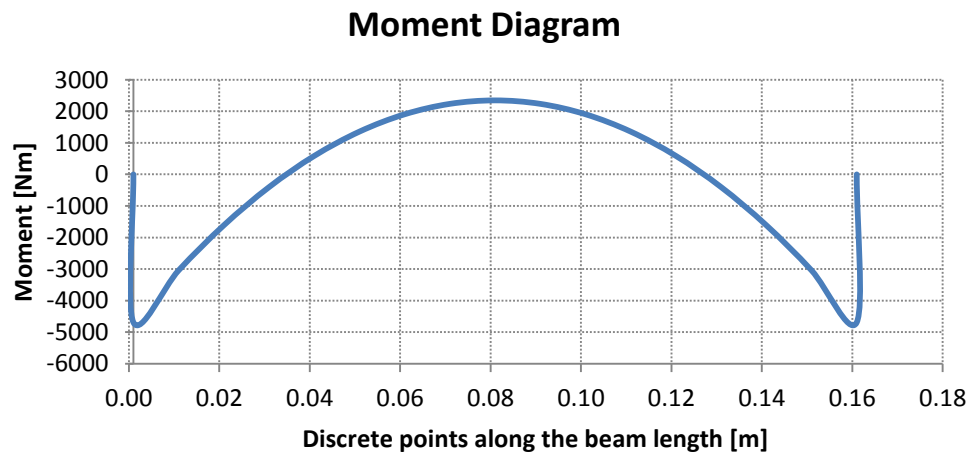
Moment Diagram

FIGURE 57 MOMENT DIAGRAM FOR THE BEAM BENEATH THE TOP CLAMP BEAM OF THE QUADRO-CAGE-CLAMP'S REAR SUPPORT FRAME.

The rear support is also constructed from 40 mm plates and to the same dimensions as the front support even though it carries far less forces in order to reduce the number of thickness plates required in the design. Manufacturing four of the same size supports is easier than two sets of different supports. Having the front and rear supports the same size and strength allows the entire assembly to be installed any way around lessening the change of incorrect installation. The oversize rear support is excessively strong with a safety factor of 28.4 on the loaded beam illustrated by the great distance between $\sigma_{element}$ and $\sigma_{yield}{}^{2}$ in the graph below.
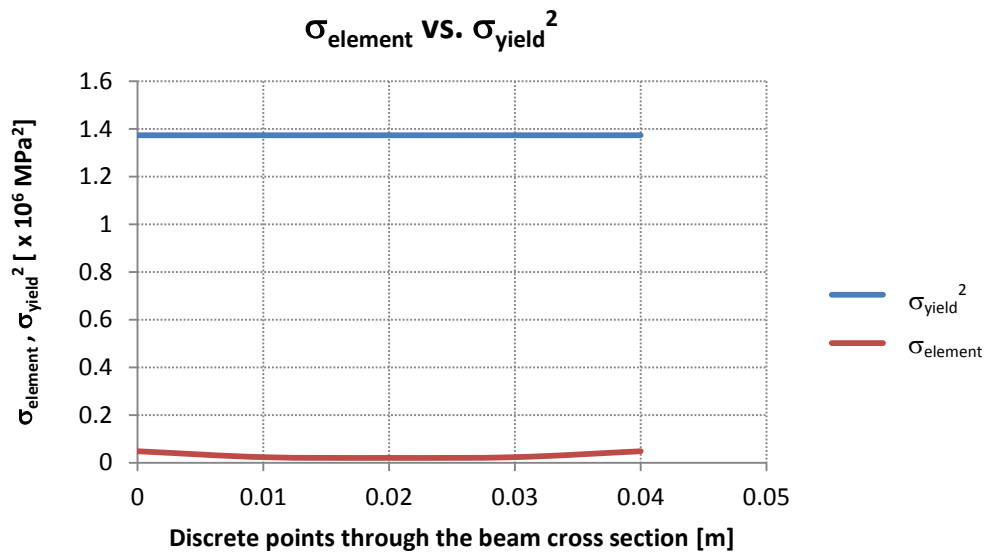
FIGURE 58 GRAPH OF THE ELEMENT STRESS VS. THE SQUARE OF THE YIELD STRESS IN THE BEAM BENEATH THE TOP CLAMP BEAM OF THE QUADRO-CAGE-CLAMP'S REAR SUPPORT FRAME.

The legs on the rear support experiences a compressive stress requiring column buckling to be considered. From the Rear Support tab in the Excel Program Side Mount Support Calculations it can be seen that a force of 3.1×10^3 kN is required to buckle the support leg about the Y-Y axis which is far in excess of the 176 kN applied concentrically about the Y-Y axis of the support leg. The stress developed in the beam about the X-X axis due to the eccentric loading on the beam is found as 283 MPa resulting in a safety factor of 4.1 in the support leg. The support legs are sufficiently strong and will resist buckling. In the case where the bottom clamp beam is subjected to load the beam above the bottom clamp beam will experience an upwards force with the same magnitude as above. The reaction force and moment will induce a pull on the legs of the bottom part of the support beams resulting in a tensile stress. The combined tensile stress of the pull and the moment equals 275 MPa far below the allowed stress of 1172 MPa delivering a safety factor of 4.3.

5.3. SUPPORT LINERS

In this sub-section the support liners shown below in blue of the Quadro-cage-clamp is considered.
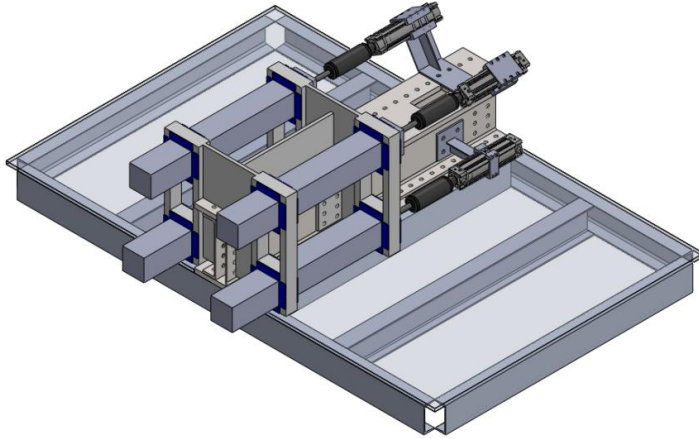
FIGURE 59 3D MODEL ILLUSTRATING THE SUPPORT LINERS OF THE QUADRO-CAGE-CLAMP.

The passage of the clamp beams through the openings in the support frame, during engagement and disengagement, wears away at both the clamp beam and the support. To reduce this wear liners made from ToughMet 3 CX 105 are installed to both reduce the sliding friction and to provide a sacrificial wear surface. ToughMet 3 CX 105 is used due to its low coefficient of friction and high yield strength [36] making it suitable for this high pressure application. The liners are manufactured to two sizes a top / bottom liner and a side liner from 5 mm plate welded together. The top / bottom-liners are installed first followed by the side-liners, using two screws, to the support frame. The difference in length, between the two liners, is to allow the side-liners to fit in the now reduced opening in the support following the installation of the top / bottom-liners. The liners are illustrated below.
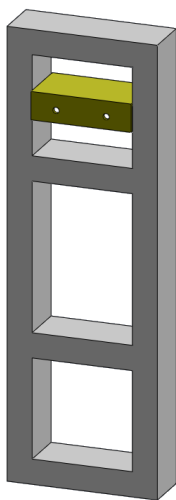
FIGURE 60 3D MODEL OF THE INSTALLATION OF A TOP / BOTTOM-LINER TO THE SUPPORT FRAME.
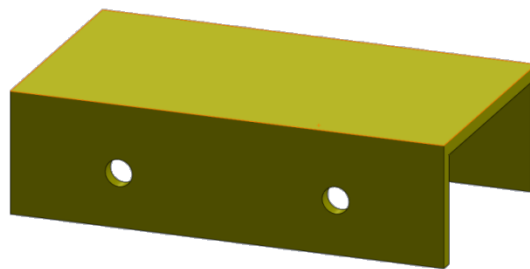
FIGURE 61 3D MODEL OF A TOP / BOTTOM-LINER USED IN THE QUADRO-CAGE-CLAMP.

5.4.   SUPPORT FIXTURES

Different positions for mounting the arresting device to the conveyance are considered in this section. Mounting the device to the rear of the conveyance will have the clamp beams settle onto the pipe dividers connecting the Buntons. The layout has the front and rear support mounted to a bottom beam which is simply a thick plate designed to transfer the forces to the channel and I beam structure of the conveyance roof. The top of the supports are then connected to a channel beam that transfers the forces to the Transom. Figure 60 illustrates the layout. The load sharing between the bottom and top beam is controlled by the ratio of the beam stiffness and the positions of the supports. The EES program Rear Support, provided in Appendix F, was used to vary the bottom beam thickness and support positions until the forces transferred to the roof support beams reached the maximum allowed magnitude as presented in Appendix G. The top beam was then sized to transmit the remainder of the force to the Transom. Due to the large force applied to the clamp beam and excessive distance from the Transom the force and moment transferred to the Transom exceeds its load carrying ability as shown in Appendix G. The use of this mounting layout is not feasible as the force cannot be carried by the conveyance structure.
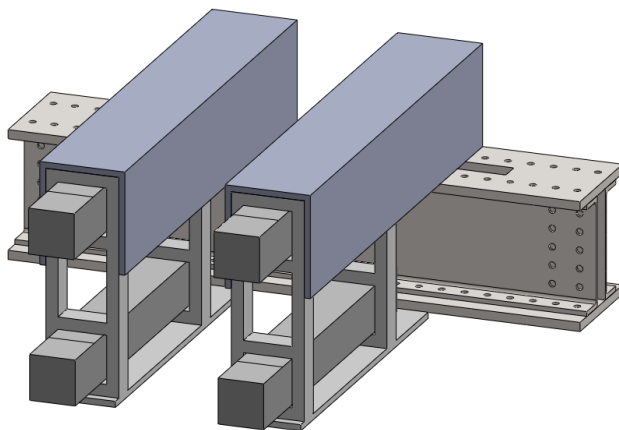
FIGURE 62 3D MODEL OF THE CLAMP BEAMS POSITIONED TO EXTEND FROM THE BACK OF THE CONVEYANCE.

The supports are therefore mounted to the side of the conveyance where they are directly affixed to the Transom. Mounting the supports to one side of the Transom imposes a torque onto the Transom and sets up complex stress distributions. The preferred layout is to mount the two arresting devices to opposite sides of the Transom to have the moments generated by each device neutralise each other. The final layout is illustrated on the next page.
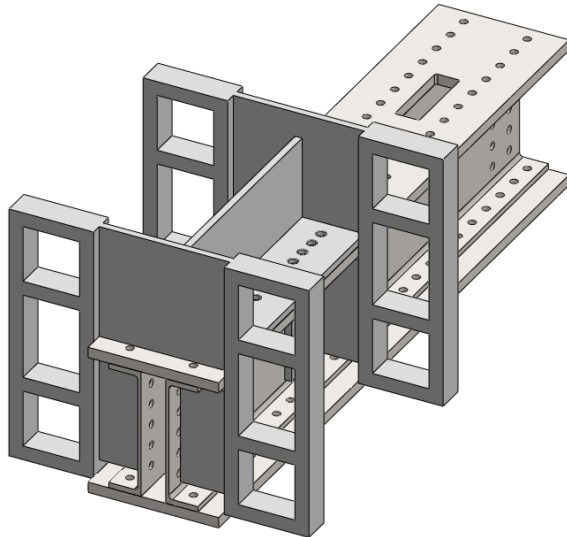
FIGURE 63 3D MODEL OF THE SUPPORT FRAME FIXTURE INSTALLED ON TOP OF THE TRANSOM.

The forces transferred to the supports are ultimately carried by the top and bottom beams bolted to the Transom. The deflection of the top beam is equal to the deflection of the bottom beam and bottom connecting plate under the assumption that the support legs does not stretch. The forces carried by the top beam and bottom beam are shared based on the ratio of the beam stiffness influenced by its moment of inertia. In the EES program Side Mount Supports the dimensions of the top beam web was altered to obtain a stress distribution that lowered the number of bolts required on the top beam to 26.

By reducing the number of bolts the overall length between the supports is reduced influencing the forces on the clamp beam. With this balance of forces 1061 kN is transmitted from each front support to the top beam through the 17-4 PH stainless steel top connecting plate shown in blue on the figure below.
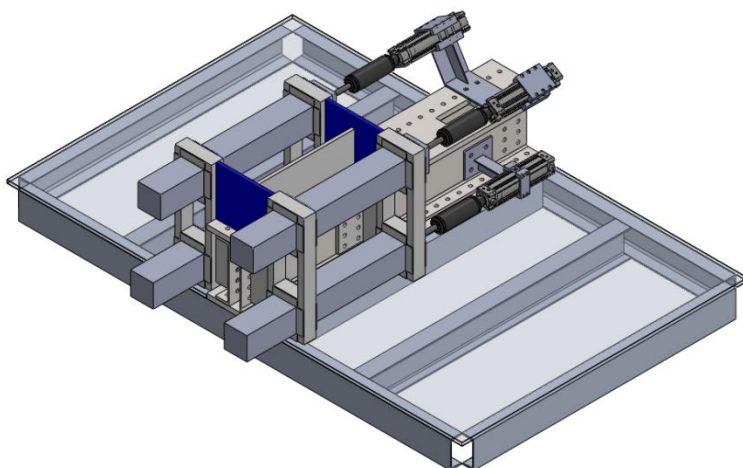
FIGURE 64 3D MODEL ILLUSTRATING THE TOP CONNECTING PLATE OF THE QUADRO-CAGE-CLAMP.

The base of the top connecting plate is joined to the top beam resulting in a tensile and shear stress distribution in the top connecting plate as illustrated below. Both the shear and tensile stress in the top connecting plate is at a maximum at position 1 where $\sigma_{element}$ is equal to 267.8 x 10^3 MPa^2 resulting in a safety factor of 5.1.
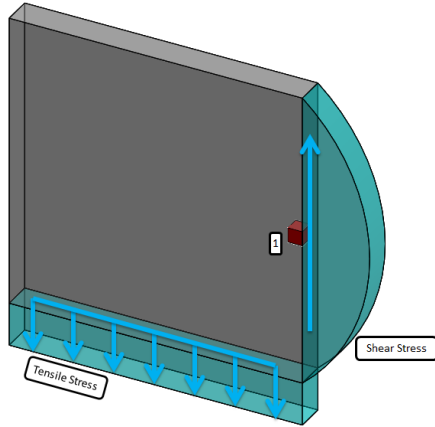
FIGURE 65 STRESS DISTRIBUTION IN HALF OF THE TOP CONNECTING PLATE (CUT SYMETRICALLY) INDICATING THE POSITION OF STRESS ANALYSIS.

The top connecting plate transfers the force from the front supports to the 17-4 PH stainless steel T-shaped top beam shown in the figure below in blue.
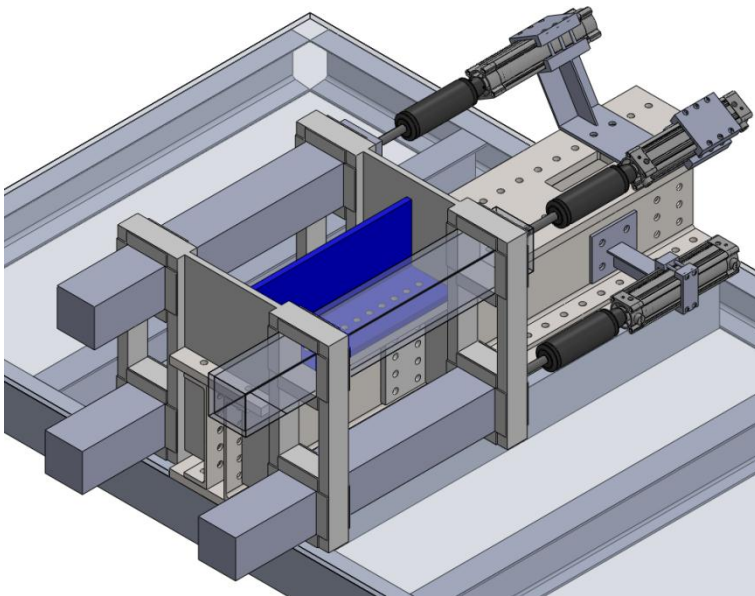
FIGURE 66 3D MODEL ILLUSTRATING THE TOP BEAM OF THE QUADRO-CAGE-CLAMP.

The beam is modelled as a cantilever beam fixed at the first row of bolts in the bolt block. The bolt block consists of twenty-six 20 mm MHP Huckbolts each capable of carrying a load of 82.5 kN [37]. The overall length of the bolt block is reduced by setting the spacing at 50 mm and in line with the existing holes in the Transom. This reduced spacing requires a new transom to be drilled to the dimensions of the bolt block. Huck 360 bolts [38] which can be installed with standard tools are inserted in the holes closest to the top connecting plate where a normal Huck bolting machine will not fit. Huckbolts are used in the assembly as it ensures the correct pre-tension in the bolt block as well as preventing vibration loosening. The resulting shear force and moment sets up a shear stress and tensile stress in the top beam with a maximum value adjacent to the bolt block. The stress in the beam, illustrated below, is calculated at position 1 at the top of the beam where the tensile stress is the greatest and at position 2 at the centre of the beam where the shear stress is the greatest. The maximum combined stress, $\sigma_{element\_Top\_Beam\_2}$ is found as 1.1×10^{6} MPa^2 resulting in a safety factor of 1.3 at position 2 in the top beam.
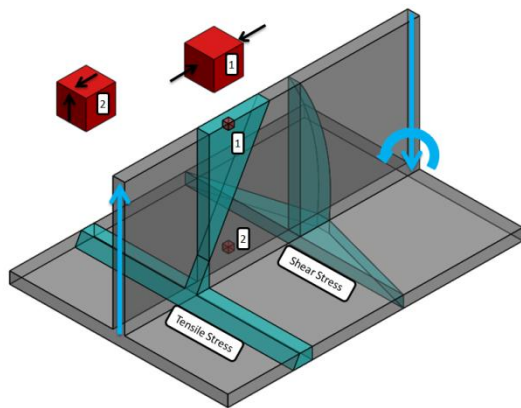
FIGURE 67 STRESS DISTRIBUTION IN THE TOP BEAM INDICATING THE POSITIONS OF STRESS ANALYSIS.

The 17-4 PH stainless steel bottom connecting plate, shown in blue below, transfers 174 kN to the bottom beam.
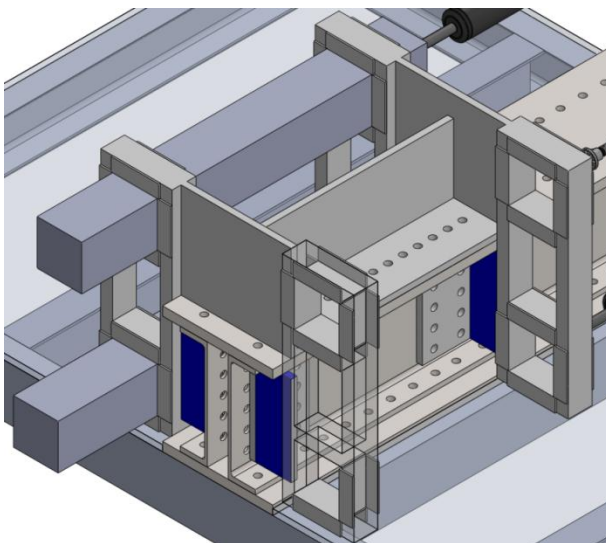
FIGURE 68 3D MODEL ILLUSTRATING THE BOTTOM CONNECTING PLATE OF THE QUADRO-CAGE-CLAMP.

The bottom connecting plate welded to the bottom beam is modelled as a cantilever beam where the force and moment reactions at the junction of the plate and bottom beam sets up a shear and tensile stress. The stress in the plate, illustrated below, is calculated at position 1 at the top of the plate where the tensile stress is the greatest and at position 2 at the centre of the plate where the shear stress is the greatest. The maximum combined stress, $\sigma_{element\_BCP\_2}$ is found as 5.7×10^3 MPa^2 resulting in a safety factor of 243 at position 2 in the bottom connecting plate. Although this beam is far stronger than it needs to be its size cannot be reduced as it needs to increase the stiffness of the bottom beam assembly to ensure the correct force distribution.
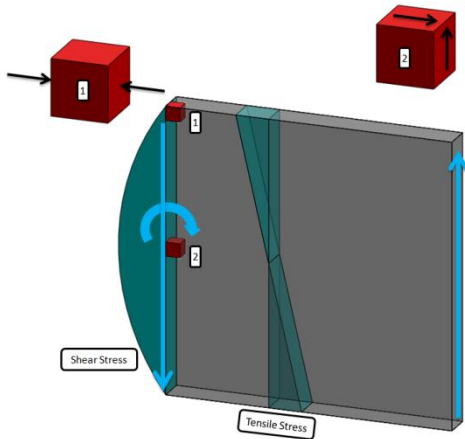
FIGURE 69 STRESS DISTRIBUTION THROUGHOUT THE BOTTOM CONNECTING PLATE INDICATING THE POSITIONS OF STRESS ANALYSIS.

The 17-4 PH stainless steel bottom beam, shown in blue below, modelled as a cantilever beam is subjected to a force and a torque transferred from the bottom connecting plate.
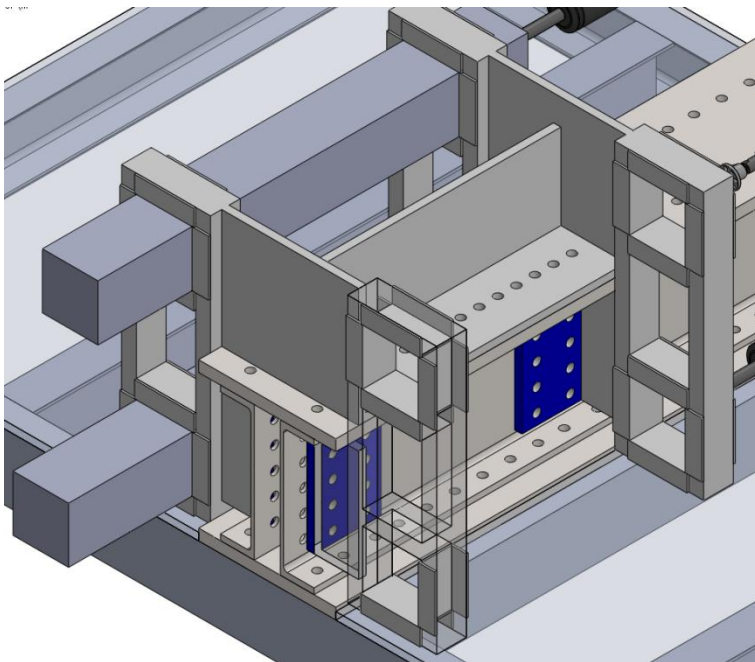
FIGURE 70 3D MODEL ILLUSTRATING THE BOTTOM BEAM OF THE QUADRO-CAGE-CLAMP.

The maximum shear force, torque and moment are obtained adjacent to the bolt block where tensile and shear stresses are set up in the beam. The Prandtl elastic membrane analogy states that the shear stress set up by torque is proportional to the slope of a membrane extending normal to the cross section of the bar subjected to the torque [39].

For a narrow rectangular cross section the stress at the short edge of the section will thus be small and it will be at its largest at the longest edge. The stress in the beam, illustrated below, is calculated at position 1 at the top of the beam where the tensile stress is the greatest and the shear stress due to the torque is small, and disregarded, as described above and at position 2 at the centre of the beam where the shear stress due to the shear force and the torque is the greatest. The maximum combined stress, $\sigma_{element\_Bottom\_Beam\_2}$ is found as 1.1×10^6 MPa^2 resulting in a safety factor of 1.3 at position 2 in the bottom beam. The bottom beam is affixed to the Transom with ten 20 mm MHP Huckbolts, more than the six required to ensure a friction joint. The decision to use ten Huckbolts of the specific size is made to keep the spacing of the bolts the same as that used on brackets already connected to the Transom. The decision to use the same size and strength of bolts was made to eliminate the possibility of mixing up the top and bottom beam bolts. Huck 360 bolts are used in the first row of the bolt block where a bolting machine cannot fit.
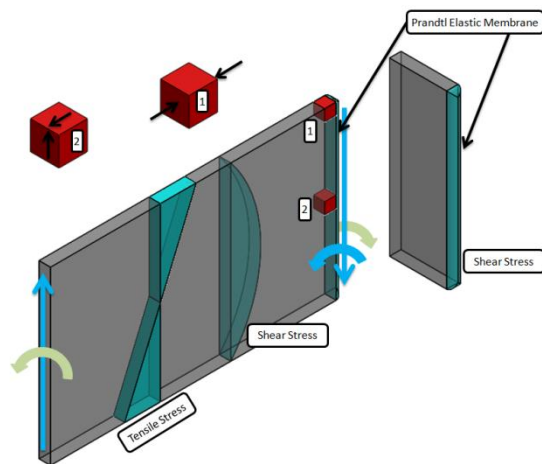
FIGURE 71 STRESS DISTRIBUTION IN THE BOTTOM BEAM INDICATING THE POSITIONS OF STRESS ANALYSIS.

The entire support fixture is manufactured from 20 mm 17-4 PH stainless steel plate to reduce the number of plate thicknesses used in the design. The height of the top connecting plate is thus flush with the top of the supports and the width of the top beam (370 mm) is the same as the width of the Transom. The height of the top beam web (250 mm) is chosen to obtain the desired stiffness ratio between the top and bottom beam. The height of the bottom beam (300 mm) is the same as that of brackets already used on the Transom.

The entire frame consisting of the supports and support fixtures are welded together and slid over the Transom during assembly of the conveyance. Because Huckbolts are used in the design for safety purposes the assembly must be done at the workshop, any damage to the device also requires a thorough examination of the conveyance at the workshop and the removal of the bolts without damaging the conveyance or arresting device structure. Because the assembly of the system must be done by the workshop the decision was taken not to split the frame such that it can be mounted to the conveyance from either side of the Transom as it would simply increase the weight and number of fasteners required in the design.

5.5. PNEUMATIC DRIVE SYSTEM
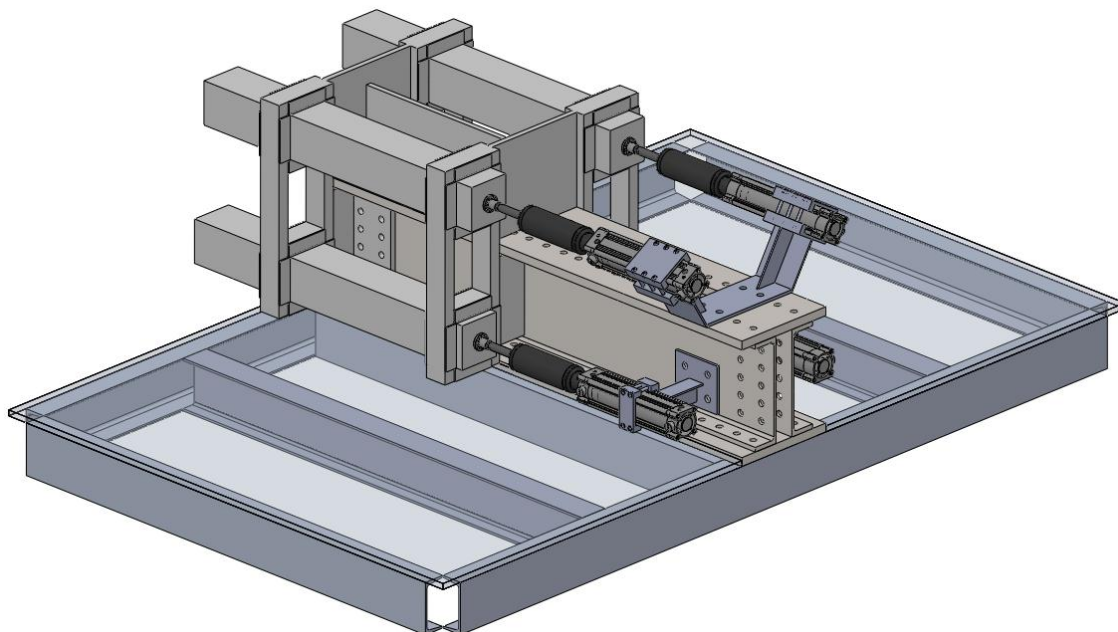
FIGURE 72 3D MODEL ILLUSTRATING THE PNEUMATIC DRIVE SYSTEM OF THE QUADRO-CAGE-CLAMP.

Numerous methods exist to actuate the clamp beams. It was decided to make use of a pneumatically actuated system as it is possible to rapidly charge the system when docked on a station. The clamp beams are actuated through 80 mm pneumatic cylinders with strokes of 300 mm. By using standard components from Festo the cost is reduced and the reliability improved. A standard DSBC cylinder [40] with end position locking and an extended piston rod is selected. The extended cylinder rod allows a bellow to be installed over the piston rod protecting the cylinder from water, dust and debris improving the reliability in the harsh shaft environment. The end locking on the cylinder works at both the extended and retracted position. Applying air pressure to the cylinder in either direction lifts the end of position spring applied pawls out of their seat on the piston rod and allows the piston to move. Should a failure of air pressure occur while the cylinder is extended or retracted the spring applied pawl engages with the piston rod and prevents it from moving, the rod can only be moved by resupplying the air pressure or through manually retracting the pawl. This feature improves the system safety by preventing movement of the cylinder should an air pressure failure occur while the conveyance is docked.

The cylinder is further fitted with PPV cushioning. This cushioning works at the end of travel to prevent the cylinder coming to a harsh stop and damaging the piston, cylinder housing or attached equipment. The PPV cushioning controls the exhaust rate of the air and is adjustable through a set screw. The release rate is set to the desired value during testing of the system at the workshop. Using a slightly oversize cylinder allows the cylinder to still actuate the beams even if the supply pressure is slightly lower than normal and ensures that the system remains functional even when the sliding friction increase due to dust or dirt. Using standard cylinders rated to 6 bar ensures that the cylinder will be safe from rupture under working pressures. The cylinder is affixed to the clamp beam using a standard flange mounting.

A 10 litre standard Festo reservoir [41] pressurised to 400 kPa will be used to power the two 1.5 l top clamp beam cylinders when the conveyance approaches and departs from the station. The 10 l reservoir ensures that the pressure in the cylinders will not fall beneath 300 kPa during its stroke. As the conveyance approach the station an electromagnet is activated in the shaft through the signal given by the onsetter opening a magnetic switch in the power circuit from the battery installed on the conveyance roof to trigger the solenoid connected to the 5/3-way valve connected to the top two cylinders. The solenoid pulls the valve out of its blocked position (Position 2) into position 1 and opens the pressure line between the reservoir and the back of the cylinder to extend it. The conveyance with the extended clamp beam now settles on the supporting steelwork where a pneumatic connection and data linkage is made. The air supply from the station passes through a pneumatic service unit where it is filtered, dried and lubricated before passing through to the pneumatic connection where it is blocked by a check valve when not connected to the conveyance. As the conveyance settles onto the pneumatic connection the check valve on the station is opened and air passes into the reservoir through the check valve connected to the reservoir installed to keep it pressurised during travel. When the clamp beam settles onto the steelwork the data linkage closes an electric bridge which triggers the solenoid on the bottom clamp beams to extend the cylinder now powered with air from the station. With all the cylinders extended the conveyance is safely docked.

When releasing the conveyance the solenoid on the bottom cylinders is triggered into position 3 to supply air to the annulus side of the cylinder to retract the beams. Upon complete return of the clamp beam the valve return to the neutral position 2 where it is blocked in all directions. As the conveyance moves away the top valve is switched to position 3 to retract the cylinders connected to the top beams. When the proximity switch fitted in the slot provided for it in the cylinder housing indicates that the cylinders are fully retracted the valve is returned to the neutral position 2 where all ports are blocked. To ensure that the top beams are fully retracted before the conveyance passes the next Bunton the proximity switch is also connected to a transmitter that will activate when the cylinder is fully retracted. If the electromagnet positioned in the shaft detects the conveyance but not the signal from the transmitter the winder is tripped. The conveyance will need to be lowered back to the station and investigated why the beams failed to retract. A 5/3-way valve is used instead of a normal 3/2-way valve in order to switch the pressure line from the reservoir to a neutral blocked position during travel. Blocking the pressure line with a valve is better than having the pressure line connected to the annulus side of the piston as the leakage will be less and the volume of air required in the reservoir reduced. The pneumatic power circuit allows effective and simple control over the device using solenoids and affords the opportunity to store energy for use at the next station. The system is considered more robust and lighter than a motor circuit requiring battery packs and gearing. The pneumatic circuit drawn using FluidDraw S5 [42] for the device is provided below.

FIGURE 73 DIAGRAMATIC ILLUSTRATION OF THE PNEUMATIC CIRCUIT OF THE QUADRO-CAGE-CLAMP USING STANDARD PNEUMATIC SYMBOLS.

5.6.   PNEUMATIC CYLINDER MOUNTS

The pneumatically actuated Quadro-cage-clamp makes use of four cylinders connected to the four clamp beams. In order to secure the cylinders a top cylinder mount as illustrated below in blue is used to secure the two top cylinders.

FIGURE 74 3D MODEL ILLUSTRATING THE TOP CYLINDER MOUNT OF THE QUADRO-CAGE-CLAMP.

The cylinders line up with the centre of the clamp beams and a bracket is required to maintain the cylinders fixed on this line. Various mounting devices are available from Festo most mounting to the rear end of the cylinder. One standard cylinder mounting however allows mounting around the cylinder body and based on that design the top support bracket is developed. The bracket is 157 mm wide in order to allow two rows of Huckbolts to be fitted when mounting to the Transom offering better resistance to bending compared to a single row. The bracket shaped as a T-section has a wide flange to handle the maximum force exerted by the cylinder. The shear stress in the bracket will be a maximum at the centre of the bracket flange and the tensile stress maximum at the outer edge of the bracket flange at the point where the bracket is mounted to the Transom. At the maximum operating pressure of the cylinder the bracket constructed from 6061-T6 Aluminium has a safety factor of 43 against shear failure and 17 against tensile failure. The web and flange thickness is 6 mm to match the thickness of the bottom bracket reducing the various thickness sheets required. The bracket is more than adequately strong to support the 5.5 kg cylinder with safety factors exceeding 400 in the vertical direction. The decision to use 6061-T6 Aluminium is based on the lower weight of Aluminium and its corrosion resistant properties in a wet shaft. It is further a common material used in the construction of the cage shell. Illustrated below is a model of the top clamp bracket used to secure the top cylinders when they are clamped using a clamp cap.
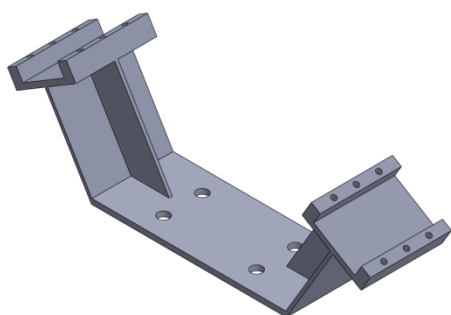
FIGURE 75 3D MODEL OF THE TOP CYLINDER MOUNT USED IN THE QUADRO-CAGE-CLAMP.

The bottom cylinders are positioned next to the Transom and a straight mounting bracket can be used to secure them. The mounting bracket used to secure the bottom cylinders ensuring they line up properly with the clamp beams are shown below in blue.
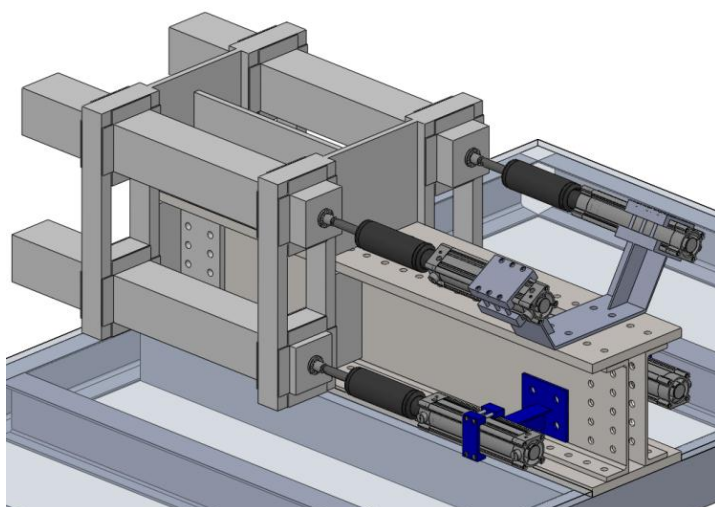
FIGURE 76 3D MODEL ILLUSTRATING THE BOTTOM CYLINDER MOUNT OF THE QUADRO-CAGE-CLAMP.

The bottom mounting cylinders consist of a straight T-section beam extending from the Transom side to the bottom cylinders. Because there is no existing holes in the side of the Transom a narrower beam section can be used to secure the bracket in comparison to the top cylinder mount that requires a mounting plate wide enough to fit bolts at the existing Transom holes. The bottom cylinder mount is therefore constructed from 6 mm 6061-T6 Aluminium sheet sections. The height of both the flange and web is 60 mm. These dimensions are based on the geometry of the clamp section required to fit about the cylinder body while ensuring proper clearance between the two M10 cylinder securing bolts. Stresses in the bracket is considered at four positions. The bracket will be subjected to the maximum force of the cylinder if the clamp beams jam for some reason. Under this assumption the cylinder force at the maximum mine pressure of 4.5 bar is considered. The maximum shear stress found at the centre of the bracket flange next to the fixed end of the cantilever beam is 10 MPa resulting in a factor of safety of 15 at this point. The maximum tensile stress due to the cylinder force is found at the edge of the flange next to the fixed end of the cantiler beam as 128 MPa resulting in a factor of safety of 2.2. This factor of safety is below the safety factor of 10 used in the rest of the design but is more than adequate considering the application. The cylinder mounting is not a direct load carrying component on which the safe suspension of the cage depends and is not exposed to extreme shock loads. Should the bracket fail while the cage is locked it will not influence the secure suspension of the conveyance. The bracket will further only be subjected to this maximum force should the mine operate at its maximum pressure and the clamp beams jam completely. Apart from the above mentioned points the bracket is found to have a safety factor of 1.6 when the pressure in the cylinder reaches the maximum rated capacity of the cylinder. The bracket is further more than adequately sized to carry the weight of the cylinder with safety factors in excess of 165 in the vertical direction. The bottom cylinder mounting bracket is illustrated below. Appendix H provides the detailed calculations of the clamp beams.
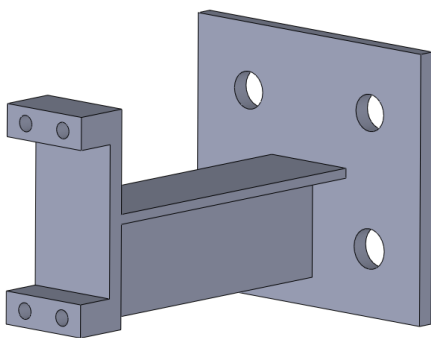
FIGURE 77 3D MODEL OF THE BOTTOM CYLINDER MOUNTING OF THE QUADRO-CAGE-CLAMP.

5.7.   DESIGN SUMMARY

Throughout this section the various components making up the Quadro-cage-clamp was considered. A decision was made to use a box shape clamp beam in order to reduce the weight of the beams. The support frame for the clamp beams are fitted with ToughMet liners to reduce friction and wear during the operation of the system. The Quadro-cage-clamp is mounted directly to the Transom in order to reduce any bending of the Transom and greatly reduces the forces on the Transom compared to a rear mounted arrangement. The entire load carrying portion of the system is made from 17-4 PH stainless steel due to its high strength and corrosion resistance to deliver a safety factor throughout the device in excess of 10 as is required of cage arresting devices. The system is affixed to the Transom using vibration resistant Huckbolts of the same size and strength to eliminate the possibility of incorrect application. The clamp beams of the system are actuated through a pneumatic system consisting of four cylinders powered either from the conveyance mounted reservoir or the station supplied compressed air. These cylinders are securely attached to the Transom through 6061-T6 Aluminium mounting brackets adequately sized to withstand the force applied when a cylinder pushes against a jammed clamp beam at a supplied air pressure equal to the maximum rated capacity of the cylinder. The conventional calculations contained in Appendix C through to Appendix H indicate an adequately sized device with the results verified in the next section.

CHAPTER 6.   FINITE ELEMENT ANALYSIS

Solidworks is a powerful computer aided design (CAD) software package used extensively in this project. The program's primary function is the three dimensional modelling of components and assemblies but it also provides valuable analysis capabilities.

6.1.   CLAMP BEAM

To assure that the design is of adequate strength the system and its components are subjected to Finite Element Analysis (FEA) using Solidworks-Simulation. The clamp beam is modelled as a simply supported beam with joints placed at the support positions and the position where the force will act. Modelling the beam in this manner simplifies the model greatly. The clamp beam is first modelled by selecting the option to model the part as a beam. A custom material is defined with the properties of 17-4 PH with H900 heat treatment and applied to the model before analysis. The joints at the support positions are restrained from movement and a force of 883 kN applied at the end of the beam. The analysis delivered reaction forces of 1235 kN and 352 kN which is in agreement with the calculated values in section 5.1. The results of the analysis are shown below.
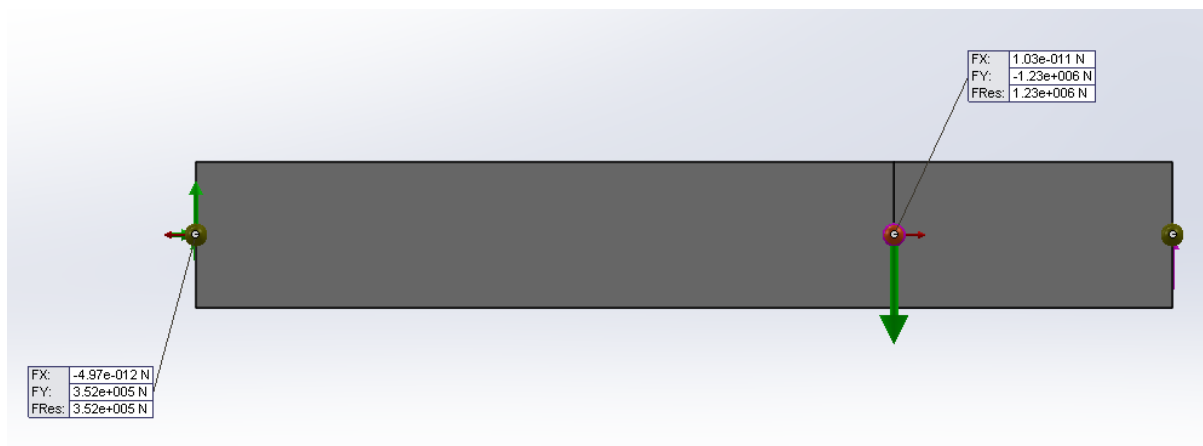
FIGURE 78 SIDE VIEW OF THE CLAMP BEAM ILLUSTRATING THE REACTION FORCES

The stress throughout the clamp beam when modelled as a beam is shown in the image below. In this modelling method the average stress is calculated through a cross section and does not vary across the section. The maximum stress is indicated at the beam perimeter where the front support reaction works with axial and bending stress equal to 976 MPa the same as the 976 MPa obtained through calculation.
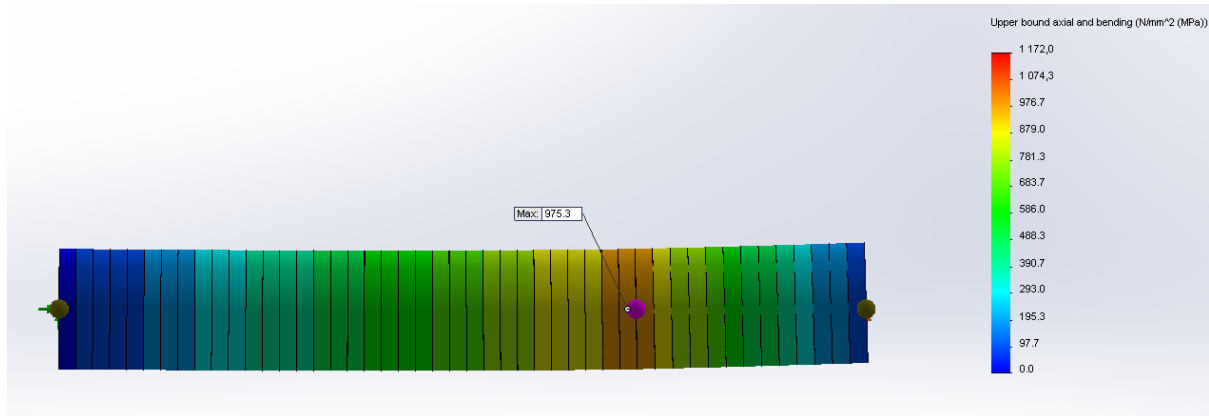
FIGURE 79 STRESS DISTRIBUTION THROUGHOUT THE CLAMP BEAM WHEN MODELLED AS A BEAM.

Modelling the beam as a solid delivers slightly different results. The force acting over the beam shown in purple acts over the 166 mm width of the Bunton on which it rests. The Front support works in as a distributed load over the 80 mm support width with a reaction force of 1147kN while the rear support has a reaction force of 264 kN. Due to the distributed loads the forces on the clamp beam is slightly smaller.

FIGURE 80 SIDE VIEW OF THE CLAMP BEAM ILLUSTRATING THE REACTION FORCE ON THE FRONT SUPPORT WHEN MODELLED AS A SOLID.

FIGURE 81 SIDE VIEW OF THE CLAMP BEAM ILLUSTRATING THE REACTION FORCE ON THE REAR SUPPORT WHEN MODELLED AS A SOLID.

Modelling the beam as a solid calculates the stress along the entire beam length at all the different positions on the cross sections. From the figure below it is shown that the maximum stress of 1.18×10^3 MPa occurs next to the front support, as expected, and is in agreement with the 1.13×10^3 MPa calculated in section 5.1.
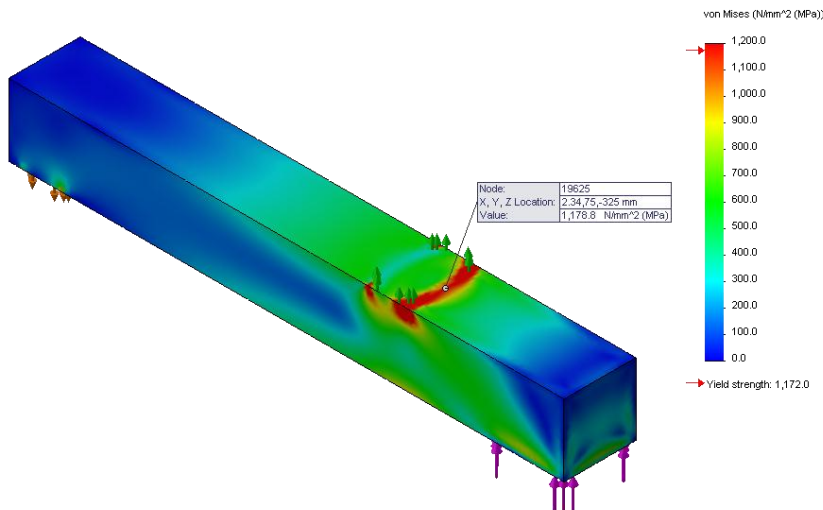
FIGURE 82 STRESS DISTRIBUTION THROUGHOUT THE CLAMP BEAM WHEN MODELLED AS A SOLID.

In this section the calculated and modelled results corresponded well and are attributed to the simplicity of the design. The constant cross section and fair assumption to calculate the forces as concentrated loads allowed the beam to be calculated using basic mechanics of materials principles with good results.

6.2.   SUPPORT STRUCTURE

The support structure was modelled by constraining the area where the bottom connecting plate attaches to the support and applying the 1235kN, calculated from the clamp beam, to the top beam of the support. A force of 1061 kN is applied to the area where the top connecting plate attaches to the support. The resultant of these forces found from the simulation is 174 kN on the bottom beam connection plate as illustrated in the figure below.
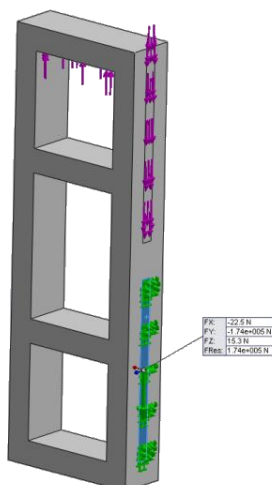
FIGURE 83 3D MODEL OF THE SUPPORT FRAME ILLUSTRATING THE REACTION FORCE ON THE BOTTOM CONNECTING PLATE.

Subjecting the beam to these loads causes a stress throughout the support load carrying beam and legs. In section 5.2 the force and moment distribution was calculated and the stress induced determined. The positions of critical stress were identified in the top load carrying beam adjacent to the leg junction at the bottom face with a calculated stress of 771 MPa. The second position of critical stress is on the inner surface of the support legs where the legs are subjected to the combined tensile stress of the pull on the leg and the moment resisting rotation of the load bearing beam. The stress at this position is calculated as 965 MPa. When considering the top section of the support shown in figure 84 below it can be seen that the stress obtained from simulation at the junction of the load carrying beam and the support leg is calculated as 681 MPa and 917 MPa on the inner surface of the support legs.
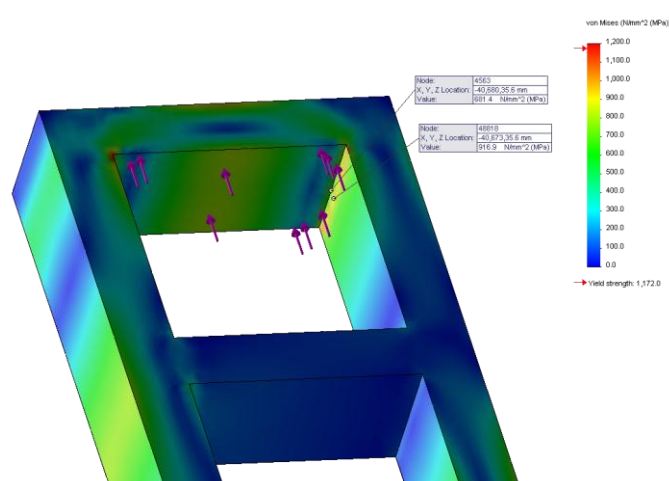
FIGURE 84 3D MODEL OF THE STRESS DISTRIBUTION IN THE TOP PORTION OF THE SUPPORT FRAME.

Comparison between the conventionally calculated and simulated values of stress shows that the stress predicted in the load carrying beam is approximately 12% less than that predicted by conventional calculation and 5% in the leg section. The difference in stress is attributed to the assumption made in the conventional calculation of the stresses in the support frame.

During the conventional calculations the load carrying beam is assumed to be a beam clamped at both ends to resist rotation resulting in a larger moment being obtained than the simulation which allows rotation of the beam ends with a resulting lower moment. In both cases the vertical force, creating a shear force in the beam and a tensile force in the legs, remains the same. The lower moment will have a more pronounced influence on the beam stress as the stress calculated at the surface of the beam is completely due to the moment size explaining the larger discrepancy in values. The stress in the leg section relies both on the magnitude of the tensile force and the moment and therefore a different moment will have a smaller effect on the value explaining the smaller discrepancy. The difference in values and stress distribution between the two cases is illustrated below where figure 85 shows the legs assumed rigid, as was done in the conventional calculations and figure 86 shows the legs deformable.
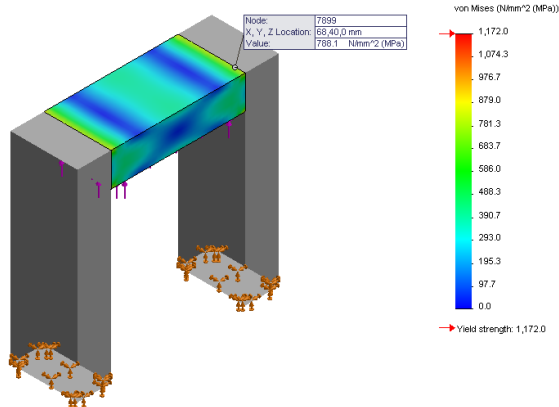
FIGURE 85 3D STRESS DISTRIBUTION THROUGHOUT THE TOP BEAM OF THE SUPPORT FRAME WITH THE SUPPORT FRAME LEGS ASSUMED RIGID.
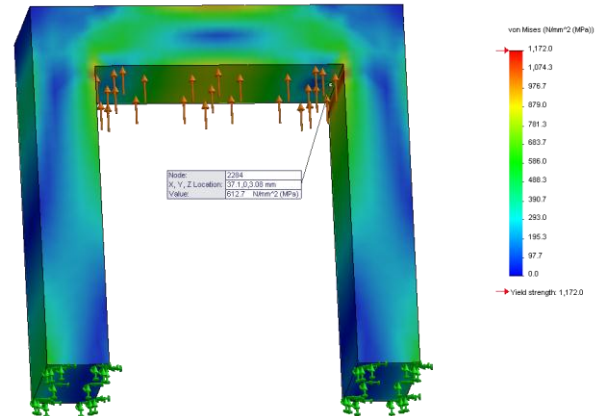
FIGURE 86 3D STRESS DISTRIBUTION THROUGHOUT THE TOP BEAM OF THE SUPPORT FRAME WITH THE SUPPORT FRAME LEGS ASSUMED DEFORMABLE.
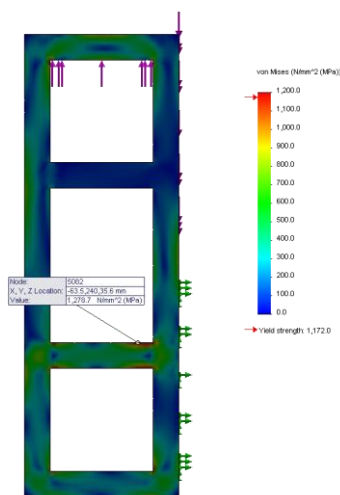
FIGURE 87 3D STRESS DISTRIBUTIONTHROUGHOUT THE SUPPORT FRAME WHEN SUBJECTED TO A LOAD TEN TIMES THE LOAD PRESCRIBED ON THE WINDER PERMIT.
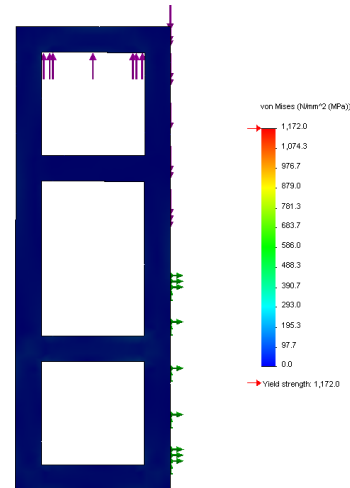
FIGURE 88 3D STRESS DISTRIBUTION THROUGHOUT THE SUPPORT FRAME WHEN SUBJECTED TO THE LOAD PRESCRIBED ON THE WINDER PERMIT.

Above the stress distribution for the entire support frame is shown and illustrates that the frame is far below the yield stress when subjected to a force 10 times greater than the allowed conveyance mass. The stress does however exceed the limit at the corners where stress concentrations occur and where the beams tend to bend relative to the support legs when loaded. Considering that the stress is only slightly above the yield stress and that a factor of safety of ten is applied the design is considered safe. The figure on the right illustrates the stress when the system is simply supporting the allowed load where it can be seen that the entire frame is blue far below the yield strength of the material indicated with a red arrow. The stresses calculated through conventional methods and simulations indicate an adequately strong design.

6.3. COMPLETE SYSTEM

The conveyance arresting device consists of an assembly of components the most important of which were analysed using conventional and computer calculation tools. The entire load carrying portion of the device is subjected to the applied load in this section to illustrate how the stresses are distributed throughout the system. The model must represent reality and the clamp beam, support and fixtures are assigned the material properties of 17-4 PH stainless steel. The clamps are extended to their full position where the load of 883 kN is applied; ten times the load required to suspend the maximally loaded conveyance. The load is transferred through the beam to the front and rear support frame as discussed earlier. The forces on the support frame are transferred to the Transom through the support fixtures connected by bolts. In order to simulate the effect these bolts have, each hole through which a bolt fit is given a split line consisting of a circle around the hole. This split line and the internal surface of the bolt hole is constrained in Solidworks to prevent the assembly moving at those locations. Internal forces works throughout the system to transfer the force from the applied position at the end of the clamp beam, over an area equal to the supporting Bunton width, to the bolt holes where the loads are transferred to the Transom which ultimately carries the conveyance load. The first figure provided below illustrates the stress distribution throughout the assembly when the load is applied to the top clamp beams simulating the conveyance settling onto the Bunton. On the right hand side of the figure the stress distribution colour chart is presented where the yield stress of the material is indicated.
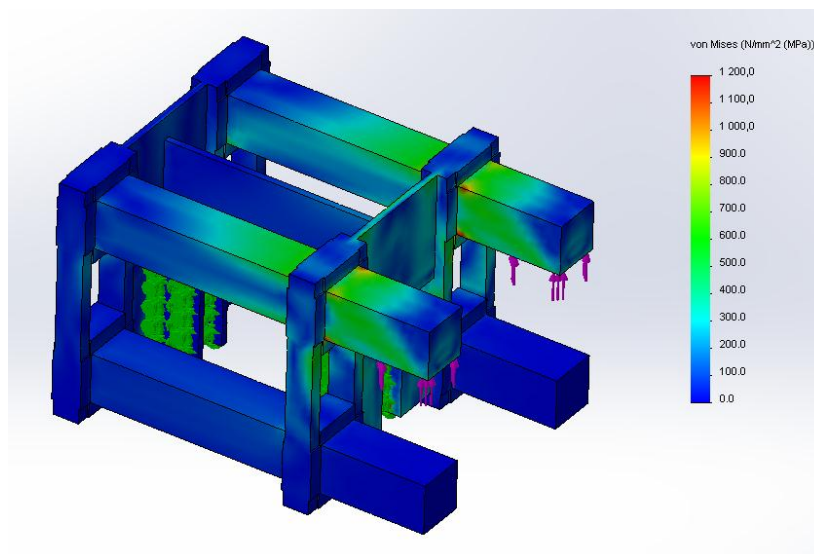
FIGURE 89 3D STRESS DISTRIBUTION THROUGH THE QUADRO-CAGE-CLAMP.

From the illustration above the applied forces can be seen in purple and the constraints in green. The stress colours show that the system only have a few highly stressed regions. These heavily stressed regions are found where the clamp beams transfer load to the front supports and where the support fixture transfers loads to the first row of bolts. The red regions on the clamp beam slightly exceed the yield stress when a load ten times larger than what is allowed for on the winder permit is applied. The simulation shows that the system is of adequate strength with safety factors in excess of 10 for all the regions highlighted blue, green, yellow and most of the red.

The clamp beam and support fixture still have a factor of safety in excess of 7 at the highly stressed red locations which is mostly due to stress concentrations and contact forces. Providing fillets and properly sized washers is important in these regions. The two images below illustrate the system from different angles where the leftmost figure provides a view to the top of the system and the rightmost figure the system seen in line with the clamps. These figures illustrate that the stresses in the support fixtures are well below the yield limit.
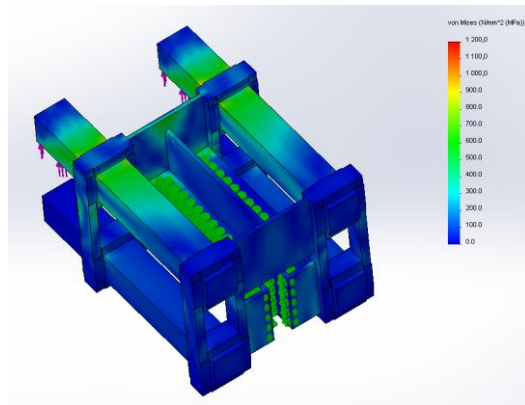
FIGURE 90 3D MODEL VIEWED FROM THE TOP SHOWING THE STRESS DISTRIBUTION THROUGHOUT THE QUADRO-CAGE-CLAMP.
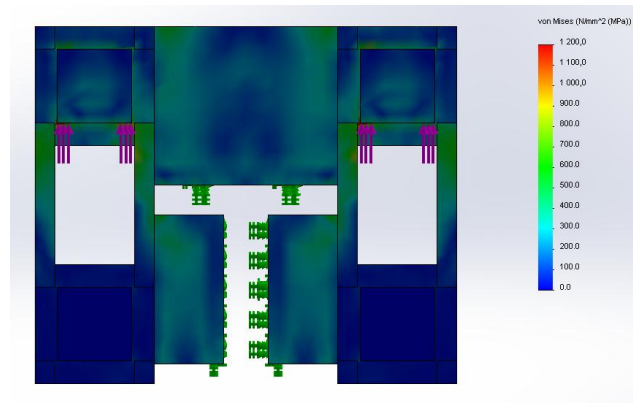
FIGURE 91 MODEL OF THE STRESS DISTRIBUTION THROUGHOUT THE QUADRO-CAGE-CLAMP WHEN LOOKING FROM THE BUNTON.

Having shown that the system is of adequate strength when loaded on the top beams it is also important to show that the system does not deform excessively. The figure below illustrates the deflection of the system when the top beams are loaded. The greatest deflection is found in the cantilever portion of the clamp beam. Due to the length by which the beam must extend a great moment arm is created resulting in deflection. A maximum deflection of 8 mm is calculated when the fully extended beam is loaded and given the size of the entire assembly and noting that an absolutely precise alignment is not a requirement the deflection is seen as allowable. The material is far from yield such that the beam will not permanently deform. Considering further that the deflection when loaded to the allowable conveyance mass is around 1 mm the beam is considered rigid enough.
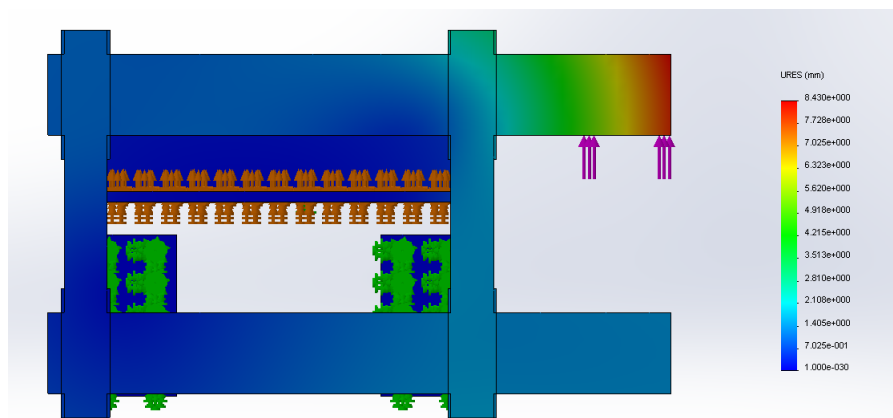
FIGURE 92 SIDE VIEW OF THE QUADRO-CAGE-CLAMP ILLUSTRATING THE SYSTEM DEFLECTIONS.

Throughout the dissertation loading on the top beam has been considered and discussed. The load on the bottom beam isn't of concern because the device will never be exposed to such a great stress as the Winder's slack/tight rope safety device will trip the winder before such a force is generated. The support frame and fixtures are also of the same strength and is able to handle the load should it be applied. The support legs are further subjected to tensile stress when the bottom beam is loaded in contrast to compression stress when the top beam is loaded making it more suitable for load carrying. To illustrate this adequacy of strength the modelled result of the system when subjected to a load on the bottom beam is provided below.
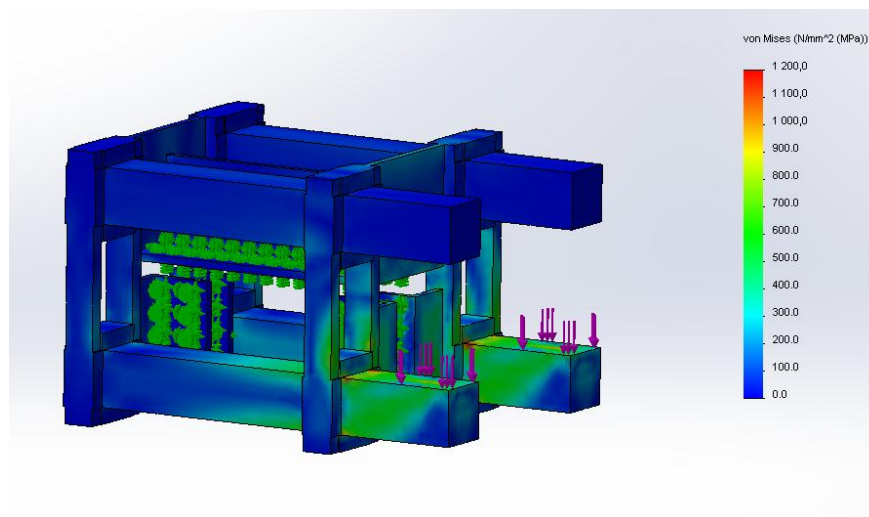
FIGURE 93 3D MODEL SHOWING THE STRESS DISTRIBUTION THROUGHOUT THE QUADRO-CAGE-CLAMP WITH THE BOTTOM CLAMP BEAMS LOADED.

The above figure illustrates that the system is of more than adequate strength when loaded on the bottom beams. The stresses throughout the system are less and a few regions of green can be seen no more than 70% towards the yield strength. The only areas of concern are the contact points on the beam and the front support similar to the top loading condition. Below two more figures are provided to show that the stresses in the support fixtures are within an allowable range. The top figure shows the system from above and the bottom figure the system when viewed in line with the beams.
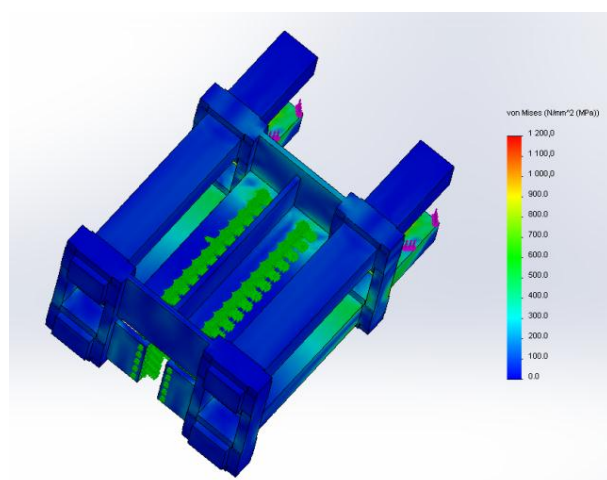
FIGURE 94 3D MODEL VIEWED FROM THE TOP SHOWING THE STRESS DISTRIBUTION THROUGHOUT THE QUADRO-CAGE-CLAMP WITH THE BOTTOM CLAMP BEAMS LOADED.
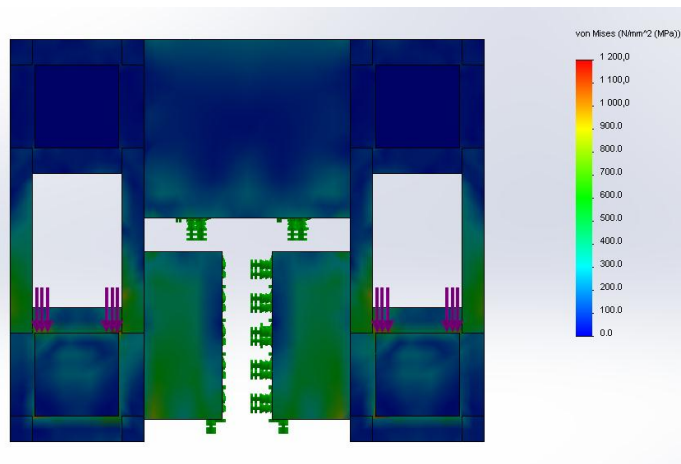
FIGURE 95 ILLUSTRATION OF THE STRESS DISTRIBUTION THROUGHOUT THE QUADRO-CAGE-CLAMP WHEN LOOKING FROM THE BUNTON WITH THE BOTTOM CLAMP BEAMS LOADED.

When defining a material in Solidworks the density of the material is included that allows the program to compute the mass of a component or assembly. In the assembly the mass of the liners made from ToughMet, with a density of 9000 kg/m^3 [36], and the system components made from 17-4 PH, with a density of 7800 kg/m^3 [33], are calculated and summed to obtain a total system mass of 637 kg from the mass properties tab. This mass excludes the cylinders but already constitutes a heavy design.

6.4.   CRITICAL STRESSES SUMMARY

To ensure an adequately strong design conventional and FEA calculations were performed on the Quadro-cage-clamp and five critical areas of stress were identified. The first critical stress is found in the clamp beam at the point where the force is transferred to the support structure. Due to the simple cross section and good slenderness ratio of the beam the conventional and FEA result is exactly the same with the maximum stress on the outer boundary of the beam.

The support structure has two areas of critical stress the first being at the edge of the top beam portion of the support where the force from the clamp beam is transferred to the support structure. Here it can be seen that the stress calculated from the FEA is 88% in agreement with that of the conventional calculation. The difference is due to the assumption made in the conventional calculation that the beam is fixed at its ends and therefore subject to a large moment at the beam ends whereas the FEA considers the deformability of the support legs which allows some rotation of the beam and an associated lower moment as explained in sub-section 6.4. The juncture of the support leg and the beam was found as a second critical stress with the conventional and FEA results agreeing 95%. This lower discrepancy in results are due to the lesser impact a reduced moment has on the stress in the legs because of the presence of a large tensile stress as explained in sub-section 6.4

The fourth critical stress in the system was found in the top T-beam transferring the forces from the support structure to the Transom. The critical stress is predicted from conventional calculation to be a shear stress located on the beam neutral axis above the first row of bolts. The FEA result for the T-beam is in agreement with the stress distribution predicted by conventional calculation but is found to be 21% less. The reason for this discrepancy is due to the fact that Solidworks-Simulation makes use of Timoshenko beam theory whereas the conventional calculations were performed using Euler-Bernoulli beam theory. Solidworks-Simulation therefore calculates transverse shear stress according to the formula below.

$$\tau = \frac{V}{(SF)(A)}$$

Where

τ = Shear stress [Pascal]

V = Shear force [Newton]

SF = Shear Factor; typically 0.84 for a short rectangular beam
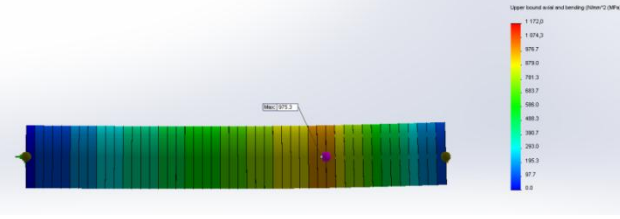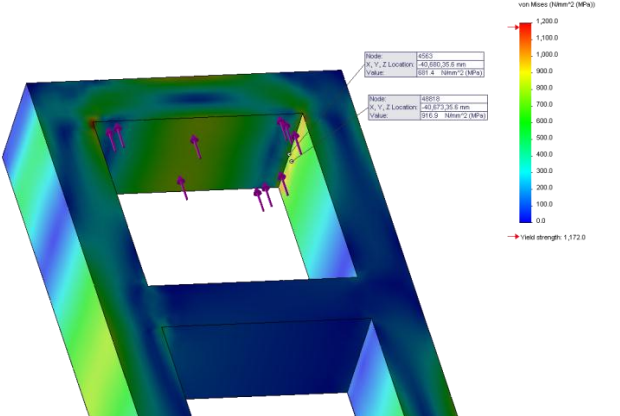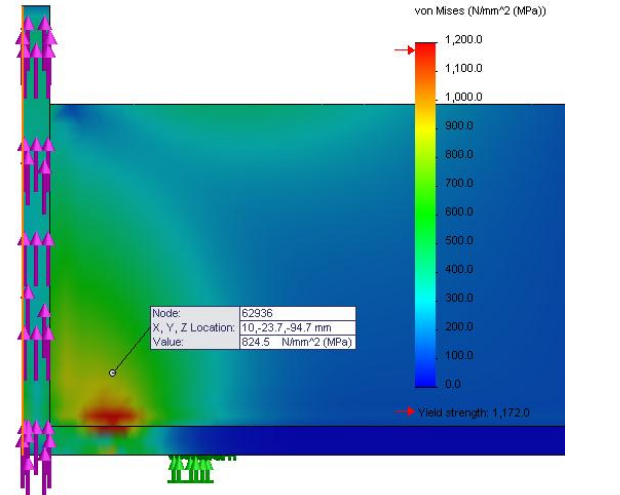
A = Cross sectional area [meters squared]

Due to the short length of the beam from the loaded end to the assumed clamped end the Euler-Bernoulli theory will deliver a shear value approximately 80% larger than that predicted by the Timoshenko theory. This approximate 80% can be found by comparing the shear stress predicted by conventional calculation, $\tau = \frac{1.5\,V}{A}$ with that predicted by Timoshenko, $\tau \cong \frac{1.2\,V}{A}$, for a rectangular cross section. Considering the difference in calculation methods the agreement of 79% between conventional calculation and FEA is satisfactory.

These critical stresses are tabulated below in order to compare the FEA result with the conventional calculations. Conventional calculations further predict a fifth critical stress in the bottom beam transferring load to the Transom. This stress is however far from that predicted by the FEA and is due to the overestimation of the shear stress caused by torque on the bottom beam. The accurate calculation of stress due to torque in a narrow rectangular section is compromised due to the complexity thereof. The overestimated as well as the assumed more accurate FEA result however indicates that the bottom beam is of adequate strength. A refined review of the complex conventional calculation is however discouraged as it won't change the outcome of the next chapter. All considered the conventional and FEA results even though not always as close as would be preferred suggest that the Quadro-cage-clamp is of sufficient strength.

TABLE 12 COMPARISON BETWEEN CONVENTIONAL CALCULATIONS AND FEA RESULTS AT LOCATIONS OF CRITICAL STRESS IN THE QUADRO-CAGE-CLAMP.

	Description	Conventional calculation	Finite Element Analysis	% Agreement
		MPa	MPa	%
	Clamp beam	975	975	100
	Top beam of the support structure	771	681	88
	Leg juncture of the support structure	965	917	95
	Top securing beam	1045	825	79

CHAPTER 7. DISCUSSION

This dissertation focused on searching for a solution to the problem of a conveyance being misaligned and capable of moving relative to a station during loading and unloading operations. No suitable solution existed and a formal design process ensued. Product design requirements were identified and grouped into 16 classes through the application of the objectives tree and functional analysis methods. The process progressed to generate 9 concepts through the application of 6 concept generation tools namely, brainstorming, Synectics, TRIZ, 2500 engineering principles, mechanical sourcebooks and a morphological chart. The tools all delivered valuable principle solutions with brainstorming contributing the most. The morphological chart is a powerful tool to combine the principle solutions into promising concepts.

Screening reduced the 9 concepts to 4 concepts that were passed to the embodiment stage. One concept was selected after applying an evaluation technique to the 4 concepts and the concept further developed by subjecting it to conventional calculations and simulations.

During the conventional calculations three important design decisions were made. A solid and a box beam section were considered for the clamp beam and the box beam selected based on its better stress distribution and lower weight. Consideration was given to mounting the system on various positions on the conveyance roof. It was decided to affix the support structure directly to the conveyance Transom with clamp beams extending on both sides of the Transom in order to eliminate moments on the Transom. This decision simplified the design and added certainty to the calculations by simplifying the load distribution and stresses. Various methods exist to actuate the clamp beams and a pneumatic solution was selected. Using pneumatics allows readily available energy to be used and adds more reliability to the device operating in a wet environment. Deciding against a motor and battery system removes the weight of a large battery installation and the danger of damaging water ingress to motors. It is further important to review how the final design complies with the product design requirement groups identified earlier to ultimately judge its suitability for the application.

The design geometry is found satisfactory as it is completely constrained within the bounds of the shaft compartment and does not obstruct the entrance to the conveyance. The system geometry however requires some modifications to the conveyance. The first and most critical change required to the conveyance is the repositioning and addition of holes to the Transom. The device is installed beneath the dolly wheel mounting surfaces requiring the dolly wheels to be raised above the system. The height of the system above the Transom requires the draw bar of the conveyance to be elongated and some modifications will be required to accommodate the shaft examination canopy frequently installed on the conveyance roof. The conveyance slinging brackets will also need to be moved as the system covers the openings through which they pass. Apart from the danger of overrun clearance in the headgear the changes to the conveyance are all surmountable.

The forces applied to the system were multiplied to ensure that the system was designed to a factor of safety of 10. Conventional calculations and Solidworks simulation indicated that the design is of adequate strength to resist the applied forces and maintain a satisfactory factor of safety. Special materials were selected and used in the design primarily to reduce the weight of the system.

A precipitation hardened stainless steel is used in the majority of the design because of its high strength, wear and corrosion resistance. ToughMet is also used because of its high strength and low friction coefficient to reduce wear on components. Both these materials are commercially available as plate. Cylinder mounts constructed from 6061-T6 Aluminium because of its lower weight and corrosion resistant properties are used to secure the cylinders in line with the clamp beams.

The primary goal of safety is achieved through dedicated design considerations. The design completely removes the onsetter from the line of fire unlike some current systems. It is interconnected with the existing lock bell system to ensure that the system is used as intended. The device incorporates features such as end of position locking and position sensors to prevent the system from releasing during engagement or from moving away from a station with extended clamp beams. To minimise the likelihood of interference with the system it is positioned on the conveyance roof out of reach of persons except during maintenance and examinations.

Production of the system is simplified through a design free of complex shapes. The device can be manufactured completely from commercially available plate cut to the correct size and welded together. The pneumatic circuit consists of standard components all available from a single manufacturer to ease resourcing and troubleshooting. The system assembly is however more complex and must be performed in a workshop environment. The entire frame is manufactured beforehand and simply slid over the Transom after which it is connected using Huckbolts. After installation of the support structure the components are simply slid into place and connected using standard fasteners. The symmetrical design ensures stable transport with a chain block and all weights are below the capacity of the smallest chain block available eliminating the possibility of using an undersized chain block. Once installed on the conveyance the system is simply transported with the conveyance.

Simple and robust design with exotic materials ensures a design suitable for use in a shaft environment. The design is very similar to current systems and does not require extensive retraining or changes in operating environment. The device eases the work of the onsetter by eliminating the need to either insert a hook beneath the conveyance or connecting an air hose and only requires the use of buttons and monitoring of indication lights. The device is compatible with all shaft operations and only requires a little extra time for maintenance and examinations.

Development cost was kept to a minimum through conventional calculations and computer simulation. The cost associated with the manufacture of the design was not calculated but is perceived to be expensive. The cost of the device will be high due to the exotic materials employed and the specialist welding skill required.

Kinematic considerations require the control of speed into the engagement position and the secure docking of the conveyance. Approach and departing speed is still controlled by the WED while positive and secure docking is assured by the design capable of withstanding overload conditions. The ability to store pneumatic energy ensures that the device is usable at all stations. The system is considered more ergonomical as the onsetter does not need to change his way of doing by a great deal while removing the manual labour involved. He is further kept informed of the status of the device through indicator lights on the level and simply transmits the necessary signals through the use of the lock bell system.

Quality control and maintenance plays an important role in ensuring reliability and safety. A more than adequate safety factor is included in the device when manufactured by a suitable workshop. Non-destructive tests by a third party and progress visits by the responsible engineering personnel are advised. The maintenance requirements are also reduced in the design. Huckbolts are used to ensure proper connection of the device to the Transom while the selected cylinder is provided with bellows to protect it against the ingress of dirt. ToughMet retains its low coefficient of friction even when running dry. The design therefore has a certain tolerance to neglected maintenance. Critical inspections however include the testing of the interlocks, which can be done without extended stoppages, and inspecting the pneumatic valves and connections for tightness and leakage.

CHAPTER 8.   CONCLUSION

The aim of this project was to obtain a solution to the problem of aligning and maintaining a conveyance aligned at an underground station in order to address the hazards to safety and equipment associated with a misaligned and moving conveyance. Failing to identify a satisfactory currently available solution or proposed patent in the literature survey necessitated the design of a potentially suitable device.

A structured and systematic design methodology was followed based on the guidelines provided in the books by Pahl and Beitz [20], Dieter [21] and Cross [19]. A fundamental step in any design process is the generation of detailed product design requirements. Product design requirements for the device were derived to address the 16 requirement groups namely, geometry, forces, material, safety, production, assembly, operation, cost, kinematics, energy, signals, ergonomics, quality control, transport, maintenance and schedule presented in chapter 3 and Appendix A. A large number of principle solutions were identified through the use of multiple creativity stimulating techniques.

Employing concept stimulating techniques as discussed in chapter 4 proved to be of great value in generating practical potential solutions and aided in overcoming the hurdle of concept synthesis. A great deal of time was spent to no avail in searching for solutions before a structured process as discussed in chapter 4 was employed. Scrutinising the concepts through a process of screening and evaluation ensured that only the strongest concept was identified and further developed. Modern day three dimensional modelling on Solidworks as employed with the embodiment of the potential concepts provides great insight into the workings and complexity of concepts. Computational models quickly highlight the potential shortcomings in obtaining a practical solution allowing these areas to be addressed earlier in the design process.

Certain design decisions had to be made in order to realise a practical design and these were done using conventional calculations in chapter 5. It would have been ideal to have the arresting device engage with the supporting steelwork behind the conveyance as there are no pipe brackets or cable clamps positioned behind the conveyance. Calculations however indicated that installing the device in that position would generate an excessive moment and force on the Transom that cannot be resisted by the Transom or conveyance roof structure. A far better and less complex solution was obtained by installing the support frame of the device directly on the Transom and having the clamp beams protrude to the side of the conveyance during docking. Choosing to use a box section beam ensures a more equally distributed stress in the beams resulting in a valuable weight reduction. Pneumatic cylinders were decided upon as the preferred drive system of the beams because of the availability of compressed air. A compressed air solution is seen as a more reliable solution in comparison to a heavier motor, rack and pinion solution. The pneumatic solution incorporates bellows to isolate the working components of the cylinder from the harsh operating environment as well an incorporating end position locking safety features. With a pneumatic solution it is further possible to store compressed air energy for use at different stations improving the flexibility of the system.

Critical components in the design was modelled in Solidworks-Simulation and corresponded to a fair degree with the conventionally calculated values. The modelled stresses were less than the conservative stresses calculated by conventional methods. The ability of the program to handle complex stress distributions and shapes delivered better results in comparison to the conventional calculations that were based on sometimes too strict assumptions.

A final design, referred to as the Quadro-cage-clamp, was presented utilising four clamp beams; each set of top and bottom beams travelling through a front and rear support with the support fixed directly to the Transom through vibration resisting Huckbolts. Both conventional and simulated calculations indicated that the device is of adequate strength to handle the stresses associated with an applied load ten times the maximum allowed stationary load of the conveyance. A safety factor in excess of ten is present throughout the entire device except where the clamp beams and the front supports contact each other. A satisfactory safety factor in excess of 7 is however still present at these locations.

The need for this large safety factor and the extreme magnitude of the forces involved justified the use of exotic material such as 17-4 PH stainless steel considered to be an intelligent choice because of its ultra-high strength and corrosion resistant properties. Using an ultra-high strength steel is the only viable method of reducing the weight of the system required to withstand the tremendous stresses created by the extreme forces. Even with the use of this special material the overall weight of the device is still excessive at 635 kg excluding the pneumatic components. This weight amounts to 5% of the allowable payload which affects the efficiency of the hoisting system. A reduction in payload necessitates an increase in trips influencing available shaft time and increasing power consumption both bringing increased operational costs. Great effort has been applied to keep the design as simple as possible and to minimize the variety of materials required. Using only a small variety of different thickness plates and designing the system to be almost entirely welded together simplifies the manufacturing process by limiting the processes required. The associated cost of manufacture was not calculated but is perceived to be expensive due to the quantity of exotic material used and the required skill level of the welder. Further contributing costs will come in the form of third party inspectors and design modifications to the conveyance and some shaft steelwork. These design alterations include the repositioning of the dolly wheel cluster, modification of the shaft examination canopy, the elongation of the draw bar, repositioning of the slinging brackets, modification to the hole spacing in the Transom and lowering of the jack catches in the headgear because of the elongated draw bar. Even though all these alterations are surmountable they will come at a great cost as all the design alterations need to be approved by a professional structural engineer.

Utilising a conveyance mounted design comes at a lower cost than installing devices at all levels. Some installations are however still required on all stations such as the electronic control panel interlinking the system with the lock bell system, adequately sized support steelwork at the same spacing as the decks to provide for all deck positioning, pneumatic and data linkage points. To maintain warranty and ensure compatibility the control panel interlinked with the lock bell system must be designed by the manufacturer of the lock bell system and falls outside the scope of this project.

On conclusion of this study a device is presented with the potential to ensure a properly aligned and secured conveyance relative to a shaft station. Utilising such a device promises to improve safety by reducing the likelihood of conveyance motion related accidents. The system simplicity should make it easily acceptable in the industry, once functionality has been proven, and promises an easy transition from current systems. The presented design is however still far from an implementable solution and will require extensive testing on a full scale prototype.

Detailed risk assessments and training literature as well as site specific alterations need to be considered before such a device is presented as a suggested solution. Currently the design provides a good platform from which further development and testing can be done. The decrease in payload, cost of prototype development and testing, cost of manufacture, required shaft modifications and design work of the control circuits counts heavily against the design and will likely stop its development to full implementation.

The study is however considered a success in that a detailed potential solution is provided along with valuable design tools in this dissertation. The dissertation is proof of the value of following a systematic design process that facilitated not only the detailed design of a potentially successful conveyance arresting device but the synthesis of many different concepts that might be altered and considered in the future all with the potential of eventually resolving this problem.

REFERENCES

[1] Storm, C. (2011, June 8). Vertical Transport Manager (Mponeng).(A.J.H. Lamprecht, Interviewer).

[2] HUGO, M. (Made.Hugo@dmr.gov.za) 15 Jun. 2011. Accidents. E-mail to: Lamprecht, A.J.H. (ALamprecht@Anglogoldashanti.com).

[3] De Winnaar, J. (2011, June 24). Health and Safety Manager (Tau Tona). (A.J.H. Lamprecht, Interviewer).

[4] TAU TONA MINE. 2004. Keps Fatal. Tau Tona.[Power Point presentation].

[5] ODENDAAL, P., compiler. 2011. Mp shaft cage project. Carletonville: Mponeng. [CD].

[6] LAMPRECHT, A.J.H., presenter. 2014. Slack Tight Rope Protection on a Koepe Winder. Presented at the AMRE central district meeting. WW AGA Mashie Golf Club.[Power Point Presentation].

[7] African Wire Ropes Limited. 1965. African Wire Ropes Limited. 2nd edition. Johannesburg: Swan Press.

[8] Haggie Rand Ltd. 1987. Steel wire ropes for Cranes and General Engineering. Johannesburg: Whitnall Simonsen.

[9] Scaw Metals Group. Haggie steel wire ropes for mining technical training manual. Fabform Graphics.

[10] APCOR, 1996, Minerals Act Regulation 16.34.1(a), Winding Ropes.

[11] AngloGold AG ENG 063. (2000). Operate a cage arresting (Levelok) system.

[12] AngloGold AG ENG 064. (200). Install a cage arresting (Levelok) system on a shaft conveyance.

[13] AngloGold AG ENG 218.(1999). Maintain a cage arrestor (K.E.P.S).

[14] AngloGold AG ENG 350. (1999). Operate a cage arrestor (K.E.P.S).

[15] AUSTIN, R. 2005. Design of a cage arresting device by using a rack and pinion. Cape Town: UCT. (Thesis - B.Eng.).

[16] Austin, R. (2011, April 6). Turbo Engineer (Tau Tona). (A.J.H. Lamprecht, Interviewer).

[17] Héiyrinen, S. 1995. Safety device arrangement. Patent: US: 5,411,117. 9 p.

[18] Bennet et al. 1995. Pretorque to unload elevator car / floor locks before retraction. Patent: US:5,862,886. 8 p.

[19] Cross N., Engineering design methods, 2nd edition, John Wiley & sons Ltd, Baffins Lake, 1999.

[20] Pahl G., Beitz W., Feldhusen J., and Grote K.H., Engineering design a systematic approach, 3rd edition, Springer, London, 2007.

[21] Dieter G. E., Engineering design, 3rd edition, McGraw-Hill, Singapore, 2000.

[22] Roukes N., Design synectics: stimulating creativity in design, Davis Publications, Worcester, 1988.

[23] Gadd K., TRIZ for engineers: enabling inventive problem solving, Wiley, Chichester, Hoboken, 2011.

[24] Orloff A., Modern TRIZ: a practical course with EASyTRIZ technology, Springer, Heidelberg, 2012.

[25] OXFORD CREATIVITY. Effects Database. http://www.triz4engineers.com.

[26] Parmley R., Illustrated Sourcebook of Mechanical Components, McGraw Hill Professional, New York, 2000.

[27] DEPARTMENT OF MINERALS AND ENERGY. Permit number: 3957 to use a winding plant at Western Deep Levels (East) mine 3 Main shaft. Department of Minerals and Energy, R.S.A., 1997.

[28] AngloGold Ashanti, 2004, ESP 7.8, Keps devices, p.3.

[29] SOUTH AFRICAN INSTITUDE OF STEEL CONSTRUCTION. Section properties of steel profiles.http://saisc.co.za/saisc/struct_sd_profiles.htm.

[30] ANGLO AMERICAN. Typical cross section through shaft showing Bunton steelwork. Drawing number: 346-SO1-RM0383. Rev: 0.

[31] ANGLO AMERICAN. ARRGT& details of roof & top transom for 4 deck man cage. Drawing number: 349-000-M0574. Rev: 18.

[32] Hibbeler R.C., Mechanics of materials, 7th edition, Pearson Prentice Hall, Upper Saddle River, New Jersey, 2008.

[33] AK Steel., 17-4 PH Stainless Steel Product Data Bulletin, West Chester: AK Steel, p. 3, table 3.

[34] INTOCO., 17-4PH / 1.4542 / S17400 Precipitation Hardening Martensitic Stainless Steel. http://www.17-4ph.co.uk.

[35] Juvinall R.C., Marshek K.M., Fundamentals of machine component design, 4th edition, John Wiley & Sons (Asia) Pte Ltd, 2006.

[36] BRUSH WELLMAN ALLOY PRODUCTS, ToughMet 3 CX 105 The Tough Alloy for Tough Environments, Distributed by: Multi Alloys, Kyalami, 2004.

[37] HUCK., Huck industrial fastening systems, Huck South Africa (Pty) Ltd.

[38] HUCK., Huck 360 Advanced Fastening System, Alcoa Fastening Systems, 2014.

[39] Boresi A.P., Schmidt R.J., Advanced Mechanics of Materials, 6th edition, John Wiley & Sons, INC., Hoboken, New Jersey, 2003.

[40] FESTO., Standard cylinders DSBC, to ISO 15552, Festo, 2014.

[41] FESTO., Air reservoirs, Festo, 2014.

[42] FESTO., FluidDraw S5, Festo, 2014.

[43] Smith F., Boersma C., 2013, Shaft Foreman and Shaft Artisan (Tau Tona), (A.J.H. Lamprecht, Interviewer).

[44] ANGLO AMERICAN. Details of new jack catch lug for 4 deck man cage. Drawing number: 034-0349-000-MO585. Rev: 4.

[45] ANGLO AMERICAN, ANGLOGOLD ASHANTI. General ARRGT of 4-deck aluminium man cage - 40 men per deck. Drawing number: 349-000-MO572. Rev: 29.

[46] ANGLO AMERICAN. ARRGT & details of intermediate decks - 4 deck AL cage. Drawing number: 349-000-MO576. Rev: 8.

[47] AngloGold Ashanti, 2012, ESP-21.02.42, Winder Dynamic Tests, p. 39.

[48] AngloGold Ashanti, 2006, AGTE-21.2.16, Cage Arresting Devices.doc, p. 7.

[49] PUZONE, M. 2005. KEPS SYSTEM.AMRE annual safety seminar.[PowerPoint presentation].

[50] CSIR, 2010, Certificate of test conducted on winding rope, Certificate number: 243530.

[51] Anglo American, 2013, Tau Tona-Main shaft rope condition assessment on the man winder ropes, Report number: C172.25437.

[52] AngloGold Ashanti, 2006, AGTE-21.2.5, Conveyor Belts, pp. 4-5.

[53] AngloGold Ashanti, 2012, OH PR 01-06, Provision for adequate illumination on surface and underground, p. 5.

[54] APCOR, 1996, Mine Health and Safety Act, Regulation 22.9(2)(b) Occupational exposure limits for physical agents.

[55] Budinski K., Budinski M., Engineering materials properties and selection, 8th edition, Pearson Prentice Hall, Upper Saddle River, New Jersey, 2005.

[56] Amirault, S.B. 2015. Strength of Materials: Mohr's Circle. http://engineering-references.sbainvent.com/strength_of_materials/mohrs-circle.php#.VSQKr_mUc0o 07 Mar. 2015.

APPENDIX A. DETAILED TASK CLARIFICATION

1. OBJECTIVES TREE METHOD

The objectives tree method is a useful procedure to obtain a clearly defined set of objectives usable as a powerful control and management tool.

The method works by extracting the broad objectives from a design brief and expanding the objectives. The objectives are sorted based on their importance and relationships resulting in a "means - ends" hierarchy. The results are presented in a diagrammatic tree showing how an objective will be met by moving down the tree and why it must be done when moving up the tree. The true value of the method is in the generation of the document as it promotes comprehension of the problem.

The objectives tree illustrated below lists the 10 main objectives in the top level of the hierarchy outlined in green. Each of these objectives requires sub-objectives in order to be achievable. This next level is given in the red blocks. In order to realise these objectives the blue objectives must be satisfied and these in turn rely on the black objectives. The lines connecting the blocks illustrate the interrelationships.

Ensure cage approaches the station smoothly
- Aids in deceleration when approaching a station
  - Deceleration device
    - Allowed deceleration rate
    - Measurement and control of deceleration rate.
- Communication with WED
- Reduce cage oscillation
- Allowed creep distance.

Reliable
- Do not cause damage
  - Mechanism not to protrude into adjacent compartments
  - Damage to shaft infrastructure
    - infrastructure strength
    - Infrastructure integrity
    - Infrastructure position
  - Damage to rails
  - Damage to cage
  - Damage to rolling stock
  - Damage to rolling stock content
- Easily maintainable
  - Minimize components
  - Reduce labour
  - Indication of deterioration
  - Easily accessible
  - Elimination of experts
- Operate in a harsh environment
  - Wet environment
    - Suitable materials
  - Dusty environment
    - Suitable ingress protection
  - Resist falling debris
    - Protective hood
- Does not create nuisance trips
  - Analyse and improve philosophy
  - Indication of equipment status

Compatibility
- Utilizable with current systems
  - Compensating sheaves
  - Communication systems
  - Locked bell system
    - Do not obstruct the view to the locked bell system
  - Call bell system
  - E-cam
  - Slack rope device
    - Maintain tension in the rope
- Minimize modifications
  - Fit inside the shaft constraints
- full manual override for slinging
  - Authorized isolation of the system
  - Indication of the deactivated status

Safety
- Prevent equipment failure
  - Adequate safety factor
  - Robust construction
  - Resistance to tampering
- Remove people from harm
  - Reduce human error
  - Do not obstruct the cage exit
    - Ease of operation of the cage doors
- System Compatibility
  - Sequencing
  - Interlocking

Ensure the cage is repositioned to the next deck
- Allow cage to be moved x meter
  - Communication with the WED
  - Maintain tension in the rope
  - Uni-directional travel

Ensure that the cage accelerates away smoothly
- Control the acceleration
  - Allowed acceleration rate
  - Measurement and control of the acceleration rate

Improve system efficiency
- Rapid operation
  - Improvement on current time usage
  - Sequence of operation
  - Reduce fatigue
    - Reduce manual labour
    - Amount of operators or assistants
- Automatic / Semi automatic system
  - Minimize human input
    - Level of education of operators
  - Minimize duplication
- Operate on multiple levels
  - Low cost per unit
    - Identified stations
- Do not negatively influence the cage payload
  - Maximum allowed weight
    - Minimize the weight of the components
- Eliminate re-alignment

Ensure the cage remains stationary while aligned
- Do not cause damage
  - Do not damage shaft infrastructure
    - Load carrying ability
  - Do not damage cage
    - Device operating forces
  - Activation mechanism
  - Latching mechanism
    - Maintain tension in rope
- Prevent vertical movement of the load
  - Detaching mechanism

Ensure the cage aligns accurately
- Alignment mechanism
  - Align rails in cage with rails on station
    - Misalignment tolerances
  - Measurement and control of alignment

Financial
- Low product cost
  - Reduce complexity
    - Use of standard parts
  - Material choices
    - Minimize parts
- Operational cost
  - Labour costs
  - Elimination of outside resources
    - Local manufacturing
  - Minimize maintenance

2. FUNCTIONAL ANALYSIS

The functional analysis method is an effective process to define a system boundary that satisfies the client's requirements while leaving room for innovation. The process starts off by identifying the inputs that is converted by the system, illustrated as a black box, into the desired outputs. The figure below illustrates this first step.

Variable mass
conveyance

Arbitrary positioned
conveyance

Unknown amount of
rope stretch

Black Box
(Material, energy and
data transformation
system)

Precisely positioned
conveyance

Stationary conveyance

Material
Energy
Information
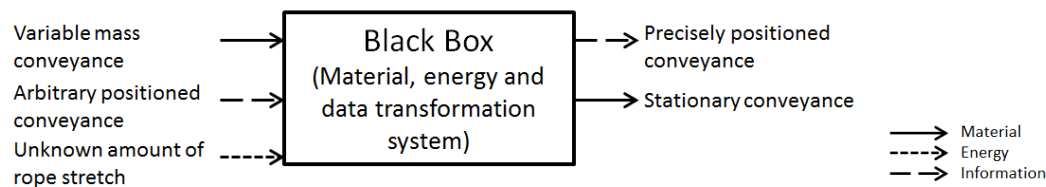
The black box system is responsible for converting material, energy and information into a new desired form. The intermediate desired forms are identified and shown in the central region of the figure below. A conveyance in the shaft has a certain position (information), velocity (energy) and mass (material), shown by the green arrows on the figure below, that must be stopped in a new position where it has a different position, velocity and mass. All the material, energy and information that is added to the system between the initial position and the new position is identified and shown as red arrows feeding into the red arrow connecting the two positions. The blue arrow on the left shows a change in the physical environment that result in a change of energy and material. The red arrows therefore also indicate functions that should occur to change the material, energy and information to the desired state. The same is done between the "conveyance stopped in position" and "conveyance maintained in position" states as well as the conveyance "maintained in position" and "conveyance in the shaft" state. The orange and purple arrows indicate that it is a cyclic process with the orange arrow indicating a smaller change in position.

Known position (P_A)

Known velocity (V_A)

Known mass (M_CA + M_RA)

Conveyance in the shaft

Change in weight

Decelerate the conveyance

Stop the conveyance

Align the conveyance

Change in length of rope

Known position (P_B)

Zero velocity (V_B)

Known mass (M_CA + M_RB)

Conveyance stopped in position

Lock or secure the conveyance weight

Rope stretch due to weight change

Compensate for rope stretch + weight change

Load or unload content

Known position (P_B)

Zero velocity (V_B)

Known mass (M_CB + M_RB)

Conveyance maintained in position

Change in weight

Prevent oscillation

Accelerate the conveyance

Change in length of rope

Known position (P_C)

Known velocity (V_C)

Known mass (M_CB + M_RC)

Conveyance in the shaft

Small change in position (Moving to next deck)

Large change in position (Moving to next station)

The multiple sub-functions, identified above (next to red arrows), required to facilitate the steps of transformation of material, energy and information are now linked together to commutatively achieve the overall function. To ensure compatibility between the sub-functions auxiliary functions may be added. The sub-functions together with their auxiliary functions, where applicable, are placed in a transparent box showing their interrelationship with arrows representing the flow of material, energy and information. The system is enclosed by a boundary clearly illustrating the limits of the problem. The figure below illustrates the system sub-functions and interrelationships.
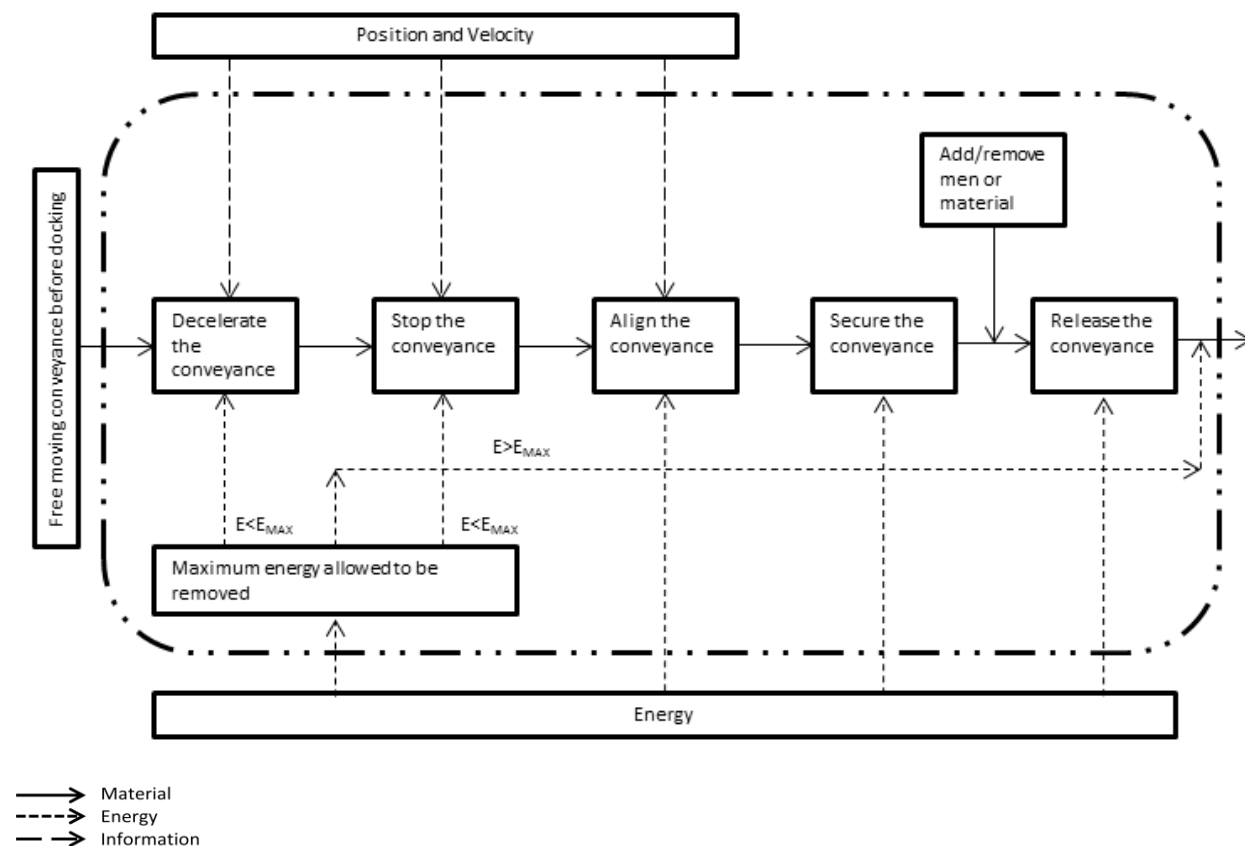
3. PRODUCT DESIGN REQUIREMENTS

A detailed set of PDR are derived using the Objectives tree and Functional Analysis methods discussed above. Sixteen topics were identified requiring quantitative definition with a summarised description of each topic given in chapter 3. These sixteen topics are geometry, kinematics, forces, energy, material, signals, safety, ergonomics, production, quality control, assembly, transport, operation, maintenance, costs and schedules. Each of these topics is tabled below where the desired value of the requirement is assigned to each entry.

A format proposed in the book, Engineering design a systematic approach [20], was used for the tabulation of the requirements. The document contains a heading defining the project for which the requirements list is prepared as well as the date on which it was issued. The subsequent tables consist of three columns where any changes made to the requirements are recorded in the first column along with the date and reason. The second column indicates whether the requirement listed in column three is a demand or a wish. Where applicable each requirement is provided with a value in curled brackets along with its reference source in block brackets.

Changes	D / W	Requirements
		Geometry Fit in between the shaft compartments
	D	Height {4 200 mm} [43] [30]
	D	Width {310 mm} [43] [30]
	D	Length {1 200 mm} [43] [30]
	W	Contact area when engaged {>28 mm} [44]
	W	Clearance between device and conveyance when not engaged {60 mm} [30]
	D	Should not obstruct loading area {Cage opening of 1 682 mm x 1 722 mm} [45] [46]

Changes	D / W	Requirements
		Kinematics What movement is desired from the conveyance
	D	Decelerate at acceptable limit {<4 m.s^{-1}} [47]
	D	Minimize or reduce oscillations during arrival and departure {< 200 mm.s^{-1}} [48]
	D	Acceptable engagement speed {<0.35 m.s^{-1}} [49]
	D	Minimal movement when released from cage arresting system {< 50 mm}
	W	Accelerate away at acceptable limit {<4 m.s^{-1}} [9]
	D	Account for stretch in the rope [9] [27] [50] [51]
	W	Operate on simple movements
	D	Reduce or eliminate nipping points {Provide guards with mesh size smaller than 10 mm x 10 mm at 100 mm from nip point / non perforated cover} [52]
	W	Reposition next deck to landing {2 057 mm} [45]

Changes	D / W	Requirements
		Forces What forces are associated with the conveyance and what should be done with these
	D	Support the conveyance for a downwards load {176 580 N} [27]
	D	Support the conveyance in the upward direction {109 872 N} [27]
	D	Ensure a proper load carrying structure {A-frames / Buntons or King post}
	D	Provide clamping or holding force in excess {Safety factor of 10} [28]
	D	Do not deform excessively under applied loads
	W	Specify cyclic life span of device based on final design

Changes	D / W	Requirements
		Energy
		What sources of energy is available and how should it be utilized
	D	Absorb the kinetic energy of the conveyance
	W	Supply energy to required systems
	W	Electrical energy is available {525 V}
	W	Compressed air pressure {350 - 410 kPa}
	W	Water pressure
	W	Storage of energy for cage mounted solutions
	W	Minimize energy consumption

Changes	D / W	Requirements
		Material
		Any material flows, material properties and mine standards
	W	Utilize low density metals
	D	Corrosion resistance {Resist corrosion in wet shaft}
	W	Ductile to handle impact stress
	W	Ease fabrication
	D	Suitable properties for application (Friction etc.)
	D	Non toxic
	W	Abrasion resistant {Prevent wear on critical components}
	D	Allow desired tolerances
	D	Adequate strength

Changes	D / W	Requirements
		Signals
		What signals are required for safety, communication and compatibility
	D	Compatible with Lock bell system
	D	Compatible with Call bell system
	D	Compatible with Slack-tight rope system
	D	Compatible with the shaft station stopping devices
	D	Inform WED with regard to docking status
	D	Provide onsetter with engagement status of the mechanism
	D	Inform the WED when it is safe to move the conveyance
	W	Necessary signals between functional components
	W	If computer control is required adequate information must be ensured
	D	Integrate with safety system to ensure safe operation
	W	Provide fault finding information
	W	Restrict access to appointed personnel

Changes	D / W	Requirements
		Safety Safety must be ensured at all time
	D	Fail to safe once engaged
	D	Resist abuse {Restricted access}
	D	Eliminate possible malpractices {Controllable only by appointed persons}
	W	Provide monitoring capabilities {Necessary signals}
	W	Forbid bridging out
	D	Provide adequate training
	D	Minimize access
	D	Prevent operation under dangerous situations {Manual lock out}
	D	Integrate with current safety systems

Changes	D / W	Requirements
		Ergonomics The device must reduce work effort by being simple and comfortable to operate and maintain
	W	Reduce physical labour {Eliminate lifting or pulling of components}
	W	Be mostly automatic {Controllable by a single person}
	W	Provide clear indication of status
	W	Simple mechanism to ease maintenance
	W	Locate in accessible location
	W	Do not change the current method of doing
	W	Ensure adequate illumination {160 LUX} [53]
	W	Provide visual appeal {confidence inspiring}

Changes	D / W	Requirements
		Production The device should increase the efficiency of the loading and unloading process
	W	Rely on simple mechanisms to promote South African manufacturing
	D	Operate time effectively {<15 sec} [48]
	W	Aid in deck repositioning
	W	Design for quick and easy installation {Fit lifting lugs + locating pins}
	W	Minimal available maintenance time {20 min a week}

Changes	D / W	Requirements
		Quality control Ensures that the docking device is of adequate design and construction
	W	Proof concept with a model
	D	Build in sufficient safety factors {SF 10} [28]
	W	Specify tight tolerances
	D	Contract a reliable manufacturer {Mine accredited}
	W	Perform necessary Non Destructive Tests (NDT's)
	D	Comply with mine standards {Verify design with Project Engineering Services (PES)}

Changes	D / W	Requirements
		Assembly What requirements are there around the assembly process
	W	Provide documentation for manual assembly
	W	Must be easy to install in location {Pre-assembled on surface}
	W	Must be easily disassembled to the degree necessary for maintenance or repair
	D	When assembling standard components must be of the correct grade and quality.

Changes	D / W	Requirements
		Transport What should be addressed to improve transport efficiency
	W	Provide connecting lugs or points for rigging gear
	D	Must be lift-able with a chain block {< 3 200 kg}

Changes	D / W	Requirements
		Maintenance What should the maintenance requirement of the mechanism be
	W	Easy to perform maintenance {grease nipples / oil fillers + bolted on components}
	W	Indication of failure to perform maintenance
	W	Easily accessible for maintenance {Accessible from station or shaft exam canopy}
	W	Have a long maintenance frequency

Changes	D / W	Requirements
		Operation What qualities is important during operation of the equipment
	D	Must not exceed acceptable noise levels {<85 dB} [54]
	D	Must not wear away at conveyance or shaft infrastructure {Wear plates at possible scuffing points}
	W	Must rely on minimal human input {<1 person}
	D	Must operate repetitively and reliably
	D	Must operate in a wet environment
	D	Must operate in a dusty environment
	W	Must be able to resist falling debris {< 5kg debris}
	W	Must be compatible with all shaft activities
	D	Have a quick reaction time {<4 sec} [48]

Changes	D / W	Requirements
		Costs What are the restrictions and procedures regarding finances
	D	Low concept development cost
	D	Low modelling and design cost
	D	Minimal cost model
	W	Financing for experimental testing of a prototype or component

Changes	D / W	Requirements
		Schedules What is the time frame for the project
	D	Submit a full dissertation {14 Nov 2014}
	W	Present project for possible future development {14 Nov 2014}

APPENDIX B. CONCEPT EVALUATION COMPARISON TABLE

Concept evaluation is a tool used to identify the strongest concept for further development. In the table below concepts 1, 6 and 9 described in chapter 4 are compared. Chapter 4 explains the working of the table and only presents an extract from the complete table below. To briefly recap the first column lists the lowest level requirements form the Objectives Tree presented in appendix A. These requirements are listed beneath the highest level requirements outlined in green blocks in the Objectives Tree. A weighting is assigned to every requirement by considering their relative importance to the problem such that all the weights in column 2 sum to 1. Each concept is considered by making use of the embodiments in chapter 4 and a value between 0 and 10, according to table 15 in chapter 4, assigned for each requirement. The column next to the value column shows the product of the value assigned for the requirement under the Concept tab and the weight assigned for the requirement under the Evaluation Criteria tab.

At the bottom of the table the overall value (OV) and overall weighted value (OWV) is given for each concept calculated by summing the entries of all the rows in the column. Beneath the overall value and the overall weighted value the ranking (R) and the weighted ranking (WR) for each concept is provided. The ranking is the sum of the values in the column divided by the potential total of the values (number of requirements timed by 10) and provides an indication of how well the requirements are perceived to be addressed by the design if all the requirements carried the same weight. Some requirements however carry more weight and the weighted ranking which is simply the overall weighted value divided by 10 provides an indication of how well the requirements are perceived to be addressed by the design. The best concept will therefore have the largest weighted ranking and concept 9 is found as the best candidate at 64 %.

Evaluation Criteria		Concept 1		Concept 6		Concept 9	
	Weight	Value	Weighted Value	Value	Weighted Value	Value	Weighted Value
Ensure cage approaches the station smoothly.							
Allowed deceleration rate	0.005	1	0.005	4	0.020	0	0.000
Measurement and control of deceleration rate.	0.005	1	0.005	5	0.025	0	0.000
Communication with WED	0.030	5	0.150	5	0.150	5	0.150
Reduce cage oscillation	0.020	7	0.140	7	0.140	8	0.160
Allowed creep distance.	0.020	5	0.100	5	0.100	5	0.100

Evaluation Criteria		Concept 1		Concept 6		Concept 9	
	Weight	Value	Weighted Value	Value	Weighted Value	Value	Weighted Value
Reliable							
Mechanism not to protrude into adjacent compartments	0.014	6	0.084	5	0.070	5	0.070
Infrastructure strength	0.002	5	0.011	5	0.011	6	0.013
Infrastructure integrity	0.002	5	0.011	5	0.011	6	0.013
Infrastructure position	0.004	5	0.021	5	0.021	6	0.025
Damage to rails	0.006	8	0.045	8	0.045	8	0.045
Damage to cage	0.008	6	0.051	7	0.059	7	0.059
Damage to rolling stock	0.006	8	0.045	8	0.045	8	0.045
Damage to rolling stock content	0.003	8	0.023	8	0.023	8	0.023
Minimize components	0.004	7	0.026	6	0.023	8	0.030
Reduce labour	0.002	7	0.013	7	0.013	7	0.013
Indication of deterioration	0.004	6	0.023	5	0.019	5	0.019
Easily accessible	0.002	7	0.013	6	0.011	6	0.011
Elimination of experts	0.004	5	0.019	5	0.019	5	0.019
Suitable materials	0.007	6	0.043	5	0.036	5	0.036
Suitable ingress protection	0.005	6	0.029	5	0.024	6	0.029
Dusty environment	0.012	6	0.072	5	0.060	6	0.072
Resist falling debris	0.006	6	0.036	6	0.036	6	0.036
Analyse and improve philosophy	0.008	5	0.038	5	0.038	5	0.038
Indication of equipment status	0.023	5	0.113	5	0.113	5	0.113
Compatibility							
Compensating sheaves	0.005	5	0.026	5	0.026	5	0.026
Communication systems	0.005	7	0.036	7	0.036	7	0.036
Do not obstruct the view to the locked bell system	0.005	6	0.031	8	0.041	8	0.041
Call bell system	0.005	6	0.031	8	0.041	8	0.041
E-cam	0.005	5	0.023	5	0.023	5	0.023
Slack rope device	0.005	6	0.031	6	0.031	6	0.031
Fit inside the shaft constraints	0.060	5	0.300	7	0.420	8	0.480
Authorized isolation of the system	0.015	6	0.090	7	0.105	7	0.105
Indication of the deactivated status	0.015	5	0.075	5	0.075	5	0.075

Continued on next page...

Evaluation Criteria		Concept 1		Concept 6		Concept 9	
	Weight	Value	Weighted Value	Value	Weighted Value	Value	Weighted Value
Safety							
Adequate safety factor	0.022	6	0.131	6	0.131	7	0.152
Robust construction	0.022	6	0.131	5	0.109	7	0.152
Resistance to tampering	0.020	5	0.102	7	0.143	7	0.143
Reduce human error	0.032	6	0.192	6	0.192	6	0.192
Ease of operation of the cage doors	0.032	4	0.128	8	0.256	8	0.256
Ease of sequencing with shaft operation	0.016	6	0.096	6	0.096	6	0.096
Ability for safety Interlocking	0.016	6	0.096	5	0.080	5	0.080
Ensure the cage is repositioned to the next deck.							
Communication with the WED	0.014	7	0.098	7	0.098	7	0.098
Maintain tension in the rope	0.020	4	0.080	6	0.120	6	0.120
Uni-directional travel	0.006	2	0.012	2	0.012	4	0.024
Ensure that the cage accelerates away smoothly							
Allowed acceleration rate	0.040	4	0.160	7	0.280	7	0.280
Measurement and control of the acceleration rate	0.040	3	0.120	5	0.200	5	0.200
Improve system efficiency							
Improvement on current time usage	0.006	4	0.024	6	0.036	6	0.036
Speed of sequenced steps in operation	0.006	5	0.030	6	0.036	6	0.036
Number of sequenced steps in operation	0.003	5	0.015	6	0.018	7	0.021
Reduce manual labour	0.002	7	0.015	7	0.015	7	0.015
Amount of operators or assistants	0.001	7	0.006	7	0.006	7	0.006
Level of education of operators	0.006	7	0.042	6	0.036	6	0.036
Number of units to serve an entire shaft	0.012	3	0.036	8	0.096	8	0.096
Cost to prepare a station for docking	0.008	3	0.024	7	0.056	7	0.056
Influence the payload of the cage	0.016	9	0.144	6	0.096	5	0.080
Eliminate re-alignment	0.020	7	0.140	7	0.140	8	0.160

Evaluation Criteria		Concept 1		Concept 6		Concept 9	
	Weight	Value	Weighted Value	Value	Weighted Value	Value	Weighted Value
Ensure the cage remains stationary while aligned							
Seriousness of infrastructure damage	0.006	5	0.030	5	0.030	5	0.030
Probability of damage to infrastructure due to forces involved	0.006	6	0.036	6	0.036	6	0.036
Seriousness of cage damage	0.006	4	0.024	6	0.036	6	0.036
Probability of damage to cage due to forces involved	0.006	5	0.030	7	0.042	7	0.042
Vulnerability of damage to the activation mechanism	0.012	5	0.060	7	0.084	7	0.084
Vulnerability of damage to the latching mechanism	0.012	5	0.060	7	0.084	7	0.084
Vulnerability of damage to the detaching mechanism	0.012	4	0.048	6	0.072	7	0.084
Likelihood of damage to the activation device resulting in vertical movement	0.020	7	0.139	6	0.119	6	0.119
Likelihood of damage to the latching device resulting in vertical movement	0.020	4	0.082	7	0.143	7	0.143
Likelihood of damage to the detaching device resulting in vertical movement	0.020	6	0.119	6	0.119	6	0.119
Ensure the cage aligns accurately							
Misalignment tolerances	0.072	7	0.504	7	0.504	7	0.504
Measurement and control of alignment	0.048	6	0.288	6	0.288	7	0.336
Financial							
Use of standard parts	0.013	4	0.050	4	0.050	5	0.063
Minimize parts	0.013	6	0.076	5	0.063	6	0.076
Local manufacturing	0.008	6	0.050	6	0.050	6	0.050
Material choices	0.014	5	0.072	5	0.072	4	0.058
Labour costs	0.010	7	0.067	7	0.067	7	0.067
Elimination of outside resources including power draw	0.013	3	0.038	7	0.090	7	0.090
Minimize maintenance	0.010	6	0.058	6	0.058	6	0.058
	Sum Wt	**OV 1**	**OWV 1**	**OV 6**	**OWV 6**	**OV 9**	**OWV 9**
	1.000	404	5.41	447	6.16	456	6.39
		R 1	**WR 1**	**R 6**	**WR 6**	**R 9**	**WR 9**
		0.546	0.54	0.60	0.62	0.62	0.64

APPENDIX C. SPREADSHEET BASED CALCULATIONS - CLAMP BEAM STRENGTH

In this chapter the Microsoft Excel document titled, "Clamp Beam Two Supports Side Mount Extended Base" is used to calculate the stresses in the clamp beam. Two sets of calculations are performed to compare a solid beam and a box section beam.

1. SOLID BEAM

Seven dimensions govern the geometry of the solid beam. The first dimension "overlap" is an arbitrary dimension referring to the distance by which the beam will protrude past the rear support when fully extended and past the front support when fully retracted. The stroke is calculated from the shaft arrangement [30] such that the beam will extend beyond the clearance between the conveyance and the steelwork to the furthest edge of the supporting steelwork. The widths of the supports are then considered under support 1 and support 2 where, x, gives the distance between the centres of the two supports. It is shown that, x, can vary between 420 mm and 830 mm where the 420 mm accounts for the stroke and half the widths of the support beams as well as 40 mm for a potential stopper. The 830 mm is the maximum length before the beam will extend past the conveyance edge when retracted. Further down the spreadsheet a scroll bar is provided to change the value of, x, to see what the influence on the beam forces are. The width and height of the beam is also variable to lower the stresses to an allowable value. Based on these 7 dimensions other geometrically important calculations are made including the total beam length, beam cross sectional area, beam volume, beam mass and the beam's moment of inertia about the X-X axis.

The material properties are provided for stress and weight calculations. Having defined the geometry the forces on the beam can be calculated by applying 883 kN (F1) to the beam and then summing the forces in the vertical direction as well as summing the moments about point A defined at the point where F3 acts. The calculated forces are simply summarised under the Force Analysis heading and used to generate the shear force (graph on the left) and moment diagram (graph on the right) for the beam along its length. These diagrams are illustrated in the graphs and changes for a change in the value of x. Decreasing the value of, x, increases the forces on the supports while the moment due to the constant F1 and constant length of the cantilever remains the same. Increasing the distance between the support centres, x, decreases the forces on the supports but increases the beam mass. A balance must thus be found between lowering the support forces and increasing the beam mass. The bolts used to secure the support fixture to the Transom must however fit between the supports and if the support forces increase so do the required number of bolts. The value of, x, was therefore changed and the number of bolts required determined in the EES program "Side mount supports same side extended base". The bolts need to be spaced at least 50 mm apart and a balance point is obtained at an, x, value of 720 mm. At this distance the support forces require 26 bolts which are more than the 700 mm required to accommodate 13 pairs of bolts.

Beam Geometry

Overlap	30	mm		0.03	m			
Stroke	300	mm		0.3	m			
Support 1	80	mm		0.08	m			
Support 2	80	mm		0.08	m			
x	720	mm		0.72	m	420 <x>	830	mm
						0.42 <x>	0.83	m
Length	1,160.00	mm		1.16	m			
B	80	mm		0.08	m			
H	130	mm		0.13	m			
Area	10400	mm²		0.0104	m²			
Volume	12,064,000.00	mm³		0.012064	m³			
Mass				94.1	kg	Mass of 4 beams	376.3968	kg
Ixx	14,646,666.67	mm⁴		1.46467E-05	m⁴			

Mechanical Properties

ρ	7,800.00	kg/m³			
σy	1172	MPa	1,172,000,000.00	Pa	
E	197	GPa	1.97E+11	Pa	

Force Analysis

F1	882,900.00	N	@	1.077	m
F2	1,234,833.75	N	@	0.79	m
F3	351,933.75	N	@	0.07	m

Sum of vertical forces

F3 - F2 + F1 = 0
F2 = F1+F3   ..... (1)

Sum of Moments about A

F2(x) - F1(x + Support1/2 + Stroke + Overlap - 0.083) = 0		.... (2)
(F1 + F3)(x) - F1(x + Support1/2 + Stroke + Overlap - 0.083) = 0		(1) in (2)
F3 = (F1(x + Support1/2 + Stroke + Overlap - 0.083) - F1(x))/x		
F3	351,933.75	N

Force Diagrams

x	V	M
m	N	Nm
0	0	0
0.07	0	0
0.07	351,933.75	-
0.79	351,933.75	253,392.30
0.79	- 882,900.00	253,392.30
1.08	- 882,900.00	-
1.08	-	-
1.16	-	-

Shear Force Diagram

Moment Diagram

Having defined the length of the beam the forces on the beam is also fixed. The stresses throughout the beam are calculated in the spreadsheet section shown below. The first column provides discrete steps through the cross section of the beam starting at the bottom of the beam. The next three columns provide the constant moment of inertia, the maximum shear stress and moment found next to F2 at 790 mm from the left edge of the beam as shown on the graphs above. The next four columns are used to calculate the shear stress and tensile stresses at the discrete steps throughout the section in both Pa and MPa.

The resultant shear stresses are plotted in the graph below on the left and shows the expected parabolic distribution along the height of the beam which refers to the discrete points along the beams height.

The centre graph illustrates the tensile stress distribution throughout the beam cross section. The next two columns contain the values of the thickness and Q the product of the area to the discrete point of concern and the distance between the centroid of this area and the neutral axis. The last three columns contain the square of the material's yield stress and the value of $\sigma_{element}$ calculated as described in chapter 5. Dividing the square of the yield stress by the value of $\sigma_{element}$ the safety factors at the discrete points are calculated. The graph on the right shows the values of $\sigma_{element}$ in red and the value of the square of the yield stress in blue. As long as the red curve lies beneath the blue line the factor of safety is above 1 and because a force ten times the permitted load of the conveyance is used the factor of safety is greater than 10.

Shear stress							Compressive stresses					
				$\tau = VQ/It$			$\sigma = Mc/I$					
h	I	V	M	τ	τ	σ	σ	Q	t	σ_{yield}^2	$\sigma_{element}$	SF
m	m^4	N	N/m	Pa	Mpa	Pa	Mpa	m^3	m	MPa^2	MPa^2	
0	1.46467E-05	882,900.00	253,392.30	0.00	0.00	1,124,522,041.42	1,124.52	0	0.080	1,373,584.00	1,264,549.82	1.09
0.01	1.46467E-05	882,900.00	253,392.30	36167956.30	36.17	951,518,650.43	951.52	0.000048	0.080	1,373,584.00	909,312.11	1.51
0.02	1.46467E-05	882,900.00	253,392.30	66307919.89	66.31	778,515,259.44	778.52	0.000088	0.080	1,373,584.00	619,276.23	2.22
0.03	1.46467E-05	882,900.00	253,392.30	90419890.76	90.42	605,511,868.46	605.51	0.00012	0.080	1,373,584.00	391,171.89	3.51
0.04	1.46467E-05	882,900.00	253,392.30	108503868.91	108.50	432,508,477.47	432.51	0.000144	0.080	1,373,584.00	222,382.85	6.18
0.05	1.46467E-05	882,900.00	253,392.30	120559854.35	120.56	259,505,086.48	259.51	0.00016	0.080	1,373,584.00	110,946.93	12.38
0.06	1.46467E-05	882,900.00	253,392.30	126587847.06	126.59	86,501,695.49	86.50	0.000168	0.080	1,373,584.00	55,555.99	24.72
0.07	1.46467E-05	882,900.00	253,392.30	126587847.06	126.59	- 86,501,695.49	- 86.50	0.000168	0.080	1,373,584.00	55,555.99	24.72
0.08	1.46467E-05	882,900.00	253,392.30	120559854.35	120.56	- 259,505,086.48	- 259.51	0.00016	0.080	1,373,584.00	110,946.93	12.38
0.09	1.46467E-05	882,900.00	253,392.30	108503868.91	108.50	- 432,508,477.47	- 432.51	0.000144	0.080	1,373,584.00	222,382.85	6.18
0.1	1.46467E-05	882,900.00	253,392.30	90419890.76	90.42	- 605,511,868.46	- 605.51	0.00012	0.080	1,373,584.00	391,171.89	3.51
0.11	1.46467E-05	882,900.00	253,392.30	66307919.89	66.31	- 778,515,259.44	- 778.52	8.8E-05	0.080	1,373,584.00	619,276.23	2.22
0.12	1.46467E-05	882,900.00	253,392.30	36167956.30	36.17	- 951,518,650.43	- 951.52	4.8E-05	0.080	1,373,584.00	909,312.11	1.51
0.13	1.46467E-05	882,900.00	253,392.30	0.00	0.00	- 1,124,522,041.42	- 1,124.52	1.44329E-19	0.080	1,373,584.00	1,264,549.82	1.09
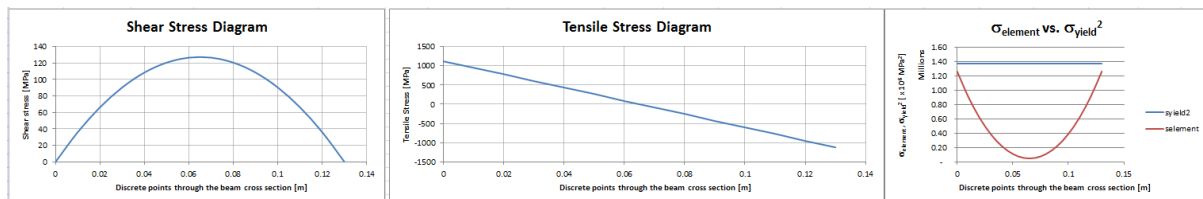
Even though the calculations above are based on the Mohr circle the last section in the spreadsheet generates a Mohr circle. Under the plot circle heading four columns are found where the first column contains values from 0 to 360 degrees which is converted for calculation purposed to radians in column two. This angular divisions are then used in conjunction with the calculated radius to calculate x and y coordinates in the third and fourth column used to plot the circle. The midpoint is defined at zero on the vertical axis and at the radius on the x axis because the value of σ_y is zero. σ_{avg} as shown in figure 42 in chapter 5 is thus equal to the radius. The circle centre defines the first point of the line with its end point corresponding to the shear stress and tensile stress calculated at the point of concern. For the Mohr circle presented below σ_x and τ_{xy} is taken at the top of the section. Using the equations presented in figure 42 in chapter 5 and the distortion energy equations presented in chapter 5 the values $\sigma 1$, $\sigma 2$, τ_{max}, θ, $\sigma_{element}$, σ_y^2 and the safety factor are calculated. The values of $\sigma_{element}$ calculated using the Mohr circle agrees with that calculated in the table above because plane stresses are considered. Below the data used to generate the Mohr circle and the Mohr circle is presented.

Mohr circle

σx	1,124.52	MPa
σy	0	Mpa
τxy	0.00	MPa
σ1	1124.52	Mpa
σ2	0.00	MPa
τmax	562.26	MPa
θ	0.00	°

Maximum distortion Energy Theory

σelement	1,264,549.82	MPa
σy^2	1,373,584.00	MPa
SF	1.09	
R	562.26	MPa
Midpoint		
X	Y	
562.261021	0	

Plot circle

		X	Y
0	0	1124.522041	0
10	0.174532925	1115.980033	-97.63560162
20	0.34906585	1090.613553	-192.3045949
30	0.523598776	1049.193348	-281.1305104
40	0.698131701	992.9779512	-361.4144175
50	0.872664626	923.6754382	-430.7169305
60	1.047197551	843.3915311	-486.9323275
70	1.221730476	754.5656156	-528.3525321
80	1.396263402	659.8966223	-553.7190124
90	1.570796327	562.2610207	-562.2610207
100	1.745329252	464.6254191	-553.7190124
110	1.919862177	369.9564258	-528.3525321
120	2.094395102	281.1305104	-486.9323275
130	2.268928028	200.8466032	-430.7169305
140	2.443460953	131.5440902	-361.4144175
150	2.617993878	75.32869322	-281.1305104
160	2.792526803	33.90848859	-192.3045949
170	2.967059728	8.542008298	-97.63560162
180	3.141592654	0	-6.88853E-14
190	3.316125579	8.542008298	97.63560162
200	3.490658504	33.90848859	192.3045949
210	3.665191429	75.32869322	281.1305104
220	3.839724354	131.5440902	361.4144175
230	4.01425728	200.8466032	430.7169305
240	4.188790205	281.1305104	486.9323275
250	4.36332313	369.9564258	528.3525321

260	4.537856055	464.6254191	553.7190124
270	4.71238898	562.2610207	562.2610207
280	4.886921906	659.8966223	553.7190124
290	5.061454831	754.5656156	528.3525321
300	5.235987756	843.3915311	486.9323275
310	5.410520681	923.6754382	430.7169305
320	5.585053606	992.9779512	361.4144175
330	5.759586532	1049.193348	281.1305104
340	5.934119457	1090.613553	192.3045949
350	6.108652382	1115.980033	97.63560162
360	6.283185307	1124.522041	1.37771E-13
0	0	1124.522041	0

Plot line

	X	Y
	562.2610207	0
	1124.522041	0
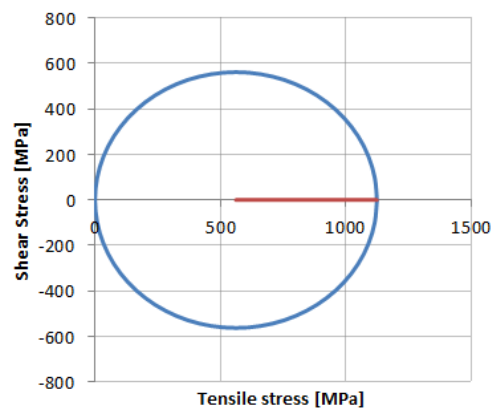
2. BOX BEAM 17-4 PH H900

The calculations for the box section beam is done under the Box Beam 17-4 PH H900 tab and presented below. The geometry contains the same variables as the solid beam with the thickness of the plates used on the sides of the beam (tb) and at the top and bottom of the beam (th) added. The thickness of these plates can be changed through scroll bars lower in the spreadsheet along with the overall width and height of the beam to obtain geometry that can handle the stresses. The forces, shear force diagram and moment diagram calculated are exactly the same as for the solid beam.

Beam Geometry

Overlap	30	mm	0.03	m				
Stroke	300	mm	0.3	m				
Support 1	80	mm	0.08	m				
Support 2	80	mm	0.08	m				
x	720	mm	0.72	m	420	<x>	1442	mm
					0.42	<x>	1.442	m
Length	1,160.00	mm	1.16	m				
Bo	150	mm	0.15	m	tb	13 mm	0.013	m
Ho	150	mm	0.15	m	th	10 mm	0.01	m
Area	6380	mm²	0.00638	m²				
Volume	7,400,800.00	mm³	0.0074008	m³				
Mass			57.7	kg	Mass of 4 beams		230.90	kg
Ixx	19,485,166.67	mm⁴	1.94852E-05	m⁴				

Mechanical Properties (AK Steel)

ρ	7,800.00	kg/m³		
σy	1172	MPa	1,172,000,000.00	Pa
E	197	GPa	1.97E+11	Pa

Force Analysis

F1	882,900.00	N	@	1.077	m
F2	1,234,833.75	N	@	0.79	m
F3	351,933.75	N	@	0.07	m

Sum of vertical forces

F3 - F2 + F1 = 0
F2 = F1+F3   ..... (1)

Sum of Moments about A

F2(x) - F1(x + Support1/2 + Stroke + Overlap - 0.083) = 0	.... (2)
(F1 + F3)(x) - F1(x + Support1/2 + Stroke + Overlap - 0.083) = 0	(1) in (2)
F3 = (F1(x + Support1/2 + Stroke + Overlap - 0.083) - F1(x))/x	
F3 351,933.75 N	

Force Diagrams

x	V	M
m	N	Nm
0	0	0
0.07	0	0
0.07	351,933.75	-
0.79	351,933.75	253,392.30
0.79 -	882,900.00	253,392.30
1.08 -	882,900.00	-
1.08	-	-
1.16	-	-

Shear Force Diagram

Moment Diagram

The calculations performed in the portion of the spreadsheet shown below are mostly the same as that of the solid beam. The first column shows the discrete points along the beam height where the stresses are calculated with the blue entries showing the areas where the shear stress is equal to the average shear stress calculated at the centroid of the top and bottom plates. The moment of inertia, shear force, moment and tensile stresses are calculated as before. The extract shown beneath the table below forms part of the table below and is simply cut off to show more clearly. In this portion of the spreadsheet the height is taken at the centre of the bottom plate, the centre of the beam and the centre of the top plate all measured from the bottom of the beam. The shear force is then calculated at each of these points using standard calculation methods. It is known that the shear distribution should be parabolic and the equation of a parabolic curve is therefore derived beneath the three shear stresses. The turning point of the parabola is defined by p and is equal to the centre height of the beam due to the beam symmetry. At the turning point the maximum shear stress will be present as calculated at the beam centre and assigned to the variable q according to the parabolic equation. Another point on the curve is needed to fix the equation and the height of the centre of the bottom plate is assigned to, x, with its corresponding shear stress assigned to, y. The variable, a, can now be solved and the equation of the curve established. The values of the discrete points along the beam height, h, are fed into the parabolic equation to deliver the associated shear stress in column 5 and 6 in the table below. From these values the shear stress distribution graph on the left, the tensile stress distribution graph in the centre and the $\sigma_{element}$ vs. σ_y^2 graph on the right on the next page is generated. The values of the plate thicknesses were then manipulated using the scroll bars along with the overall external dimensions of the beam to obtain as flat a red curve on the rightmost graph all located beneath the blue line as possible. This resulted in an adequately strong beam with a more equal stress distribution and lower weight in comparison to the solid beam.

Shear stress							Compressive stresses				
				$\tau = VQ/It$			$\sigma = Mc/I$				
h	I	V	M	τ	τ	σ	σ	σY^2	$\sigma_{element}$	SF	$\sigma_{element}{}^{0.5}$
m	m⁴	N	N/m	Pa	Mpa	Pa	MPa	MPa²	MPa²		MPa
0	1.94852E-05	882,900.00	253,392.30	334258643.82	334.26	975,327,685.16	975.33	1373584	1,286,450.62	1.07	1,134.22
0.0050	1.94852E-05	882,900.00	253,392.30	334258643.82	334.26	910,305,839.48	910.31	1373584	1,163,843.24	1.18	1,078.82
0.01	1.94852E-05	882,900.00	253,392.30	364999879.44	365.00	845,283,993.81	845.28	1373584	1,114,179.77	1.23	1,055.55
0.02	1.94852E-05	882,900.00	253,392.30	419650964.97	419.65	715,240,302.45	715.24	1373584	1,039,889.49	1.32	1,019.75
0.03	1.94852E-05	882,900.00	253,392.30	465193536.25	465.19	585,196,611.10	585.20	1373584	991,670.15	1.39	995.83
0.04	1.94852E-05	882,900.00	253,392.30	501627593.28	501.63	455,152,919.74	455.15	1373584	962,054.91	1.43	980.84
0.05	1.94852E-05	882,900.00	253,392.30	528953136.05	528.95	325,109,228.39	325.11	1373584	945,070.27	1.45	972.15
0.06	1.94852E-05	882,900.00	253,392.30	547170164.56	547.17	195,065,537.03	195.07	1373584	936,236.13	1.47	967.59
0.07	1.94852E-05	882,900.00	253,392.30	556278678.81	556.28	65,021,845.68	65.02	1373584	932,565.75	1.47	965.69
0.08	1.94852E-05	882,900.00	253,392.30	556278678.81	556.28	- 65,021,845.68	- 65.02	1373584	932,565.75	1.47	965.69
0.09	1.94852E-05	882,900.00	253,392.30	547170164.56	547.17	- 195,065,537.03	- 195.07	1373584	936,236.13	1.47	967.59
0.1	1.94852E-05	882,900.00	253,392.30	528953136.05	528.95	- 325,109,228.39	- 325.11	1373584	945,070.27	1.45	972.15
0.11	1.94852E-05	882,900.00	253,392.30	501627593.28	501.63	- 455,152,919.74	- 455.15	1373584	962,054.91	1.43	980.84
0.12	1.94852E-05	882,900.00	253,392.30	465193536.25	465.19	- 585,196,611.10	- 585.20	1373584	991,670.15	1.39	995.83
0.13	1.94852E-05	882,900.00	253,392.30	419650964.97	419.65	- 715,240,302.45	- 715.24	1373584	1,039,889.49	1.32	1,019.75
0.14	1.94852E-05	882,900.00	253,392.30	364999879.44	365.00	- 845,283,993.81	- 845.28	1373584	1,114,179.77	1.23	1,055.55
0.145	1.94852E-05	882,900.00	253,392.30	334258643.82	334.26	- 910,305,839.48	- 910.31	1373584	1,163,843.24	1.18	1,078.82
0.15	1.94852E-05	882,900.00	253,392.30	334258643.82	334.26	- 975,327,685.16	- 975.33	1373584	1,286,450.62	1.07	1,134.22

h	τ	τ	yA	y	A	y	A
m	MPa	Pa	m³	m	m²	m	m²
0.0050	334.2586438	334258643.8	0.0000959	0.07	0.00137		
0.0750	557.4172431	557417243.1	0.00015993	0.07	0.00124	0.0375	0.000975
0.1450	334.2586438	334258643.8	0.0000959				

y = a(x-p)2 + q		Parabolic equation for known turning point					
p	0.075						
q	557417243.1						
y	334258643.8						
x	0.0050						
a	-45542571281						

	tb		th	Mass	
	mm		mm	kg	
	13		10	57.73	
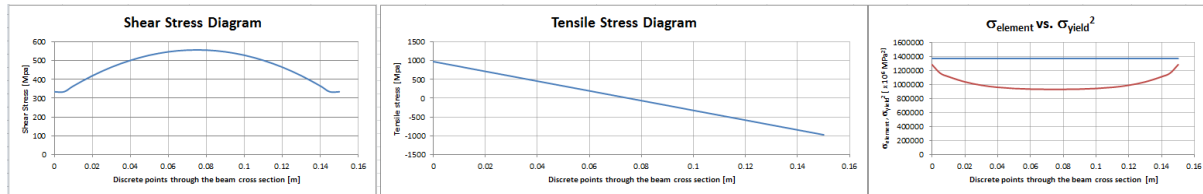
Above from left the shear stress distribution, tensile stress distribution and $\sigma_{element}$ vs. σ_y^2 graph is presented for discrete values through the box section. The Mohr circle for the beam is calculated below and the circle presented at the end of the section. The calculations are the same as with the solid beam and calculated at the top of the beam where the average shear stress throughout the top plate is present.

Mohr circle

σx	975.33	MPa
σy	0	MPa
τxy	334.26	MPa
$\sigma 1$	1078.89	Mpa
$\sigma 2$	-103.56	MPa
τmax	591.22	MPa
θ	17.21	°

Maximum distortion Energy Theory

$\sigma element$	1,286,450.62	MPa
σy^2	1,373,584.00	Mpa
SF	1.07	
R	591.22	Mpa

Midpoint

X	Y
487.663843	0

Plot circle

		X	Y
0	0	1078.887036	0
10	0.174532925	1069.905027	-102.6648301
20	0.34906585	1043.231915	-202.2102413
30	0.523598776	999.6781473	-295.6115967
40	0.698131701	940.5670845	-380.0309432
50	0.872664626	867.6947858	-452.9032419
60	1.047197551	783.2754392	-512.0143047
70	1.221730476	689.8740839	-555.568072
80	1.396263402	590.3286727	-582.2411846
90	1.570796327	487.6638426	-591.2231933
100	1.745329252	384.9990125	-582.2411846
110	1.919862177	285.4536013	-555.568072
120	2.094395102	192.0522459	-512.0143047
130	2.268928028	107.6328994	-452.9032419
140	2.443460953	34.76060069	-380.0309432
150	2.617993878	-24.35046215	-295.6115967
160	2.792526803	-67.90422943	-202.2102413
170	2.967059728	-94.57734197	-102.6648301
180	3.141592654	-103.5593507	-7.24336E-14
190	3.316125579	-94.57734197	102.6648301
200	3.490658504	-67.90422943	202.2102413
210	3.665191429	-24.35046215	295.6115967
220	3.839724354	34.76060069	380.0309432
230	4.01425728	107.6328994	452.9032419
240	4.188790205	192.0522459	512.0143047
250	4.36332313	285.4536013	555.568072

260	4.537856055	384.9990125	582.2411846
270	4.71238898	487.6638426	591.2231933
280	4.886921906	590.3286727	582.2411846
290	5.061454831	689.8740839	555.568072
300	5.235987756	783.2754392	512.0143047
310	5.410520681	867.6947858	452.9032419
320	5.585053606	940.5670845	380.0309432
330	5.759586532	999.6781473	295.6115967
340	5.934119457	1043.231915	202.2102413
350	6.108652382	1069.905027	102.6648301
360	6.283185307	1078.887036	1.44867E-13
0	0	1078.887036	0

Plot line

X	Y
487.6638426	0
975.3276852	-334.2586438
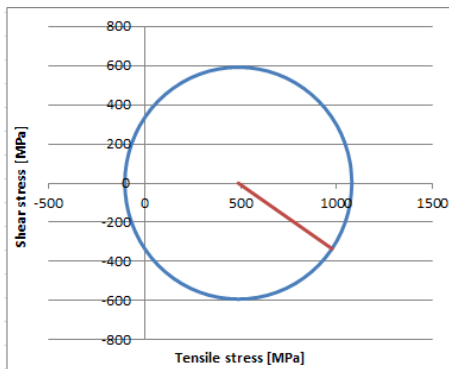
APPENDIX D. EES PROGRAM - SIDE MOUNT SUPPORTS SAME SIDE EXTENDED BASE

This appendix presents an extract from the EES program entitled "Side mount supports same side extended base" in which the strength of the components constituting the fixture that connects the support frame to the Transom are calculated. Both the programming and solutions are presented.

1. FORMATTED EQUATIONS

The formatted equations presented below are grouped under seven headings and a group without a heading at the top of the program. The program uses the force on the front support (F2) as an input value as this is the greatest value to which the system will be exposed. The material data required in the program is also included at the top of the program with the square of the yield in MPa. Throughout the program Standard International (SI) units are used. The first heading groups all the geometrical calculations where the thicknesses and heights of the components were changed to influence the stresses until a satisfactory solution was found. The front support is connected to the top connecting plate and induces a tensile stress throughout the plate as it is connected to the top beam at its base. A shear stress is also generated where the support want to tear away from the top connecting plate. The maximum stress will thus be in the centre of the plate where both the shear stress and tensile stress is a maximum as shown in chapter 5.

$$F2 = 1.23483 \times 10^{6}$$

$$E = 197 \cdot 10^{9}$$

$$\sigma_{yield2} = 1172^{2}$$

Geometry

$$Bo_{Clamp,Beam} = \frac{150}{1000}$$

$$t_{liner} = \frac{5}{1000}$$

$$h_{support} = \frac{40}{1000}$$

$$b_{support} = \left[0.065 + \frac{t_{Top,Web}}{2} - 0.024 \right] \cdot 2$$

$$h_{Top,Web} = \frac{320}{1000}$$

$$h_{Top,T,Web} = \frac{250}{1000}$$

$$h_{Bottom,Web} = \frac{300}{1000}$$

$$b_{Top,Base} = \frac{370}{1000}$$

$$t_{Top,T,Web} = \frac{20}{1000}$$

$$t_{Top,Web} = \frac{20}{1000}$$

$$t_{Top,Base} = \frac{20}{1000}$$

$$t_{Bottom,Web} = \frac{20}{1000}$$

$$t_{Bottom,Base} = \frac{20}{1000}$$

Top Connecting plate

$$\sigma_{tensile,Pull,TCP} = \frac{2 \cdot \dfrac{F_{SP1,y}}{t_{Top,Web} \cdot b_{Top,Base}}}{10^6}$$

$$\tau_{TCP} = \frac{1.5 \cdot \dfrac{F_{SP1,y}}{t_{Top,Web} \cdot h_{Top,Web}}}{10^6}$$

$$\sigma_{element,TCP} = \sigma_{tensile,Pull,TCP}^2 + 3 \cdot \tau_{TCP}^2$$

$$SF_{TCP} = \frac{\sigma_{yield2}}{\sigma_{element,TCP}}$$

The top connecting plate transfers a share of the total load to the top beam which is connected with bolts to the Transom. The beam is therefore modelled as a cantilever beam as if it is clamped at the first bolt in the bolt block. This assumption was made to obtain a simple approximation for the beam deflection. The deflection of the beam is dependent upon its stiffness and the ratio between the stiffness of the top beam and the bottom beam determines the load sharing between the beams. The approximation will be slightly in error as the support is assumed rigid and will in reality stretch somewhat, the top and bottom beams assumed as cantilever beams will also experience some stretch in the bolts and deflection along the webs. The approximation provides a feel for the forces distribution. The length between the first bolt in the bolt block and the top connecting plate is used to calculate the moment expected in the top beam. Because the top beam has a T section a neutral axis is first calculated followed by the moment of inertia. As shown in chapter 5 there are two locations where the stress can be a maximum and this is either at the top of the beam where the tensile stress is the greatest or at the neutral axis where the shear stress is the greatest. The stresses at both these locations are calculated and the associated safety factors calculated based on the derived maximum distortion energy equation presented in chapter 5. The deflection of the end of the beam where the top connecting plate is attached is calculated as $\delta1$.

Top Beam

$$L_{Lever,Top,Beam} = 0.06$$

$$M_{Top,Beam,xx} = 2 \cdot F_{SP1,y} \cdot L_{Lever,Top,Beam}$$

$$Yneutral_{Top,T} = \frac{b_{Top,Base} \cdot t_{Top,Base} \cdot \dfrac{t_{Top,Base}}{2} + t_{Top,T,Web} \cdot (h_{Top,T,Web} - t_{Top,Base}) \cdot \left[\dfrac{h_{Top,T,Web} - t_{Top,Base}}{2} + t_{Top,Base}\right]}{b_{Top,Base} \cdot t_{Top,Base} + (h_{Top,T,Web} - t_{Top,Base}) \cdot t_{Top,T,Web}}$$

$$Ixx_{Top,Beam} = \frac{1}{12} \cdot b_{Top,Base} \cdot t_{Top,Base}^3 + b_{Top,Base} \cdot t_{Top,Base} \cdot \left[Yneutral_{Top,T} - \frac{t_{Top,Base}}{2}\right]^2$$

$$+ \frac{1}{12} \cdot t_{Top,T,Web} \cdot (h_{Top,T,Web} - t_{Top,Base})^3 + t_{Top,T,Web} \cdot (h_{Top,T,Web} - t_{Top,Base}) \cdot \left[\frac{h_{Top,T,Web} - t_{Top,Base}}{2} + t_{Top,Base} - Yneutral_{Top,T}\right]^2$$

$$\sigma_{tensile,Top,Beam,xx,1} = \frac{M_{Top,Beam,xx} \cdot \left[\dfrac{h_{Top,T,Web} - Yneutral_{Top,T}}{Ixx_{Top,Beam}}\right]}{10^6}$$

$$\sigma_{element,Top,Beam,1} = \sigma_{tensile,Top,Beam,xx,1}^2$$

$$SF_{Top,Beam,1} = \frac{\sigma_{yield2}}{\sigma_{element,Top,Beam,1}}$$

$$\tau_{Top,Beam,Base,F,SP1,y} = \frac{2 \cdot F_{SP1,y} \cdot \left[b_{Top,Base} \cdot t_{Top,Base} \cdot \left(Yneutral_{Top,T} - \dfrac{t_{Top,Base}}{2}\right) + t_{Top,T,Web} \cdot (Yneutral_{Top,T} - t_{Top,Base}) \cdot \left(\dfrac{Yneutral_{Top,T} - t_{Top,Base}}{2}\right)\right]}{Ixx_{Top,Beam} \cdot t_{Top,Base} \cdot 10^6}$$

$$\sigma_{element,Top,Beam,2} = 3 \cdot \tau_{Top,Beam,Base,F,SP1,y}^2$$

$$SF_{Top,Beam,2} = \frac{\sigma_{yield2}}{\sigma_{element,Top,Beam,2}}$$

$$\delta1 = \frac{2 \cdot F_{SP1,y} \cdot L_{Lever,Top,Beam}^3}{3 \cdot E \cdot Ixx_{Top,Beam}}$$

The support is also connected to a bottom beam through a bottom connecting plate with a height of 300 mm which is equal to the existing brackets previously used on the Transom. The bottom connecting plate is affixed to the support at the one end and to the bottom beam at the other end and is therefore modelled according to the approximation of a cantilever beam. The reality will differ somewhat from this approximation as the bottom beam can twist and will therefore experience a little more deflection than what is calculated. The length of the bottom connecting plate modelled as a beam is calculated first followed by the moment and the beam's moment of inertia. Because of the forces imposed on the plate the stresses can be maximal at either one of two positions, at the top of the beam where the tensile stress is at its maximum or at the centre of the beam where the shear stress is at its maximum as illustrated in chapter 5. Both the shear stress and tensile stress is calculated at these positions and the safety factors calculated. The deflection of the beam end affixed to the support is now calculated relative to the end affixed to the bottom beam as $\delta21$. A continuity equation is obtained stating that the deflection of the point on the support where the bottom connecting plate is attached must be equal to the displacement of the top connecting plate because the support is assumed not to stretch. The displacement of the point where the bottom connecting plate attaches is due to both the deflection of the bottom connecting plate ($\delta21$) and the deflection of the bottom beam ($\delta22$). The next continuity equation states that the total force on the support (F2) must be resisted by the two forces acting on the top beam through the top connecting plate and the bottom beam acting through the bottom connecting plate.

Bottom Connecting Plate

$$L_{lever,BCP} = \frac{\frac{370}{2} - 35 - 9.1}{1000} - t_{Bottom,Base}$$

$$M_{BCP} = F_{SP2,y} \cdot L_{lever,BCP}$$

$$Ixx_{BCP} = \frac{1}{12} \cdot t_{Bottom,Web} \cdot h_{Bottom,Web}^{3}$$

$$\sigma_{tensile,BCP} = \frac{M_{BCP} \cdot \frac{h_{Bottom,Web}}{2 \cdot Ixx_{BCP}}}{10^{6}}$$

$$\tau_{BCP} = \frac{\frac{1.5 \cdot F_{SP2,y}}{t_{Bottom,Web} \cdot h_{Bottom,Web}}}{10^{6}}$$

$$\sigma_{element,BCP,1} = \sigma_{tensile,BCP}^{2}$$

$$\sigma_{element,BCP,2} = 3 \cdot \tau_{BCP}^{2}$$

$$SF_{BCP,1} = \frac{\sigma_{yield2}}{\sigma_{element,BCP,1}}$$

$$SF_{BCP,2} = \frac{\sigma_{yield2}}{\sigma_{element,BCP,2}}$$

$$\delta21 = \frac{F_{SP2,y} \cdot L_{lever,BCP}^{3}}{3 \cdot E \cdot Ixx_{BCP}}$$

$$\delta1 = \delta21 + \delta22$$

$$F_{SP2,y} + F_{SP1,y} = F2$$

The bottom connecting plate transfers the share of the load not carried by the top beam to the bottom beam which is also modelled as a cantilever beam with a length equal to the distance between the centre of the connecting plate and the bolt block. Apart from the shear force and moment the beam is also subjected to a torque. After calculation of the stress at the top edge of the beam and the moment of inertia a ratio is calculated which is used to select the correct k_2 factor from the Advanced mechanics of materials book [39]. This is then used to calculate the shear stress due to the torque on the beam. As shown in chapter 5 the stress can be a maximum at either the top of the beam due to tensile stress or in the centre of the beam next to the longest edge due to shear stress induced by the shear force and shear stress induced by the torque. After completing the safety factor calculations the displacement of the beam edge where the connecting plate is attached is calculated relative to the edge secured by the bolt block as δ_{22}.

Bottom Beam

$$L_{Lever,Bottom,Beam} = 0.03 + \frac{t_{Bottom,Web}}{2}$$

$$M_{Bottom,Beam,y} = F_{SP2,y} \cdot L_{Lever,Bottom,Beam}$$

$$Iyy_{Bottom,Beam} = \frac{1}{12} \cdot t_{Bottom,Base} \cdot h_{Bottom,Web}^{3}$$

$$\sigma_{tensile,Bottom,Beam,y,1} = \frac{M_{Bottom,Beam,y} \cdot \frac{h_{Bottom,Web}}{2 \cdot Iyy_{Bottom,Beam}}}{10^{6}}$$

$$Ratio_{Bottom,Beam,Base} = \frac{h_{Bottom,Web}}{t_{Bottom,Base}}$$

$$k_2 = 0.312$$

$$\tau_{max,Bottom,Beam,Torque} = \frac{\frac{M_{BCP}}{k_2 \cdot h_{Bottom,Web} \cdot t_{Bottom,Base}^{2}}}{10^{6}}$$

$$\tau_{Bottom,Beam,FSP2,y,2} = \frac{\frac{1.5 \cdot F_{SP2,y}}{h_{Bottom,Web} \cdot t_{Bottom,Base}}}{10^{6}}$$

$$\sigma_{element,Bottom,Beam,1} = \sigma_{tensile,Bottom,Beam,y,1}^{2}$$

$$SF_{Bottom,Beam,1} = \frac{\sigma_{yield2}}{\sigma_{element,Bottom,Beam,1}}$$

$$\sigma_{element,Bottom,Beam,2} = 3 \cdot (\tau_{max,Bottom,Beam,Torque} + \tau_{Bottom,Beam,FSP2,y,2})^{2}$$

$$SF_{Bottom,Beam,2} = \frac{\sigma_{yield2}}{\sigma_{element,Bottom,Beam,2}}$$

$$\delta_{22} = \frac{F_{SP2,y} \cdot L_{Lever,Bottom,Beam}^{3}}{3 \cdot E \cdot Iyy_{Bottom,Beam}}$$

The decision was made to use high strength Huckbolts to resist loosening under vibration and with the resistance provided by a bolt known the force that must be resisted by bolts is calculated in kN. The number of bolts required is simply the force that must be resisted divided by the resistance provided by a bolt. The assumption is used that all the bolts carry the same loading where in reality the bolts closest to the edge connected to the front support will carry the most. Due to the large safety factor this assumption is considered fair.

Bolts on top Beam

$$F_{Bolts,tension} = 2 \cdot \frac{F_{SP1,y}}{1000}$$

$$F_{Bolt,Resistance,tension} = 82.5$$

$$N_{bolts,tension} = \frac{F_{Bolts,tension}}{F_{Bolt,Resistance,tension}}$$

Similar to the calculations above the force in shear that needs to be resisted is calculated and divided by the shear resistance provided by a bolt to obtain the number of bolts required. The shear resistance per bolt takes account for a friction grip and will thus resist the beam slipping.

Bolts in shear at bottom beam

$$F_{Bolts,shear} = \frac{F_{SP2,y}}{1000}$$

$$F_{Bolt,Resistance,Shear} = 30.4$$

$$N_{boltws,shear} = \frac{F_{Bolts,shear}}{F_{Bolt,Resistance,Shear}}$$

2. RESULTS

The extract below provides the answers to the variables calculated above. All the safety factors are highlighted in yellow and can be seen to exceed 1 by far except for the bottom beam which is at 1.25 indicating safety factors far in excess of the required 10. The thicknesses of the plates were varied until one of the beams' safety factor was as close as possible to 1 and the same thickness plate used all over to minimise the number of different thickness plates required. The thicknesses and heights also determine the load share and is therefore larger than needed to simply handle the stress at most points.

Unit Settings: SI C kPa kJ mass deg

$Bo_{Clamp,Beam} = 0.15$	$b_{support} = 0.102$	$b_{Top,Base} = 0.37$	$\delta 1 = 0.00001196$
$F2 = 1.235E+06$	$F_{Bolts,shear} = 173.7$	$F_{Bolts,tension} = 2122$	$F_{Bolt,Resistance,Shear} = 30.4$
$h_{Bottom,Web} = 0.3$	$h_{support} = 0.04$	$h_{Top,T,Web} = 0.25$	$h_{Top,Web} = 0.32$
$k_2 = 0.312$	$L_{Lever,BCP} = 0.1209$	$L_{Lever,Bottom,Beam} = 0.04$	$L_{Lever,Top,Beam} = 0.06$
$N_{bolts,tension} = 25.72$	$N_{boltws,shear} = 5.714$	$Ratio_{Bottom,Beam,Base} = 15$	$SF_{BCP,1} = 280.3$
$SF_{TCP} = 5.129$	$SF_{Top,Beam,1} = 9.656$	$SF_{Top,Beam,2} = 1.256$	$\sigma_{element,BCP,1} = 4901$
$\sigma_{element,TCP} = 267803$	$\sigma_{element,Top,Beam,1} = 142258$	$\sigma_{element,Top,Beam,2} = 1.093E+06$	$\sigma_{tensile,BCP} = 70.01$
$\sigma_{yield2} = 1.374E+06$	$\tau_{BCP} = 43.43$	$\tau_{Bottom,Beam,FSP2,y,2} = 43.43$	$\tau_{max,Bottom,Beam,Torque} = 561$
$t_{Bottom,Web} = 0.02$	$t_{liner} = 0.005$	$t_{Top,Base} = 0.02$	$t_{Top,T,Web} = 0.02$
$\delta_{21} = 0.00001154$	$\delta_{22} = 4.180E-07$	$E = 1.970E+11$	
$F_{Bolt,Resistance,tension} = 82.5$	$F_{SP1,y} = 1.061E+06$	$F_{SP2,y} = 173714$	
$Ixx_{BCP} = 0.000045$	$Ixx_{Top,Beam} = 0.00006485$	$Iyy_{Bottom,Beam} = 0.000045$	
$M_{BCP} = 21002$	$M_{Bottom,Beam,y} = 6949$	$M_{Top,Beam,xx} = 127334$	
$SF_{BCP,2} = 242.8$	$SF_{Bottom,Beam,1} = 2560$	$SF_{Bottom,Beam,2} = 1.253$	
$\sigma_{element,BCP,2} = 5658$	$\sigma_{element,Bottom,Beam,1} = 536.5$	$\sigma_{element,Bottom,Beam,2} = 1.096E+06$	
$\sigma_{tensile,Bottom,Beam,y,1} = 23.16$	$\sigma_{tensile,Pull,TCP} = 286.8$	$\sigma_{tensile,Top,Beam,xx,1} = 377.2$	
$\tau_{TCP} = 248.7$	$\tau_{Top,Beam,Base,F,SP1,y} = 603.7$	$t_{Bottom,Base} = 0.02$	
$t_{Top,Web} = 0.02$	$Yneutral_{Top,T} = 0.05792$		

APPENDIX E. SPREADSHEET BASED CALCULATIONS - SIDE MOUNT SUPPORT

In this chapter the Microsoft Excel document titled, "Side mount support calculations" is used to calculate the stresses in the front and rear support frames.

1. FRONT SUPPORT

The force transferred to the front support from the clamp beam when the conveyance settles onto the supporting steelwork is equal to F2 and works in at the top beam section of the support. This contact area is therefore calculated as a beam with a distributed loading summing to the magnitude of F2. The spreadsheet is used to input values for the beam height and width that were changed to come to a beam geometry where the stresses are maintained at a satisfactory level. The length of the beam is due to the width of the clamp beam and the liners used between the support and the beam. Important material properties are also provided and geometry based calculations such as the moment of inertia performed. With the assumption that the beam behaves as a beam clamped at both ends, thus that the legs are rigid, the distributed loading, reaction forces and moments at the beam-leg juncture was calculated in accordance with the shear, moment and deflection equations for beams presented in Appendix D-1 of the book Fundamentals of machine component design [35]. The shear force and moment was calculated at discrete points along the beam length starting at the left beam-leg juncture.

Beam Properties					Support Mass				
L	160	mm	0.16	m				b	h
h	40	mm	0.04	m	Asolid	172800	mm^2	240	720
b	80	mm	0.08	m	Acutout	89600	mm^2	160	560
σy	1172	MPa	1172000000	Pa	Atotal	83200	mm^2	mm	mm
E	197	GPa	1.97E+11	Pa		0.0832	m^2		
Ixx	426666.6667	mm^4	4.26667E-07	m^4	V	0.006656	m^3		
					ρ	7800	kg/m^3		
Distributed load					Mass	51.9	kg		
F	- 1,234,833.75	N							
w	- 7,717,710.94	N/m							
FL	wL/2	- 617,416.88	N						
FR	wL/2	- 617,416.88	N						
ML	,-wL^2/12	16,464.45	Nm						
MR	wL^2/12	- 16,464.45	Nm						

Force distribution

x	V	M
m	N	Nm
0	0	0
0	- 617,416.88	16,464.45
0.01	- 540,239.77	10,676.17
0.02	- 463,062.66	5,659.65
0.03	- 385,885.55	1,414.91
0.04	- 308,708.44	- 2,058.06
0.05	- 231,531.33	- 4,759.26
0.06	- 154,354.22	- 6,688.68
0.07	- 77,177.11	- 7,846.34
0.08	-	- 8,232.23
0.09	77,177.11	- 7,846.34
0.1	154,354.22	- 6,688.68
0.11	231,531.33	- 4,759.26
0.12	308,708.44	- 2,058.06
0.13	385,885.55	1,414.91
0.14	463,062.66	5,659.65
0.15	540,239.77	10,676.17
0.16	617,416.88	16,464.45
0.16	-	-

The calculated values at the discrete points along the beam were used to generate the shear force distribution graph shown below on the left and the moment diagram shown below on the right. These graphs show how the forces and moments along the beam vary and assist to show the cross section where the shear force and moment is a maximum in this case next to the beam-leg junctures.
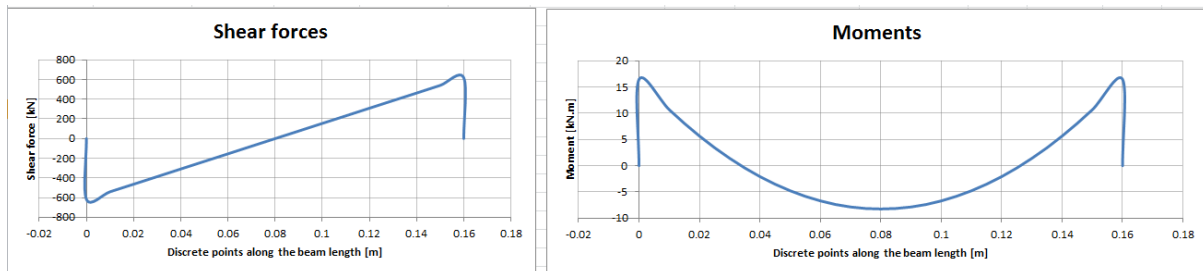
Knowing the position of the cross section exposed to the greatest load and moment allows the stresses at that section to be calculated at discrete points along its height. The method used for the calculations are the same as that for the calculations in appendix C. Again a parabolic equation is derived for the shear stress distribution and used to calculate the shear stresses at the discrete points along the beam height. The spreadsheet extract below shows the calculations of the discrete points (h), the moment of inertia (I), the shear force (V), the moment (M), the shear stresses (τ), the tensile stresses (σ), the square of the yield stress (σY), $\sigma_{element}$ and the safety factors. It shows that the safety factors are in excess of 2 and thus in reality in excess of 20 indicating that a thinner plate can be used as a beam. The thicker plate is however used to match the thickness plate required in the leg section.

Stress Analysis Beam section

h	I	V	M	τ	τ	σ	σ	sY	σelement	SF	σelement$^{0.5}$
m	m^4	N	N/m	Pa	Mpa	Pa		Mpa	MPa^2	MPa^2		MPa
0	4.26667E-07	617,416.88	16,464.45	0.00	0	771,771,093.75	771.77	1373584	595,630.62	2.31	771.77
0.01	4.26667E-07	617,416.88	16,464.45	217060620.12	217.0606201	385,885,546.88	385.89	1373584	290,253.59	4.73	538.75
0.02	4.26667E-07	617,416.88	16,464.45	289414160.16	289.4141602	-	-	1373584	251,281.67	5.47	501.28
0.03	4.26667E-07	617,416.88	16,464.45	217060620.12	217.0606201 -	385,885,546.88 -	385.89	1373584	290,253.59	4.73	538.75
0.04	4.26667E-07	617,416.88	16,464.45	0.00	0 -	771,771,093.75 -	771.77	1373584	595,630.62	2.31	771.77

h	τ	τ	yA	y	A	
m	MPa	Pa	m^3	m	m^2	
0	0	0	-	0.02	0	1.5V/A
0.02	289.41	289,414,160.16	0.000016	0.01	0.0016	289,414,160.16
0.04	0	0	-			

y = a(x-p)2 + q						
p	0.02		h			
q	289,414,160.16			40 mm		
y	0					
x	-					
a	-7.23535E+11					

Below on the left a graph is shown illustrating the tensile stress throughout the beam height at the discrete points. The centre graph shows the shear stress distribution throughout the beam height and the rightmost graph a comparison between the square of the yield stress in blue and $\sigma_{element}$ in red. It can be seen that the red curve is below the blue line indicating an excessively strong beam.
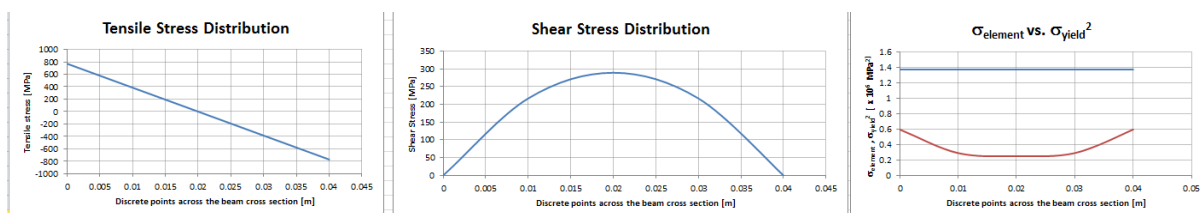
The forces carried over to the support frame legs induce stresses as calculated below. The leg is assumed to have a constant tensile force throughout equal to the support reaction at the beam-leg juncture. For simplicity the beams further down the leg section is assumed pin connected such that the moment is constant throughout the beam. Both these simplifying assumptions vary from reality in that the leg is not completely rigid and will have different tensile stresses throughout changing at the points where the top connecting plate and bottom connecting plate attaches. The beams are also not pin connected but will resist some of the moment as will the connections to the top and bottom connecting plate resulting in a different internal moment along the leg length. For stress calculations only the maximum tensile stress and moment is of interest and this more complex tensile and internal moment distribution further down the leg is not of major importance in determining an adequately strong leg profile. Due to the excessive safety factor a slight error attributed to this simplification should not be a concern. Below the tensile stress is calculated and added to the tensile stress caused by the internal moment and compared with the material's yield strength to obtain a safety factor. At a safety factor of 1 an odd material thickness is obtained and the plate thickness is rounded up to 40 mm. The graph below illustrates this tensile stress distribution across the height of the leg profile.

Stress Analysis Leg section					
Moment is constant throughout					
Tensile stress is constant throughout					
bleg	80	mm		0.08	m
hleg	40	mm		0.04	m
Ixx	426666.6667	mm^4		4.26667E-07	m^4
σmoment	Mc/I	@	c		0.02 m
	771771093.8	Pa		771.7710938	MPa
σtensile	F/A				
	192,942,773.44	Pa		192.9427734	Mpa
σsum	964.7138672				
SF	σy/(σmoment + σtensile)				
	1.21				
Stress profile					
x	σ				
m	MPa				
0	964.7138672				
0.02	192.9427734				
0.04	-578.8283203				

Leg Stresses

Tensile stress [MPa] vs Discrete points across the leg section's cross section [m]
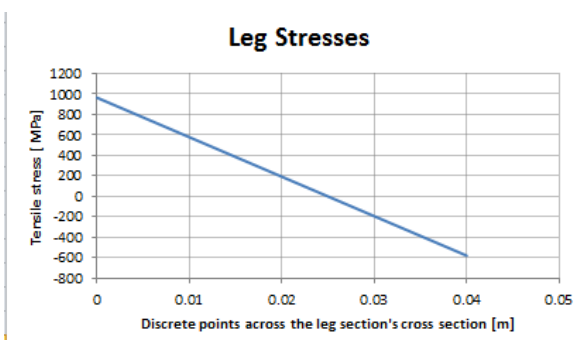
2. REAR SUPPORT

The calculations for the rear supports are similar to that of the front support. The rear support however experiences a smaller force (F3) pushing down on the support. With this load configuration consideration is also given to buckling. The decision was made to manufacture the rear support from the same material and to the same dimensions as that of the front support in order to minimise the number of different thickness plates required, to minimize the different setting on machines and to provide a symmetrical design that cannot accidentally be installed the wrong way around. The beam properties are thus the same and the force analysis and distribution determined the same as with the front support. A graph showing the shear stress distribution along the beam length is provided below on the left and a graph showing the moment distribution along the beam length on the right.

Beam Properties					Support Mass				b	h	
L	160	mm	0.16	m							
h	40	mm	0.04	m	Asolid	172800	mm²		240		720
b	80	mm	0.08	m	Acutout	89600	mm²		160		560
σy	1172	MPa	1172000000	Pa	Atotal	83200	mm²	mm	mm		
E	197	GPa	1.97E+11	Pa		0.0832	m²				
Ixx	426666.6667	mm⁴	4.26667E-07	m⁴	V	0.006656	m³				
					ρ	7800	kg/m³				
Force Analysis					Mass	51.9	kg				
F	351,933.75	N									
w	2,199,585.94	N/m									
FL	wL/2		175,966.88	N							
FR	wL/2		175,966.88	N							
ML	,-wL²/12	-	4,692.45	Nm							
MR	wL²/12		4,692.45	Nm							

Force distribution

x	V		M	
m	N		Nm	
0	0		0	
0	175,966.88	-	4,692.45	
0.01	153,971.02	-	3,042.76	
0.02	131,975.16	-	1,613.03	
0.03	109,979.30	-	403.26	
0.04	87,983.44		586.56	
0.05	65,987.58		1,356.41	
0.06	43,991.72		1,906.31	
0.07	21,995.86		2,236.25	
0.08	-		2,346.23	
0.09	-	21,995.86	2,236.25	
0.1	-	43,991.72	1,906.31	
0.11	-	65,987.58	1,356.41	
0.12	-	87,983.44	586.56	
0.13	-	109,979.30	-	403.26
0.14	-	131,975.16	-	1,613.03
0.15	-	153,971.02	-	3,042.76
0.16	-	175,966.88	-	4,692.45
0.16	-		-	

Shear Force Diagram

Moment Diagram
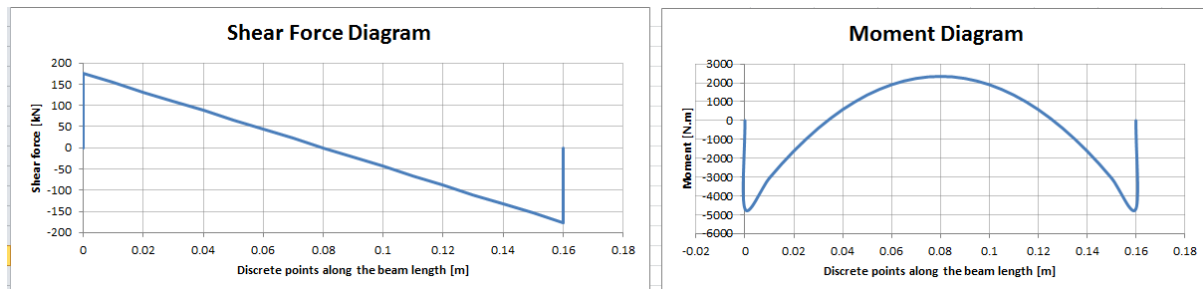
The stress analysis is performed exactly the same also making use of a parabolic equation. Because the beam geometry is the same as that of the front support and the force acting on the beam considerably less an excessive safety factor is found at all the discrete points along the beam height. The tensile stress at the various points is shown on a graph below on the left, the shear stress at the points on the graph in the centre and the comparison between the square of the yield stress and $\sigma_{element}$ on the right.

Stress Analysis Beam section

h	I	V	M	τ	τ	σ	σ	σY	σelement	SF
m	m^4	N	N/m	Pa	MPa	Pa	Mpa	MPa^2	MPa^2	
0	4.26667E-07	175,966.88	4,692.45	0.00	0	219,958,593.75	219.96	1373584	48,381.78	28.39
0.01	4.26667E-07	175,966.88	4,692.45	61863354.49	61.86335449	109,979,296.88	109.98	1373584	23,576.67	58.26
0.02	4.26667E-07	175,966.88	4,692.45	82484472.66	82.48447266	-	-	1373584	20,411.06	67.30
0.03	4.26667E-07	175,966.88	4,692.45	61863354.49	61.86335449	- 109,979,296.88	- 109.98	1373584	23,576.67	58.26
0.04	4.26667E-07	175,966.88	4,692.45	0.00	0	- 219,958,593.75	- 219.96	1373584	48,381.78	28.39

h	τ	τ	yA	y	A		
m	MPa	Pa	m^3	m	m^2		
0	0	0	-	0.0200	0	1.5 V/A	
0.0200	82.48	82,484,472.66	0.000016	0.0100	0.0016	82484473	
0.040	0	0	-			Pa	

$y = a(x-p)2 + q$

p	0.02	h	
q	82,484,472.66	40 mm	
y	0		
x	-		
a	-2.06211E+11		

Tensile Stress Distribution

Shear Stress Distribution

$\sigma_{element}$ vs. σ_{yield}^2
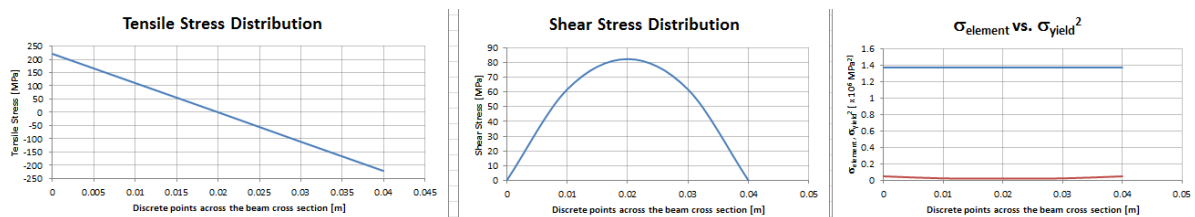
The stress in the rear support legs differs from that of the front support as buckling needs to be considered. Because buckling can occur about either the X-X axis or the Y-Y axis both I_{xx} and I_{yy} is calculated. Looking at buckling about the Y-Y axis the leg is considered as a column fixed at the base and free at the top as the entire frame will buckle in line with the clamp beam. The calculations show that a 3.1 x10^3 kN force is required to buckle the column about the Y-Y axis which is in excess of the force experienced in the leg indicating that the beam is safe from buckling about the Y-Y axis.

Stress Analysis Leg section

Moment is constant throughout
Tensile stress is constant throughout

bleg	80	mm	0.08	m	
hleg	40	mm	0.04	m	"Increased to 40 to match Front support"
Ixx	426666.6667	mm^4	4.26667E-07	m^4	
Iyy	1706666.667	mm^5	1.70667E-06	m^5	
A	3200	mm^2	0.0032	m^2	

About the yy axis

K	2			"Free end at top and fixed at the bottom"
L	520	mm	0.52 m	
Pcr	$\pi^2 EI/(KL)^2$	3,067,948.03	N	

When considering bending about the X-X axis it is taken into consideration that the column has a slight eccentric loading in that the reaction force is determined at the edge of the clamp beam a small distance from the centre of the leg. To bring this eccentric loading into consideration the secant formula is used on the column assumed to be braced at the position of the beam above the bottom clamp beam. Comparing the stress in the leg with the maximum allowed that will initiate buckling it can be seen that the stress is beneath this threshold value and will not buckle about the X-X axis.

About the xx axis

K	0.7			"Braced thus assume pin connected"
L	520	mm	0.52 m	
M	4692.45	Nm		
P	175,966.88	N		
e	0.03	m		
r	$(I/A)^{0.5}$	0.011547005 m		
c	0.02	m		
σmax	$(P/A)(1+(ec/r^2)sec((L/2r)((P/EA)^{0.5})))$			"pg 718 Hibbeler"
	282,801,576.18	Pa	282.80	Mpa
SF	σy/σmax	4.14		

When the bottom clamp beam is loaded a force equal in magnitude is imposed on the beam above the bottom clamp beam and the stresses in that beam is therefore exactly the same as that in the beam beneath the top clamp beam considered above. The leg section is however exposed to a tensile stress due to the pull and a tensile stress due to the internal moment. These stresses are calculated the same as those in the front support and provided below. A graph showing the tensile stresses in the legs are provided at the bottom.

When the lower beam is loaded					
Support beam					
"The forces is exactly the same and thus the support beam is the same"					
Stress Analysis Leg section					
Moment is constant throughout					
Tensile stress is constant throughout					
FL	175,966.88	N			
ML	4692.45	Nm			
bleg	80	mm		0.08	m
hleg	40	mm		0.04	m
Ixx	426666.6667	mm^4		4.26667E-07	m^4
A	3200	mm^2		0.0032	m^2
σmoment	Mc/I		@	c		0.02	m
	219958593.8	Pa		219.9585938	MPa
σtensile	F/A				
	54,989,648.44	Pa		54.98964844	Mpa
SF	σy/(σmoment + σtensile)				
	4.3			274.9482422	Mpa
Stress profile					
x	σ				
0	274.9482422				
0.02	54.98964844				
0.04	-164.9689453				

Tensile Stresses in Support Leg
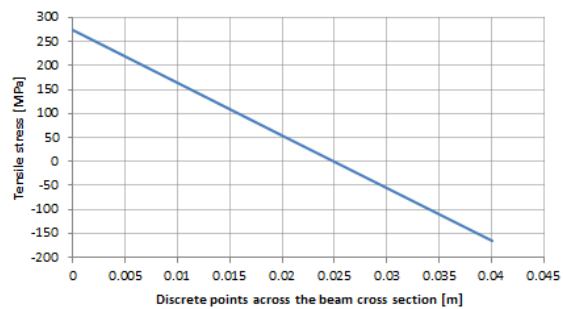
APPENDIX F. EES PROGRAM - REAR SUPPORT

In this appendix an EES program entitled "Rear support" is provided that was used to calculate the dimensions and stresses of the support fixtures required to secure the support frames such that the clamp beams are able to extend from the rear of the conveyance. Placing the device in this position has the advantage that the support steelwork is free of clamp brackets. Ultimately this layout was discarded in favour of the layout described in the previous appendixes due to the strength limitations on the conveyance roof beams and Transom.

1. PROGRAM

A previous version of the excel program "clamp beam two supports" were used to calculate the magnitude of F2 the force on the rear support and F5 the force on the front support. These forces are larger than that in the previous section as a shorter beam was considered. The layout of the fixture has the front and rear support frame bolted to a bottom beam with the ends of the beam bolted to the I-beam next to the trap door and the channel at the rear edge of the conveyance roof. The top of the support frames are then bolted to a channel beam that extends to the Transom where it is joined with a bolted connection. The graph of the displacements provides an illustration of the layout.

To calculate the forces at the various points continuity equations are derived. It is known that the displacement of the top beam at the point where the rear support is affixed $\delta 1$ must be equal to the displacement of the rear support $\delta 2$ and that of the displacement of the bottom beam at the base of the rear support $\delta 3$. Similar the displacement of the top beam at the point where the front beam is affixed $\delta 4$ should be equal to the sum of the displacement of the front support frame $\delta 5$ and the displacement of the bottom beam at the base of the front support $\delta 6$.

Known Constraints and forces

$$F2 = 482146 \quad \text{From Clamp Beam Two Supports}$$

$$F5 = 1.36505 \times 10^{6} \quad \text{From Clamp Beam Two Supports}$$

$$\delta 1 = \delta 2 + \delta 3$$

$$\delta 4 = \delta 5 + \delta 6$$

The calculations associated with the bottom beam are presented on the next page. The length from the leftmost edge of the bottom beam is calculated to both the rear support (L1), front support (L2) and to the end of the beam (L3) connected to the channel on the conveyance's roof rear edge. The width of the beam corresponds to the width of the support frame and the height to the minimum thickness plate required to secure an M20 bolt used to fasten the supports to the bottom beam. With this geometry known the moment of inertia, cross sectional area, volume and mass of the bottom beam is calculated using the material properties provided. The bottom beam is assumed pin connected at the ends where the left end connected to the I-beam next to the trap door experiences a force F8 and the end connected to the channel at the conveyance's roof edge a force of F9. The force from the rear support (F3) and from the front support (F6) is summed along with the forces on the beam ends to obtain vertical equilibrium. An equation is also generated for the moments due to these forces about the left end of the beam where F8 works in. These forces will cause a deflection in the beam where $\delta 3$ corresponds to the vertical displacement of the bottom beam at the base of the rear support and $\delta 6$ to the vertical displacement of the bottom beam at the front support. These deflections are calculated by taking into consideration the deflection caused at each point ($\delta 3_1$, $\delta 3_2$, $\delta 6_1$ and $\delta 6_2$) by both forces F3 and F6.

Bottom Beam afixed to conveyance roof

$L1 = L2 - 0.6$ L2 - x from Clamp Beam Two Supports

$L2 = L3 - 0.03 - \dfrac{b_{support,leg}}{2}$ L3 - overlap - half of support leg

$L3 = 1.5 - 0.759$ Drawing 000 M-05488

$b_{Bottom,Beam} = 2 \cdot 0.04 + 0.15 + 2 \cdot 0.005$

40 mm x 2 for legs + width of clamp beam +2 x 5 mm for liners

$h_{Bottom,Beam} = 0.015$

Minimum thickness since a thread length of 18 mm is required as with a M20
nut plus the increased tap length to accomodate bolt stretch

$I_{Bottom,Beam} = \dfrac{1}{12} \cdot b_{Bottom,Beam} \cdot h_{Bottom,Beam}^3$

$Area_{Bottom,Beam} = b_{Bottom,Beam} \cdot h_{Bottom,Beam}$

$Volume_{Bottom,Beam} = Area_{Bottom,Beam} \cdot L3$

$Mass_{Bottom,Beam} = Volume_{Bottom,Beam} \cdot \rho_{Bottom,Beam}$

$E_{Bottom,Beam} = 197 \cdot 10^9$

$\rho_{Bottom,Beam} = 7800$

$sigmaY_{Bottom,Beam} = 1172$

$sigmaY2_{Bottom,Beam} = sigmaY_{Bottom,Beam}^2$

$F8 - F3 + F6 - F9 = 0$

$F3 \cdot L1 - F6 \cdot L2 + F9 \cdot L3 = 0$

$\delta3_1 = \dfrac{-1 \cdot F3 \cdot L1 \cdot (L3 - L1)}{6 \cdot E_{Bottom,Beam} \cdot I_{Bottom,Beam} \cdot L3} \cdot (L3^2 - L1^2 - (L3 - L1)^2)$

$\delta6_1 = \dfrac{-1 \cdot F3 \cdot L1 \cdot (L3 - L2)}{6 \cdot E_{Bottom,Beam} \cdot I_{Bottom,Beam} \cdot L3} \cdot (L3^2 - L1^2 - (L3 - L2)^2)$

$\delta3_2 = \dfrac{F6 \cdot (L3 - L2) \cdot L1}{6 \cdot E_{Bottom,Beam} \cdot I_{Bottom,Beam} \cdot L3} \cdot (L3^2 - (L3 - L2)^2 - L1^2)$

$\delta6_2 = \dfrac{F6 \cdot (L3 - L2) \cdot L2}{6 \cdot E_{Bottom,Beam} \cdot I_{Bottom,Beam} \cdot L3} \cdot (L3^2 - (L3 - L2)^2 - L2^2)$

$\delta3 = \delta3_2 + \delta3_1$

$\delta6 = \delta6_2 + \delta6_1$

The stresses throughout the bottom beam is calculated at discrete points throughout the bottom beam height denoted as *hxBottom,Beam*. An equation is presented to calculate the tensile stress at the discrete points using the maximum Bottom Beam Moment (BBM$_5$) found at position 5. The shear stress is calculated at the bottom edge of the beam and at the beam centre then used to generate a parabolic equation to calculate the shear stress at any point in the bottom beam. With equations for the shear stress and tensile stress throughout the beam the safety factor can be calculated at any discrete point along the height of the beam. These stress calculations are provided below.

Bottom Beam Stresses

$h_{x,Bottom,Beam} = 0.01$

$\sigma_{Bottom,Beam} = \dfrac{|BBM_5| \cdot \left[\dfrac{h_{Bottom,Beam}}{2} - h_{x,Bottom,Beam} \right]}{\dfrac{I_{Bottom,Beam}}{10^6}}$

$h_{x,Bottom,Beam,1} = 0$

$\tau_{Bottom,Beam,1} = 0$

$h_{x,Bottom,Beam,3} = \dfrac{h_{Bottom,Beam}}{2}$

$$\tau_{Bottom,Beam,3} = 1.5 \cdot \frac{\left| BBS_5 \right|}{Area_{Bottom,Beam}}$$

$$p_{Bottom,Beam} = \frac{h_{Bottom,Beam}}{2}$$

$$q_{Bottom,Beam} = \tau_{Bottom,Beam,3}$$

$$a_{Bottom,Beam} = \frac{\tau_{Bottom,Beam,1} - q_{Bottom,Beam}}{\left(h_{x,Bottom,Beam,1} - p_{Bottom,Beam} \right)^2}$$

$$\tau_{Bottom,Beam} = \frac{a_{Bottom,Beam} \cdot \left(h_{x,Bottom,Beam} - p_{Bottom,Beam} \right)^2 + q_{Bottom,Beam}}{10^6}$$

$$sigmaE_{Bottom,Beam} = \sigma_{Bottom,Beam}^2 + 3 \cdot \tau_{Bottom,Beam}^2$$

$$SF_{Bottom,Beam} = \frac{sigmaY2_{Bottom,Beam}}{sigmaE_{Bottom,Beam}}$$

The top beam connecting the two support frames to the Transom is handled similar to the bottom beam. The beam length is calculated as the length from the centre of the Transom to the rear support (L4) and to the front support (L5). The channel beam is placed over the supports and must therefore be wider than the support width and the thicknesses were manipulated until the load share was such that the bottom beam carried its maximum allowable load. The height of the beam is such that it will fit over the supports with the sides of the channel resting on the Transom. Making use of the material properties and the geometry the cross sectional area, volume, mass, neutral axis, and moment of inertia of the beam were calculated. The beam is subjected to three forces; F7 at the Transom connection, F1 at the rear support and F4 at the front support. These forces were summed to give vertical equilibrium and their associated moments about the left end of the beam determined. The moments are summed about the end of the beam to obtain equilibrium. The deflections of the top beam at the rear support $\delta 1$ and at the front support $\delta 4$ were calculated by considering the deflections on the beam ($\delta 1_1$, $\delta 1_2$, $\delta 4_1$ and $\delta 4_2$) caused by the two forces F1 and F4.

Top beam afixed to the conveyance Transom

$$L4 = L1 + 0.759$$

$$L5 = L4 + 0.6$$

$$t_T = 0.04$$

$$b_T = 0.15 + 2 \cdot 0.04 + 2 \cdot 0.005 \quad \text{Must fit over the support} \quad \text{40 mm x 2 for legs + width of clamp beam +2 x 5 mm for liners}$$

$$t_B = 0.03$$

$$h_{Top,Beam} = \frac{h_{Bottom,Beam} \cdot 1000 + 15 + 25 + 5 + 155 + 330 + 155 + 5 + 40 - 417}{1000} + t_T$$

$$E_{Top,Beam} = 197 \cdot 10^9$$

$$sigmaY_{Top,Beam} = 1172$$

$$\rho_{Top,Beam} = 7800$$

$$Area_{web} = t_B \cdot h_{Top,Beam}$$

$$Area_{Flange} = b_T \cdot t_T$$

$$Volume_{Top,Beam} = \left(2 \cdot Area_{web} + Area_{Flange} \right) \cdot L5$$

$$Mass_{Top,Beam} = Volume_{Top,Beam} \cdot \rho_{Top,Beam}$$

$$Y_{neutral} = \frac{2 \cdot Area_{web} \cdot \frac{h_{Top,Beam}}{2} + Area_{Flange} \cdot \left[h_{Top,Beam} - \frac{t_T}{2} \right]}{2 \cdot Area_{web} + Area_{Flange}}$$

$$I_{Top,Beam} = 2 \cdot \left[\frac{1}{12} \cdot t_B \cdot h_{Top,Beam}^3 + Area_{web} \cdot \left(Y_{neutral} - \frac{h_{Top,Beam}}{2} \right)^2 \right] + \frac{1}{12} \cdot b_T \cdot t_T^3 + Area_{Flange} \cdot \left[h_{Top,Beam} - \frac{t_T}{2} - Y_{neutral} \right]^2$$

$$- F7 - F1 + F4 = 0$$

$$M1 + F1 \cdot L4 - F4 \cdot L5 = 0$$

$$\delta1_1 = \frac{-1 \cdot F1 \cdot L4^2}{6 \cdot E_{Top,Beam} \cdot I_{Top,Beam}} \cdot (3 \cdot L4 - L4)$$

$$\delta4_1 = \frac{-1 \cdot F1 \cdot L4^2}{2 \cdot E_{Top,Beam} \cdot I_{Top,Beam}} \cdot (L5 - L4) + \delta1_1$$

$$\delta1_2 = \frac{F4 \cdot L4^2}{6 \cdot E_{Top,Beam} \cdot I_{Top,Beam}} \cdot (3 \cdot L5 - L4)$$

$$\delta4_2 = \frac{F4 \cdot L5^2}{6 \cdot E_{Top,Beam} \cdot I_{Top,Beam}} \cdot (3 \cdot L5 - L5)$$

$$\delta1 = \delta1_1 + \delta1_2$$

$$\delta4 = \delta4_1 + \delta4_2$$

An equation is presented for the tensile stress at any discrete distance, *hxTop,Beam*, through the beam cross section as determined at position 2 along the beam's length where the Top Beam Moment (TBM2) is at its maximum. The shear flow was calculated at various positions to determine the shear stresses at various heights across the top beam cross section in order to generate a parabolic equation that is used to determine the shear stress at any position across the cross section. The stresses at these positions are then summed as per the Maximum Distortion Energy Theory and used to calculate the safety factors at any arbitrary position on the beam cross section.

Top Beam stresses

$$h_{x,Top,Beam} = 0$$

$$\sigma_{Top,Beam} = \frac{|TBM_2| \cdot \left[\dfrac{Y_{neutral} - h_{x,Top,Beam}}{I_{Top,Beam}}\right]}{10^6}$$

Shear flow at various positions

$$Q_1 = \left[h_{Top,Beam} - Y_{neutral} - \frac{t_T}{2}\right] \cdot t_T \cdot (b_T + t_B)$$

$$\tau_{sf,1} = \frac{|TBS_5| \cdot Q_1}{I_{Top,Beam} \cdot t_B}$$

$$Q_2 = 2 \cdot \left[\left(\frac{h_{Top,Beam} - Y_{neutral}}{2}\right) \cdot t_B \cdot (h_{Top,Beam} - Y_{neutral})\right] + \left[h_{Top,Beam} - Y_{neutral} - \frac{t_T}{2}\right] \cdot t_T \cdot b_T$$

$$\tau_{sf,2} = \frac{|TBS_5| \cdot Q_2}{I_{Top,Beam} \cdot t_B}$$

$$Q_3 = 2 \cdot \left[h_{Top,Beam} - \frac{h_{Top,Beam}}{4} - Y_{neutral}\right] \cdot \frac{h_{Top,Beam}}{2} \cdot t_B + \left[h_{Top,Beam} - Y_{neutral} - \frac{t_T}{2}\right] \cdot t_T \cdot b_T$$

$$\tau_{sf,3} = \frac{|TBS_5| \cdot Q_3}{I_{Top,Beam} \cdot t_B}$$

$$\tau_{sf,1} = a \cdot \left[h_{Top,Beam} - \frac{t_T}{2}\right]^2 + b \cdot \left[h_{Top,Beam} - \frac{t_T}{2}\right] + c$$

$$\tau_{sf,2} = a \cdot Y_{neutral}^2 + b \cdot Y_{neutral} + c$$

$$\tau_{sf,3} = a \cdot \left[\frac{h_{Top,Beam}}{2}\right]^2 + b \cdot \frac{h_{Top,Beam}}{2} + c$$

$$\tau_{Top,Beam} = \frac{a \cdot h_{x,Top,Beam}^2 + b \cdot h_{x,Top,Beam} + c}{10^6}$$

Combined stresses and SF

$$sigmaY2_{Top,Beam} = sigmaY_{Top,Beam}^2$$

$$sigmaE_{Top,Beam} = \sigma_{Top,Beam}^2 + 3 \cdot \tau_{Top,Beam}^2$$

$$SF_{Top,Beam} = \frac{sigmaY2_{Top,Beam}}{sigmaE_{Top,Beam}}$$

The support frame legs were split into two lengths L6 and L7 respectively where L6 is loaded in tension and L7 in compression for the rear support and L6 in compression and L7 in tension for the front support. Further it is known that the forces imposed on the supports from the clamp beams way back at the beginning of the program must be resisted by the force acting between the top beam and the support and the bottom beam and the support. These relationships provide the final continuity equations. Due to the tensile and compression forces on the support frame legs the frame either elongates or compresses and this is taken into consideration in the final displacement of the beams. This program therefore accounts for all the component deflections and calculates the force distribution throughout the system based on the component's stiffness. The program further calculates the stresses across the beams' cross sections at the maximally loaded positions.

Rear support

$L6 = 0.04$

$$L7 = \frac{15 + 25 + 5 + 155 + 330 + 155 + 5 + 40}{1000} - L6$$

$b_{support,leg} = 0.135$

$h_{support,leg} = 0.04$

$A_{support,leg} = b_{support,leg} \cdot h_{support,leg}$

$E_{support,leg} = 197 \cdot 10^9$

$F1 + F3 = F2$

$$\delta2_1 = F2 \cdot \frac{L6}{A_{support,leg} \cdot E_{support,leg}}$$

$$\delta2_2 = \frac{-F2 \cdot L7}{A_{support,leg} \cdot E_{support,leg}}$$

$\delta2 = \delta2_1 + \delta2_2$

Front support

$F4 + F6 = F5$

$$\delta5_1 = -1 \cdot F5 \cdot \frac{L6}{A_{support,leg} \cdot E_{support,leg}}$$

$$\delta5_2 = \frac{F5 \cdot L7}{A_{support,leg} \cdot E_{support,leg}}$$

$\delta5 = \delta5_1 + \delta5_2$

Various graphs are generated by the program and the data presented in the table on the next page is used for the generation of the displacement, Top beam shear force, Top Beam moment, Bottom Beam shear force and Bottom beam moment diagrams.

Graphics	Rear support	Top Beam Shear Force Diagram	Bottom Beam Shear Force Diagram
Top Beam displacement	$x3_1 = x2_2$	$TBS_1 = 0$	$BBS_1 = 0$
$x1_1 = 0$	$y3_1 = y2_2$	$TBS_2 = -F7$	$BBS_2 = F8$
$y1_1 = 0 + 0.1$	$x3_2 = x1_2$	$TBS_3 = -F7$	$BBS_3 = BBS_2$
$x1_2 = L4$	$y3_2 = y1_2$	$TBS_4 = -F7 - F1$	$BBS_4 = F8 - F3$
$y1_2 = \delta1 + 0.1$	**Front support**	$TBS_5 = -F7 - F1$	$BBS_5 = BBS_4$
$x1_3 = L5$	$x4_1 = x2_3$	$TBS_6 = -F7 - F1 + F4$	$BBS_6 = F8 - F3 + F6$
$y1_3 = \delta4 + 0.1$	$y4_1 = y2_3$	**Top Beam Moment Diagram**	$BBS_7 = BBS_6$
Bottom Beam Displacement	$x4_2 = x1_3$	$TBM_1 = 0$	$BBS_8 = F8 - F3 + F6 - F9$
$x2_1 = 0.759$	$y4_2 = y1_3$	$TBM_2 = M1$	**Bottom Beam Moment Diagram**
$y2_1 = 0$	**Top Beam x axis**	$TBM_3 = M1 - F7 \cdot L4$	$BBM_1 = 0$
$x2_2 = x2_1 + L1$	$TB_1 = 0$	$TBM_4 = TBM_3$	$BBM_2 = 0$
$y2_2 = \delta3$	$TB_2 = 0$	$TBM_5 = M1 - F7 \cdot L5 - F1 \cdot (L5 - L4)$	$BBM_3 = F8 \cdot L1$
$x2_3 = x2_1 + L2$	$TB_3 = L4$	$TBM_6 = TBM_5$	$BBM_4 = BBM_3$
$y2_3 = \delta6$	$TB_4 = L4$	**Bottom Beam x axis**	$BBM_5 = F8 \cdot L2 - F3 \cdot (L2 - L1)$
$x2_4 = x2_1 + L3$	$TB_5 = L5$	$BB_1 = 0$	$BBM_6 = BBM_5$
$y2_4 = 0$	$TB_6 = L5$	$BB_2 = 0$	$BBM_7 = F8 \cdot L3 - F3 \cdot (L3 - L1) + F6 \cdot (L3 - L2)$
		$BB_3 = L1$	$BBM_8 = BBM_7$
		$BB_4 = BB_3$	
		$BB_5 = L2$	
		$BB_6 = BB_5$	
		$BB_7 = L3$	
		$BB_8 = BB_7$	

The extract from the program provided below gives the results off all the calculations performed. The forces calculated are given in yellow and compared to the allowable limits of the beams used in the conveyance roof. The beam geometries were varied in discrete 1 mm intervals until the forces at F8 and F9 were as close as possible to the conveyance beam limits.

Unit Settings: SI C kPa kJ mass deg

(Table 1, Run 10)

$a = -3.101E{+}09$	$Area_{Bottom,Beam} = 0.0036$	$Area_{Flange} = 0.0096$	$Area_{web} = 0.01104$
$b_{support,leg} = 0.135$	$b_T = 0.24$	$c = -2.785E{+}06$	$\delta1 = 0.004487$
$\delta2_2 = -0.0003127$	$\delta3 = 0.004782$	$\delta3_1 = 0.00253$	$\delta3_2 = 0.002252$
$\delta5_1 = -0.00005133$	$\delta5_2 = 0.0008854$	$\delta6 = 0.01091$	$\delta6_1 = 0.003134$
$F1 = 563382$	$F2 = 482146$ [N]	$F3 = -81236$	$F4 = 1.307E{+}06$
$F9 = 55471$	$h_{Bottom,Beam} = 0.015$ [m]	$h_{support,leg} = 0.04$	$h_{Top,Beam} = 0.368$
$I_{Bottom,Beam} = 6.750E{-}08$	$I_{Top,Beam} = 0.0004304$	$L1 = 0.0435$	$L2 = 0.6435$
$L7 = 0.69$	$M1 = 1.380E{+}06$	$Mass_{Bottom,Beam} = 20.81$	$Mass_{Top,Beam} = 346.6$
$q_{Bottom,Beam} = 1.214E{+}06$	$\rho_{Bottom,Beam} = 7800$ [kg/m^3]	$\rho_{Top,Beam} = 7800$	$SF_{Bottom,Beam} = 0.6986$
$sigmaY2_{Top,Beam} = 1.374E{+}06$	$sigmaY_{Bottom,Beam} = 1172$	$sigmaY_{Top,Beam} = 1172$	$\sigma_{Bottom,Beam} = -1402$
$\tau_{sf,1} = 1.249E{+}08$	$\tau_{sf,2} = 1.658E{+}08$	$\tau_{sf,3} = 1.583E{+}08$	$\tau_{Top,Beam} = 124.9$
$Y_{neutral} = 0.2337$			

$a_{Bottom,Beam} = -2.158E{+}10$	$A_{support,leg} = 0.0054$	$b = 1.446E{+}09$	$b_{Bottom,Beam} = 0.24$
$\delta1_1 = -0.001145$	$\delta1_2 = 0.005632$	$\delta2 = -0.0002946$	$\delta2_1 = 0.00001813$
$\delta4 = 0.01174$	$\delta4_1 = -0.002428$	$\delta4_2 = 0.01417$	$\delta5 = 0.0008341$
$\delta6_2 = 0.007775$	$E_{Bottom,Beam} = 1.970E{+}11$	$E_{support,leg} = 1.970E{+}11$	$E_{Top,Beam} = 1.970E{+}11$
$F5 = 1.365E{+}06$ [N]	$F6 = 58384$	$F7 = 743279$	$F8 = -84149$
$h_{x,Bottom,Beam} = 0.025$	$h_{x,Bottom,Beam,1} = 0$	$h_{x,Bottom,Beam,3} = 0.0075$	$h_{x,Top,Beam} = 0.348$
$L3 = 0.741$	$L4 = 0.8025$	$L5 = 1.403$	$L6 = 0.04$
$p_{Bottom,Beam} = 0.0075$	$Q_1 = 0.001234$	$Q_2 = 0.001638$	$Q_3 = 0.001564$
$SF_{Top,Beam} = 7.58$	$sigmaE_{Bottom,Beam} = 1.966E{+}06$	$sigmaE_{Top,Beam} = 181213$	$sigmaY2_{Bottom,Beam} = 1.374E{+}06$
$\sigma_{Top,Beam} = -366.6$	$\tau_{Bottom,Beam} = -5.395$	$\tau_{Bottom,Beam,1} = 0$	$\tau_{Bottom,Beam,3} = 1.214E{+}06$
$t_B = 0.03$	$t_T = 0.04$	$Volume_{Bottom,Beam} = 0.002668$	$Volume_{Top,Beam} = 0.04443$

2. PARAMETRIC TABLE FOR THE REAR SUPPORT

The parametric table provided below was used to calculate the tensile and shear stresses for both the top and bottom beams similar to that done in the Excel calculations in the previous appendixes. The $\sigma_{element}$ values, square of the yield stress and safety factors for the top and bottom beams are also calculated. The mass of both the beams and the magnitude of F8, F9 and F4 are shown. The parametric table is useful in showing the important data and for plotting the graphs of the stress distributions across the beam cross sections.

Table 1

	$h_{x,Bottom,Beam}$	$h_{x,Top,Beam}$	$\sigma_{Bottom,Beam}$	$\tau_{Bottom,Beam}$	sigmaE$_{Bottom,B}$	sigmaY2$_{Bottom,I}$	SF$_{Bottom,Beam}$	$\sigma_{Top,Beam}$
Run 1	0	0	600.9	-2.623E-15	361127	1.374E+06	3.804	749.5
Run 2	0.001667	0.04089	467.4	0.4795	218460	1.374E+06	6.288	618.4
Run 3	0.003333	0.08178	333.9	0.8392	111461	1.374E+06	12.32	487.2
Run 4	0.005	0.1227	200.3	1.079	40129	1.374E+06	34.23	356.1
Run 5	0.006667	0.1636	66.77	1.199	4463	1.374E+06	307.8	225
Run 6	0.008333	0.2044	-66.77	1.199	4463	1.374E+06	307.8	93.82
Run 7	0.01	0.2453	-200.3	1.079	40129	1.374E+06	34.23	-37.32
Run 8	0.01167	0.2862	-333.9	0.8392	111461	1.374E+06	12.32	-168.5
Run 9	0.01333	0.3271	-467.4	0.4795	218460	1.374E+06	6.288	-299.6
Run 10	0.015	0.368	-600.9	4.547E-19	361127	1.374E+06	3.804	-430.7

$\tau_{Top,Beam}$	sigmaE$_{Top,Beam}$	sigmaY2$_{Top,Bea}$	SF$_{Top,Beam}$	Mass$_{Bottom,Bea}$	Mass$_{Top,Beam}$	F8	F9	F4
-2.786	561825	1.374E+06	2.445	20.81	346.6	-84149	55471	1.307E+06
51.15	390259	1.374E+06	3.52	20.81	346.6	-84149	55471	1.307E+06
94.73	264331	1.374E+06	5.196	20.81	346.6	-84149	55471	1.307E+06
127.9	175912	1.374E+06	7.808	20.81	346.6	-84149	55471	1.307E+06
150.8	118803	1.374E+06	11.56	20.81	346.6	-84149	55471	1.307E+06
163.2	88743	1.374E+06	15.48	20.81	346.6	-84149	55471	1.307E+06
165.3	83405	1.374E+06	16.47	20.81	346.6	-84149	55471	1.307E+06
157.1	102397	1.374E+06	13.41	20.81	346.6	-84149	55471	1.307E+06
138.4	147261	1.374E+06	9.328	20.81	346.6	-84149	55471	1.307E+06
109.4	221475	1.374E+06	6.202	20.81	346.6	-84149	55471	1.307E+06

3. GRAPHS PORTRAYING IMPORTANT RESULTS OBTAINED FROM THE REAR SUPPORT EES PROGRAM

The graph below provides an illustration of the deflection of the system when viewed from the conveyance's right side. The black line shows the top beam where it is connected to the Transom at the vertical axis. The red line illustrates the rear support and the green line the front support. The blue line shows the displacement of the bottom beam. In order to enlarge the deflections so that they can be clearly seen the length of the support frames were reduced.
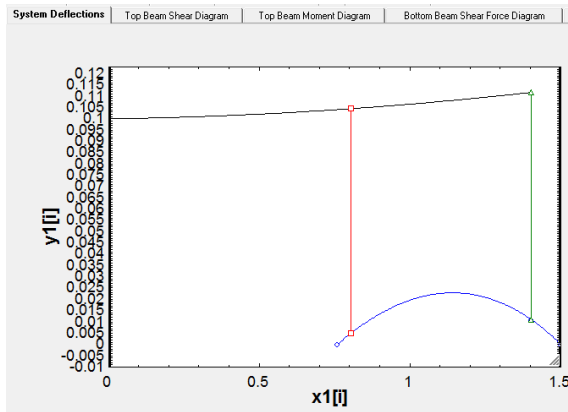
The graph below shows the shear force distribution along the top beam. The influence of the three forces F7 at the left end, F1 near the middle and F4 at the right end is clearly shown. The maximum shear force is found between force F1 and F4.
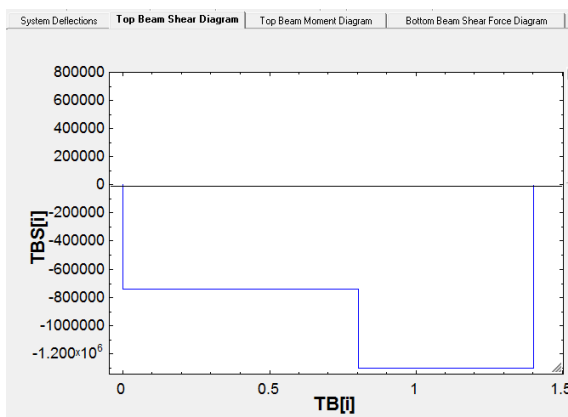
The graph below shows the moment distribution along the top beam. Because the beam is fixed at its left end the beam behaves as a cantilever beam with a force F4 acting in on the right end and a force F1 just right of the middle. Because the direction of the forces differ a decrease in the slope of the moment curve can be seen left of the point where F1 acts. The moment is thus a maximum at the clamped point on the left end of the beam.
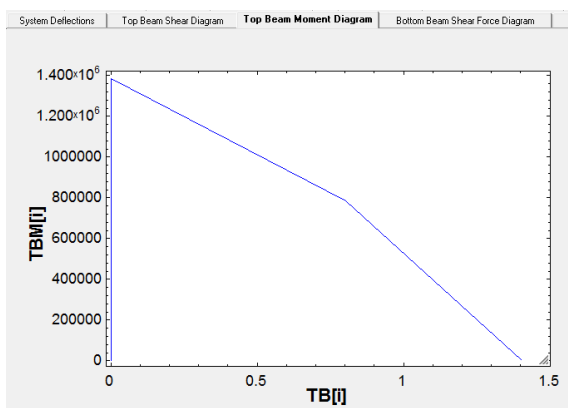
With the forces along the top beam known the tensile stresses and shear stresses across the cross section where the maximum shear force or moment acts can be calculated. The graph below shows the tensile stress distribution across the cross section of the top beam at point 2 adjacent to the left most end connected to the Transom where the moment is at its maximum value. Because of the asymmetry of the top beam it can be seen that the graph is not symmetrical about the vertical axis and that a large tensile stress is developed at the outer fibre of the channel beam's side panels.
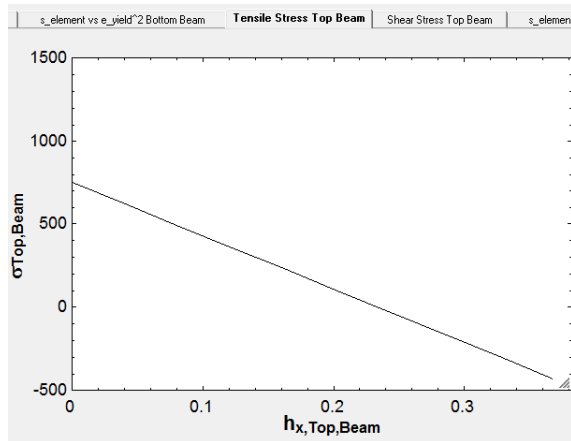
The graph below shows the shear stress distribution across the cross section of the top beam at point 5, adjacent to the point where force F4 acts, where the shear force is maximum. It can be seen that the shear stress has a parabolic curve as is expected. The curve seems lopsided and is due to the fact that the neutral axis of the channel section beam does not lie in the centre of the beam but closer to the flange. The rightmost value corresponds to the average shear stress in the flange. The stress therefore starts of at zero at the bottom of the beam in the outer fibres of the beam side panels and increases to a maximum at the neutral axis before declining to the average shear stress across the flange at the top of the beam.
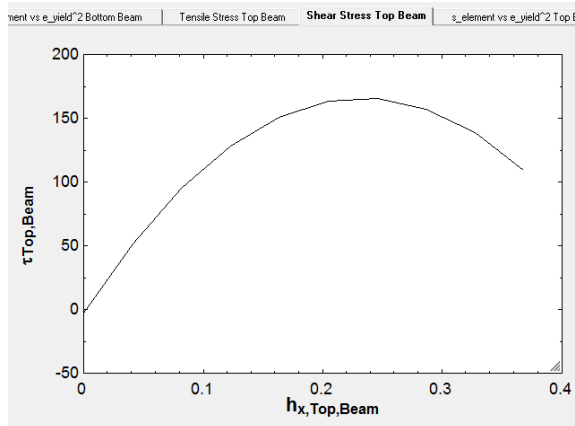
The graph below shows a comparison between the square of the yield stress and $\sigma_{element}$ across the top beam cross section and is slightly in error as the maximum tensile stress and shear stress is used even though they occur at different positions along the beam length. It can however be seen that even though larger stresses are used that what is found at a specific point that the distribution of $\sigma_{element}$ indicated by the black line remains beneath the blue line indicating the square of the yield stress. The beam is therefore more than adequately strong, but the dimensions cannot be decreased as the stiffness ratio must be maintained not to overload the bottom beam.
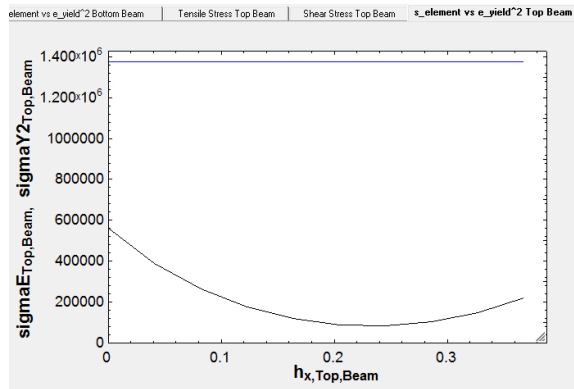
The graph below shows the shear force distribution along the bottom beam. The influence of the four forces F8 at the left end, F3 left of the middle, F6 right of the middle and F9 at the right end is clearly shown. The maximum shear force is found between force F8 and F3. It can further be seen that the reaction forces at the ends of the beam is downward while both supports pull upward on the bottom beam.
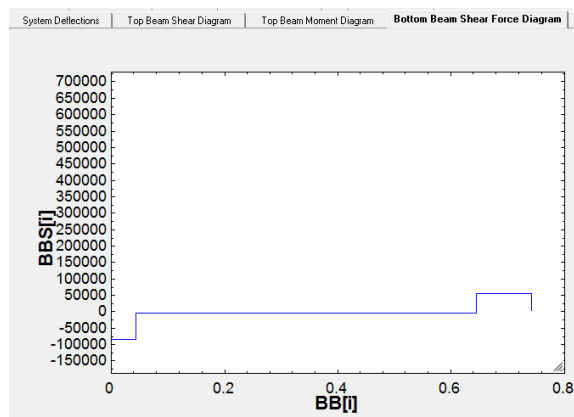
The graph below shows the moment distribution along the bottom beam. The beam behaves as a simply supported beam and therefore doesn't have a moment at the ends of the beam. The moment increases rapidly from the left end of the beam to the point where F3 acts after which it slightly increases to its maximum value at the point where F6 acts before decreasing to zero at the right end.
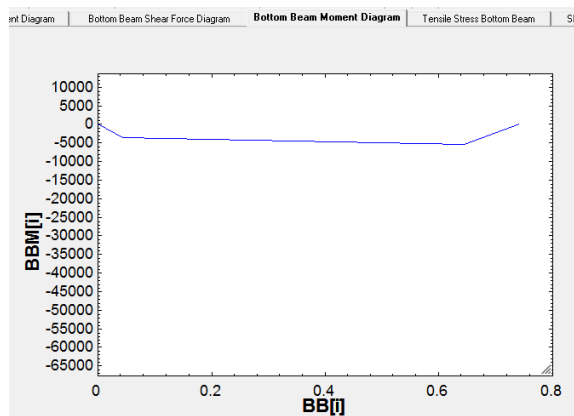
The graph below shows the tensile stress distribution across the cross section of the bottom beam at point 5 the location of force F6 where the moment is at its maximum value. It can be seen that the stress distribution is symmetrical about the vertical axis because the neutral axis is located at the centre of the beam. The outer fibres of the beam are therefore subjected to the same magnitude tensile and compression stress.
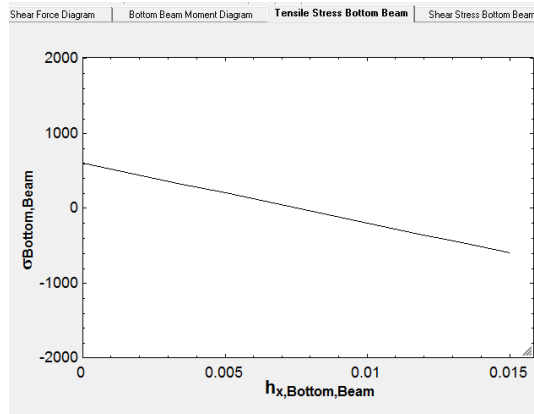
The graph below shows the shear stress distribution across the cross section of the bottom beam at point 5 the location of force F6 where the moment is at its maximum value. The shear stress distribution forms a symmetrical parabola about the centre of the beam.
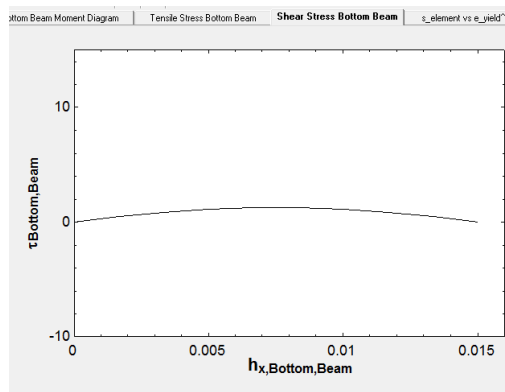
The graph below shows a comparison between the square of the yield stress and $\sigma_{element}$ for the bottom beam across the cross section located at point 5. It is shown that $\sigma_{element}$ indicated by the black line lies beneath the square of the yield strength blue line and that the bottom beam is therefore adequately strong. Even though the graph shows that the beam geometry is more that strong enough to resist the tensile and yield stresses it cannot be reduced as it must be thick enough for a screw to tighten properly. This is important because the base of the support needs to be fastened to the bottom beam by screws.
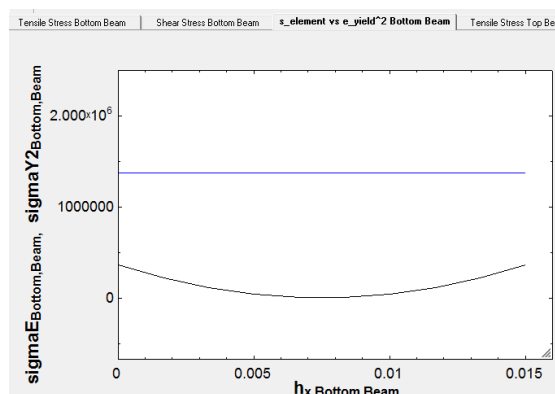
APPENDIX G. CONVEYANCE BEAM LIMITS

This appendix covers the calculations of the conveyance roof structure. The load carrying ability of the beams were calculated and used to determine whether the conveyance roof is able to support the conveyance arresting device.

1. CHANNEL AT THE REAR OF THE CONVEYANCE

The conveyance roof is constructed from Aluminium channels around the periphery with I-beams parallel to the Transom. The bottom beam supporting the partial load of the rear support fixture will be fastened to this channel beam at the rear of the conveyance and to the I-beam next to the trap door in the conveyance roof. The calculations below show the geometry of the channel and the mechanical properties of the 6061-T6 Aluminium from which it is constructed. Because two arresting devices are used symmetrically about the conveyance centre; forces of the same magnitude works in at 420 mm from either end of the conveyance. The graph on the left below shows the force distribution through the beam while the graph on the right shows the moments along the beam. The maximum shear force and moment is found at the point where the force acts and the tensile and shear stresses calculated in the same manner as in the previous appendixes. Two scroll bars are provided, one to increase the magnitude of the force acting on the beam and the second to change the position where the force acts. The magnitude of the force was increased until the red curve touched the blue line in the graph on the right. This indicated that a safety factor of 1 is obtained at a force of 90 kN. The beam can thus handle a maximum load of 90 kN and is therefore used as the limiting force for F9 in the preceding appendix.

Channel Geometric properties

t	9	mm	0.009	m
b	76	mm	0.076	m
h	178	mm	0.178	m
A	2808	mm^2	0.002808	m^2
Mass	7.6	kg/m	14.3	kg
L	1882	mm	1.882	m
I	12849096	mm^4	1.28491E-05	m^4

Mechanical Properties

ρ	2700	kg/m^3		
σY	276	MPa	276000000 Pa	(6061-T6)
E	68.9	GPa	68900000000 Pa	

Force Analysis

Force applied	90	kN	@	420 mm
	90000	N		0.42 m	from beam edge

x	V	M
m	N	Nm
0	0	0
0	-90000	0
0.42	-90000	37800
0.42	0	37800
1.462	0	37800
1.462	90000	37800
1.882	90000	0
1.882	0	0

Shear Force Diagram

Moment Diagram

						σ = Mc/I												
h	I	V	M	τ	τ	σ	σ	σY²	σelement	SF		h	τ	τ	yA	y	A	y	A
m	m⁴	N	Nm	Pa	MPa	Pa	MPa	MPa²	MPa²			m	MPa	Pa	m³	m	m²	m	m²
0	1.28491E-05	90000	37800	42318736	42.31874	2.62E+08	261.8239	76176	73924.36	1.030459		0.0045	42.31873589	42318736	5.43758E-05	0.0845	0.000644		
0.0045	1.28491E-05	90000	37800	42318736	42.31874	2.49E+08	248.5856	76176	67167.42	1.134121		0.089	67.39618102	67396181	0.000086598	0.0445	0.000801	0.0845	0.000603
0.01	1.28491E-05	90000	37800	45477014	45.47701	2.32E+08	232.4055	76176	60216.77	1.26503		0.1735	42.31873589	42318736	5.43758E-05				
0.02	1.28491E-05	90000	37800	50674957	50.67496	2.03E+08	202.987	76176	48907.59	1.55755									
0.03	1.28491E-05	90000	37800	55170477	55.17048	1.74E+08	173.5686	76176	39257.41	1.940423		y = a(x-p)2 + q	Parabolic equation for known turning point						
0.04	1.28491E-05	90000	37800	58963571	58.96357	1.44E+08	144.1502	76176	31209.39	2.440804									
0.05	1.28491E-05	90000	37800	62054240	62.05424	1.15E+08	114.7318	76176	24715.57	3.082105		p	0.089						
0.06	1.28491E-05	90000	37800	64442485	64.44248	85313395	85.31339	76176	19736.88	3.859577		q	67396181.02						
0.07	1.28491E-05	90000	37800	66128304	66.1283	55894983	55.89498	76176	16243.11	4.689743		y	42318735.89						
0.08	1.28491E-05	90000	37800	67111699	67.1117	26476571	26.47657	76176	14212.95	5.35962		x	0.0045						
0.09	1.28491E-05	90000	37800	67392669	67.39267	-2941841	-2.94184	76176	13633.97	5.587221		a	-3512124245						
0.1	1.28491E-05	90000	37800	66971214	66.97121	-3.2E+07	-32.3603	76176	14502.62	5.252569									
0.11	1.28491E-05	90000	37800	65847334	65.84733	-6.2E+07	-61.7787	76176	16824.22	4.527759									
0.12	1.28491E-05	90000	37800	64021030	64.02103	-9.1E+07	-91.1971	76176	20612.98	3.695535			Force		Position				
0.13	1.28491E-05	90000	37800	61492300	61.4923	-1.2E+08	-120.615	76176	25892.01	2.942066			N		mm				
0.14	1.28491E-05	90000	37800	58261146	58.26115	-1.5E+08	-150.034	76176	32693.25	2.330022			90,000.00		420				
0.15	1.28491E-05	90000	37800	54327567	54.32757	-1.8E+08	-179.452	76176	41057.59	1.855345									
0.16	1.28491E-05	90000	37800	49691563	49.69156	-2.1E+08	-208.871	76176	51034.73	1.49263									
0.17	1.28491E-05	90000	37800	44353134	44.35313	-2.4E+08	-238.289	76176	62683.31	1.215252									
0.1735	1.28491E-05	90000	37800	42318736	42.31874	-2.5E+08	-248.586	76176	67167.42	1.134121									
0.178	1.28491E-05	90000	37800	42318736	42.31874	-2.6E+08	-261.824	76176	73924.36	1.030459									

Shear Stress Distribution

Tensile Stress Distribution

$\sigma_{element}$ vs. σ_{yield}^2
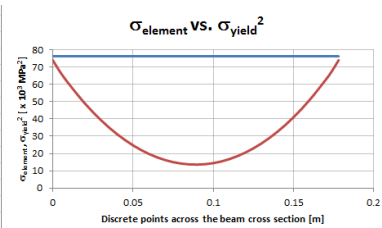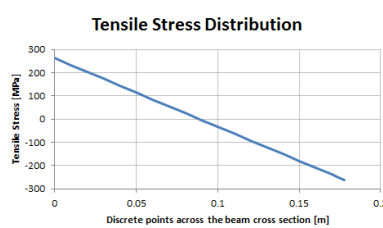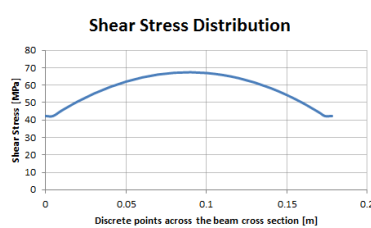
Shown above on the left is a graph illustrating the shear stress distribution through the channel section located at the conveyance roof edge at the position where the force acts. The centre graph shows the tensile stress distribution across the cross section where the force acts in on the channel section. The graph on the right is a comparison between the square of the yield stress and $\sigma_{element}$ showing that the beam has a safety factor of 1 when the applied load is equal to 90 kN.

2. I-BEAM POSITIONED NEXT TO THE TRAP DOOR

The exact same calculations were performed on the I-beam where the rear end of the bottom beam is connected. It is found that the beam can withstand a force of 120 kN. Force F8 in the preceding appendix is therefore allowed to go up to 120 kN before the beam's safety factor decreases to below 1.

I Beam Geometric properties			
t_{flange} (t1)	11.11 mm	0.01111 m	(Hulamin Databook)
t_{web} (t2)	7.94 mm	0.00794 m	
W (B)	101.6 mm	0.1016 m	
H (A)	177.8 mm	0.1778 m	
A	3492.8572 mm²	0.003492857 m²	
Mass	9.4 kg/m	17.7 kg	
L	1882 mm	1.882 m	
I	18196783.21 mm⁴	1.81968E-05 m⁴	
Mechanical Properties			
ρ	2700 kg/m³		
σY	276 MPa	276000000 Pa	(6061-T6)
E	68.9 GPa	68900000000 Pa	
Force Analysis			
Force applied	120 kN	@	420 mm
	120000 N		0.42 m	from beam edge

x	V	M
m	N	Nm
0	0	0
0	-120000	0
0.42	-120000	50400
0.42	0	50400
1.462	0	50400
1.462	120000	50400
1.882	120000	0
1.882	0	0

The graph below on the left illustrates the shear force distribution along the I-beam and the graph on the right the moment distribution along the I beam.

Shear Force Diagram   **Moment Diagram**

The results of the stress calculations shown above are displayed in the graphs below. The graph on the left shows the shear stress distribution across the I-beam cross section where the force works in. The centre graph shows the tensile stress distribution across the beam cross section and the rightmost graph a comparison between the square of the yield stress and $\sigma_{element}$. As shown above and displayed below it is seen that the I beam can carry 120 kN and thus the maximum allowed value of F8.

Shear Stress Distribution   **Tensile Stress Distribution** $\sigma_{element}$ vs. σ_{yield}^2
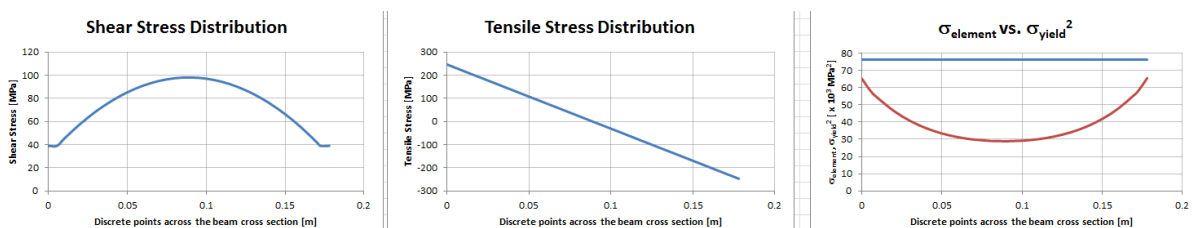
2. TRANSOM WEB STRENGTH

Having obtained the load carrying ability of the conveyance roof's I and channel beam it is necessary to determine whether the Transom can handle the remaining load. From the preceding chapter the beam geometries were altered until F9 was approximately at its maximum allowed value and the force and moment needed to be resisted by the Transom calculated. The geometry and material properties of the Transom constructed from structural steel is provided below. From the preceding appendix it is seen that the Transom must resist a force of 743 kN and a moment of 1.4×10^3 kNm.

This force and moment is considered as a force and moment applied on a simply supported beam where the supports are the two webs of the channel sections comprising the Transom. The reaction force in each of the webs, FA and FB were then calculated.

The forces that will cause the webs of the Transom to yield or buckle were then calculated and compared to the forces that need to be resisted by the Transom. It can be seen that the forces that will cause yielding or buckling is highlighted in red as it is beneath the forces that works in on the Transom channel's webs. The Transom is therefore not able to withstand the applied load. It can be seen that the applied load is far in excess of the load carrying ability of the Transom and that the load cannot be radically reduced. Because the forces carried by the bottom beam is nearly equal to the maximum load carrying ability of the roof beams the bottom beam cannot be made to carry more load. Even if the I-beam and channel in the conveyance roof was loaded to its maximum value, the force and moment that needs to be carried by the Transom would still overload the Transom webs. The decision was therefore taken to go with the support fixture presented in the dissertation body.

Transom Geometric properties

H	356	mm	0.356	m
W	171	mm	0.171	m
t	12.5	mm	0.0125	m
Area	8412.5	mm^2	0.0084125	m^2
Mass	66	kg/m	123.49214	kg
L	1882	mm	1.882	m
x	82.5	mm	0.0825	m

Mechanical Properties

ρ	7800	kg/m^3		
σY	355	MPa	355000000	Pa
E	200	GPa	2E+11	Pa

Force Analysis

F7	743279	N
M	1380000	Nm
FA	16,355,633.23	N
FB	17,098,912.23	N

Sum of vertical forces

FA + F7 - FB = 0		
FB = FA + F7		......(1)

Sum of moments

FB(x) - M - F7(x/2) = 0		
(FA + F7)(x) - M - F7(x/2) = 0		
FA	16355633.23	N

Force limits for channel A (Compresion)

Yielding

Area	0.023525	m^2
σ=FA/Area		
FA	8,351,375.00	N

Buckling

K	1	(Assume it behaves as pinned)
L	0.331	m
I	3.06315E-07	m^4
Pcr = π^{2}EI/(KL)^2		
Pcr	5,518,768.36	N

Force limits for channel B

Area	0.023525	m^2
σ=FB/Area		
FB	8,351,375.00	N

APPENDIX H. CYLINDER MOUNTING BRACKETS

This appendix covers the calculations of the cylinder mounting brackets. These brackets must resist both a force exerted by the cylinder should the clamp beams become jammed and the load imposed by the weight of the cylinder.

1. TOP CYLINDER MOUNTING BRACKET

The first part of the EES program, Cylinder top mount, lists the cylinder details. It is known that an 80 mm cylinder is used with mine pressure able to go up to 4.5 bar. The bracket needs to position the cylinder such that it aligns with the clamp beams and the length of the mount is obtained from a three dimensional model. The geometry of the flange and web of the T-section beam can be adjusted to obtain a design of adequate strength to resist the forces generated by the cylinder. Other important geometrical calculations are performed for use later in the program. The area of the cylinder is important to calculate the force generated by the cylinder. The moments of inertia about the X-X and Y-Y axis is calculated where the Y-Y axis is parallel to the flange of the T-section. Because of the asymmetry of the T-section about the Y-Y axis the neutral axis is calculated first. It is also known that the maximum shear stress occurs at the neutral axis and as such Q is calculated at the neutral axis when the beam is loaded either horizontally or vertically. The mass of the cylinder is obtained according to the guidelines given in the Festo standard cylinder document [40]. Because the weight of the cylinder acts downwards and the top mounting beam connects to the cylinder at an angle;θ is introduced to obtain the force component perpendicular to the beam. The extract of the EES program Cylinder top mount is given below.

Cylinder information

$$D_{cylinder} = \frac{80}{1000}$$

$$Pressure = 450000$$

Geometric properties

$$L_{top,mount} = \frac{180}{1000}$$

$$t_{flange} = \frac{6}{1000}$$

$$h_{flange} = \frac{157}{1000}$$

$$h_{web} = \frac{60}{1000}$$

$$t_{web} = \frac{6}{1000}$$

$$\theta = 30$$

$$A_{cylinder} = \pi \cdot \frac{D_{cylinder}^2}{4}$$

$$I_{xx} = \frac{1}{12} \cdot t_{flange} \cdot h_{flange}^3 + \frac{1}{12} \cdot h_{web} \cdot t_{web}^3$$

$$Y_{neutral} = \frac{t_{web} \cdot h_{web} \cdot \frac{h_{web}}{2} + h_{flange} \cdot t_{flange} \cdot \left[h_{web} + \frac{t_{flange}}{2} \right]}{t_{flange} \cdot h_{flange} + t_{web} \cdot h_{web}}$$

$$I_{yy} = \frac{1}{12} \cdot t_{web} \cdot h_{web}^3 + t_{web} \cdot h_{web} \cdot \left[Y_{neutral} - \frac{h_{web}}{2} \right]^2 + \frac{1}{12} \cdot h_{flange} \cdot t_{flange}^3 + t_{flange} \cdot h_{flange} \cdot \left[h_{web} + \frac{t_{flange}}{2} - Y_{neutral} \right]^2$$

$$Q_{max} = t_{flange} \cdot \frac{h_{flange}}{2} \cdot \frac{h_{flange}}{4} + h_{web} \cdot \frac{t_{web}}{2} \cdot \frac{t_{web}}{4}$$

$$Q_{max,vert} = t_{flange} \cdot h_{flange} \cdot \left[h_{web} + \frac{t_{flange}}{2} - Y_{neutral} \right] + t_{web} \cdot (h_{web} - Y_{neutral}) \cdot \left[\frac{h_{web} - Y_{neutral}}{2} \right]$$

$$Mass_{cylinder} = \frac{2660 + 30 \cdot 92}{1000}$$

With the geometry of the brackets fixed the forces working in on the bracket must be determined. The extract below shows the forces and stresses due to the push of the cylinder. The force exerted by the cylinder is equal to the pressure times the area should the clamp beam jam which is assumed to be the case. A resultant shear force equal in magnitude is therefore set up in the beam's fixed end. Because the beam behaves as a cantilever beam the moment at the fixed end is simply the product of the beam length and applied force. Below the calculations on the left the shear force diagram for the beam in the horizontal direction (VH) is shown where x is discrete points along the beam length. The graph on the right shows the moments (MH) in the beam.

Forces

$$F_{cylinder} = Pressure \cdot A_{cylinder}$$

$$V_{top,mount} = F_{cylinder}$$

$$M_{top,mount} = F_{cylinder} \cdot L_{top,mount}$$
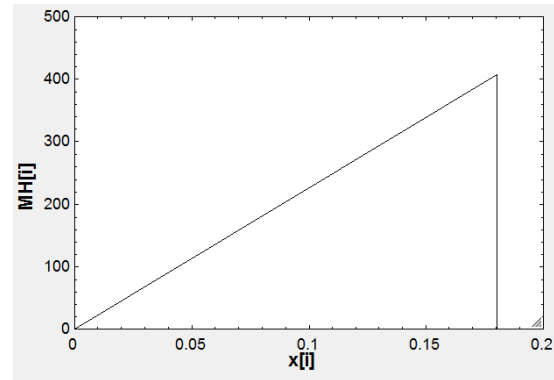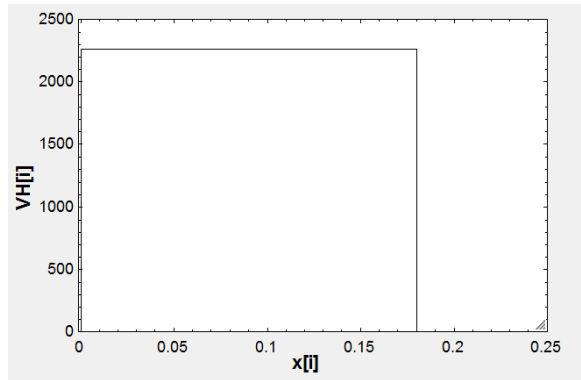
With the forces according to the graphs above it can be seen that the maximum stress will occur at the section where the bracket is fixed to the Transom as the shear force and moment is a maximum. The maximum shear force is calculated at the centre of the flange and the tensile stress at the outer edge of the flange. The equation for determining the stress across the beam cross section is then added for both the tensile and shear stress. The shear stress takes the form of a parabola of which the equation is determined using the maximum stress at the centre of the flange and the knowledge of zero stress at the outer edge of the flange. Below the extract of the calculations the tensile stress distribution (σ) for discrete points (x) across the cross section of the beam adjacent the beam fixed end is given. On the right of the tensile stress distribution the shear stress (τ) distribution at discrete points (x) across the cross section of the beam is given.

Stresses

$$\tau_{max} = V_{top,mount} \cdot \frac{Q_{max}}{I_{xx} \cdot t_{flange}}$$

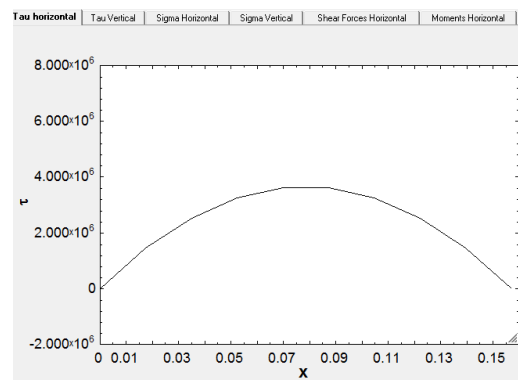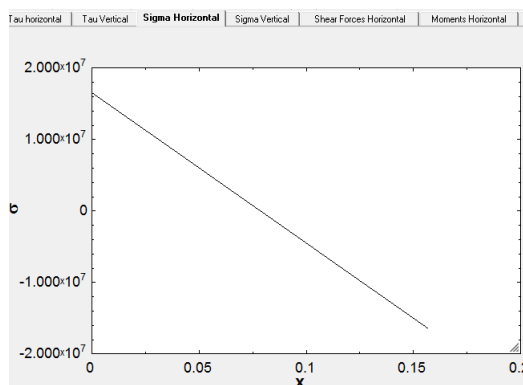$$\sigma_{max} = M_{top,mount} \cdot \frac{h_{flange}}{2 \cdot I_{xx}}$$

$$\tau = a \cdot (x - p)^2 + q$$

$$\sigma = M_{top,mount} \cdot \left[\frac{\frac{h_{flange}}{2} - x}{I_{xx}} \right]$$

$$p = \frac{h_{flange}}{2}$$

$$q = \tau_{max}$$

$$0 = a \cdot (0 - p)^2 + q$$

The beam also needs to support the weight of the cylinder which is calculated in the extract provided below. A reaction force equal to the magnitude of the weight of the cylinder is developed at the beam fixed end as well as a moment. Below the extract of the calculations the shear force (VV) distribution in the vertical direction is provided on the left and the moment (MV) distribution on the right along the beam length (x).

"Vertical forces"

F_vertical = (mass_cylinder*9.81)*cos(90-theta)

V_top_mount_vert = F_vertical
M_top_mount_vert = F_vertical*L_top_mount
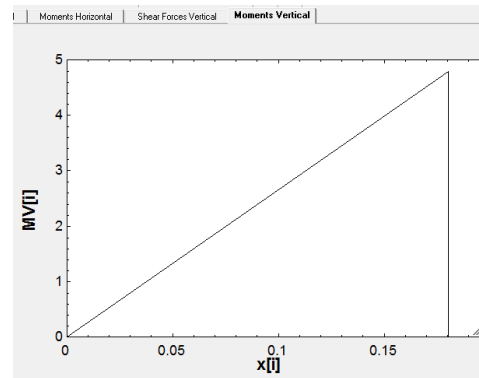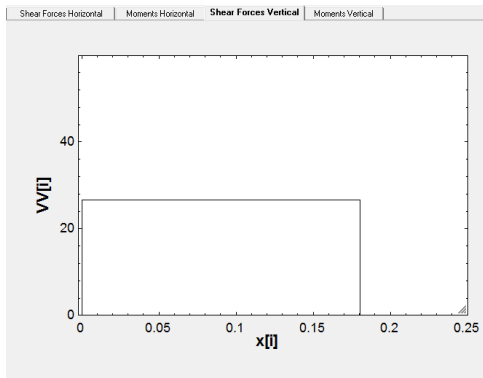
With the forces acting perpendicular to the beam about the Y-Y axis known as illustrated above the stresses in the beam is calculated. The maximum shear stress occurs at the neutral axis in the cross section immediately adjacent to the beam's fixed end. The maximum tensile stress is found at the edge furthest away from the neutral axis and thus at the outer edge of the T-section beam's web. The calculations for the maximum stresses and the stress distributions are provided below. Beneath the calculations the tensile stress distribution (σvert) across discrete points (x) through the cross section of the beam next to the beam's fixed end is shown. On the right the shear stress (τvert) distribution at discrete points (x) across the beam cross section next to the beam's fixed end is shown. It can be seen that because of the asymmetry of the beam about the Y-Y axis that the tensile stress isn't symmetrical but greatest at the web's base. The shear stress starts off at zero and increases to a maximum value at the neutral axis before decreasing to the average shear stress across the beam's flange.

"stresses"

tau_max_vert = V_top_mount_vert*Q_max_vert/(I_yy*t_web)
sigma_max_vert = M_top_mount_vert*Y_neutral/I_yy

tau_vert = a_vert*(x_vert - p_vert)^2 +q_vert
sigma_vert = M_top_mount_vert*(Y_neutral - x_vert)/I_yy

p_vert = Y_neutral
q_vert = tau_max_vert
0 = a_vert*(0 - p_vert)^2 + q_vert

"x_vert = 0.01"
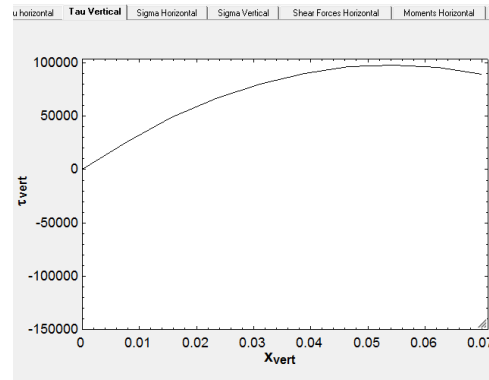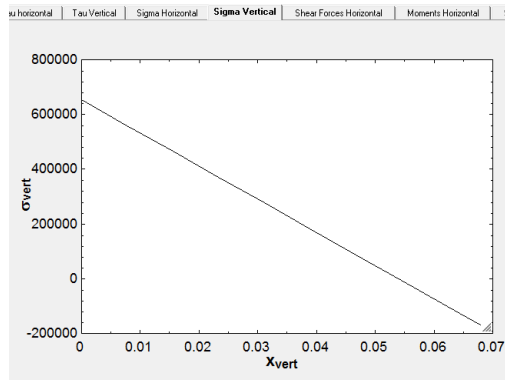
Having calculated the maximum stresses the safety factors against yield can be calculated when using 6061-T6 Aluminium. The calculations below show how the four safety factors are determined.

"Safety Factors"

sigma_yield = 275*10^6
SF_tensile = sigma_yield/sigma_max
SF_shear = ((1/3^0.5)*sigma_yield)/tau_max
SF_tensile_vert = sigma_yield/sigma_max_vert
SF_shear_vert = ((1/3^0.5)*sigma_yield)/tau_max_vert

In order to generate the shear force and moment graphs presented so far in the appendix the following data points given below are needed.

"Graph data"

"x axis"

x[0] = 0
x[1] = x[0]
x[2] = L_top_mount
x[3] = x[2]

"Forces"

VH[0] = 0
VH[1] = F_cylinder
VH[2] = VH[1]
VH[3] = 0

VV[0] = 0
VV[1] = F_vertical
VV[2] = VV[1]
VV[3] = 0

"Moments"

MH[0] = 0
MH[1] = MH[0]
MH[2] = M_top_mount
MH[3] = 0

MV[0] = 0
MV[1] = MV[0]
MV[2] = M_top_mount_vert
MV[3] = 0

All calculations in the program are done using SI units and the results obtained are also in SI units. The table presented below shows the results obtained. The four maximum stresses calculated are shown in yellow and the safety factors in green.

(Table 1, Run 10)

a = -5.927E+08	$A_{cylinder}$ = 0.005027	a_{vert} = -3.370E+07	$D_{cylinder}$ = 0.08	$F_{cylinder}$ = 2262	$F_{vertical}$ = 26.59
$Mass_{cylinder}$ = 5.42	$M_{top,mount}$ = 407.2	$M_{top,mount,vert}$ = 4.785	p = 0.0785	Pressure = 450000	p_{vert} = 0.05388
$SF_{shear,vert}$ = 1623	$SF_{tensile}$ = 16.66	$SF_{tensile,vert}$ = 420.8	σ = -1.651E+07	σ_{max} = 1.651E+07	$\sigma_{max,vert}$ = 653568
τ_{vert} = 89048	θ = 30	t_{flange} = 0.006	t_{web} = 0.006	$V_{top,mount}$ = 2262	$V_{top,mount,vert}$ = 26.59
h_{flange} = 0.157	h_{web} = 0.06	I_{xx} = 0.000001936	I_{yy} = 3.945E-07	$L_{top,mount}$ = 0.18	
q = 3.652E+06	Q_{max} = 0.00001876	$Q_{max,vert}$ = 0.000008708	q_{vert} = 97809	SF_{shear} = 43.47	
σ_{vert} = -195607	σ_{yield} = 2.750E+08	τ = 1.137E-12	τ_{max} = 3.652E+06	$\tau_{max,vert}$ = 97809	
x = 0.157	x_{vert} = 0.07	$Y_{neutral}$ = 0.05388			

The parametric table used to calculate the stresses across the beam cross sections is presented below.

Table 1

	x	x_{vert}	σ	τ	$σ_{vert}$	$τ_{vert}$
Run 1	0	0	1.651E+07	0	653568	-7.105E-15
Run 2	0.01744	0.007778	1.284E+07	1.443E+06	559216	26202
Run 3	0.03489	0.01556	9.172E+06	2.525E+06	464863	48327
Run 4	0.05233	0.02333	5.503E+06	3.247E+06	370510	66375
Run 5	0.06978	0.03111	1.834E+06	3.607E+06	276157	80347
Run 6	0.08722	0.03889	-1.834E+06	3.607E+06	181805	90241
Run 7	0.1047	0.04667	-5.503E+06	3.247E+06	87452	96058
Run 8	0.1221	0.05444	-9.172E+06	2.525E+06	-6901	97798
Run 9	0.1396	0.06222	-1.284E+07	1.443E+06	-101254	95462
Run 10	0.157	0.07	-1.651E+07	1.137E-12	-195607	89048

2. CYLINDER BOTTOM MOUNT

The calculation of the bottom cylinder mount is similar to that of the top cylinder mount with differences in the vertical forces where the weight of the cylinder works in perpendicular to the beam. The EES program Cylinder bottom mount starts off with the cylinder properties and the geometrical calculations. The length of the beam is longer than the top mount at 205 mm and the heights of the flange and web is less. The heights are less because the mounting base isn't stretched to fit onto existing bolt holes but can be of the dimension required to simply accommodate the clamp section. Under the geometrical calculation section the flange and web dimensions are fixed and the moment of inertia about the X-X and Y-Y axis calculated. The cylinder area and neutral axis about the asymmetrical side of the T-section beam is also calculated. The values of Q for the horizontal force and vertical force are also calculated at the neutral axis. The cylinder and geometrical calculations are shown below.

Table 1

	x	x_{vert}	σ	τ	$σ_{vert}$	$τ_{vert}$
Run 1	0	0	1.651E+07	0	653568	-7.105E-15
Run 2	0.01744	0.007778	1.284E+07	1.443E+06	559216	26202
Run 3	0.03489	0.01556	9.172E+06	2.525E+06	464863	48327
Run 4	0.05233	0.02333	5.503E+06	3.247E+06	370510	66375
Run 5	0.06978	0.03111	1.834E+06	3.607E+06	276157	80347

Cylinder information

$$D_{cylinder} = \frac{80}{1000}$$

$$Pressure = 450000$$

Geometric properties

$$L_{bottom,mount} = \frac{205}{1000}$$

$$t_{flange} = \frac{6}{1000}$$

$$h_{flange} = \frac{60}{1000}$$

$$h_{web} = \frac{60}{1000}$$

$$t_{web} = \frac{6}{1000}$$

$$A_{cylinder} = \pi \cdot \frac{D_{cylinder}{}^2}{4}$$

$$I_{xx} = \frac{1}{12} \cdot t_{flange} \cdot h_{flange}{}^3 + \frac{1}{12} \cdot h_{web} \cdot t_{web}{}^3$$

$$Y_{neutral} = \frac{t_{web} \cdot h_{web} \cdot \frac{h_{web}}{2} + h_{flange} \cdot t_{flange} \cdot \left[h_{web} + \frac{t_{flange}}{2} \right]}{t_{flange} \cdot h_{flange} + t_{web} \cdot h_{web}}$$

$$I_{yy} = \frac{1}{12} \cdot t_{web} \cdot h_{web}{}^3 + t_{web} \cdot h_{web} \cdot \left[Y_{neutral} - \frac{h_{web}}{2} \right]^2 + \frac{1}{12} \cdot h_{flange} \cdot t_{flange}{}^3 + t_{flange} \cdot h_{flange} \cdot \left[h_{web} + \frac{t_{flange}}{2} - Y_{neutral} \right]^2$$

$$Q_{max} = t_{flange} \cdot \frac{h_{flange}}{2} \cdot \frac{h_{flange}}{4} + h_{web} \cdot \frac{t_{web}}{2} \cdot \frac{t_{web}}{4}$$

$$Q_{max,vert} = t_{flange} \cdot h_{flange} \cdot \left[h_{web} + \frac{t_{flange}}{2} - Y_{neutral} \right] + t_{web} \cdot (h_{web} - Y_{neutral}) \cdot \left[\frac{h_{web} - Y_{neutral}}{2} \right]$$

$$Mass_{cylinder} = \frac{2660 + 30 \cdot 92}{1000}$$

The geometrical properties are used to calculate the forces working in on the beam. When the cylinder presses against a jammed clamp beam a reaction force equal in magnitude is developed at the beam clamped end. The maximum moment is also obtained at the cantilever beam's clamped end. The figure below the calculations on the left shows the shear force (VH) distribution at discrete points (x) along the length of the beam and the figure on the right the moment (MH) distribution.

Forces

$$F_{cylinder} = Pressure \cdot A_{cylinder}$$

$$V_{bottom,mount} = F_{cylinder}$$

$$M_{bottom,mount} = F_{cylinder} \cdot L_{bottom,mount}$$
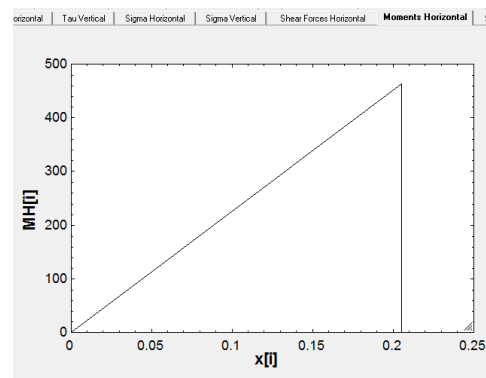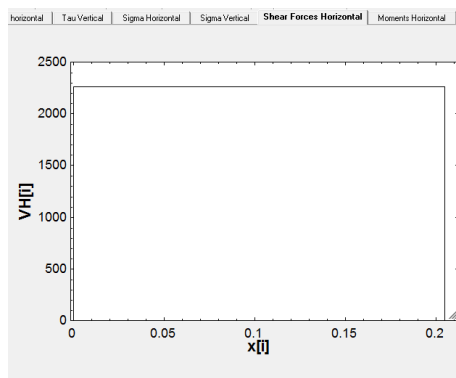
The forces set up stresses in the beam where the maximum tensile stress is found at the outer edge of the flange and the maximum shear stress at the centre of the flange. After calculating the maximum stresses formula is presented to calculate the shear and tensile stress at discrete points along the cross section of the beam at the clamped end of the beam. In order to calculate the shear stresses a parabolic equation is derived using the maximum shear stress at the neutral axis and the zero stress at the edge of the flange. The calculations are shown below.

Stresses

$$\tau_{max} = V_{bottom,mount} \cdot \frac{Q_{max}}{I_{xx} \cdot t_{flange}}$$

$$\sigma_{max} = M_{bottom,mount} \cdot \frac{h_{flange}}{2 \cdot I_{xx}}$$

$$\tau = a \cdot (x - p)^2 + q$$

$$\sigma = M_{bottom,mount} \cdot \left[\frac{\frac{h_{flange}}{2} - x}{I_{xx}} \right]$$

$$p = \frac{h_{flange}}{2}$$

$$q = \tau_{max}$$

$$0 = a \cdot (0 - p)^2 + q$$

Using the equations in conjunction with a parametric table presented later on; the graphs shown below are generated. The graph on the left shows the tensile stress (σ) distribution at discrete points (x) across the beam cross section adjacent to the clamped end. The graph on the right shows the shear stress (τ) distribution at discrete points (x) across the beam cross section adjacent to the clamped end.
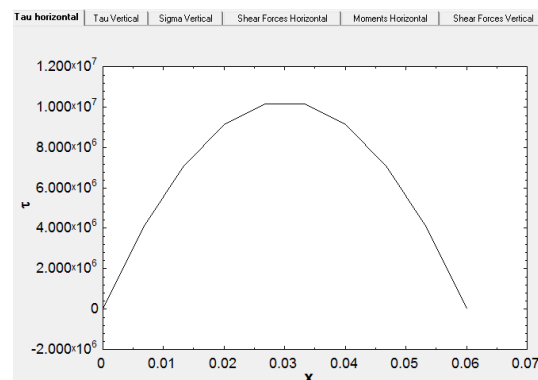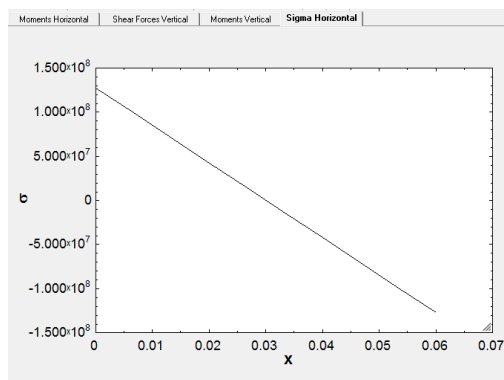

Having completed the horizontal forces the vertical forces due to the weight of the cylinder is calculated. The weight of the cylinder works in perpendicular to the beam and therefore differs from the top beam. The reaction forces and moments are calculated. Below the calculations the shear force (VV) distribution along the length (x) of the beam and the moment distribution (MV) along the length of the beam (X) are shown on the left and right respectively.

Vertical forces

$$F_{vertical} = Mass_{cylinder} \cdot 9.81$$

$$V_{bottom,mount,vert} = F_{vertical}$$

$$M_{bottom,mount,vert} = F_{vertical} \cdot L_{bottom,mount}$$
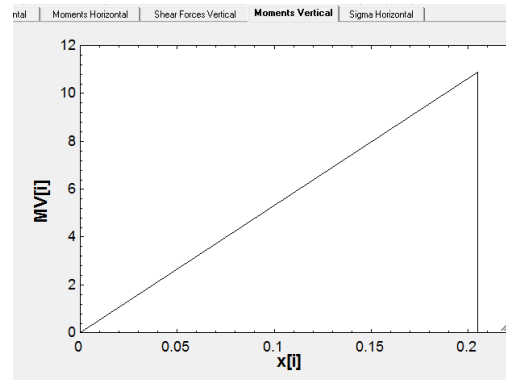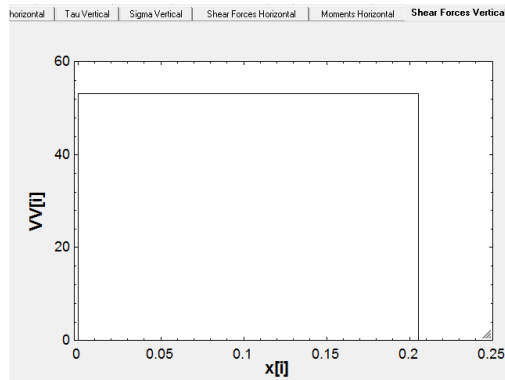
The maximum shear stress is calculated at the neutral axis and the maximum tensile stress at the base of the web similar to the top mount. Equations are also provided for the shear and tensile stress distribution with the shear stress calculated from a parabolic equation. The equation is derived using the maximum stress at the neutral axis and the zero stress at the base of the web. Beneath the calculations on the left the tensile stress (σvert) distribution at discrete points (x) across the cross section of the beam adjacent to the clamped end is shown. The graph on the right shows the shear stress distribution (τvert) at discrete points (x) across the cross section of the beam adjacent to the clamped end.

stresses

$$\tau_{max,vert} = V_{bottom,mount,vert} \cdot \frac{Q_{max,vert}}{I_{yy} \cdot t_{web}}$$

$$\sigma_{max,vert} = M_{bottom,mount,vert} \cdot \frac{Y_{neutral}}{I_{yy}}$$

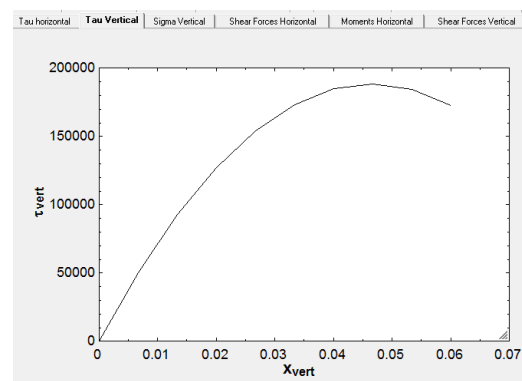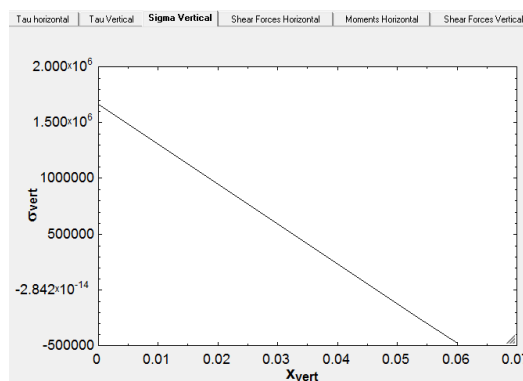$$\tau_{vert} = a_{vert} \cdot (x_{vert} - p_{vert})^2 + q_{vert}$$

$$\sigma_{vert} = M_{bottom,mount,vert} \cdot \left[\frac{Y_{neutral} - x_{vert}}{I_{yy}} \right]$$

$$p_{vert} = Y_{neutral}$$

$$q_{vert} = \tau_{max,vert}$$

$$0 = a_{vert} \cdot (0 - p_{vert})^2 + q_{vert}$$

From the graph above on the left it can be seen that the tensile stress distribution is asymmetric due to the asymmetry of the T-section. The tensile stress is zero at the neutral axis and a maximum at the base of the web. The graph on the right shows the shear stress starting off from zero at the base of the web and increasing to a maximum at the neutral axis after which it decreases to the average stress across the flange.

Having calculated the maximum stresses the safety factors against yield can be calculated when using 6061-T6 Aluminium. The calculations below show how the four safety factors are determined.

Safety Factors

$$\sigma_{yield} = 275 \cdot 10^6$$

$$SF_{tensile} = \frac{\sigma_{yield}}{\sigma_{max}}$$

$$SF_{shear} = \frac{\frac{1}{3^{0.5}} \cdot \sigma_{yield}}{\tau_{max}}$$

$$SF_{tensile,vert} = \frac{\sigma_{yield}}{\sigma_{max,vert}}$$

$$SF_{shear,vert} = \frac{\frac{1}{3^{0.5}} \cdot \sigma_{yield}}{\tau_{max,vert}}$$

In order to plot the shear force and moment diagrams presented in this appendix the graph data provided below was generated.

Graph data

x axis

$$x_0 = 0$$

$$x_1 = x_0$$

$$x_2 = L_{bottom,mount}$$

$$x_3 = x_2$$

Forces

$$VH_0 = 0$$

$$VH_1 = F_{cylinder}$$

$$VH_2 = VH_1$$

$$VH_3 = 0$$

$$W_0 = 0$$

$$W_1 = F_{vertical}$$

$$W_2 = W_1$$

$$W_3 = 0$$

Moments

$MH_0 = 0$

$MH_1 = MH_0$

$MH_2 = M_{bottom,mount}$

$MH_3 = 0$

$MV_0 = 0$

$MV_1 = MV_0$

$MV_2 = M_{bottom,mount,vert}$

$MV_3 = 0$

A parametric table was used to vary the position at which both the tensile and shear stresses were calculated in order to generate the tensile and shear stress distribution graphs. The parametric table used is shown below.

Table 1	x	x_{vert}	σ	τ	σ_{vert}	τ_{vert}
Run 1	0	0	1.275E+08	-9.095E-13	1.661E+06	1.421E-14
Run 2	0.006667	0.006667	9.919E+07	4.055E+06	1.423E+06	50151
Run 3	0.01333	0.01333	7.085E+07	7.097E+06	1.185E+06	92557
Run 4	0.02	0.02	4.251E+07	9.124E+06	946729	127218
Run 5	0.02667	0.02667	1.417E+07	1.014E+07	708558	154133
Run 6	0.03333	0.03333	-1.417E+07	1.014E+07	470388	173303
Run 7	0.04	0.04	-4.251E+07	9.124E+06	232217	184728
Run 8	0.04667	0.04667	-7.085E+07	7.097E+06	-5954	188407
Run 9	0.05333	0.05333	-9.919E+07	4.055E+06	-244125	184340
Run 10	0.06	0.06	-1.275E+08	-2.728E-12	-482296	172529

All the calculations performed in this program were done using SI units and the results obtained are also in SI units. The safety factors obtained are highlighted in green and the maximum stresses in yellow. It can be seen that the bracket is of adequate strength according to the results presented below.

(Table 1, Run 10)

$a = -1.141E+10$	$A_{cylinder} = 0.005027$	$a_{vert} = -8.714E+07$	$D_{cylinder} = 0.08$	$F_{cylinder} = 2262$
$L_{bottom,mount} = 0.205$	$Mass_{cylinder} = 5.42$	$M_{bottom,mount} = 463.7$	$M_{bottom,mount,vert} = 10.9$	$p = 0.03$
$q_{vert} = 188409$	$SF_{shear} = 15.47$	$SF_{shear,vert} = 842.7$	$SF_{tensile} = 2.156$	$SF_{tensile,vert} = 165.5$
$\tau = -2.728E-12$	$\tau_{max} = 1.026E+07$	$\tau_{max,vert} = 188409$	$\tau_{vert} = 172529$	$t_{flange} = 0.006$
$Y_{neutral} = 0.0465$				

$F_{vertical} = 53.17$	$h_{flange} = 0.06$	$h_{web} = 0.06$	$I_{xx} = 1.091E-07$	$I_{yy} = 3.051E-07$
$Pressure = 450000$	$p_{vert} = 0.0465$	$q = 1.026E+07$	$Q_{max} = 0.00000297$	$Q_{max,vert} = 0.000006487$
$\sigma = -1.275E+08$	$\sigma_{max} = 1.275E+08$	$\sigma_{max,vert} = 1.661E+06$	$\sigma_{vert} = -482296$	$\sigma_{yield} = 2.750E+08$
$t_{web} = 0.006$	$V_{bottom,mount} = 2262$	$V_{bottom,mount,vert} = 53.17$	$x = 0.06$	$x_{vert} = 0.06$